

Early-age thermal crack control in concrete

P B Bamforth



CIRIA *sharing knowledge ■ building best practice*

Classic House, 174-180 Old Street, London EC1V 9BP

TELEPHONE 020 7549 3300 FAX 020 7253 0523

EMAIL enquiries@ciria.org

WEBSITE www.ciria.org

Errata

Readers are advised of the following:

1. Figure 4.13 on page 61 is incorrect. The corrected image and caption reference should be as follows:

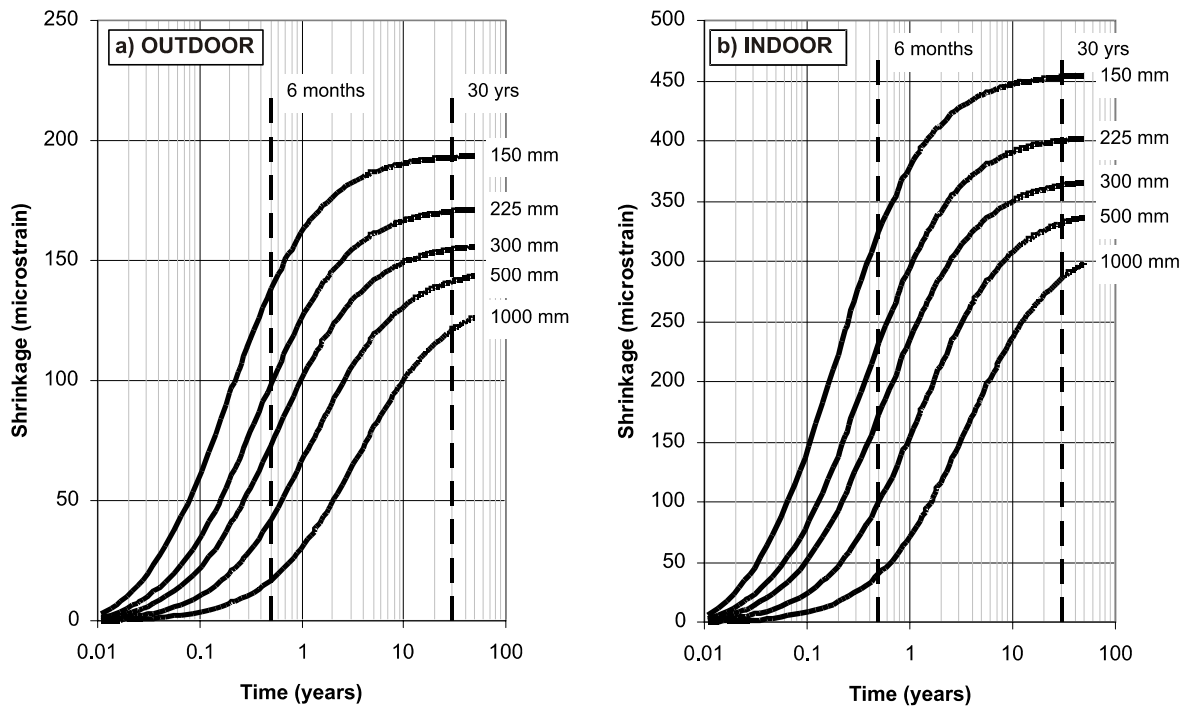


Figure 4.13 *Drying shrinkage curves estimated using the method of EN1992-1-1 for a) outdoor conditions (45 per cent rh) and b) UK indoor conditions (85 per cent rh)*

2. On page 111 under “British Standards” BS8500 Parts 1 and 2 were updated in 2006 and should be listed as:

BS8500-1:2006 Concrete – Part 1: Complementary British Standard to BS EN206-1 – Part 1: Method of specifying and guidance for the specifier

BS8500-2:2006 Concrete – Part 2: Complementary British Standard to BS EN206-1 – Part 2: Specification for constituent materials for concrete

We apologise for any inconvenience this may have caused.

Early-age thermal crack control in concrete

Bamforth, P

CIRIA

CIRIA C660

© CIRIA 2007

RP722

ISBN 978-8-86107-660-2

British Library Cataloguing in Publication Data

A catalogue record for this book is available from the British Library.

Keywords Reinforced concrete, early-age behaviour, thermal cracking, shrinkage, design, reinforcement, crack control	
Reader interest Reinforced concrete designers and specifiers, construction planners and engineers, concrete technologists	Classification AVAILABILITY Unrestricted CONTENT Design and construction guidance STATUS Committee-guided USER Structural and civil engineers in design and construction

Published by CIRIA, Classic House, 174–180 Old Street, London EC1V 9BP, UK.

This publication is designed to provide accurate and authoritative information on the subject matter covered. It is sold and/or distributed with the understanding that neither the authors nor the publisher is thereby engaged in rendering a specific legal or any other professional service. While every effort has been made to ensure the accuracy and completeness of the publication, no warranty or fitness is provided or implied, and the authors and publisher shall have neither liability nor responsibility to any person or entity with respect to any loss or damage arising from its use.

All rights reserved. No part of this publication may be reproduced or transmitted in any form or by any means, including photocopying and recording, without the written permission of the copyright-holder, application for which should be addressed to the publisher. Such written permission must also be obtained before any part of this publication is stored in a retrieval system of any nature.

If you would like to reproduce any of the figures, text or technical information from this or any other CIRIA publication for use in other documents or publications, please contact the Publishing Department for more details on copyright terms and charges at: publishing@ciria.org Tel: +44 (0)20 7549 3300.

Summary

Early-age thermal cracking occurs when the tensile strain, arising from either restrained thermal contraction or a temperature differential within the concrete section, exceeds the tensile strain capacity of the concrete. Autogenous shrinkage may also contribute to early contraction. Numerous factors influence the risk of early-age cracking including the temperature rise, the coefficient of thermal expansion of the concrete, the restraint to movement offered either by adjacent elements or by differential strain within an element, and the ability of the concrete to resist tensile strain. Temperature rise depends on the heat generating capacity of the concrete affected by the cement content and type, the element thickness and the conditions into which the concrete is cast, in particular the formwork type.

This guide provides a method for estimating the magnitude of crack-inducing strain and the risk of cracking; and where cracking is predicted guidance is provided on the design of reinforcement to control crack widths. For specific situations where cracking should be avoided, or where the use of reinforcement to achieve acceptable crack widths is uneconomic or impractical, measures are described to minimise the risk including selection of materials and mix design, planning pour sizes and construction sequence, the use of insulation to reduce thermal gradients, the use of movement joints, and cooling of the concrete either prior to placing or *in situ*.

Significant changes since the last revision to report R91 – *Early-age thermal crack control in concrete* (CIRIA, 1992) which this report replaces, include:

- ↻ compatibility with EN1992-3:2006 and EN1992-1-1 with regard to the properties of concrete and the design of reinforcement
- ↻ an increase in the heat generating capacity of CEM I and peak temperature values
- ↻ additional data on temperature rise for concretes containing fly ash and ggbs
- ↻ additional data and methods for estimating critical parameters such as restraint and tensile strain capacity
- ↻ different methods for calculating crack width depending on the form of restraint
- ↻ advice on specification, measurement and testing.

Although the title of this guide refers specifically to early-age thermal cracking, the design of the reinforcement should take into account the effect of both short- and long-term strains. Guidance is also provided on how to deal with long-term thermal strains and drying shrinkage.

Acknowledgements

Authors

Phil Bamforth BSc (Hons), PhD, C Eng, MICE

After graduating from Leeds University in 1970 Phil joined Taywood Engineering, the Consultancy arm of Taylor Woodrow, and spent the next 33 years undertaking and managing construction consultancy and research, primarily in the area of concrete technology. During this time he completed his PhD with Aston University. Since 2003 he has been an independent consultant supporting design and construction activities in concrete. He is experienced in the performance, specification, investigation and repair of concrete structures.

Steering group

Following CIRIA's usual practice, the research project was carried out under contract to CIRIA by Dr Phil Bamforth who has authored the report. The project was guided throughout by the CIRIA Project Steering Group comprising:

Chair

Keith Wilson

Faber Maunsell

Members

Chris Clear

BCA

Steve Denton

Parsons Brinkerhoff

Ravindra Dhir

University of Dundee (CTU)

Charles Goodchild

The Concrete Centre

Tom Harrison (corresponding)

QPA-BRMCA

Neil Henderson

Mott MacDonald

Denis Higgins

CSMA

Tony Jones

Arup

Rob Lewis

Elkem

Jon Knights

Halcrow

Bryan Marsh

Arup Materials

Andrew Pitchford

CIRIA

Ben Sadka

Highways Agency

Lindon Sear

UKQAA

Jonathan Wood

Consultant (representing ICE)

CIRIA managers

CIRIA's research manager for the project was Alan Gilbertson.

Project funders

The project was funded by CIRIA Core programme members and by special contributions from The Institution of Civil Engineers Research and Development Enabling Fund, The Concrete Centre, The British Cement Association, The Cementitious Slag Makers Association, The UK Quality Ash Association.

The author wishes to thank the Steering Group for their guidance and technical input, and in particular Steve Denton, of Parsons Brinkerhoff, who made a substantial contribution in developing an understanding of the design method of EN1992-1-1 and EN1992-3 as it applies to early-age cracking. Thanks are also extended to Tom Harrison, the author of CIRIA R91, as much of the content is based upon his work.

Contents

Summary	3
Acknowledgements	4
Notation	8
Abbreviations	10
Glossary	10
List of figures	11
List of tables	12
1 Introduction	15
1.1 Scope	15
1.2 Background to updating the former report R91	16
1.3 The cause of early-age thermal cracking	17
1.4 The design process	20
1.5 Responsibilities	21
1.6 Other effects of temperature	21
1.7 Advances	22
1.8 Format of the guide	22
2 Significance of cracking	24
2.1 The acceptability of cracking	24
2.2 The relationship between crack width and functionality	24
2.3 Cracks which lead to durability problems	25
2.4 Cracks which lead to a malfunction of the structure	26
2.5 Cracks which are aesthetically unacceptable	27
2.6 The role of autogenous healing	28
2.7 Measures to avoid cracking	29
3 The design process	30
3.1 Introduction	30
3.2 Estimating the risk of cracking and the crack-inducing strain	31
3.2.1 External restraint	31
3.2.2 Internal restraint	33
3.2.3 Input data	33
3.3 Minimum reinforcement area $A_{s,min}$	35
3.3.1 General equation	36
3.3.2 Tensile strength of concrete	37
3.3.3 Tensile strength of steel	37
3.4 Crack spacing	37
3.5 Crack width	38
3.5.1 The requirements of EN1992-3	38
3.5.2 A member restrained along one edge	38
3.5.3 A member restrained at its ends only	38

3.5.4	A member subject to internal restraint	39
3.6	The Simplified Method with default values	39
3.6.1	Estimating the risk of cracking and the crack-inducing strain	39
3.6.2	Crack control	41
3.7	Selecting options to reduce the risk of cracking	41
4	Factors affecting early-age cracking and data required for design	45
4.1	Information and assumptions	45
4.2	Temperature rise	47
4.2.1	Influencing factors	47
4.2.2	Estimating T_1	49
4.2.3	Adjustments to T_1	53
4.3	Annual temperature change, T_2	54
4.4	Temperature differentials, ΔT	56
4.5	Coefficient of thermal expansion, α_c	57
4.6	Shrinkage strains	58
4.6.1	Autogenous shrinkage, ε_{ca}	58
4.6.2	Drying shrinkage, ε_{cd}	60
4.6.3	Appropriate use of shrinkage strains	61
4.7	Restraint, R	62
4.7.1	General guidance	62
4.7.2	External edge restraint	65
4.7.3	End and local restraint	66
4.7.4	Internal restraint	67
4.7.5	Combined internal and external restraint	68
4.8	Tensile strain capacity, ε_{ctu}	68
4.9	Coefficients and inherent safety factors	69
4.9.1	Coefficient for creep, K_1	70
4.9.2	Coefficient for sustained loading, K_2	70
4.9.3	Inherent safety factors	70
4.10	Tensile strength of concrete, f_{ct}	71
4.11	Estimating the minimum area of reinforcement, $A_{s,min}$	72
4.11.1	Changes in approach	72
4.11.2	External restraint	73
4.11.3	Internal restraint is dominant	74
4.12	The steel ratio used in calculating crack spacing, $\rho_{e,eff}$	75
4.13	The ratio of tensile strength to bond strength f_{ct}/f_b	76
5	Application of the design process using worked examples	78
5.1	Example 1: Retaining wall on a rigid foundation (continuous edge restraint)	79
5.2	Example 2: Suspended slab cast between core wall and columns (end restraint)	81
5.3	Example 3: Massive raft foundation (internal restraint)	83
6	Measures to mitigate cracking and minimise crack widths	85
6.1	Planning pour sizes and construction sequence	85

6.2	Movement joints	.87
6.3	Additional measures to cool the concrete	.90
6.3.1	Pre-cooling the constituent materials	.90
6.3.2	Cooling of the fresh concrete before placing	.92
6.3.3	<i>In situ</i> cooling	.92
6.3.4	Application of cooling techniques	.93
7	Specification, testing and monitoring	.94
7.1	Specification	.94
7.2	Test methods for obtaining relevant concrete properties	.97
7.2.1	Heat generation and temperature rise	.97
7.2.2	Coefficient of thermal expansion	.98
7.2.3	Tensile strain capacity	.99
7.3	Measurement and assessment of <i>in situ</i> temperature and strain	.99
7.3.1	Measuring temperature differentials	.99
7.3.2	Deriving restraint factors	.102
7.4	Measurement of crack width	.103
7.5	Actions in the event of non compliance	.104
8	Conclusions and recommendation	.105
9	References	.106

Appendices included on the CD

A1	Heat generation, temperature rise and temperature differentials
A2	A model for predicting the temperature rise and temperature differentials using adiabatic temperature data
A3	Estimating drying shrinkage using the method of EN1992-1-1
A4	Estimating autogenous shrinkage
A5	Estimating restraint
A6	Estimating tensile strain capacity
A7	Evaluating risk/extent of cracking using a strain based approach
A8	Reinforcement design to control crack widths
A9	The effect of peak temperature on the <i>in situ</i> strength
A10	Assessment of the <i>in situ</i> tensile strength of concrete

Spreadsheet calculators included on the CD

Model for prediction of temperature rise and thermal gradients
EN1992-1-1 drying shrinkage calculator
EN1992-1-1 autogenous shrinkage calculator
Restraint calculator based on the ACI method for walls on rigid foundations
Crack width calculator for edge restraint, end restraint and internal restraint

Notation

A_c	concrete cross-section used in the calculation of drying shrinkage
A_{ct}	area of concrete in the tensile zone used in the calculation of minimum area of reinforcement
$A_{c,eff}$	effective area of concrete in tension surrounding the reinforcement used in the calculation of crack spacing
A_o	cross sectional area of old (restraining) concrete section
A_n	cross sectional area of new (restrained) concrete section cast against A_o
$A_{s,min}$	minimum area of tensile reinforcement
c	cover to reinforcement
E_{cm}	mean elastic modulus of concrete
E_s	elastic modulus of reinforcement
E_o	elastic modulus of old (restraining) concrete section
E_n	elastic modulus of new (restrained) concrete section
ε_{ctu}	ultimate strain capacity of concrete in tension (tensile strain capacity)
f_{ck}	characteristic cylinder strength at 28 days
$f_{ck,cube}$	characteristic cube strength at 28 days
f_{bd}	steel-concrete bond strength
$f_{ct,eff}$	mean value of tensile strength effective at the time when cracks may first occur
f_{ctm}	mean concrete strength in tension at 28 days
$f_{ctm}(t)$	mean value of tensile strength at time, t, if cracking is expected earlier than 28 days
f_{ky}	characteristic strength of reinforcement
h	section thickness
$h_{e,ef}$	effective depth describing the effective area of concrete in tension surrounding the reinforcement
h_n	thickness of new (restrained) concrete section cast against A_o
h_o	thickness of old (restraining) concrete section
h_0	notional thickness used in shrinkage calculations
h_p	pressure head
H	height of an element
K_1	coefficient for the effect of creep on stress relaxation
K_2	coefficient for the effect of sustained loading on the tensile strength of concrete
K	coefficient combining the effect of creep on stress relaxation and the effect of sustained loading on the tensile strength of concrete
k	<i>coefficient which allows for the effect of non-uniform self-equilibrating stress which lead to a reduction in restraint forces</i>
k_c	coefficient which takes account of stress distribution within a section immediately prior to cracking
k_l	coefficient which takes account of the bond properties of reinforcement
k_h	coefficient depending on the notional size of the cross section, h_0 using in calculation of drying shrinkage

L	length of an element
R	restraint factor (R_1, R_2, R_3 etc at different stages in the life of the element)
R_{ax}	EN1992-1-1 notation for factor defining the of external restraint
R_j	restraint at the joint between new and old concrete
S	crack spacing
$S_{r,max}$	maximum crack spacing, defined as the characteristic crack spacing with a five per cent probability of being exceeded
S_0	minimum crack spacing
t_s	the time at which drying begins
T_1	difference between the centreline peak temperature and the mean ambient temperature
T_2	difference between the mean ambient temperature at the time of casting and the minimum mean ambient temperature
T_p	the peak temperature achieved at the centre of a concrete section
T_m	the mean temperature through a concrete section
T_s	the temperature at the surface of a concrete section (T_{s1}, T_{s2} etc for difference surfaces)
u	perimeter of that part of a concrete section exposed to drying
w_k	crack width defined in EN1992-1-1 with a five per cent probability of being exceeded
w_{max}	crack width defined in the UK National Annex to EN1992-1-1. This may be assumed to be equivalent to w_k
w/b	water to binder ratio by weight
α_c	free coefficient of thermal expansion of concrete
α_e	the modular ratio
α_r	coefficient of thermal expansion of concrete in a structure
$\beta_{ad}(t, t_s)$	time function for drying shrinkage
$\beta_{as}(t)$	time function for autogenous shrinkage
ΔT	temperature difference between the mid point of a section and the surface
ε_{ca}	autogenous shrinkage strain
$\varepsilon_{ca}(\infty)$	ultimate autogenous shrinkage strain
$\varepsilon_{ca}(t)$	autogenous shrinkage strain at time t after casting
ε_{cd}	drying shrinkage strain
$\varepsilon_{cd,0}$	nominal unrestrained drying shrinkage
$\varepsilon_{cd}(t)$	drying shrinkage strain at time t after casting
ε_{free}	the strain which would occur if a member was completely unrestrained
ε_r	restrained strain in concrete
ε_{cr}	crack-inducing strain in concrete defined as the proportion of restrained strain that is relieved when a crack occurs.
$\mu\varepsilon$	microstrain = 1×10^{-6} mm/mm
ρ	percentage of steel based on the area of concrete in tension A_{ct}
$\rho_{p,eff}$	effective steel percentage based on the area $A_{c,eff}$
σ_s	absolute value of maximum stress permitted in the reinforcement immediately after the formation of a crack
ϕ	bar diameter

Abbreviations

GGBS	Ground granulated blast-furnace slag
NDP	Nationally determined parameter
RH	Relative humidity
LINAC	Linear accelerator x-ray facility

Glossary

Binder	The total content of cementitious material in the concrete, including Portland cement and any additions such as fly ash, ground granulated blast-furnace slag, limestone powder, silica fume or metakaolin.
Crack-inducing strain	The component of restrained strain that is relieved when a crack occurs and is exhibited as crack width. This is the restrained strain less the residual strain in the concrete after a crack has occurred.
Crack width	The crack width at the surface of the concrete. “Maximum” crack widths designed to EN1992-1-1 are design “target” characteristic values with only a five per cent chance of being exceeded.
Early-age	Typically up to seven days.
Free strain	The strain that would occur in the concrete if it was completely unrestrained.
Full design method	A comprehensive approach which takes advantage of knowledge of the concrete and its behaviour and which is compliant with Eurocode 2.
Long-term	Beyond the period of the early-age temperature cycle, typically beyond 28 days.
Microstrain	1×10^{-6} strain.
Restrained strain	The component of free strain which is restrained and which generates stresses in the concrete.
Simplified method	An approximate approach using conservative assumptions and default values which are compliant with Eurocode 2.

List of figures

- Figure 1.1 Build-up of stresses and strains as a result of early-age thermal movements and restraint
- Figure 2.1 Aesthetically acceptable crack widths
- Figure 2.2 Limiting crack width for self-healing related to pressure gradient across the section (EN1992-3)
- Figure 3.1 Values of crack-inducing strain
- Figure 3.2 Flow chart showing the design process for control of early-age and long-term cracking
- Figure 4.1 The effect of wall thickness on the temperature rise (for 350 kg/m³ CEM I, 18 mm plywood formwork removed after seven days)
- Figure 4.2 The effect of formwork type on the temperature rise in 500 mm thick walls (for 350 kg/m³ CEM I)
- Figure 4.3 The effect of formwork type on the temperature profile in 500 mm thick walls achieved at the time of the peak temperature (for 350 kg/m³ CEM I)
- Figure 4.4 The effect of placing temperature on the temperature rise in a 500 mm thick wall using concrete with 350 kg/m³ CEM I cast in steel formwork
- Figure 4.5 T_I values for CEM I in walls
- Figure 4.6 T_I values for concretes containing 35, 50 and 70 per cent ggbs in walls
- Figure 4.7 T_I values for concretes containing 20, 35 and 50 per cent fly ash in walls
- Figure 4.8 Temperature rise per unit weight of binder in massive sections (to obtain values of T_I 5 °C should be added to the temperature rise calculated)
- Figure 4.9 The estimated change in T_I (per 100 kg/m³ CEM I) with placing temperatures for elements of varying thickness
- Figure 4.10 Mean monthly temperatures over each decade since 1916 (Met Office, 2006)
- Figure 4.11 Variation in ground temperature recorded for a heat pump installation in Croydon (Witte, 2001). The data points were provided and the curves fitted assuming a sinusoidal variation
- Figure 4.12 Autogenous shrinkage for different strength classes estimated using the method of EN1992-1-1
- Figure 4.13 Drying shrinkage curves estimated using the method of EN1992-1-1 for a) indoor conditions (45 per cent rh) and b) UK outdoor conditions (85 per cent rh)
- Figure 4.14 Total shrinkage of C40/50 concrete in a 500 mm thick wall at 65 per cent relative humidity
- Figure 4.15 Recommended values of restraint given in EN 1992-3
- Figure 4.16 Early thermal cracking in the walls of a box-section tunnel wall
- Figure 4.17 The relationship between restraint and distance from the joint including data for a wall with $L/H = 4$

Figure 4.18	Schematic representation of the development of crack in a massive element due to temperature differentials assuming no external restraint (such cracking may occur in both the vertical and horizontal orientation)
Figure 4.19	Values of tensile strain capacity at three and 28 days derived using concrete property estimates from EN1992-1-1
Figure 4.20	Surface zones of influence of reinforcement used to estimate the minimum reinforcement area, also presented as the area reduction factor, k
Figure 4.21	Development of cracking in an externally restrained, thick section during cooling
Figure 4.22	Simplified stress distribution used to determine the coefficient, k_c , for a member subjected to a temperature profile
Figure 4.23	Surface zones used in estimating $A_{s,min}$ in sections that are dominated by internal restraint
Figure 4.24	The ratio f_{ct}/f_b in relation to cube strength and age
Figure 6.1	Pour configuration as it affects restraint and delay between casting adjacent bays
Figure 6.2	The superposition of internal and external restraint
Figure 6.3	Expansion joint detail
Figure 6.4	Full and partial contraction joint details
Figure 6.5	Nomogram for estimating concrete mix temperatures
Figure 6.6	The use of liquid nitrogen to cool concrete on site immediately before placing
Figure 7.1	BP Harding gravity base constructed using lightweight aggregate concrete
Figure 7.2	Semi adiabatic test results for concretes containing ggbs and fly ash
Figure 7.3	Results from a 1 m ³ hot-box test where the placing temperature was 25 °C. The value of α_c is determined during cooling
Figure 7.4	Proposed location and fixing of thermocouple to monitor temperature variation
Figure 7.5	Estimated temperature difference between the reinforcement and the surface as affected by cover depth and the maximum centre-surface differential
Figure 7.6	<i>In situ</i> stress-strain curves used to derived restraint factors
Figure 7.7	Crack comparator

List of tables

Table 2.1	Limiting crack widths
Table 2.2	Recommended values of crack width, w_{max} (mm). Note: w_{max} is equivalent to w_k used in EN1992-1-1
Table 2.3	Provisions for achieving EN1992-3 tightness class
Table 3.1	Coefficients used in the estimation of $A_{s,min}$ for different restraint conditions

Table 3.2	Values of early-age and long-term tensile strength estimated in accordance with EN1992-1-1
Table 3.3	T_I values (°C) for different strength classes and section thicknesses (in mm) cast in the summer with a mix temperature of 20 °C and a mean ambient temperature of 15 °C. Adjustment values are given for winter casting
Table 3.4	Summary of the options available to prevent, minimize or control early-age thermal cracking
Table 4.1	Assumptions made in the estimation of the risk of cracking and the design of reinforcement to control crack widths (this table is included on the accompanying CD)
Table 4.2	Cement contents for different strength classes
Table 4.3	Estimated values of temperature differential in walls assuming a placing temperature of 20 °C and a mean ambient temperature of 15 °C (assuming thermal conductance values of 18.9 and 5.2 W/m ² K for steel and plywood formwork respectively with a wind speed of about 3.5 m/s. Solar gain has not been included)
Table 4.4	Coefficients of thermal expansion
Table 4.5	Values of autogenous shrinkage ($\mu\epsilon$) calculated using the method of EN1992-1-1
Table 4.6	Nominal unrestrained drying shrinkage values (in microstrain) with CEM I Class N
Table 4.7	Values of k_h for use in equation 4.4
Table 4.8	Estimated values of drying shrinkage ($\mu\epsilon$) in 300 mm and 500 mm thick walls for UK external exposure (RH = 85 per cent)
Table 4.9	Estimated values of drying shrinkage ($\mu\epsilon$) in 300 mm and 500 mm thick for internal (RH = 45 per cent)
Table 4.10	External restraint values, R , for different conditions
Table 4.11	Estimated values of ϵ_{ctu} for strength class C30/37 under sustained short term loading using different aggregate types
Table 7.1	Limiting temperature drop $T_{I,max}$ and temperature differentials ΔT_{max} to avoid early-age cracking, based on assumed typical values of α_c (Table 4.4) and ϵ_{ctu} (Table 4.7) as affected by aggregate type (for $K_I = 0.65$ and $\epsilon_{ca} = 15\mu\epsilon$)
Table 7.2	Example specification – control of concrete temperatures during hardening

1 Introduction

1.1 Scope

This guide is intended primarily for designers, but information is also included to support contractors in meeting the specifications which they have been provided with. The principal objective is to give a method for checking that the reinforcement provided will be sufficient to control early-age cracking, while also being adequate for controlling cracks that may develop due to long-term deformations caused by temperature change and shrinkage. Design guidance provided is in accordance with EN1992, Eurocode 2, in particular Part 1-1: *General rules and rules for buildings* and Part 3: *Liquid retaining and containment structures*. Guidance on concrete and its constituents is in accordance BS8500, Parts 1 and 2.

The aim is to help both designers and contractors to understand why early-age thermal cracking occurs; to recognise the influencing factors; to understand when cracking is most likely; to appreciate the significance of cracking; and to have methods for its avoidance and/or control.

There are numerous factors which influence the early thermal behaviour of concrete and consequently there is no single rule that defines when cracking will occur. However, the conditions under which the risk of cracking increases can be qualified as follows:

- ⌘ increasing Portland cement content
- ⌘ increasing placing temperature
- ⌘ increasing pour thickness
- ⌘ increasing restraint.

As a rule of thumb, any concrete element cast against an adjacent element of the same thickness or greater, and which achieves a temperature rise in excess of about 20 °C, has a significant risk of early thermal cracking if the length of the joint exceeds about 5 m. A 20 °C rise would typically be achieved in a 300 mm thick wall cast in plywood formwork using C30/37 concrete with CEM I. Cracking can not be ruled out if these conditions are not met, however they offer some guidance as to when early-age thermal cracking might be expected. Such conditions commonly apply in walls cast onto rigid foundations, tunnel linings (where the rock provides the restraint), tank walls cast onto a thick base and large slabs cast as a series of bays. When there is doubt about the likelihood and/or consequences of early-age thermal cracking expert advice should be sought.

There are many situations within normal concreting practice when early-age thermal cracking may be difficult to avoid. Additionally even in structures that have no special requirements, cracking can be a source of dispute. It is important that clients appreciate that early thermal cracking can be consistent with good construction practice, provided that it has been dealt with properly in the design and construction process. In many cases it may be either unnecessary or uneconomical to avoid cracking entirely. Indeed, the avoidance of cracking is contrary to the concept of reinforced concrete design, which assumes that concrete has no tensile capability and uses the

reinforcement to carry the tensile stresses and to control crack widths. If concrete does not crack then the reinforcement is not being used effectively. When specific performance requirements call for cracking to be avoided, special measures are available, but these may have significant cost implications that the client should be aware of.

1.2

Background to updating the former report R91

The last revision to report R91 (Harrison, 1992) noted a trend towards large continuous pours and the development of Portland cements to give higher early strengths and shorter striking times. In combination, these changes exacerbated the problems associated with the heat generated by the hydration of cements and the resulting early-age thermal cracking. Since that time, changes have continued to occur, with the increasing use of additions such as ground granulated blast-furnace slag (ggbfs), fly ash (previously referred to as pulverised fuel ash, pfa), silica fume and metakaolin and with the development of high performance concretes.

In addition, EN1992-3:2006: Eurocode 2 – *Design of concrete structures – Part 3: Liquid retaining and containment structures*, has superseded BS8007 which previously provided the basis for design to control early-age cracking. EN1992-3 refers extensively to EN1992-1-1:2004, Eurocode 2 – *Design of concrete structures - General rules and rules for buildings*, which has superseded BS8110, for both the estimation of concrete properties and the equations for estimating the design crack spacing and width. This publication follows the requirements of EN1992-3 and EN1992-1-1. Compared with the approach of BS8007 the following changes should be noted:

- ☞ in estimating the minimum area of reinforcement, $A_{s,min}$, to achieve a state of controlled cracking (formerly defined by the critical steel ratio) and the design crack width, w_k , different surface zones, or areas of concrete in tension, are used. The difference is greatest in sections thicker than 800 mm for which EN1992-1-1 requires higher values
- ☞ in estimating the steel ratio for calculating crack spacing, much lower values of surface zone are used for sections thicker than about 300 mm
- ☞ the equation for estimating crack spacing includes an additional term related to cover
- ☞ the term f_{ct} / f_b which influences crack spacing has been replaced by the coefficient k_1 which also includes a factor which relates the mean and the minimum crack spacing
- ☞ the way in which cracking develops is assumed to differ depending on whether the element is subject to edge restraint or end restraint (Beeby and Forth, 2005) and this is reflected in different expressions that are used to calculate crack width
- ☞ autogenous shrinkage is assumed to occur in all grades of structural concrete
- ☞ design to EN1992-1-1 is based on the 28-day characteristic cylinder strength, f_{ck} . Recognising that testing in the UK uses cubes, where necessary other properties are related to the 28-day characteristic cube strength $f_{ck,cube}$.

With regard to concreting materials and mix design, the guide is in accordance with BS EN 206-1:2000 – Part 1: *Specification, performance, production and conformity*, BS8500-1:2000, *Concrete – Complementary British Standard to BS EN206-1 – Part 1: Method of specifying and guidance for the specifier*, and BS8500-2:2002, *Concrete – Complementary British Standard to BS EN206-1 – Part 2: Specification for constituent materials for concrete*.

The terminology relating to cement has also changed. OPC is now replaced by CEM I followed by the strength class, eg CEM I 42.5 and this may also be referred to as Portland cement. Cements containing additions such as fly ash (previously referred to as pulverised fuel ash, pfa) or ground granulated blast-furnace slag, ggbs, are classified as CEM II, CEM III or CEM IV depending on the level of addition (Appendix A1 Table A1.1). For clarity, when such cements are referred to, the percentage addition is defined. Although it is not a recognised term within Eurocodes, for general convenience the term BINDER is used to represent the total content of binder material, including additions such as fly ash, ggbs, silica fume and metakaolin, and the term w/b is used to represent the water/binder ratio.

In addition, considerable research over the past 15 years has led to a greater understanding of the way in which the principal factors contribute to the development of early-age thermal cracking, and how these may be used in the assessment of risk. A range of models is now available for predicting temperature rise and temperature differentials, thermal strains, and the resulting thermal stresses enabling, where appropriate, a much more rigorous approach to design. Some simple spreadsheet models for predicting temperatures, strains and restraint are included with this guide.

While EN1992-1-1 provides some guidance on shrinkage strains (autogenous and drying) neither EN1992-3 nor EN1992-1-1 provides significant guidance on the prediction of early thermal strain, and in this respect the guide is supplementary.

1.3

The cause of early-age thermal cracking

Early-age thermal cracking is associated with the release of the heat of hydration from the binder and is the result of either differential expansion within an element during heating causing **internal restraint** or by **external restraint** to contraction of an element on cooling from a temperature peak. Early-age thermal cracking occurs within a few days in thinner sections, but it may take longer to develop in thicker sections which cool more slowly.

The process of early-age thermal cracking is complex and in order to achieve a procedure for routine design it is necessary to make a number of simplifying assumptions. To do this in a safe and rigorous way the process and the predominant factors should be understood fully.

As cement hydrates it generates heat, initially at a rate greater than the heat loss to the environment, and this causes an increase in the temperature of the concrete. As the rate of heat generation progressively reduces heat loss becomes dominant and the concrete cools and contracts. If unrestrained and fully insulated (preventing temperature differentials and internal restraint) the concrete would expand and contract without creating any stresses. In practice partial restraint is always present leading to the development of stresses. If the concrete properties were constant, a restrained element would generate compressive stresses during heating and relieve these stresses during cooling. The elastic modulus of concrete changes considerably during the first few days after casting, being relatively low during the heating period compared with the value during cool down. For a given magnitude of restrained thermal strain, the compressive stress generated during heating is lower than the tensile stress generated during cooling, resulting in a residual tensile stress at the end of the heat cycle (Bamforth, 1982). This is illustrated in Figure 1.1.

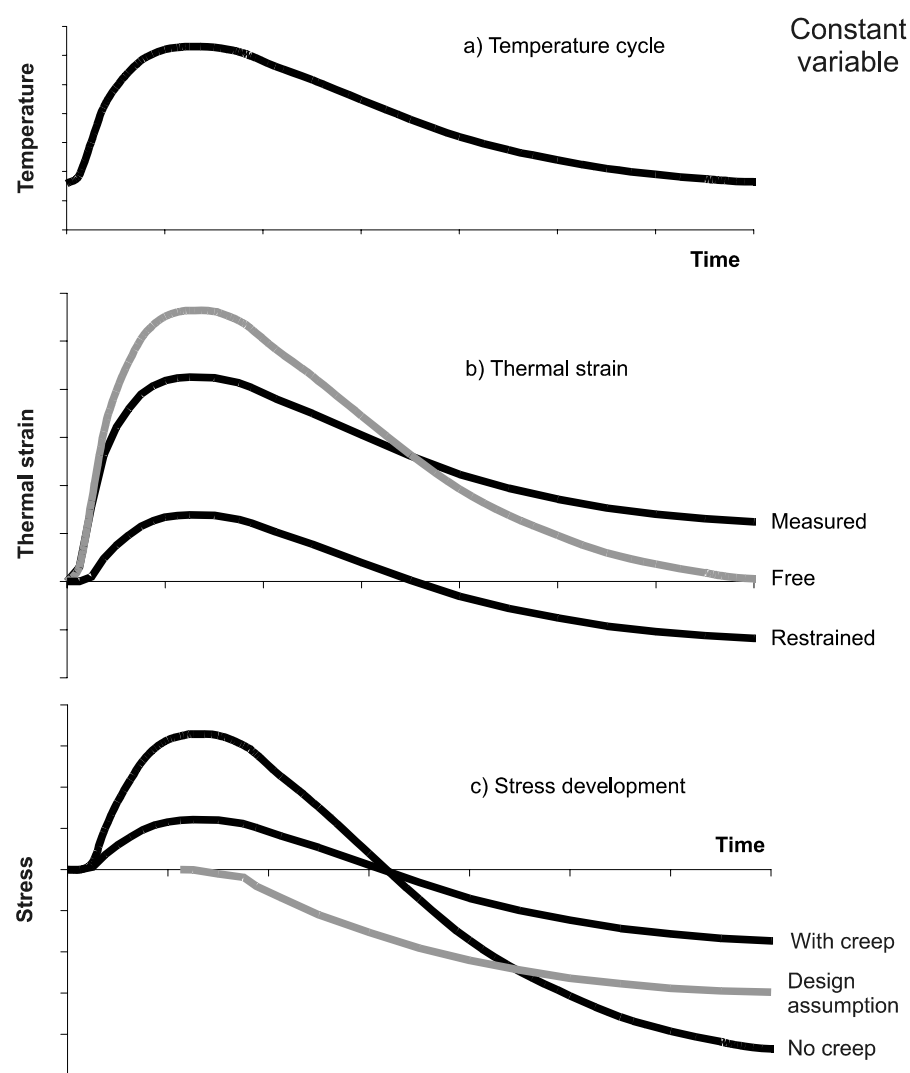


Figure 1.1 Build-up of stresses and strains as a result of early-age thermal movements and restraint (Bamforth, 1982)

Figure 1.1a shows the temperature change at the centre of a large concrete element during the early thermal cycle. The free thermal strain which develops at the same location is shown in Figure 1.1b together with the measured strain and the “restrained strain” (ie the difference between the free and the measured strain). It is only this restrained movement which induces stresses in the concrete which, subsequently, can cause cracking.

Figure 1.1c shows the stress associated with the restrained strain both with and without creep being taken into account and demonstrates the significant role that creep plays in reducing the magnitude of early thermal stresses.

The stresses developed during the early thermal cycle are difficult to calculate precisely because of the rapidly changing elastic modulus of the concrete and modifying influence of creep (deformation under sustained loading) which, due to both the young age of the concrete and the accelerating effect of temperature, can cause significant relaxation of these induced stresses as shown in Figure 1.1c. The stress curve in Figure 1.1c has been obtained by calculation but is very similar to measurements obtained using stress simulators (Blundell and Bamforth,1975, Kanstad *et al*, 2001, van Breugel and Lokhorst, 2001, van Beek *et al*, 2001, Pane and Hansen, 2002) in which specimens

of concrete are subjected to the same thermal and moisture regime as the concrete in the pour. The stresses needed to maintain the same strains as those measured on site are recorded. Figure 1.1c shows that the restraint to expansion during heating causes compressive stresses which are relieved during cool-down before tensile stresses develop. The compressive stresses resulting from external restraint are unlikely to cause any problems but if the tensile stresses are excessive, cracking occurs.

For design purposes it is generally assumed that for conditions of external restraint, compressive stresses induced during the heating phase are entirely relieved by creep and that tensile stresses are induced during the cooling phase from the time of the peak temperature (shown as the design assumption in Figure 1c). To simplify the design process further, a strain based approach was developed (Hughes, 1971) in which the restrained tensile strain induced during the period of cooling from peak to ambient temperature is compared with the tensile strain capacity of the concrete. In its simplest form the restrained strain, ε_r , is estimated using the equation:

$$\varepsilon_r = \alpha_c T_l K R \quad (1.1)$$

where

- ε_r = the restrained strain
- T_l = temperature drop from peak temperature to mean ambient (ie $T_p - T_a$) (see Section 4.2)
- α_c = coefficient of thermal expansion of concrete (see Section 4.5)
- R = restraint factor (see Section 4.7)
- K = coefficient which takes account creep and stress relaxation under sustained loading (Section 4.9)

When cracking is caused by temperature differentials that generate internal restraint in thick sections the assumptions employed will differ. In this case the tensile strain at the surface may be caused by restrained contraction (for example, if formwork or insulation is removed allowing rapid cooling of the surface) but may also be the result of expansion of the core of the section, which achieves a higher temperature rise and thermal expansion than the surface. In either case, for sufficient tension to develop at the surface, compression should be developed at the centre of the section and the assumption that all compressive stresses are relieved by creep is no longer conservative.

Estimating the likelihood of cracking due to internal restraint may be dealt with using Equation 1.1. In this case the temperature T_l is replaced by the centre to surface temperature differential ΔT and a value of restraint is derived from the shape of the temperature profile through the thickness.

Equation 1.1 is presented in various forms (BS8110:Part 2:1985, EN 1992-3:2006, HA BD28/87) but in every case it is assumed that to avoid cracking, the restrained-strain ε_r should be less than the tensile strain capacity ε_{ctu} of the concrete.

In some cases the restrained tensile strain developed may be insufficient to cause early-age thermal cracking but may contribute to strains that cause cracking in the longer term and it is important to recognise the significance of these residual strains within the design process. It is also important to recognise other deformations that may be occurring during the early heat cycle, in particular autogenous shrinkage which, in accordance with EN1992-1-1:2004, occurs to some degree in all structural concretes.

1.4

The design process

Recognising that, at the design stage, there may be very limited information on the concrete (in the most extreme case only the strength class will be known) two approaches are offered for estimating the deformations that lead to cracking. The design of reinforcement is the same in each case, following the recommendations of EN1992-1-1 and EN1992-3.

- ↳ the **full method** that can be applied when information is available on the concrete to be used for estimating thermal strain, ($T_I \alpha_c$) and pours sizes, and casting sequence for estimating restraint (R) both at early-age and in the long-term. This approach may be appropriate where the consequences of cracking are most severe: where the specification includes limits on materials and mix proportions: and where it is apparent that significant savings may be achieved. It may also be used by contractors to identify the most effective means for meeting the requirements of the specification with regard to early thermal cracking and for negotiating appropriate changes where the design assumptions differ from practice
- ↳ the **simplified method** for routine design and where the designer has limited information on the details of the concrete materials and mix proportions. This will involve the use of conservative “default” assumptions as it will have to deal with all possible scenarios.

In each case the process is as follows:

1 Define the design crack width, w_k

Section 2 discusses appropriate crack widths for different design criteria.

The crack width may change over time and in such circumstances the early-age (ie a few days) design crack width may be different from the permanent condition (see Section 2.2).

2 Estimate the magnitude of restrained-strain ε_r and the risk of cracking

Restrained strain is the restrained component of the free strain and is determined by the concrete materials and mix proportions (in particular the cement type and content and the aggregate type), the section geometry, and the environment into which the element is cast (with regard to restraint imposed by previously cast concrete). The risk of cracking is the ratio of the restrained-strain, ε_r , to the strain capacity of the concrete ε_{ctu} . Where it is critical that early-age cracking is avoided a declared safety factor should be introduced. The risk is assessed at both early-age and in the long-term to determine when cracking is most likely.

3 Estimate the crack-inducing strain ε_{cr}

The crack-inducing strain is that proportion of restrained strain that is relieved by forming cracks and is equal to the restrained strain less the average residual tensile strain in the concrete after cracking.

4 Design the reinforcement to control the crack spacing and width

This is in two stages:

- a Ensure that the area of steel A_s exceeds the minimum reinforcement area $A_{s,min}$ required for crack control. This is related to the ratio of the tensile strength of the concrete at the time of cracking being considered $f_{ctm}(t)$ to the yield strength of the reinforcement f_{ky} ($A_{s,min}$ was previously described in BS8007 through ρ_{crit}). Where it is critical that crack widths are adequately controlled a declared safety factor should be introduced.
- b Check that the area of steel, A_s achieves the specified crack width. The crack width is proportional to the crack spacing S which is determined by the bar diameter, the bond characteristics of the reinforcement, and the cover. If A_s is insufficient then either increase the steel ratio or use more smaller diameter bars until the specified crack width is achieved or use measures to reduce the magnitude of crack-inducing strain.

1.5

Responsibilities

The practical outcome of the number and size of cracks is influenced by decisions made by both the designer and the constructor. In a traditional situation, namely *design first then tender for contracting against a specification* the responsibilities will typically be as follows:

Designer's decisions

- ☞ selecting the element geometry
- ☞ specifying the concrete strength class (and possibly cement type and minimum cement content)
- ☞ design of reinforcement
- ☞ specifying the location of movement and (some) construction joints

Contractor's decisions

- ☞ procuring concrete to meet the specification and buildability requirements
- ☞ planning the construction sequence
- ☞ selecting the type of formwork, and striking and curing times
- ☞ employing any additional measures.

As there is a joint responsibility it is important that the assumptions made in the design process are very clearly stated within the specification documents and a proforma for this purpose is provided (Section 4.1, Table 4.1). In this respect, there are clear advantages for the designer and constructor working together. This may be achieved on many projects where the contract permits such as design and build partnering, where input from the lead constructor and the larger supply chain can be achieved earlier. However, regardless of the procurement route used, it will always be necessary to work forwards from a "clean sheet" situation logically.

1.6

Other effects of temperature

In addition to influencing the risk of early-age cracking, the temperatures achieved during early hydration also affect the strength and other properties of the concrete to

varying degrees (Bamforth, 1977, Barnett *et al*, 2005, Concrete Society, 2004, Sato *et al*, 2001, Sugiyama *et al* 2000) and some guidance is given on the nature and extent of these changes in relation to their potential impact on *in situ* performance (Appendix A9). This may be particularly important in relation to the development of tensile strength and the determination of the minimum area of steel $A_{s,min}$ for controlled cracking.

1.7

Advances

Considerable advances have been made since the last revision of this report as follows:

- ✦ extensive data have been generated on the heat generation characteristic of modern cements (Dhir *et al*, 2006) and combinations, and the T_I values have been revised accordingly. It has been noted that current CEM I cements generate more heat than those used in developing T_I values when R91 (CIRIA, 1992) was last revised
- ✦ a better understanding of the factors affecting early thermal cracking has been established, especially in relation to the stress cycle and the point at which tensile stresses are first initiated; and the effects of creep and sustained loading
- ✦ restraint factors may be estimated more reliably for some common element geometries, eg walls on rigid foundations, adjacent slabs
- ✦ additional data on tensile strain capacity, ε_{ctu} , have been generated, enabling this property to be related to the tensile strength and elastic modulus of the concrete and to the strength class
- ✦ guidance on predicting autogenous shrinkage is provided
- ✦ the impact on the variability of the input parameters to the design model can be accommodated by the use of probabilistic (risk) analysis and the results of such analyses may be used in the decision making process
- ✦ it has been identified that the way in which cracks form and the resulting crack widths are related to the nature of the restraint. End restraint generally leads to significantly larger crack widths but fewer cracks compared with the continuous edge restraint condition
- ✦ guidance is provided for controlling cracks caused by temperature differentials
- ✦ the influence on the early thermal cycle has been investigated and a better understanding has been established of the impact the peak temperature has on the development of strength.

There is a significant margin of safety within the method of R91 (CIRIA, 1992), and in many circumstances this has been sufficient to more than offset the risk in situations where T_I may have been underestimated. Nevertheless, it is estimated that there is still a small risk that without modification R91 (CIRIA, 1992) would (for current cements) underestimate the magnitude of crack-inducing strain and crack width, and that exceedence of the design target crack width would occur more often.

1.8

Format of the guide

The format of this guide broadly follows the design process described in Section 1.4.

Chapter 2 provides information on the significance of cracking in relation to various performance requirements.

Chapter 3 describes the design process, the way in which the magnitude of crack-inducing strain may be estimated, and the method for reinforcement design for crack control.

Chapter 4 provides input data covering temperature rise, strain (thermal and shrinkage), tensile strength, and strain capacity and restraint. Detailed supporting data are provided in appendices on the CD.

Chapter 5 gives worked examples to demonstrate how the process may be applied.

Chapter 6 provides guidance on mitigating measures which may be required in some cases. Options include planning pour sizes and construction sequence, the inclusion of movement joints and measures for cooling the concrete before and after placing. Again, details are provided in appendices.

Chapter 7 provides advice on specification, testing and monitoring, and on actions that may be taken in the event of non-compliance.

In addition to the text, some parts of the process are provided as spreadsheet calculators and these are included on the CD provided with this guide. For the benefit of the reader the appendices, also provided on the CD, are written as stand-alone documents and there is considerable replication of information between the appendices and the guide.

2 Significance of cracking

2.1 The acceptability of cracking

Before getting involved in the complexities of early-age thermal cracking it is important to understand why it is important. Cracking in reinforced concrete is not a defect; indeed the very basis of reinforced concrete design is that concrete has no significant tensile strength and that sufficient reinforcement should be provided to control crack widths.

EN1992-1-1, Cl 7.3.1 states that: “Cracking is normal in reinforced concrete structures subject to bending, shear, torsion or tension resulting from either direct loading or restraint to imposed deformations”.

Problems may arise however when cracks occur unpredictably, or are of sufficient magnitude to render the structure unserviceable.

This section deals with the nature of cracks in concrete and their significance in relation to the performance requirements of the structure. The designer should make the client aware that cracking is an inherent part of reinforced concrete and that if controlled, will not be detrimental to the performance of the structure. In this way, the potential for disputes will be minimised.

2.2 The relationship between crack width and functionality

Before considering the methods used to control or prevent early-age thermal cracking, it is appropriate to consider the significance of cracking, so that the objectives of the control methods are clear. Cracking is an integral part of reinforced concrete and assessing the acceptable crack distribution is an important part of the design process. The significance of cracking can be considered under three categories:

- 1 Cracks which lead to durability problems and consequently a reduction in structural capacity.
- 2 Cracks which lead to a loss of serviceability of the structure (eg the leakage of water or radiation, sound transfer or damage to finishes).
- 3 Cracks which are aesthetically unacceptable.

Under serviceability conditions, crack widths may only be excessive if the minimum reinforcement area $A_{s,min}$ is not achieved and the steel yields. As the achievement of $A_{s,min}$ is an essential part of the design process, crack widths that jeopardise structural integrity are avoided.

Limiting cracks widths appropriate for each of these categories of cracking are given in Table 2.1.

Table 2.1 Limiting crack widths

Limit state	Limiting crack width (mm)	Comments
Durability	0.3	For all exposure classes except X0 and XC1 (National Annex to EN1992-1-1, Table NA.4) in which case appearance is often the main criterion, although the preservation of aggregate interlock for shear strength should be considered (see also Table 2.2).
Serviceability (in water retaining structures)	0.05 to 0.2	For sealing under hydrostatic pressure (EN1992-3 Cl.7.3.1).
Appearance	0.3. or greater	Depends upon specific requirements for appearance (National Annex to EN1992-1-1, Table NA.4).

It is important to appreciate that the values given in Table 2.1 are the total crack widths arising from early-age deformations, long-term deformations and loading. As stated in Section 1.4, where it is apparent that long-term effects will be additive to early-age cracking then the limiting crack width associated with early deformations should be reduced accordingly.

It should be noted that it has not been common practice to add early-age crack widths to those arising from structural loading, with no reported detriment to structural performance. This may be due to the fact that early-age thermal stresses are often self-equilibrating, with creep being a significant factor: because moment effects are generally not coincident with early-age thermal effects; or because new cracks are formed. More research in this area, including field observations, is required.

Each of these categories in Table 2.1 is now considered, and the relevance of the appropriate cracking criterion is discussed.

2.3

Cracks which lead to durability problems

Crack width limitations are used as one of the durability criteria in all Standards and Codes of Practice for reinforced concrete. Table NA.4 of the UK National Annex to EN1992-1-1 is reproduced here as Table 2.2, with additional information describing the exposure classes.

Table 2.2 Recommended values of crack width, w_{max} (mm). Note: w_{max} is equivalent to w_k used in EN1992-1-1

Exposure class	Description of exposure condition	Reinforced members and prestressed members without bonded tendons (Quasi-permanent load combination) mm	Prestressed members with bonded tendons (Frequent load combination) mm
X0, XC1		0.3 ^a	0.2
XC2, XC3, XC4	Carbonation	0.3	0.2 ^b
XD1, XD2, XD3, XS1, XS2, XS3	Chlorides, eg de-icing salt (XD) or seawater (XS)		0.2 and decompression ^c

- a For X0 and XC1 exposure classes, crack width has no influence on durability and this limit is set to produce acceptable appearance. In the absence of specific requirements for appearance this limit may be relaxed (*but consider shear strength*).
- b For these exposure classes, in addition, decompression should be checked under the quasi-permanent combination of loads.
- c $w_{max} = 0.2$ mm applies to parts of the member that do not have to be checked for decompression.

The issue of the effect of cracking on durability is still not entirely clear, but EN1992-1-1 states that the values given in Table 2.2 “*will generally be satisfactory for reinforced concrete members in buildings with respect to appearance and durability*”.

In reinforced or prestressed concrete structures, preventing excessive corrosion of the embedded steel is vital. Research into the effect of crack widths on steel corrosion has yielded interesting findings. Using site surveys, experimental evidence and theories of corrosion and crack propagation (Beeby 1978a, Beeby, 1978b) showed that there was no unique correlation between surface crack width and the crack width at the steel, nor was there any correlation between surface crack width (up to 0.5 mm) and the long-term durability of a structure. To support this, several studies have stated that it is not the crack width that is the limiting factor, but the cover and concrete quality (Ohno *et al*, 1996, Raupach, 1996). In some cases, it has been recommended that better performance is achieved with higher cover, even if this leads to greater surface crack widths (Houston *et al*, 1972, Arya and Ofori-Darko, 1996). This is an area in which additional research is needed.

Measures are available to avoid cracking, or at the very least to keep the risks low (Chapter 6). Such measures may be expensive and it is important that clients are made fully aware of the benefits and the risks.

2.4

Cracks which lead to a malfunction of the structure

Some early-age thermal cracks may be continuous through the full thickness of a section and can lead to seepage or leakage. For a water-retaining structure, water leakage is a serious malfunction of the structure, particularly if it is groundwater leaking into a drinking water tank. Even when the loss of water in itself is not serious, the crack can become visually unacceptable. EN1992-3 provides a tightness classification as shown in Table 2.3.

Cracks in walls designed as radiation shields present a potential health and safety hazard, and it should be specified that such walls are uncracked (tightness class 3).

Whether a narrow (less than 0.2 mm) crack represents a safety hazard in practice is not proven, but it is prudent to minimise potential risks and take the measures necessary to avoid cracking.

Table 2.3 Provisions for achieving EN1992-3 tightness class

Tightness class	Requirements for leakage	Provisions for achieving leakage requirements
0	Some degree of leakage acceptable, or leakage of liquids irrelevant.	General provisions for crack control (7.3.1 of EN1992-1-1) with limiting crack widths in accordance with Table 2.2 above.
1	Leakage to be limited to a small amount. Some surface staining and damp patches acceptable.	For full thickness cracks the width, w_{k1} , is related to the pressure head, h_p . For $h_p/h < 5$, $w_{k1} = 0.2$ mm while for $h_p/h > 35$, $w_{k1} = 0.05$ mm, with interpolation for intermediate values (unless given in the National Annex).
2	Leakage to be minimal. Appearance not to be impaired by staining.	Cracks which may be expected to pass through the full thickness should be avoided unless appropriate measures (eg liners or prestress) have been incorporated.
3	No leakage permitted.	Special measures (eg liners or prestress) may be required to ensure water tightness.

2.5

Cracks which are aesthetically unacceptable

There is no rational basis for defining the aesthetic implications of cracking. Campbell-Allen (1979), after reviewing the work on human reactions to cracks, proposed a graphical aid (Figure 2.1) for determining the aesthetically acceptable crack width in relation to the nature of the structure and the viewing distance. Certain surface finishes (such as bush hammering or grit blasting) break the edges of fine cracks, making them much more noticeable. It should be appreciated that these values are very subjective and for close viewing, severe.

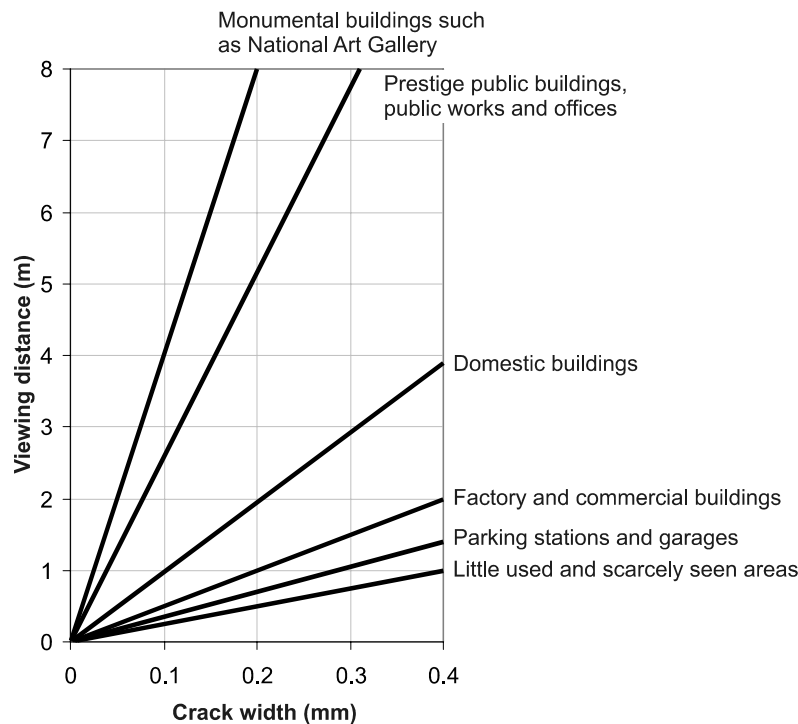


Figure 2.1 Aesthetically acceptable crack widths

2.6

The role of autogenous healing

While there has been additional research on autogenous healing and the mechanisms by which flow rate decreases are now better understood (Gerard *et al*, 1997, Khushefati, 2004), the earlier recommendations which suggests that cracks 0.2 mm or less in width tend to seal themselves have not changed substantially (Clear, 1985, BS8007, 1985) provided that the pressure gradient does not exceed 5. Guidance is now more refined with the limiting crack width being related to the pressure gradient across the section as shown in Figure 2.2 (EN1992-3). When the crack width is less than 0.05 mm self-healing will occur even when the pressure gradient is in excess of 35. While there is some evidence that flow rates may reduce under some conditions if the crack width exceeds 0.2 mm (Gerard *et al*, 1997) there is little evidence that such cracks will ultimately seal themselves either by autogenous healing or by blockage.

When cracking is caused by external restraint to early thermal contraction it is likely that a crack with a surface width of 0.2 mm will be considerably wider in the core of a section, where the temperature rise and fall is greatest (Section 4.11.2). The research on autogenous healing has often concentrated on specimens cracked under load and of uniform width. The proportion of the crack which needs to be 0.2 mm in width for self-sealing is not known. However, while there have been circumstances in which crack injection has been required to seal cracks, experience in the design of water retaining structures to BS8007, which limited surface crack widths to 0.2mm, would suggest that this is not a critical issue.

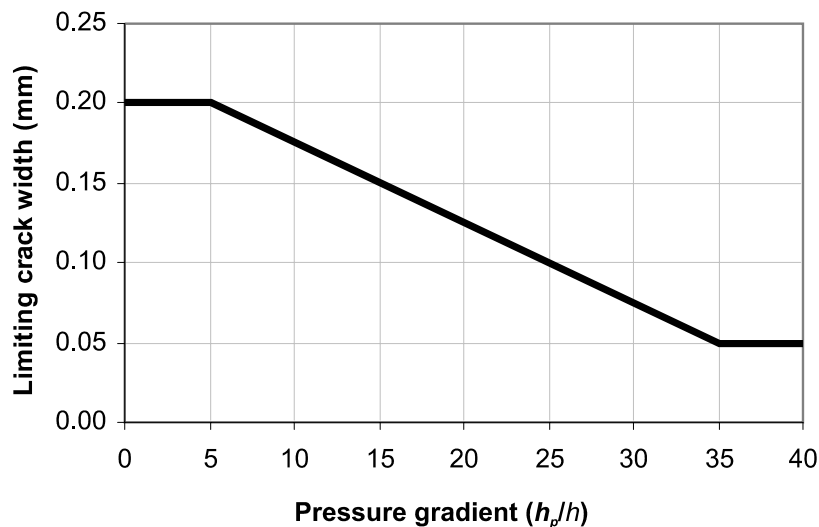


Figure 2.2 Limiting crack width for self-healing related to pressure gradient across the section (EN1992- 3)

It should be noted also that the term “self-healing” is not strictly correct in every case. Although, in water retaining structures, flow may progressively reduce and ultimately cease, this is in part due to the crack becoming blocked with fine particles and not necessarily the formation of hydration products across the crack. However, where leak tightness is a serviceability limit state, this may be sufficient (Khushefati, 2004).

2.7

Measures to avoid cracking

There are numerous measures that may be taken to avoid early thermal cracking altogether and these are described in Chapter 6. These include various methods for cooling the concrete, either before placing or *in situ*. However, these measures will add significantly to the cost of construction. In some structures, eg nuclear containments, LINAC facilities, cracking is highly undesirable and such measures may be appropriate. However, in most structural situations cracking is perfectly acceptable, provided that crack widths are within acceptable limits. Little benefit may be obtained in real terms by its avoidance.

Partial prestressing can also be used to prevent thermal and drying shrinkage cracking. This is a very expensive method of crack prevention, and is generally only used in special structures.

3 The design process

3.1 Introduction

The design process is first described in full (the **full method**) and then in a simplified form (the **simplified method**) recognising that limited information may be available at the design stage. The simplified approach (Section 3.6) uses a simplified equation for estimating the crack-inducing strain together with default values which, in combination, lead to a safe but conservative design. The full method described in Section 3.2 provides a more rigorous approach to the prediction of the crack-inducing strain. This requires more knowledge of the concrete to be used and may lead to considerable savings in reinforcement to be applied with safe default values. More detailed background information and the processes used are given in Chapter 4 and the Appendices. Spreadsheet calculators are provided on the CD for some of the calculations (see Contents). A flow chart which describe the process is provided as Figure 3.2 at the end of this section.

Both methods follow the requirements of EN1992-1-1 and EN1992-3 and involve four principal steps:

1 Define the allowable crack width associated with early-age thermal cracking (Chapter 2)

As stated in Section 2.2, it has not been common practice to add early-age crack widths to those arising from structural loading, with no apparent detriment to structural performance. However, long-term thermal contractions and drying shrinkage may cause crack widths to increase or new cracks to form, depending on the nature of the restraint. The designer should consider whether cracking due to subsequent deformations will add to early-age effects, and should design for crack widths accordingly.

2 Estimate the magnitude of restrained strain and the risk of cracking

EN1992-1-1 and EN1992-3 defines a value for the coefficient of thermal expansion of the concrete (recommended value = $10 \mu\epsilon/^\circ\text{C}$), but there is no indication of the likely magnitude of early-age thermal strains. However, EN1992-1-1 does provide guidance on autogenous shrinkage and drying shrinkage and limited information on restraint factors. More comprehensive information is given in Sections 4.2 to 4.9 as follows:

Early-age temperature change in the concrete	T_1	Section 4.2
Long term ambient temperature change	T_2	Section 4.3
Early-age temperature differential	ΔT	Section 4.4
Thermal expansion coefficient of concrete	α_c	Section 4.5
Autogenous shrinkage	ϵ_{ca}	Section 4.6.1
Drying shrinkage	ϵ_{cd}	Section 4.6.2
Restraint	R	Section 4.7
Tensile strain capacity	ϵ_{ctu}	Section 4.8
Effect of creep on stress and strain relaxation	K_1	Section 4.9.1
Effect of sustained loading on tensile properties	K_2	Section 4.9.2

The risk of cracking should be assessed both during the very early period when early temperature change and autogenous shrinkage will be the dominant forms of strain and at later life when annual temperature changes and drying shrinkage will dominate. The age at which cracking occurs will determine the level of tensile strength of the concrete used in the estimation of the minimum reinforcement area $A_{s,min}$ and, in some cases the crack width.

3 Estimate the crack-inducing strain

The crack inducing strain ε_{cr} is the proportion of restrained-strain that is relieved when a crack occurs and is equal to the restrained component of the free strain less the average residual tensile strain in the concrete after cracking.

4 Check the reinforcement of crack control, crack spacing and width

The design of reinforcement to control cracking is based on the method of EN1992-1-1 and EN1992-3.

It is normal practice to design the reinforcement to meet nominal code requirements and for structural loading and then to check that the steel ratio is adequate both to control early-age cracking and to limit the crack width.

Relevant information is provided in Chapter 4 as follows:

The tensile strength of the concrete	f_{ct}	Section 4.10
The minimum area of reinforcement	$A_{s,min}$	Section 4.11
The steel ratio for calculating crack width	$\rho_{p,eff}$	Section 4.12
The relationship between tensile strength, f_{ct} and the bond strength f_{bd}	k_1	Section 4.13

3.2 Estimating the risk of cracking and the crack-inducing strain

3.2.1 External restraint

Cracking will occur when the restrained strain, ε_r , exceeds the tensile strain capacity of the concrete, ε_{ctu} . For the case of edge restraint, eg a wall on a rigid foundation, EN1992-3 describes the restrained strain in very simple terms as follows:

$$\varepsilon_r = R_{ax} \varepsilon_{free} \quad (3.1)$$

where

R_{ax} is the restraint factor

ε_{free} is the strain that would occur if the member was completely unrestrained.

While this guide is concerned specifically with early-age thermal cracking, the reinforcement should also be designed to accommodate long-term thermal and shrinkage deformations. Recognising the individual components of strain, Equation 3.1 has been developed to form the expression for restrained strain ε_r as follows:

$$\varepsilon_r = K_1 \{[\alpha_c T_1 + \varepsilon_{ca}] R_1 + \alpha_c T_2 R_2 + \varepsilon_{cd} R_3\} \quad (3.2)$$

where

- T_1 is the difference between the peak temperature, T_p , and the mean ambient temperature T_a (Section 4.2).
- T_2 is the long-term fall in temperature which takes into account the time of year at which the concrete was cast (Section 4.3).
- α_c is the coefficient of thermal expansion of concrete (see Section 4.5).
- ε_{ca} is autogenous shrinkage (Section 4.6.1). Note: EN1992-1-1 assumes that all structural concretes exhibit some degree of autogenous shrinkage
- ε_{cd} is drying shrinkage (Section 4.6.2)
- R_1 is the restraint factor that applies during the early thermal cycle (see Section 4.7)
- $R_2 R_3$ are restraint factors applying to long-term thermal movement and drying shrinkage respectively (see Section 4.7)
- K_1 is a coefficient for the effect of stress relaxation due to creep under sustained loading ($K_1 = 0.65$, see Section 4.9.1)

The test for cracking is $\varepsilon_{cr} > \varepsilon_{ctu}$ (3.3)

Where ε_{ctu} is the tensile strain capacity of the concrete under sustained loading (Section 4.8).

This approach may be used to assess the risk of cracking for any form of external restraint, although different approaches are used to estimate crack width depending on whether the restraint is continuous edge restraint or end restraint (Section 3.5).

The risk of cracking and the crack width should be assessed at both early-age and in the long-term.

For the **early-age** calculation of ε_r using Equation 3.2, include only the terms for early-age thermal contraction and autogenous shrinkage at three days, ie assume that T_2 and ε_{cd} are zero.

For the long-term calculation include all terms in Equation 3.2. In this case use the autogenous shrinkage at 28 days as subsequent autogenous shrinkage is assumed to be included in the value of drying shrinkage (see Section 4.6.3).

The area of steel should meet the requirement for the minimum reinforcement area, $A_{s,min}$ for the latest age at which cracking is expected to occur.

To determine the maximum acceptable value of T_1 for avoidance of cracking, Equations 3.2 and 3.3 may be combined to give following:

$$\text{Maximum } T_1 \text{ for avoidance of cracking } T_{1,max} = \frac{\varepsilon_{ctu}}{K_1 \alpha_c R} - \frac{\varepsilon_{ca}}{\alpha_c} \quad (3.4)$$

Values of $T_{1,max}$ for strength class C30/37 concrete using a range of typical aggregate types have been estimated using Equation 3.4 and are given in Table 7.1.

When a crack occurs not all of the restrained strain is relieved and the **crack-inducing strain** ε_{cr} is less than the restrained strain by the amount of residual tensile strain in the concrete after cracking. The approach of EN1992-3 is cautious and does not recognise this for the condition of edge restraint and will lead to an estimate of slightly higher crack widths. It may be assumed that after cracking the average residual strain in the concrete will equal half the tensile strain capacity.

The crack-inducing strain ε_{cr} used in the derivation of crack widths, may be calculated using the expression:

$$\varepsilon_{cr} = \varepsilon_r - 0.5 \varepsilon_{ctu} \quad (3.5)$$

Combining Equations 3.2 and 3.5 gives

$$\varepsilon_{cr} = K_1 \{ [\alpha_c T_1 + \varepsilon_{ca}] R_1 + \alpha_c T_2 R_2 + \varepsilon_{cd} R_3 \} - 0.5 \varepsilon_{ctu} \quad (3.6)$$

Again, the calculation should be carried out considering both early-age and long-term strains, in the former case ignoring the long-term effects of temperature, T_2 , and drying shrinkage, ε_{cd} .

3.2.2 Internal restraint

When designing reinforcement to control cracking caused solely by temperature differentials, T_1 is replaced by ΔT , the difference in temperature between the centre and the surface of the element. In addition, autogenous strain may be omitted from the calculation as it will occur uniformly through the section and will not contribute to differential strain. Long-term strains are also omitted as the stress condition is transient and does not extend beyond the early thermal cycle. In this case the restrained strain may be estimated as follows:

$$\varepsilon_r = K_1 \Delta T \alpha_c R \quad (3.7)$$

For the condition of internal restraint it has been estimated that $R = 0.42$ (Section 4.7.4). Combining Equations 3.2 and 3.7 and substituting for $R = 0.42$, and $K_1 = 0.65$ the maximum acceptable value of ΔT for avoidance of cracking may be derived.

$$\text{Maximum } \Delta T \text{ for avoidance of cracking, } \Delta T_{max} = \frac{3.7 \varepsilon_{ctu}}{\alpha_c} \quad (3.8)$$

Values of ΔT_{max} for strength class C30/37 concrete using a range of typical aggregate types are also given in Table 7.1.

Note: When testing for compliance with limiting values of ΔT_{max} , the surface temperature is often measured at some distance from the surface, eg by fixing the thermocouple to the reinforcement. In such cases, the allowable values may need to be marginally reduced (see Section 7.3.1).

The crack inducing strain in this case is derived by combining Equations 3.5 and 3.7 to give:

$$\varepsilon_{cr} = K_1 \Delta T \alpha_c R - 0.5 \varepsilon_{ctu} \quad (3.9)$$

3.2.3 Input data

Temperature drop, T_1

While various models are available for the prediction of temperature rise and fall, the most reliable data is obtained by testing (Section 7.2.1). Data are provide in Section 4.2 for a range of concrete mixes. The T_1 values are based on modelling using semi-adiabatic data (obtained using the method of EN196-9) given as part of a comprehensive programme of testing undertaken by University of Dundee (Dhir *et al*, 2006). The model is described in Appendix A2 and on the CD.

If no information or control is available on the concrete it will be necessary to assume that CEM I is used. However, it is common practice in the UK to specify additions, in particular ground granulated blast-furnace slag (ggbs) and fly ash. These materials are beneficial to heat development, although account has to be taken of possible changes in the binder content (Table 4.2, Section 4.2.2).

Thermal strain

The coefficient of thermal expansion of the concrete α_c will determine the thermal strain associated with a particular temperature change. Values for concrete commonly used in the UK vary from about 8–13 $\mu\epsilon/^\circ\text{C}$ depending primarily on the aggregate used. Table 4.4 in Section 4.5 gives proposed design values of α_c for concretes containing a variety of aggregate types.

EN1992-1-1 recommends a value of 10 $\mu\epsilon/^\circ\text{C}$ for normal weight concretes. However, recognising that higher values may be achieved in the UK, a more cautious value of 12 $\mu\epsilon/^\circ\text{C}$ is recommended when no information on the aggregate type is available.

Autogenous shrinkage, ϵ_{ca}

EN1992-1-1 assumes that all structural concrete exhibits some degree of autogenous shrinkage, with the ultimate value $\epsilon_{ca}(\infty)$ being given by the equation:

$$\epsilon_{ca(\infty)} = 2.5(f_{ck} - 10) \quad \text{microstrain} \quad (3.10)$$

where

f_{ck} is the cylinder strength at 28 days.

EN1992-1-1 also provides a time function which enables the rate at which autogenous shrinkage develops to be determined (Section 4.6.1 and Appendix A4). Curves generated using this method for a range of strength classes are shown in Figure 4.12 (Section 4.6.1).

Values of autogenous shrinkage at three and 28 days, calculated according to EN1992-1-1 (Appendix A4), are given in Table 4.5 together with ultimate values.

EN1992-1-1 assumes that with regard to autogenous shrinkage all binders perform in the same way. There is evidence that the type of binder may significantly affect ϵ_{ca} . While further research is needed the limited evidence indicates that ϵ_{ca} is reduced with the use of fly ash, but is increased when either ggbs or silica fume are used. Further information is provided in Section 4.6.1 and in Appendix A4. A spreadsheet calculator is included on the CD for estimating ϵ_{ca} in accordance with EN1992-1-1.

Temperature drop T_2

T_2 values will only apply when the change in temperature causes differential contraction between the section under consideration and the section by which it is restrained. It may be ignored if both sections are subject to the same climatic conditions and reduced if the restraining section is affected but to a lesser extent than the section subject to restraint. In the UK values of T_2 may normally be taken as 20 °C for summer casting and 10 °C for winter casting (HA BD 28/87).

Drying shrinkage, ϵ_{cd}

Drying shrinkage may be estimated using the method of EN1992-1-1 (details are given in Section 4.6.2 and in Appendix A3. A spreadsheet calculator is also provided on the CD). Values estimated for strength class C30/37 are given in Figure 4.13 (Section 4.6.2) for typical UK outdoor conditions (assuming RH = 85 per cent) and for indoor conditions (RH = 45 per cent). Tables 4.8 and 4.9 give indoor and outdoor values for typical section thicknesses of 300 mm and 500 mm for a range of strength classes.

Restraint, R

The restraint may be derived from historical data or by calculation. Values derived from *in situ* measurements which have been used in UK codes (HA BD28.87, BS8110: Part 2) are given in Table 4.10. A method for calculating restraint for the simple case of a wall cast onto a rigid foundation is described in Section 4.7.2 with a calculator provided on the CD.

EN1992-3 uses a restraint value of $R_{ax} = 0.5$ but no coefficient is provided for the effects of creep (see Equation 3.2). If this value is adopted then it should be assumed that $K_I = 1$.

In addition, Equation 3.6 allows different values of restraint to be applied to the different components of strain. This is to take into account that strains may occur at different times and at different stages in construction. For example, when a slab is cast as a series of individual bays, the restraint in a new bay will be influenced by the bay against which it is cast. However, when the early thermal cycle is complete and the individual bays act integrally, this particular source of restraint will no longer act, although there may be other external restraints acting on the slab as a whole. The likelihood is that the restraints over the long-term, R_2 and R_3 , will be lower than the restraint to early-age strains, R_1 , and hence the single value of R_{ax} used by EN1992-3 will be conservative.

Tensile strain capacity ε_{ctu}

The tensile strain capacity of the concrete under short-term loading has been derived from the ratio of the mean tensile strength of the concrete f_{ctm} to its mean elastic modulus E_{cm} estimated using the expressions provided in EN1992-1-1. Values have been derived at three days, for early-age calculations and 28 days, for long-term calculations and are shown in Figure 4.19 for strength class C30/37. For use in design these values have been increased a factor of 1.23 to take account of sustained loading and creep (Section 4.8). The results are given in Table 4.11.

The aggregate type has a significant effect on ε_{ctu} through its influence on the elastic modulus of the concrete and values have been estimated for concrete containing a range of aggregate types. EN1992-1-1 assumes quartzite aggregate as the basis for estimating design values of E_{cm} and the value for concrete using quartzite aggregate should be used when no information is available on the aggregate type. To estimate values for different strength classes the values given in Table 4.11 should be multiplied by $0.63 + (f_{ch,cube}/100)$.

3.3

Minimum reinforcement area $A_{s,min}$

It is normal practice to design the reinforcement to meet nominal code requirements and for structural loading and then to check that the steel ratio is adequate to control early-age and long-term cracking.

3.3.1

General equation

To control the crack spacing and hence the crack widths, there should be sufficient steel such that when a crack occurs the reinforcement will not yield. Expression 7.1 of EN1992-1-1 defines the minimum area of reinforcement $A_{s,min}$ according to the expression:

$$A_{s,min} \sigma_s = k_c k f_{ct,eff} A_{ct} \quad (3.11)$$

where

- $A_{s,min}$ is the minimum area of reinforcing steel within the tensile zone
- A_{ct} is the area of concrete within the tensile zone. The tensile zone is that part of the section which is calculated to be in tension just before formation of the first crack
- σ_s is the absolute value of the maximum stress permitted in the reinforcement after formation of a crack (usually taken as the yield strength of the steel, f_{ky})
- $f_{ct,eff}$ is the mean value of the tensile strength of the concrete effective at the time when the cracks may first be expected to occur, $f_{ctm}(t)$. For early-age thermal cracking the three day value is used.
- k is a coefficient which allows for the effect of non-uniform and self-equilibrating stress which leads to a reduction in restraint forces.
- k_c is a coefficient which takes account of the stress distribution within the section immediately prior to cracking.

Substituting f_{ky} for σ_s , $f_{ctm}(t)$ for $f_{ct,eff}$ and rearranging Equation 3.11 gives:

$$A_{s,min} = k_c k A_{ct} \frac{f_{ctm}(t)}{f_{ky}} \quad (3.12)$$

The coefficients k_c and k and the area of concrete in tension, A_{ct} are all influenced by the nature of restraint and values are given in Table 3.1 for the conditions in which either external restraint or internal restraint is dominant. It is normal to estimate the area of steel on each face and this is reflected in Table 3.1 in the values for surface zone representing the area of concrete in tension.

Table 3.1 Coefficients used in the estimation of $A_{s,min}$ for different restraint conditions

Parameter		External restraint dominant	Internal restraint dominant
Coefficient	k_c	1.0 for direct tension	0.5
Coefficient	k	= 1.0 for $h < 300\text{mm}$ = 0.75 for $h > 800\text{mm}$ intermediate values are interpolated	1.0
Surface zone representing the area of concrete in tension (section thickness = h).	h	Full section thickness (0.5 h)	20% of section thickness (0.2 h)

EN1992-1-1 recommends a values of $k = 0.65$ for sections thicker than 800 mm (the basis for this value is unclear). The derivation of the more cautious value of $k = 0.75$ is given in Appendix A8 together with the basis for all values given in Table 3.1.

3.3.2

Tensile strength of concrete

Early-age (three day) and long-term (28-day) values of mean tensile strength, $f_{ctm}(t)$ for use in estimating $A_{s,min}$ are given in Table 3.2. Values are the mean tensile strength estimated using the relationships with compressive strength and age according to EN1992-1-1 (Section 4.10). A probabilistic analysis has indicated that there is less than a one per cent chance of these values being exceeded *in situ* (Appendix A10).

Table 3.2 Values of early-age and long-term tensile strength estimated in accordance with EN1992-1-1

Strength class	C20/25	C25/30	C30/37	C35/45	C40/50	C45/55	C50/60	C55/67	C60/75
Early-age tensile strength $f_{ctm}(3)$ (MPa)	1.32	1.53	1.73	1.92	2.12	2.27	2.44	2.52	2.61
Long-term tensile strength, f_{ctm} (MPa)	2.21	2.56	2.90	3.21	3.51	3.80	4.07	4.21	4.35

3.3.3

Tensile strength of steel

The characteristic yield strength of the reinforcement is taken as 500 MPa. For serviceability limit states, including early thermal cracking, the partial factor for steel γ is 1.0 (NDP).

3.4

Crack spacing

The steel ratio determines the maximum crack spacing, $S_{r,max}$, according to the expression

$$S_{r,max} = 3.4c + 0.425 \frac{k_1 \varphi}{\rho_{p,eff}} \quad (3.13)$$

where

- c is the cover to reinforcement
- k_1 is a coefficient which takes account of the bond properties of the reinforcement. EN1992-1-1 recommends value of 0.8 for high bond bars. The crack spacing is very sensitive to bond and EN1992-1-1 recommends a reduction in bond strength by a factor of 0.7 where good bond cannot be guaranteed. In this case $k_1 = 1.14$ (see Section 4.13 and Appendix A8, Section A8.5). It is recommended that, in relation to early-age thermal cracking, the higher value be used until experience with the approach of EN1992-1-1 indicates that a lower value may be appropriate
- φ is the bar diameter
- $\rho_{p,eff}$ is the ratio of the area of reinforcement to the effective area of concrete (= $A_s/A_{c,eff}$)
- $A_{c,eff}$ is the effective area of concrete in tension around the reinforcement to a depth of $h_{c,ef}$, where $h_{c,ef}$ is the lesser of $h/2$ or $2.5(c + \varphi/2)$.

$A_{c,eff}$ used to estimate the steel ratio $\rho_{p,eff}$ for controlling crack width differs from A_{ct} which is used to estimate $A_{s,min}$.

The coefficients 3.4 and 0.425 are NDPs.

3.5 Crack width

3.5.1 The requirements of EN1992-3

With regard to the calculation of crack width, EN1992-3 considers two specific conditions:

- 1 A long wall restrained along one edge.
- 2 Restraint of a member at its ends.

These conditions differ in the way in which cracks are formed and the influence of the cracks on the distribution of stresses within the element (see Appendix A8). Condition 1 may also be applied to adjacent pours in a slab, where the edge restraint occurs along the joint. It is important to understand the nature of restraint as the resulting crack widths may differ significantly.

3.5.2 A member restrained along one edge

For a member subject to restraint along one edge, the crack width, w_k , is calculated using the expression:

$$w_k = S_{r,max} \varepsilon_{cr} \quad (3.14)$$

where

ε_{cr} is the crack-inducing strain estimated using Equation 3.6.

Combining Equations 3.13 and 3.14 gives the expression:

$$w_k = \varepsilon_{cr} \left[3.4c + 0.425 \frac{k_1 \varphi}{\rho_{p,eff}} \right] \quad (3.15)$$

3.5.3 A member restrained at ends only

For a member subject to end restraint only, the crack width, w_k , is calculated using the expression:

$$w_k = \frac{0.5\alpha_e k_c k_{ct,eff}}{E_s} \left(1 + \frac{l}{\alpha_e \rho} \right) S_{r,max} \quad (3.16)$$

where

k, k_c are coefficients as defined in Table 3.1

$f_{ct,eff}$ is the mean tensile strength of the concrete at the time of cracking, $f_{ctm}(t)$

E_s is the modulus of elasticity of the reinforcement

α_e is the modular ratio

ρ is the ratio A_s/A_{ct} (Note: ρ differs from $\rho_{p,eff}$ which is used to calculate the crack width for the edge-restrained condition)

A_s is the (total) area of reinforcement

A_{ct} is the gross section in tension

$S_{r,max}$ is the crack spacing calculated using Equation 3.13.

The crack spacing and hence the crack width for a member subject end restraint only (ie with no edge restraint) is generally significantly greater than that occurring for a member subject to edge restraint, being determined by the tensile strength of the concrete rather than the magnitude of restrained strain. It is important that the nature of the restraint is properly defined.

3.5.4

A member subject to internal restraint

For a member subject to internal restraint, Equation 3.15 is used to calculate crack widths, with ε_{cr} being derived using Equation 3.9.

3.6

The Simplified Method with default values

It is recognised that at the design stage there may be limited information available and a simplified design approach which uses conservative default values is provided. This approach will lead to a conservative design.

3.6.1

Estimating the risk of cracking and the crack-inducing strain

Restrained strain, ε_r

The expression for ε_r is simplified to the following:

$$\varepsilon_r = K [\alpha_c (T_1 + T_2) + \varepsilon_{cd}] \quad (3.17)$$

K is a single coefficient which takes account of restraint R ; the coefficient K_I for creep; and the strain contribution from autogenous shrinkage.

For conditions of edge restraint $K = 0.5$.

Equation 3.17 is consistent with EN1992-3 (Equation M.3 of Informative Annex M) as the maximum restraint factor given in Informative Annex L is 0.5, and restrained-strain is estimated using the equation: $\varepsilon_r = 0.5 \varepsilon_{free}$.

Temperature drop, T_1

Values of T_1 are given in Tables 3.3 for different strength classes cast under summer conditions. CEM I has been assumed.

Table 3.3 T_1 values ($^{\circ}\text{C}$) for different strength classes and section thicknesses (in mm) cast in the summer with a mix temperature of 20°C and a mean ambient temperature of 15°C . Adjustment values are given for winter casting

	Strength class	Steel formwork					Plywood formwork				
		300	500	700	1000	2000	300	500	700	1000	2000
Summer casting	C25/30	16	25	32	39	48	25	32	37	42	49
	C30/37	18	28	35	43	54	28	36	42	47	55
	C35/45	20	31	39	48	60	31	40	46	52	60
	C40/50	22	33	42	51	64	33	43	49	56	65
Adjustment for winter casting		-6	-8	-7	-6	-2	-6	-6	-5	-5	0

Temperature drop, T_2

Summer casting	$T_2 = 20\text{ °C}$
Winter casting	$T_2 = 10\text{ °C}$

Coefficient of thermal expansion, α_c

EN1992-1-1 recommends a value of $10\text{ }\mu\epsilon/\text{°C}$ but higher values are common in the UK (Section 4.5) and a more conservative value of $12\text{ }\mu\epsilon/\text{°C}$ for normal weight concrete should be used.

Autogenous shrinkage, ϵ_{ca}

For normal structural concretes α_{ca} is no greater than about $40\text{ }\mu\epsilon$. This is equivalent to a temperature change of only $3\text{--}4\text{ °C}$ and is accommodated by the conservatively high values of T_I in Table 3.3.

Drying shrinkage, ϵ_{cd}

For members $\geq 300\text{ mm}$	$\epsilon_{cd} = 150\text{ }\mu\epsilon$ for UK external exposure conditions
	$\epsilon_{cd} = 350\text{ }\mu\epsilon$ for UK internal exposure conditions

Tensile strain capacity, ϵ_{ctu} under sustained loading

Early-age	$\epsilon_{ctu} = 70\text{ }\mu\epsilon$
Long-term	$\epsilon_{ctu} = 100\text{ }\mu\epsilon$

Limiting temperatures for avoidance of cracking

External restraint	$T_{I,max} = 13\text{ °C}$
Internal restraint	$\Delta T_{max} = 18\text{ °C}$

Crack-inducing strain, ϵ_{ct}

Early-age cracking	$\epsilon_{cr} = K \alpha_c T_I - 0.5 \epsilon_{ctu} = 6 T_I - 35$
Long term cracking	$\epsilon_{cr} = K [\alpha_c (T_I + T_2) + \epsilon_{cd}] - 0.5 \epsilon_{ctu} = 6 (T_I + T_2) + 0.5 \epsilon_{cd} - 50$

Summer casting (outdoors)	$\epsilon_{cr} = 6 T_I + 145$
Summer casting (indoors)	$\epsilon_{cr} = 6 T_I + 245$
Winter casting (outdoors)	$\epsilon_{cr} = 6 T_I + 85$
Winter casting (indoors)	$\epsilon_{cr} = 6 T_I + 185$

Values derived for the various conditions are shown in Figure 3.1.

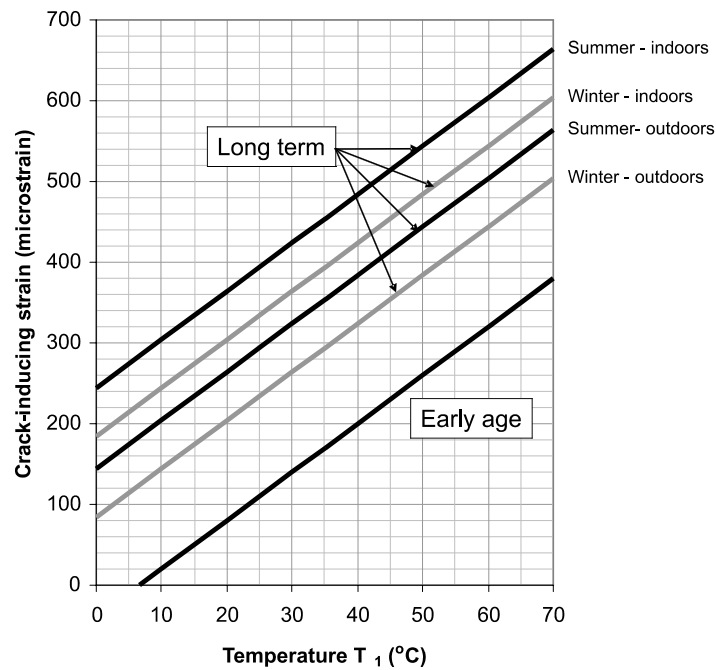


Figure 3.1 Values of crack-inducing strain

3.6.2

Crack control

The process for checking that the reinforcement is adequate to control cracks through achieving $A_{s,min}$, and estimating the crack spacing and width should follow the procedure of EN1992-1-1 described in Sections 3.3, 3.4 and 3.5.

3.7

Selecting options to reduce the risk of cracking

Table 3.4 summarises the factors which help prevent or control early-age thermal cracking and indicates where within the text further information may be found.

The selection of mix proportions to give lower thermal movements and/or higher tensile strain capacities can be fraught with difficulties, but these can be greatly reduced by clearly establishing that any concrete should first comply with requirements for durability, workability and strength.

With the introduction of EN1992-1-1, structures are designed on the basis of the characteristic cylinder strength at 28 days (although in the UK quality control is still undertaken using cubes). However, for some structures, such as dams, the concrete is usually designed to the three month strength. This principle can be applied to other structures giving both technical and economic advantages. Specifying a later age strength for compliance testing is equivalent to specifying a lower strength class. For some concretes, eg those containing fly ash or ggbs, it has been demonstrated that the *in situ* strength will be higher for a given strength class (Concrete Society, 2004). Further details are given in Appendix A9. In such circumstances a reduction in strength class may be justified subject to other specification requirements being met. For example, specifying strength does not guarantee durability; BS8500 also specifies a minimum binder content and maximum water/binder ratio for many exposure conditions. This can override the strength requirement. Conversely, lower strength does not always mean loss of durability. Concretes containing fly ash or ggbs may offer as good, or better protection to rebar in salt laden environments than CEM I concretes of a higher strength class (Bamforth, 2004).

Aggregates are expensive to haul over long distances, but if preferred aggregates are available at a competitive cost, then the design and specification should be based on their use. Normal weight concretes made with crushed aggregates have a higher tensile strain capacity than concretes made with rounded aggregates, and the preferred normal weight coarse aggregate is a crushed rock with a low coefficient of thermal expansion (ie many, but not all limestones – see Table 4.4). Even better than the normal weight aggregates are the lightweight aggregates with their very low coefficients of thermal expansion and very high tensile strain capacities. The relative merits of these aggregates are demonstrated in Table 7.1, which indicates the relative allowable temperatures for a range of aggregate types.

Commercial software is available for both thermal modelling and for the estimation of thermal strain and stresses (see Appendix A2). Such models are equally applicable for use in design and may offer further economies. However, for any predictive model to be of real value, specific information is required on the concrete to be used, the pour geometry and construction sequence and the conditions into which the concrete is to be cast.

Table 3.4 Summary of the options available to prevent, minimize or control early-age thermal cracking

Factor	Worst choice	Best choice	Best choice	Section
Concrete mix parameters				
Aggregate shape	Rounded	Angular	Better strain capacity may be partially offset by higher cement content	4.8
Aggregate modulus	High	Low	To achieve a higher f_{ctm}/E_{cm} ratio and yield a higher strain capacity	4.8
Aggregate type	High α_c	Low α_c		4.5
Binders	CEM I	Use of additions fly ash ggbs	Also silica fume to enable reduction in binder content subject to minimum specified binder limits	4.2
Admixtures (excluding latex and polymers)	None	Water reducers Superplasticisers	To reduce cement content. Check durability requirements	
Placing temperature	High	Low	Cooling of constituents using chilled water, ice or liquid nitrogen	4.2, 6.3
Construction practice				
Ambient temperature	High	Low	Night time concreting is beneficial	4.2
<i>In situ</i> cooling	Cooling pipes are effective, but expensive. Surface cooling by water spray applicable for sections under about 500 mm thick			6.3
Formwork for sections under 500 mm thick	Insulated, plywood with long striking time	GRP, steel Striking time not significant	To permit rapid heat loss and reduce T_1	4.2
Formwork material in large sections	Steel, GRP	Plywood, Insulated with long striking time	To minimise thermal gradients. Keep the upper surface insulated	4.3
Insulation for thick sections	None	Thermal blanket	Effective for isolated element, eg rafts, with low external restraint	4.3
Construction sequence	Alternate bay between lifts	Sequential construction or short infill bays	Not significant if using full movements joints	6.1
Period between successive lifts	Long	Short	First pour may be insulated to reduce differential effects. Slip-forming is beneficial as casting is continuous	6.1
Movement joints	None Partial movement joints	Full movement joints	Full movement joints require dowels and sealing	6.2
Prestressing the base			Not normally economic	
Reinforcement Distribution	Large dia. bars at wide spacing	Small dia. bars at close spacing	To increase the surface area of steel	3.5

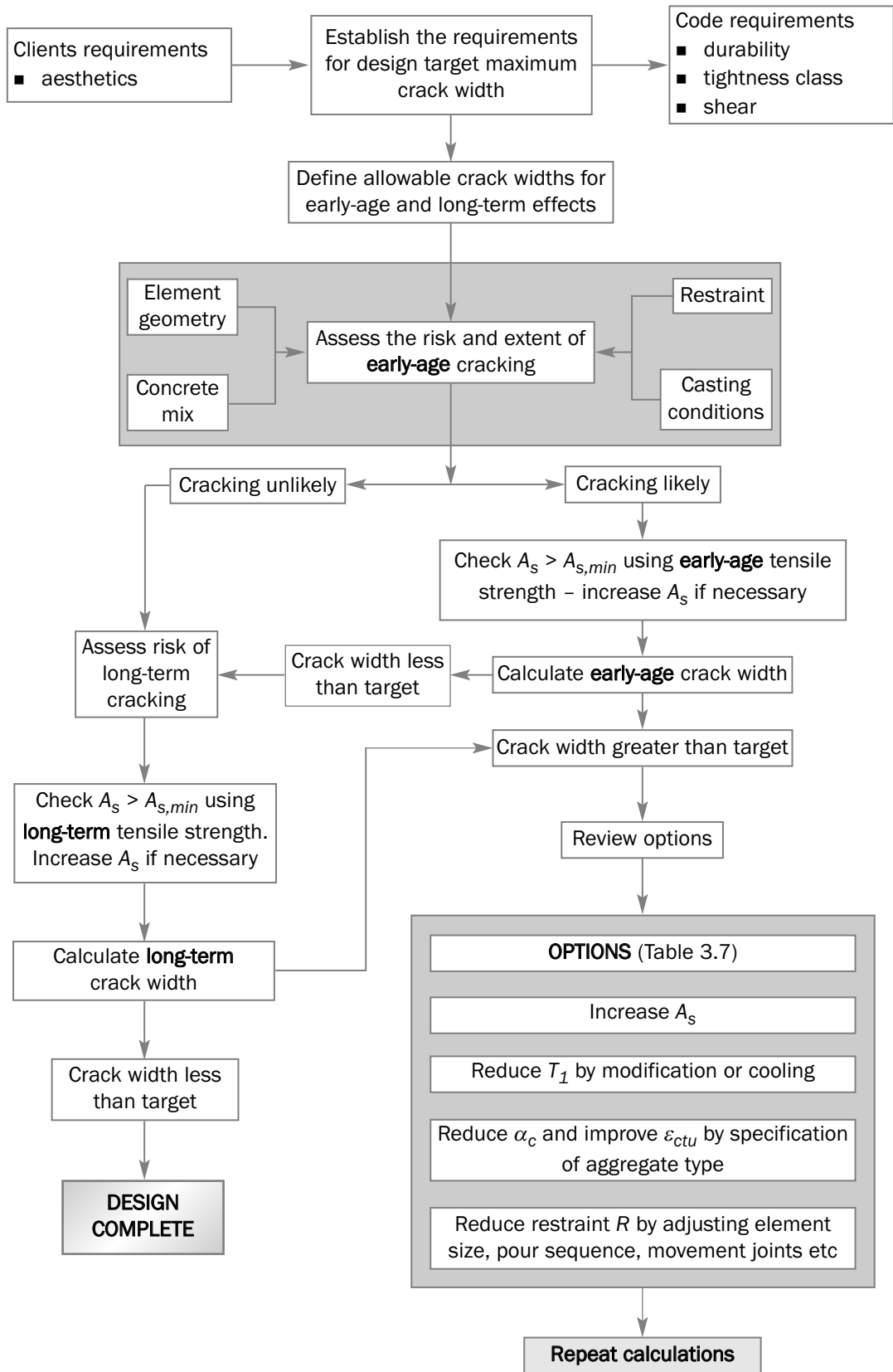


Figure 3.2 Flow chart showing the design process for control of early-age and long-term cracking

4 Factors affecting early-age cracking and data required for design

4.1 Information and assumptions

At the design stage, the designer may have limited knowledge of the concrete to be used or the construction process and conservative assumptions should be made which may not be reflected in practice. In addition, the designer has to deal with many aspects of performance (structural integrity, serviceability, durability) which may be compatible with early-age requirements, but sometimes are not. For example, specifying a minimum cement content for durability reasons may increase the risk of early thermal cracking, and the designer should be aware of the implications of such decisions.

To predict the risk of early-age cracking and to design reinforcement for crack control the following information is required:

- ☞ temperature rise (and fall) and temperature differentials
- ☞ the coefficient of thermal expansion of the concrete, to determine the free thermal strain and differential strains that develop
- ☞ the restraint to thermal movement at critical locations (involving assumptions about pour sizes and casting sequences) to determine the component of restrained strain that may result in tensile stress and cracking
- ☞ the tensile strain capacity of the concrete, to determine the extent to which the concrete is able to withstand the restrained strains
- ☞ the tensile strength of the concrete, to estimate the minimum reinforcement area needed to control any cracks which may develop and, in the case of end restraint, the crack width
- ☞ the strength of the reinforcement.

Table 4.1 is provided for the designer to record the assumptions made in relation to the control of early-age cracking. Benefits of recording this information are as follows.

- ☞ when cracking occasionally occurs that is out of specification, it is often difficult to isolate a specific cause. Being able to compare achieved concrete properties and thermal histories with the design assumptions may help with a basis for resolution
- ☞ as the design assumption are conservative it is likely that in many situation the practice will be less severe. Some advantage of this may be taken during the construction process. For example, a limestone aggregate with low thermal expansion may be available, resulting in lower than estimated thermal strain and hence a greater acceptable temperature rise and differentials.

To achieve the most cost-effective design, more information is needed about the concrete and the construction process. This may be achieved either through early interaction with the contractor through a partnering process, or by a more prescriptive specification which involves the designer in more detailed specification of the concrete type, maximum pour sizes and the construction sequence. In this case, the designer is responsible for the completed structure, provided that accepted good practice is exercised during the construction process.

Table 4.1 Assumptions made in the estimation of the risk of cracking and the design of reinforcement to control crack widths (this table is included on the accompanying CD)

Element details		NOTES
Element type	<input type="text"/>	e.g. wall, slab
Thickness	<input type="text"/> mm	This will be the value used to derive T ₁
No. of exposed faces (1 or 2)	<input type="text"/>	
Length	<input type="text"/> m	May be used in estimating restraint
Wall height / slab breadth	<input type="text"/> m	May be used in estimating restraint
Formwork type	<input type="text"/>	If not known assume 18mm plywood formwork
Insulation (for slab)	<input type="text"/>	
Concrete		
Strength Class	<input type="text"/>	e.g. C _{f_{ck}} /f _{ck,cube}
Cement content	<input type="text"/> kg/m ³	Including any additions. Table 4.2 for default values
Cement type	<input type="text"/>	If not known assume, CEM I 42.5 cement
Additions	<input type="text"/>	fly ash, ggbs, silica fume, metakaolin, etc.
Additions as percentage of binder	<input type="text"/> %	
Conditions of placing		
Mean ambient temperature if NOT 15°C	<input type="text"/> °C	If either the mean ambient temperature or placing temperature differ from their default value, indicate correction applied to T ₁
Concrete temperature if NOT 20°C	<input type="text"/> °C	
Correction applied to T ₁	<input type="text"/> °C	Add to the value of T ₁ derived from the default temperature
Any special conditions that apply?	<input type="text"/>	
Temperature drop T ₁	<input type="text"/> °C	Estimated value plus correction
Long-term temperature changed T ₂	<input type="text"/> °C	Difference between the mean ambient temperature during casting and the final operating temperature.
Thermal strain		
Coarse aggregate type	<input type="text"/>	If coarse aggregate and sand are different then estimate α _c using 0.67
Sand type	<input type="text"/>	x value for coarse type only + 0.33 x value for sand type only
Thermal expansion coefficient, α _c	<input type="text"/> με/°C	If not known use a default value of 12 με/°C
Additional early age strains		
Autogenous shrinkage, ε _{ca}	<input type="text"/> με	This strain is assumed to occur during the early thermal cycle
Drying shrinkage ε _{cd}	<input type="text"/> με	This strain is assumed to occur over the long term and to include any long term autogenous shrinkage
Restraint factors		
R ₁ during the early thermal cycle	<input type="text"/>	This restraint factor applies to the early age thermal contraction and autogenous shrinkage
R ₂ for annual temperature variation	<input type="text"/>	This value applies to T ₂
R ₃ for long term deformation	<input type="text"/>	This value applies to drying shrinkage
Coefficients		
K ₁	<input type="text"/>	for creep (default = 0.65)
K ₂	<input type="text"/>	for sustained loading (default = 0.80)
Resistance to cracking		
Tensile strain capacity, ε _{ctu}	<input type="text"/> με	This is the value obtained under short term loading
Control of cracking		
Tensile strength of concrete, f _{ctm}	<input type="text"/> MPa	This is the mean value at the age at which cracking first occurs
Yield strength of reinforcement, f _{ky}	<input type="text"/> MPa	This is the characteristic value

4.2 Temperature rise

4.2.1 Influencing factors

The main variables influencing the temperature rise are described in detail in Appendix A1 – **Heat generation, temperature rise and temperature differentials** and are summarised as follows:

- ⊗ cement content
- ⊗ types and sources of cementitious, (ie binder) material
- ⊗ other concrete constituents and mix proportions that influence the thermal properties of the concrete
- ⊗ section thickness (Figure 4.1)
- ⊗ formwork and insulation (Figure 4.2 and 4.3)
- ⊗ concrete placing temperature (Figure 4.4)
- ⊗ ambient conditions
- ⊗ active forms of temperature control such as internal cooling pipes.

Models are available for predicting the temperature rise and temperature profiles through a section and one such model is described in Appendix A2. It has been used to derive the information shown in Figures 4.1, 4.2, 4.3 and 4.4.

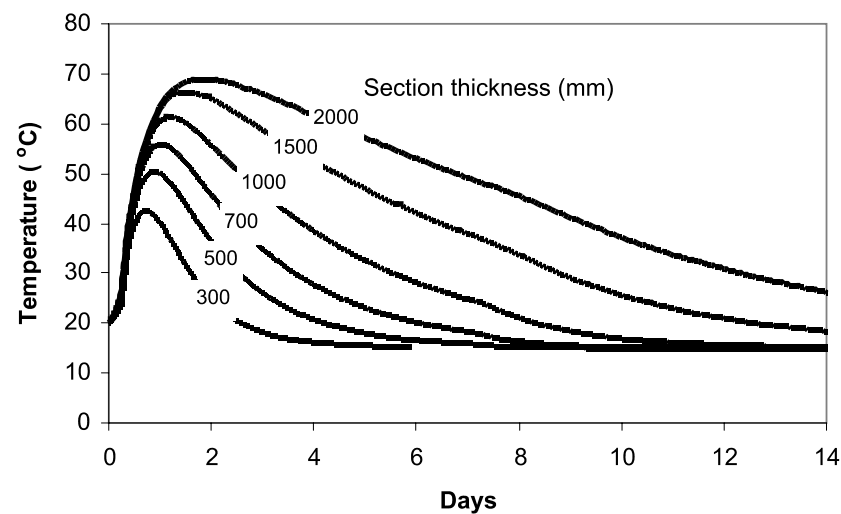


Figure 4.1 The effect of wall thickness on the temperature rise (for 350 kg/m³ CEM I, 18 mm plywood formwork removed after seven days)

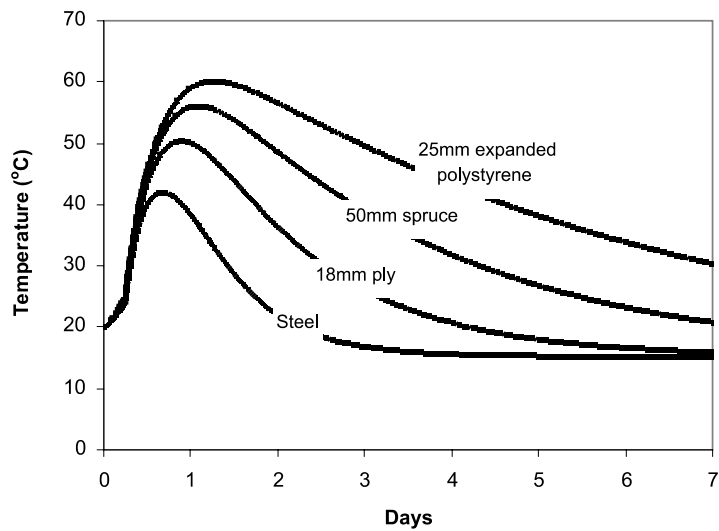


Figure 4.2 The effect of formwork type on the temperature rise in 500 mm thick walls (for 350 kg/m³ CEM I)

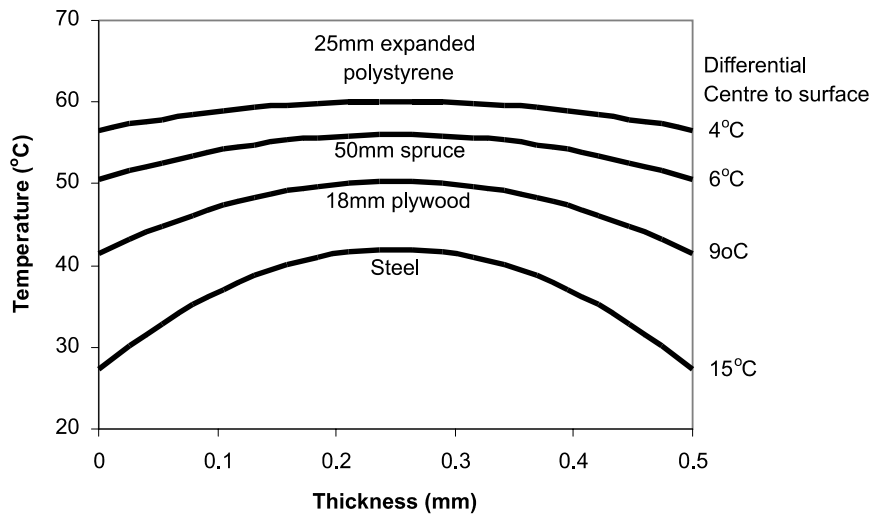


Figure 4.3 The effect of formwork type on the temperature profile in 500 mm thick walls achieved at the time of the peak temperature (for 350 kg/m³ CEM I)

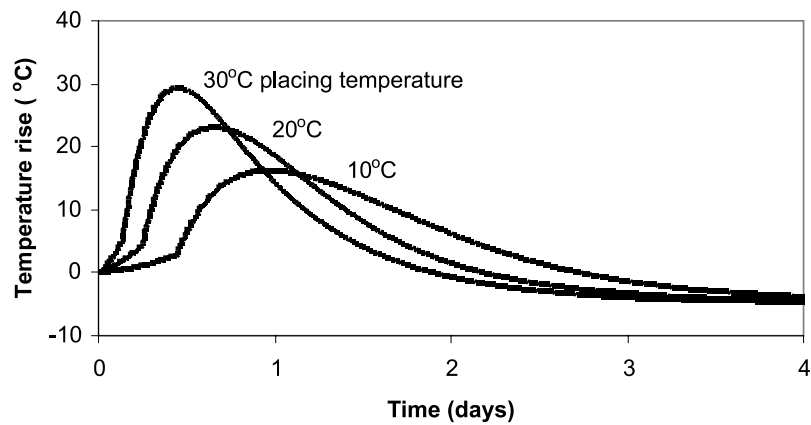


Figure 4.4 The effect of placing temperature on the temperature rise in a 500 mm thick wall using concrete with 350 kg/m³ CEM I cast in steel formwork

4.2.2

Estimating T_1

The design process requires the T_1 value as an input and a comprehensive programme of testing undertaken at University of Dundee has provided a basis upon which to modify the T_1 values to reflect the behaviour of modern CEM I materials (Dhir *et al*, 2006). It also provides information, previously unavailable, on combinations with fly ash and ggbs. In CIRIA 91 (Harrison, 1992) T_1 values were presented in tabular form for concretes with specific cement contents and for elements of specific thickness. In many cases interpolation was required. In this guide T_1 values are presented graphically.

While the designer will determine the section thickness, the only information available about the concrete may be the strength grade. To predict T_1 , the cement content is required. Table 4.2 is provided to give an indication of the cement content likely to be associated with different grades of concrete using different cement types. Advice should be sought from local concrete producers but where none is available the values in Table 4.2 may be used. **These values should not be used for mix design or specification purposes. They are indicative only and are deliberately at the high end of the range that might be expected.**

While a reduction in the heat generation of the binder is likely to be beneficial, it is the temperature rise in the resulting concrete that is of principal concern with regard to early thermal cracking. It can be seen in Table 4.2 that when additions are used, different binder contents are often required to achieve the same strength class of concrete and it is important that this is taken into account when assessing the benefits or otherwise of a particular mix design.

Table 4.2 Cement contents for different strength classes. (Note: These values are indicative only and at the high end of the range that may be expected in practice and should not be used for specification purposes)

Strength class	Binder content (kg/m ³)										
	Not specified	CEM I	up to 20% fly ash	30% fly ash	40% fly ash	50% fly ash	up to 40% ggbs	50% ggbs	60% ggbs	70% ggbs	80% ggbs
C20/25	275	275	295	300	315	330	275	285	300	325	345
C25/30	300	300	320	325	340	360	300	310	330	355	385
C30/37	340	340	360	365	380	400	340	355	375	410	450
C35/45	380	380	405	410	430	450	380	395	430	480	540
C40/50	410	410	440	445	465	485	410	430	470	530	
C45/55	440	440	470	475	500	525	440	465	515		
C50/60	475	475	505	515	535		475	505			

Note: The shaded values are those which may be necessary without the use of admixtures. However, it is common practice to use water-reducing admixtures for the higher strength classes to enable a reduction in cement content. Values greater than 550 kg/m³ have not been included as they would not normally be permitted.

It is recognised that silica fume and metakaolin may also be used to achieve equivalent strength classes with a reduced binder content and hence lower heat output. However, such mixes are dependent on the use of high range water reducing admixtures and it is difficult to offer specific binder contents in relation to strength class. Where this option is considered, advice should be sought from material suppliers.

Values of T_I for CEM I are given in Figure 4.5 for walls cooling from both faces. Values for combinations with 30, 50 and 70 per cent ggbs are given in Figure 4.6 and combinations with 20, 35 and 50 per cent fly ash, are given in Figure 4.7. These values were derived using the model described in Appendix A2 assuming CEM I with an ultimate heat output of 380 kJ/kg (about 15.8 °C/100kg in concrete with a specific heat of 1 kJ/kg°C and a density of 2400 kg/m³) and represent values with only a 10 per cent chance of being exceeded. The data on heat generation were derived from semi-adiabatic temperature rise measurements by the University of Dundee (Dhir *et al*, 2006). Values are based on a mean ambient temperature of 15 °C and a placing temperature of 20 °C. The difference of 5 °C is typical and has been derived from observations (Appendix A1). For pours thicker than 1000 mm, values may be derived from Figure 4.8.

When using silica fume or metakaolin, it is recommended that, with regard to heat generation, and T_I values, these are equivalent to CEM I. Limestone filler may be assumed to be inert (Appendix A1).

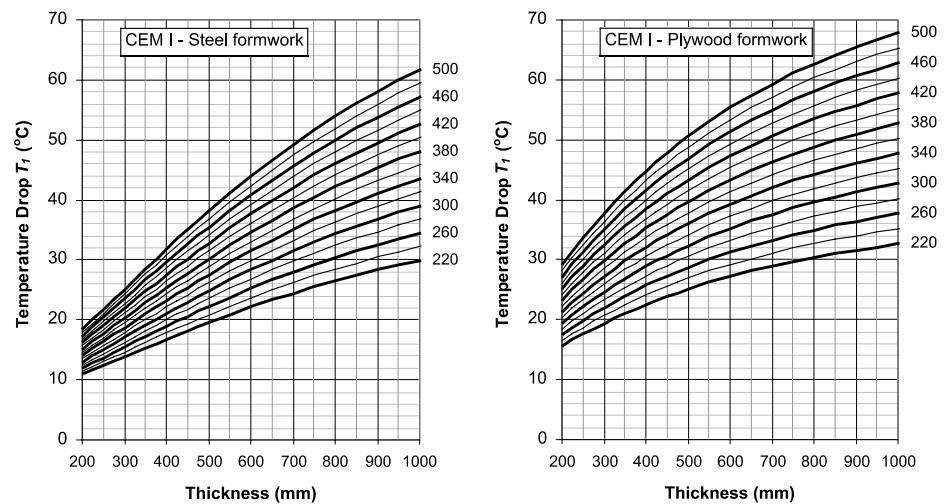


Figure 4.5 T_I values for CEM I in walls

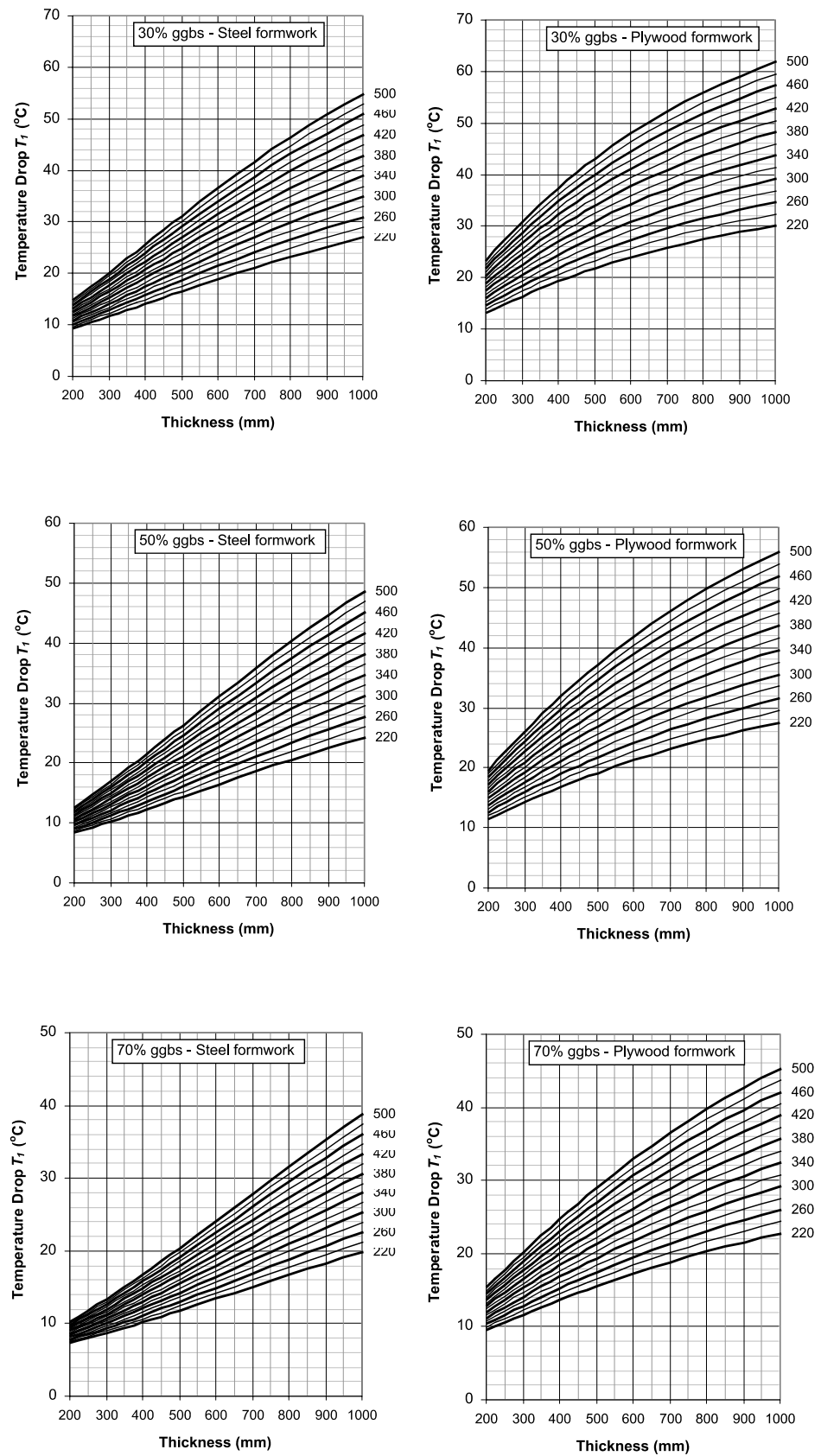


Figure 4.6 T_1 values for concretes containing 35, 50 and 70 per cent ggbs in walls

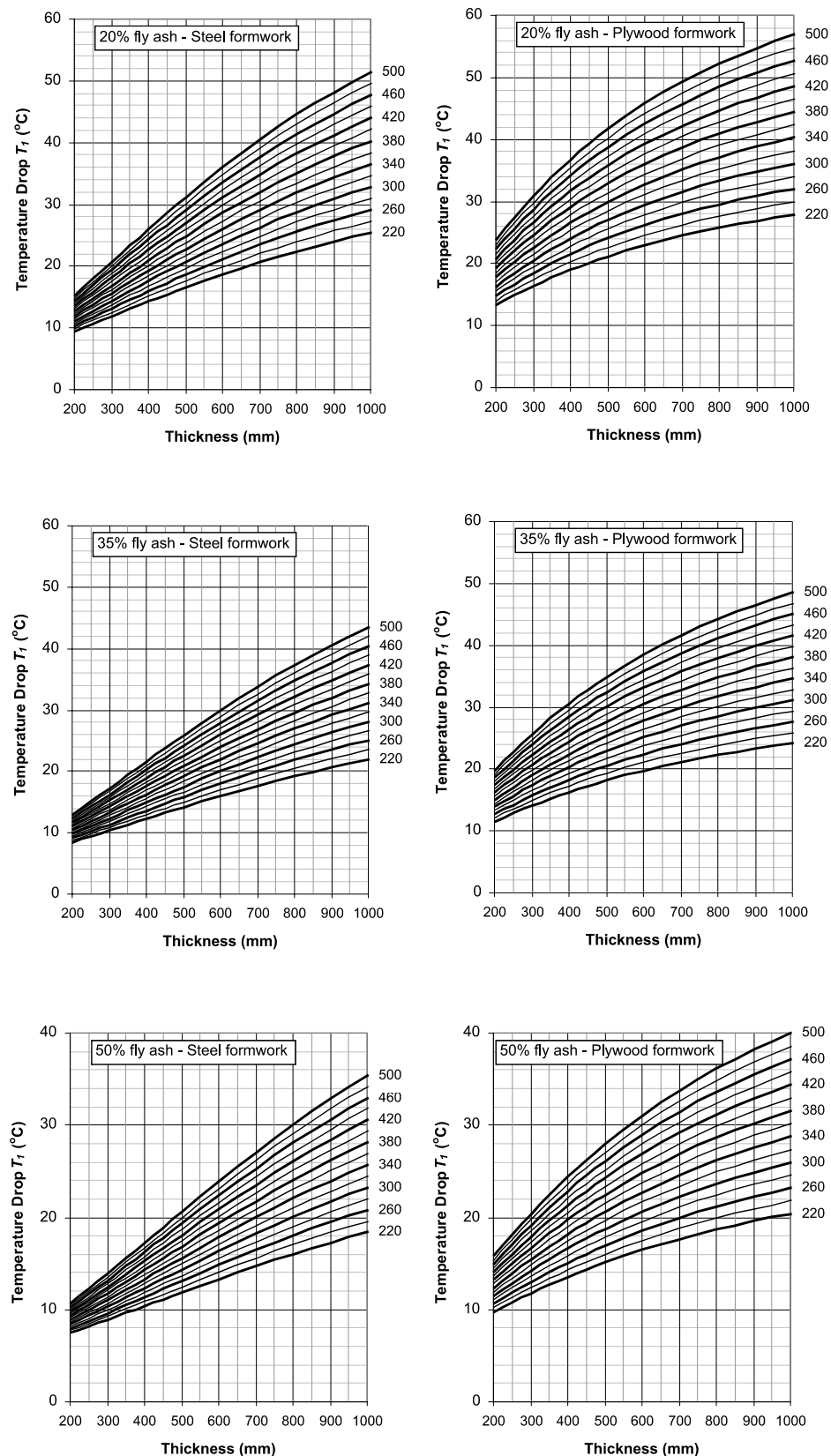


Figure 4.7 T_1 values for concretes containing 20, 35 and 50 per cent fly ash in walls

For sections thicker than 1000 mm the temperature rise is approximately proportional to the binder content (Appendix A1). CIRIA Report 135 (Bamforth and Price, 1995) provides an indication of the likely temperature rise in large volume pours in relation to pour thickness, cement/addition combination and temperature rise by weight of

binder. These curves were derived empirically from measurements in large pours (Bamforth, 1980) and have been modified to reflect the performance of modern cements (Dhir *et al.*, 2006) as shown in Figure 4.8. The original curves from CIRIA 135 are also shown.

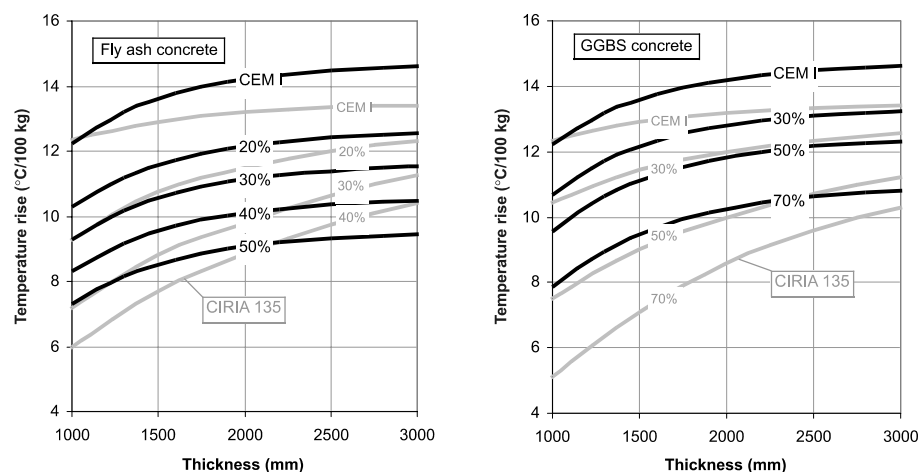


Figure 4.8 Temperature rise per unit weight of binder in massive sections (to obtain values of T_1 5 °C should be added to the temperature rise calculated)

4.2.3

Adjustments to T_1

Variation between sources of cement

The estimates given in Figures 4.5, 4.6 and 4.7 represent design values, but cements may vary considerably. Occasionally, marginally higher values may occur but in general lower values would be expected in practice. Based on the comparison between estimated and measured values and knowledge of the variation for cement (see Appendix A1) it may be assumed that the variation about the mean value will be as high as ± 6 °C. Part of this variation is due to the difference between the placing temperature and the ambient temperature deviating from the assumed 5 °C (see Appendix A1).

When there is knowledge of the cement to be used and it can be reliably demonstrated by testing or modelling that a lower value will be achieved, the value of T_1 may be reduced accordingly.

Heating or cooling the concrete

In special circumstances the difference between the placing temperature and the mean ambient temperature may differ predictably from the assumed 5 °C. For example in winter conditions the materials may be heated; in summer materials may be cooled; or when there is a long haulage time the temperature of the concrete may increase more than normal. Under such circumstances an appropriate margin should be added to the values of T_1 derived from Figures 4.5, 4.6 and 4.7.

Placing temperature

An adjustment is also required if the concrete placing temperature varies significantly from the assumed value of 20 °C. Recommended adjustments for placing temperature related to section thickness are given in Figure 4.9.

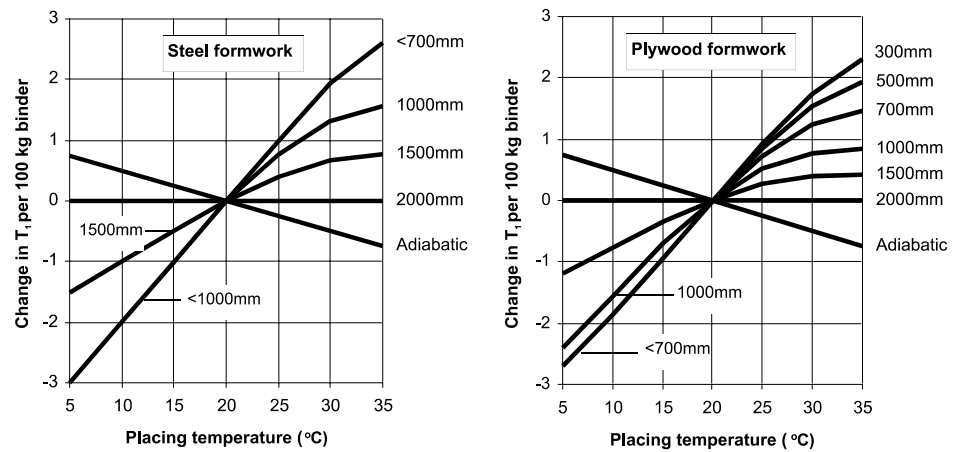


Figure 4.9 The estimated change in T_1 (per 100 kg/m³ CEM I) with placing temperatures for elements of varying thickness

Differential with adjacent concrete

T_1 may also be modified when a new pour is cast against adjacent concrete that is still at a temperature appreciably higher than the mean ambient temperature. This may be the case when the delay between adjacent pours is short, or when the previous pour is insulated to slow down the rate of cooling.

Ground slabs

For ground slabs up to 500 mm thick, without surface insulation, the value of T_1 may be obtained by estimating the value for a wall cast into steel formwork which has a thickness that is 1.3 times that of the slab. When surface insulation is applied, as a first approximation, T_1 may be assumed to be the same as that for a wall of the same thickness cast into plywood formwork.

The most reliable way to determine T_1 is by measurement (Section 7.2.1). To avoid errors that may arise in adjusting mix temperature when very high or very low placing temperatures are expected, the temperature rise in concrete samples should be measured from a placing temperature which is close to that likely to be achieved.

4.3

Annual temperature change, T_2

In the long-term the concrete will respond to changing ambient conditions. This is taken into account using the term T_2 . The annual change in temperature is shown in Figure 4.10, expressed as the mean monthly temperature for each decade since 1916. It can be seen that the variation in summer to winter temperature when presented on this basis is about 12 °C and has remained so for many decades, although the average annual temperature would appear to have increased by over 1 °C over the period investigated.

Data for the first half of 2006 is also included which indicates that in individual years both the peak temperature and the annual variation may be higher, in this case up to 19 °C and 15 °C respectively.

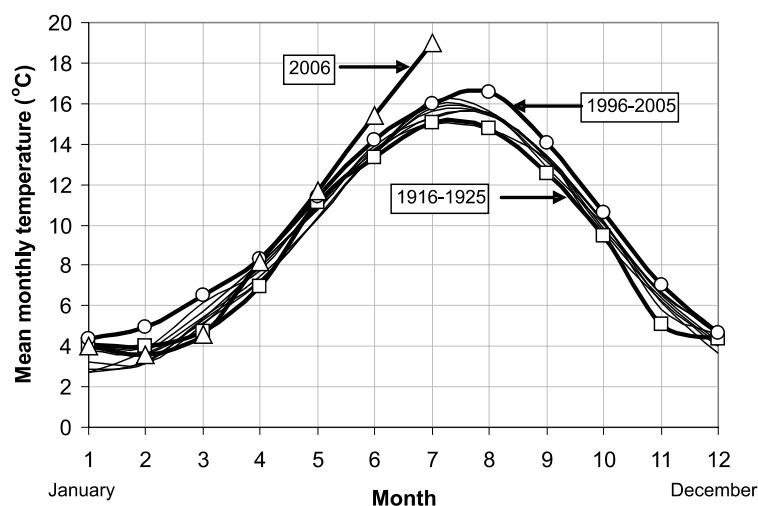


Figure 4.10 Mean monthly temperatures over each decade since 1916 (Met Office, 2006)

In selecting appropriate design values for T_2 , consideration has to be given to the following:

- ☞ the time of year when the concrete is cast. As shown in Figure 4.10, concrete cast in the summer months may experience a drop in temperature of at least 12 °C more than concrete cast in the winter
- ☞ concrete is generally cast during the day when the actual temperature is higher than the average. This is taking into the difference between the placing temperature and the mean ambient temperature in the T_1 value
- ☞ temperature variations within each month will result in periods when the ambient temperature is appreciably higher or lower than the mean monthly average.

For annual temperature changes recommended values of T_2 are 20 °C for concrete cast in the summer and 10 °C for concrete cast in the winter (HA BD28/87, 1987).

It is now rare to have prolonged periods of sub-zero temperature in the UK and these recommended values will take account of concrete cast at 25 °C in the summer when the ambient temperature is 20 °C and concrete cast in the winter at 15 °C, when the ambient temperature is 10 °C, and in each case cooling to 0 °C at some time during the winter months while the concrete against which it is cast remains at the original casting temperature. Where it is clear that conditions will apply in which the old concrete providing the restraint remains at a constant temperature then these values should be used. However, in many situations, eg concrete in the ground, the old concrete will also respond to ambient changes as shown in Figure 4.11. Under these conditions the T_2 values may be reduced to reflect the relative, rather than the absolute change in temperature. When foundations are more than 5 m deep, the temperature should be assumed to remain constant.

While the recommended T_2 values will cover most conditions, the trend towards hotter periods in the summer (eg the unusually hot July of 2006 shown in Figure 4.10) may lead to occasional situations in which the T_2 value for summer casting will be exceeded if steps are not taken to control the placing temperature of the concrete.

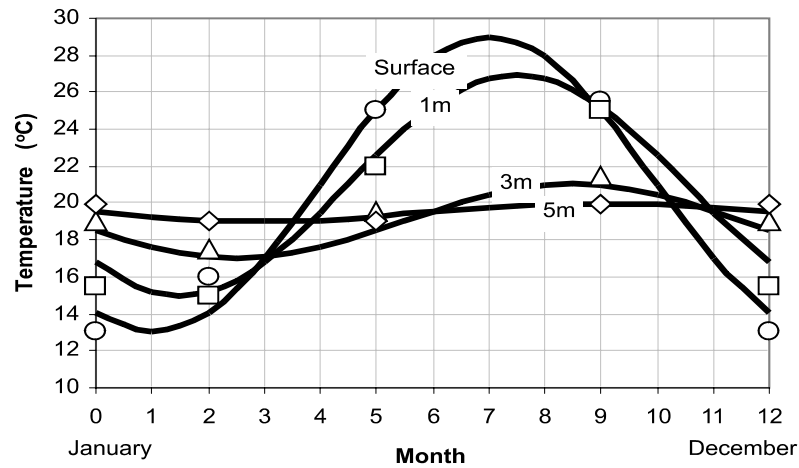


Figure 4.11 Variation in ground temperature recorded for a heat pump installation in Croydon (Witte, 2001). The data points were provided and the curves fitted assuming a sinusoidal variation

4.4

Temperature differentials, ΔT

In order to estimate the likely temperature differentials that will occur it is necessary to undertake thermal modelling. Some indicative values are provided however, in Table 4.3. These values have been obtained using the model described in Appendix A2 which can be used to undertake comparative assessments.

Table 4.3 Estimated values of temperature differential in walls assuming a placing temperature of 20 °C and a mean ambient temperature of 15 °C (assuming thermal conductance values of 18.9 and 5.2 W/m²K for steel and plywood formwork respectively with a wind speed of about 3.5 m/s. Solar gain has not been included)

Section thickness (mm)	Steel formwork				18 mm plywood formwork			
	Cement content (kg/m ³)				Cement content (kg/m ³)			
	280	320	360	400	280	320	360	400
300	8	9	10	11	4	5	5	6
500	14	15	17	19	7	8	9	10
700	18	20	22	25	10	12	13	14
1000	23	26	29	31	15	17	19	21
1500	31	35	39	41	20	22	25	27
2000	35	39	44	48	24	27	30	33

The temperature differential will be highly dependent on the following:

- ☞ the thermal diffusivity of the concrete
- ☞ the surface conditions, in particular the type of formwork and the time at which it is removed
- ☞ the environmental conditions such as wind speed and effects of solar gain.

While the values in Table 4.3 provide an indication of temperature differentials for a particular concrete under a specific set of conditions, they may not be applicable when different conditions apply. Where limiting the temperature differentials is critical to the design, thermal modelling is therefore required. Commercial software is available for this purpose and a simple spreadsheet model is described in Appendix A2.

Cracking that is caused by temperature differentials is usually localised to the surface and cracks will often close as an element cools down. More serious through-cracks arise from external restraint. Using excessive or unnecessary insulation to minimise temperature differentials will increase the mean temperature of the section and hence the risk of through cracks. Careful consideration should be given to the nature of the problem and the appropriate solution.

4.5

Coefficient of thermal expansion α_c

For a given temperature change, the free thermal expansion of the concrete is determined by the coefficient of thermal expansion α_c . A concrete with a low coefficient of thermal expansion can significantly reduce the risk of early-age thermal cracking and the percentage of reinforcement required for the control of thermally-induced cracks. The value of α_c can be estimated from a knowledge of the coefficients of thermal expansion of the aggregates using Table 4.4 (Browne, 1972) where proposed design values are given. While there is insufficient data to provide values with a defined level of statistical significance, the proposed values are at the high end of the observed range and represent safe values for use in design.

EN1992-1-1 recommends that unless more reliable information is available, the coefficient of thermal expansion should be assumed to be $10 \mu\epsilon/^\circ\text{C}$. While this is a representative value for a wide range of aggregates there are some commonly used materials in the UK, in particular flint gravels, that lead to higher values in the order of $12 \mu\epsilon/^\circ\text{C}$, as shown in Table 4.4. This 20 per cent difference in α_c may be the difference between compliant and non-compliant crack widths. The higher value should be assumed, therefore, if no data are available.

Table 4.4 Coefficients of thermal expansion (Browne, 1972)

Coarse aggregate/ rock group	Thermal expansion coefficient (microstrain/ $^\circ\text{C}$)		
	Rock	Saturated concrete	Design value
Chert or flint	7.4–13.0	11.4–12.2	12
Quartzite	7.0–13.2	11.7–14.6	14
Sandstone	4.3–12.1	9.2–13.3	12.5
Marble	2.2–16.0	4.4–7.4	7
Siliceous limestone	3.6–9.7	8.1–11.0	10.5
Granite	1.8–11.9	8.1–10.3	10
Dolerite	4.5–8.5	Average 9.2	9.5
Basalt	4.0–9.7	7.9–10.4	10
Limestone	1.8–11.7	4.3–10.3	9
Glacial gravel	-	9.0–13.7	13
Lytag (coarse and fine)	-	5.6	7
Lytag coarse and natural aggregate fines	-	8.5–9.5	9

The internal moisture content also has a significant effect on α_c and this is changing significantly during the early period of rapid hydration (Sellevold, 2006). To provide more reliable data for design, tests to measure α_c of potential materials should be considered (Section 7.2.2). At early ages, the presence of reinforcement has only a small effect on the coefficient of expansion of the concrete (Berwanger *et al*, 1976) and for practical purposes this can be ignored.

It is recognised that the peak temperature achieved during the early thermal cycle may adversely affect the strength (Appendix A9). The differential expansion between the aggregates and cement paste ($\alpha_c = 20 \mu\epsilon/^\circ\text{C}$) could contribute to these property changes. A study of *in situ* strength undertaken by the Concrete Society (2004) investigated two aggregate types, gravel and crushed limestone which would be expected to have very different coefficients of thermal expansion, and was unable to detect any significant difference with peak temperatures up to about 60 °C.

Differential expansion can also cause problems when concrete is cast against or around a material with a different coefficient of expansion. Depending on the relative coefficients of expansion, the materials can be put into tension by movement of the concrete or vice versa.

4.6 Shrinkage strains

4.6.1 Autogenous shrinkage

Autogenous shrinkage ϵ_{ca} is not a new phenomenon but it has been assumed that it will only occur in concretes with very low w/c ratios, typically below about 0.40 (Pigeon *et al*, 2004). Historically, no strain contribution from autogenous shrinkage has been included in the assessment of early-age cracking for the range of strength classes commonly used in structural concrete.

The EN1992-1-1 method for estimating autogenous shrinkage is based solely on the strength class of the concrete (Appendix A4) and assumes some degree of autogenous shrinkage occurs in all concretes with a characteristic cylinder strength greater than 10 MPa. The ultimate value (in microstrain) is given by the expression:

$$\epsilon_{ca(\infty)} = 2.5 (f_{ck} - 10) \quad (4.1)$$

A time function is provided to enable the autogenous shrinkage $\epsilon_{ca}(t)$, after time t to be calculated as follows:

$$\epsilon_{ca}(t) = \beta_{as}(t) \cdot \epsilon_{ca(\infty)} \quad (4.2)$$

where

f_{ck} is the characteristic cylinder strength
 $\beta_{as}(t)$ is a function defining the time dependent development of autogenous shrinkage and

$$\beta_{as}(t) = 1 - \exp(-0.2 \cdot t^{0.5}) \quad (4.3)$$

Using this method, autogenous shrinkage curves have been developed for different strength classes as shown in Figure 4.12.

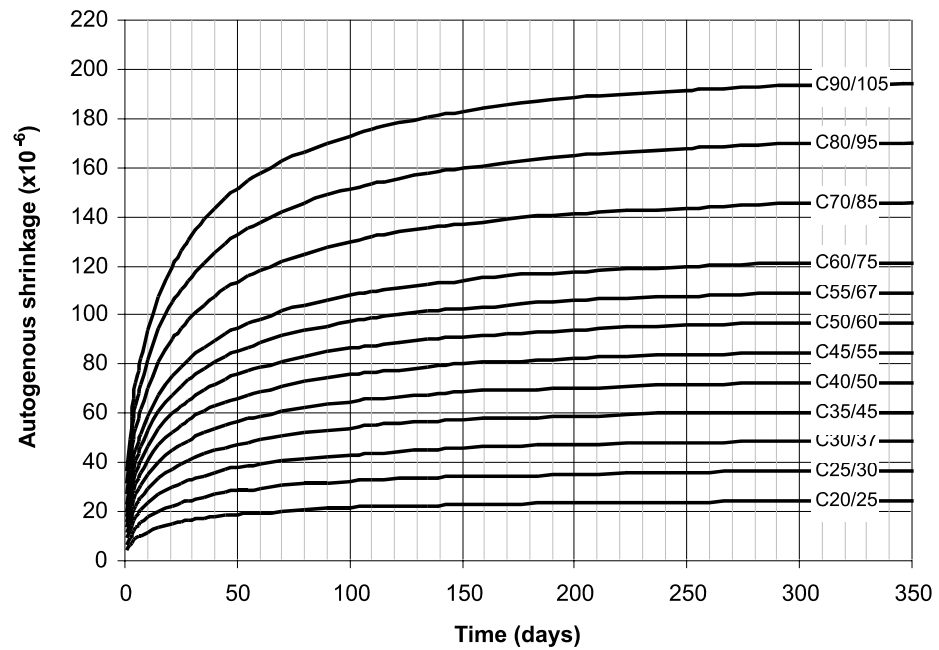


Figure 4.12 Autogenous shrinkage for different strength classes estimated using the method of EN1992-1-1

Estimated autogenous shrinkage strains at three and 28 days are given in Table 4.5 together with the ultimate values.

Table 4.5 Values of autogenous shrinkage ($\mu\epsilon$) calculated using the method of EN1992-1-1

Strength class	C20/25	C25/30	C30/37	C35/45	C40/50	C45/55	C50/60	C55/67	C60/75
3 days	7	11	15	18	22	26	29	33	37
28 days	16	24	33	41	49	57	65	73	82
Ultimate	25	38	50	63	75	88	100	113	125

This represents a significant change from R91 (CIRIA, 1992), adding early-age shrinkage strains of about $20 \mu\epsilon$ for a typical C30/37 concrete and more for higher strength classes. For design in accordance with EN1992-1-1 these strains should be included in the design process.

A review of published data (Appendix A4) has identified that the cement type has a significant effect on autogenous shrinkage but the method of EN1992-1-1 takes no account of this. While this is an area that needs further research, the limited evidence indicates that, at a constant w/b ratio, autogenous shrinkage is lower when fly ash is used, but increases with both ggbs and silica fume. However, for a given strength class the w/b will also vary, being lower for concretes containing fly ash and ggbs and higher for concrete containing silica fume which should also be accounted for when estimating the net effect for a particular strength class. There is also evidence that the magnitude of stress associated with autogenous shrinkage is not directly proportional to the shrinkage strain, due in part to the fact that the very early shrinkage (within the first 24 hours) is easily relieved by creep. Additional information is provided in Appendix A4.

4.6.2

Drying shrinkage, ε_{cd}

EN1992-1-1 provides a method for the calculation of drying shrinkage based on the ambient relative humidity (RH), the dimensions of the element and the strength class of the concrete. This is described in Appendix A3 and a spreadsheet calculator is provided on the CD.

The drying shrinkage at time t (days after casting), $\varepsilon_{cd}(t)$ is calculated using the equation:

$$\varepsilon_{cd}(t) = \beta_{ds}(t, t_s) \cdot k_h \cdot \varepsilon_{cd,0} \quad (4.4)$$

where

$\varepsilon_{cd,0}$ is the nominal unrestrained drying shrinkage with values given in Table 4.6 (values for intermediate strength classes and RH may be interpolated or derived using the equations provided in Appendix A3).

Table 4.6 Nominal unrestrained drying shrinkage values (in microstrain) with CEM I Class N

$f_{ck}/f_{ck,cube}$ (MPa)	Relative humidity (%)					
	20	40	60	80	90	100
20/25	620	580	490	300	170	0
40/50	480	460	380	240	130	0
60/75	380	360	300	190	100	0
80/95	300	280	240	150	80	0
90/105	270	250	210	130	70	0

k_h is a coefficient depending on the notional size of the cross-section, $h_o = 2 A_c/u$. Values of k_h are given in Table 4.7

A_c is the concrete cross-sectional area

u is the perimeter of that part of the cross section which is exposed to drying
For a wall drying from both faces $h_o \approx h$
For a slab drying from one face $h_o \approx 2h$.

Table 4.7 Values of k_h for use in equation 4.4

h_o	100	200	300	≥ 500
k_c	1.00	0.85	0.75	0.7

$$\beta_{ds}(t, t_s) \text{ is the time function} = (t - t_s) / \{ (t - t_s) + 0.04 \sqrt{h_o^3} \} \quad (4.5)$$

t_s is the age of the concrete (days) at the beginning of drying, normally the end of the curing period

Shrinkage curves estimated using this approach for a C30/37 concrete in walls drying from both faces are shown in Figure 4.13 for indoor conditions (RH = 45 per cent) and typical UK outdoor conditions (RH = 85 per cent). Tables 4.8 and 4.9 give ultimate values for a range of strength classes in walls 300 mm and 500 mm thick.

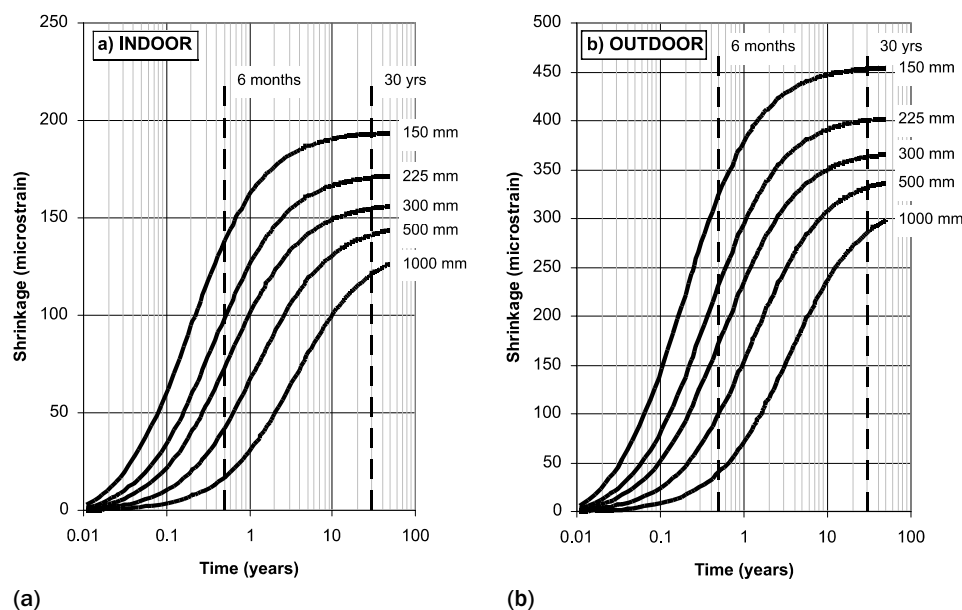


Figure 4.13 Drying shrinkage curves estimated using the method of EN1992-1-1 for a) indoor conditions (45 per cent rh) and b) UK outdoor conditions (85 per cent rh)

Table 4.8 Estimated values of drying shrinkage ($\mu\epsilon$) in 300 mm and 500 mm thick walls for UK external exposure (RH = 85 per cent)

Strength class	C20/25	C25/30	C30/37	C35/45	C40/50	C45/55	C50/60	C55/67	C60/75	C70/85	C80/95
300 mm	178	170	158	145	139	132	126	118	109	98	89
500 mm	166	158	148	136	130	124	118	110	102	92	83

Table 4.9 Estimated values of drying shrinkage ($\mu\epsilon$) in 300 mm and 500 mm thick for internal (RH = 45 per cent)

Strength class	C20/25	C25/30	C30/37	C35/45	C40/50	C45/55	C50/60	C55/67	C60/75	C70/85	C80/95
300 mm	420	400	373	344	328	312	297	277	256	231	210
500 mm	392	373	348	321	306	291	277	258	239	216	196

4.6.3

Appropriate use of shrinkage strains

When deriving shrinkage values, if the principal source of restraint is previously cast concrete, it is only the differential shrinkage strain that needs be included. In the relatively short-term, drying shrinkage, even in relatively thin sections, will be small. For example, according to the EN1992-1-1 *Method of estimation*, a 300 mm section in an environment at RH = 65 per cent will exhibit drying shrinkage of less than 10 microstrain with the first two weeks. **In general, when assessing the risk of early-age cracking, drying shrinkage may be ignored.** Autogenous shrinkage occurs much more rapidly and differential autogenous shrinkage between adjacent sections may be significant.

While providing predictive models for estimating both autogenous and drying shrinkage, EN1992-1-1 does not provide guidance on how the strains should be combined. For the purpose of this guide it is assumed that the autogenous shrinkage beyond 28 days will have been included when making long-term drying shrinkage measurements from which the drying shrinkage model was derived. This is because while autogenous shrinkage without drying shrinkage may be measured by preventing drying, autogenous shrinkage cannot be excluded when making long-term measurements of drying shrinkage. When considering long-term deformation, autogenous shrinkage is ignored beyond 28 days, except in cases where high strength, low w/c ratio concrete is used under conditions where moisture loss, and hence drying shrinkage, will be prevented.

An example is shown in Figure 4.15 for C40/50 concrete cast in a 500 mm thick wall at 65 per cent relative humidity. Autogenous shrinkage predominates up to 28 days and beyond this time the drying shrinkage is assumed to include the component of autogenous shrinkage. Hence the total shrinkage beyond 28 days is the 28 day autogenous shrinkage plus the change in drying shrinkage from 28 days onwards.

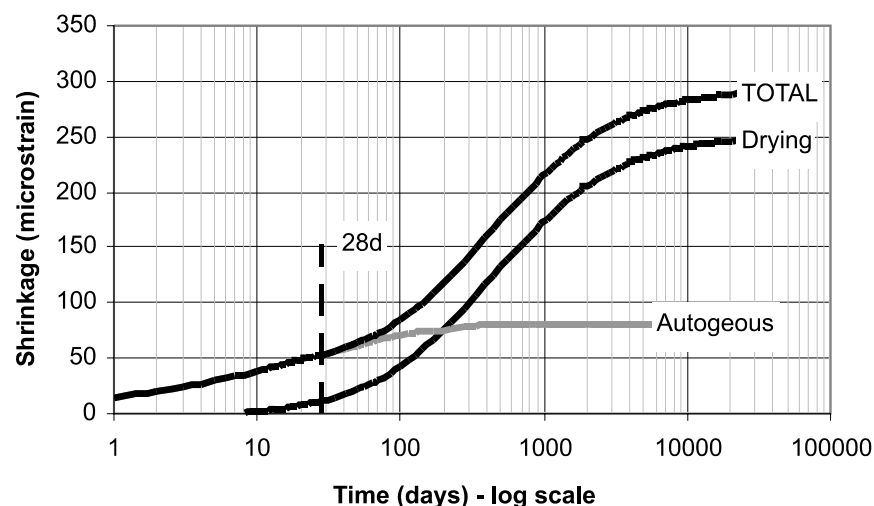


Figure 4.14 Total shrinkage of C40/50 concrete in a 500 mm thick wall at 65 per cent relative humidity

4.7

Restraint, *R*

4.7.1

General guidance

Various industry documents provide guidance on restraint with a review of values for different restraint conditions being given in Table 4.10. However, care should be taken when interpreting of the values as the way in which they are applied also vary. For example, while BS8110:Part 2 and HA BD 28/87 provide restraint factors that reflect the true restraint, BS 8007 and EN1992-3 both include, within the restraint factor, a modification factor of 0.5 to take account of creep under sustained loading.

Table 4.10 External restraint values, *R*, for different conditions

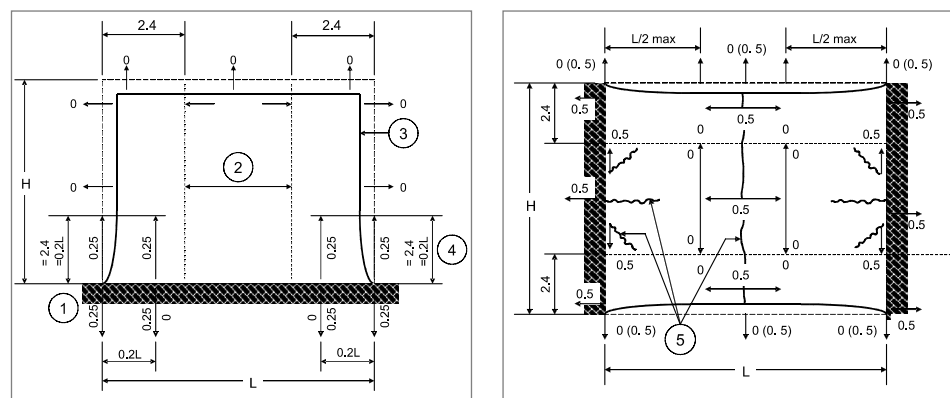
Restraint condition		BS 8110 Part 2	HA BD 28/87	CIRIA 91 1992 [1]	BS 8007 [2]	EN 1992-3 [2]
A	Base of a wall cast on to a massive base	0.6 to 0.8	0.6	1.0	0.5	0.5
B	Top of a wall cast on to a massive base	0.1 to 0.2		0 to 1.0	0 to 0.5	0 to 0.5
C	Edge restraint in box type deck cast in stages		0.5			
D	Edge element cast onto a slab		0.8			
E	Massive pour cast onto blinding	0.1 to 0.2	0.2			
F	Base of massive pour cast onto existing mass concrete	0.3 to 0.4				
G	Suspended slabs	0.2 to 0.4				
H	Infill bays, eg rigid restraint	0.8 to 1.0	1.0	1.0	0.5	0.5

Notes

- 1 CIRIA Report 91 recommends that a modification factor of 0.5 is applied to take account of simplifying assumptions and notes that this factor is applied in BS 8007 by modifying the restraint factor from 1 to 0.5.
- 2 These values represent effective restraint which takes into account sustained loading and creep using a factor of 0.5.

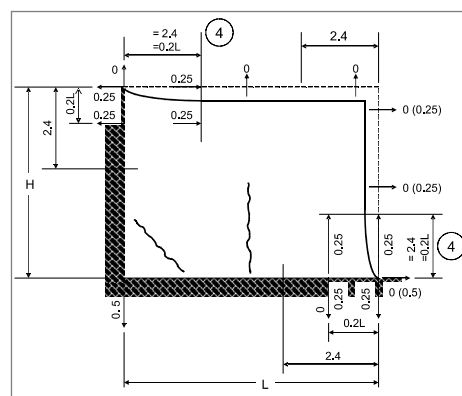
The values recommended by BS8110 and HA BD 28/87 were derived from measurements on concrete structures and where no more detailed analysis of restraint is to be undertaken these may be used in the full design method.

Guidance on restraint under various conditions is also provided in EN1992-3 (Figure 4.15). EN1992-3 has adopted broadly the same approach as BS8007 with regard to restraint and has included the modification factor for creep. Where these values are adopted the K_1 factor for creep should be assumed to be 1.

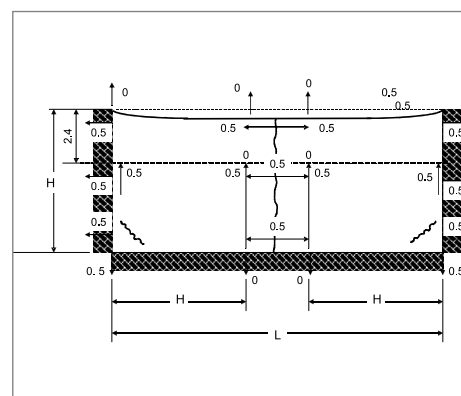


(a) Wall on a base

(b) Horizontal restraint between rigid restraints



(c) Sequential bay wall construction (with construction joints)



(d) Alternate bay wall construction (with construction joints)

Key	
1	Vertical restraint factors
2	Horizontal restraint factor
3	Expansion or free contraction joints
4	Whichever value is greater
5	Potential primary cracks

Restraint factors for central zone of walls		
Ratio L/H	Restraint factor at base	Restraint factor at top
1	0.5	0
2	0.5	0
3	0.5	0.05
4	0.5	0.5
>8	0.5	0.5

Figure 4.15 Recommended values of restraint given in EN 1992-3

Restraint to movements occur both externally and internally. External restraint can be complex, arising from continuous edge restraint, end restraint and intermittent restraint. Internal restraint arises when one part of the freshly placed section expands or contracts differently to another part of the same section. In very thick sections, internal restraint tends to dominate, while in thinner sections external restraint is dominant. In a few situations both types of restraint need to be considered.

When the element geometry is simple an estimate of restraint can be made using relatively simple methods. However, where the geometry is complex and various forms of restraint exist, eg a slab subject to both edge restraint and local restraint from core walls, determining restraint levels is more difficult and reliant on simplifying assumptions. Local features such as box-outs are also influential in crack generation.

4.7.2

External edge restraint

The most commonly recognised form of restraint is edge restraint, an example of which is shown in Figure 4.16. and is represented by conditions A and B in Table 4.10. This form of restraint is specifically addressed in EN1992-3. A method for estimating edge restraint was developed by ACI (ACI, 1990) and is described in Appendix A5. This method first estimates restraint at the joint, R_j , based on the relative geometry and stiffness of the new and old concrete according to the equation:

$$\text{Restraint at the joint, } R_j = \frac{I}{I + \frac{A_n E_n}{A_o E_o}} \quad (4.6)$$

where

A_n cross-sectional area (c.s.a) of the new (restrained) pour

A_o c.s.a. of the old (restraining) concrete

E_n modulus of elasticity of the new pour concrete

E_o modulus of elasticity of the old concrete

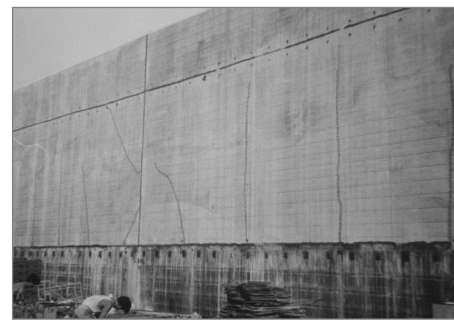
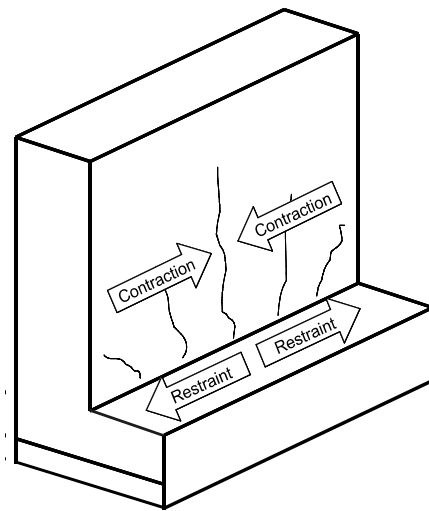


Figure 4.16

Early thermal cracking in the walls of a box-section tunnel wall

R_j is then adjusted to take account of the reduction in restraint with distance from the joint using a chart relating restraint to the length/height ratio of the pour and the height as shown in Figure 4.17. The original ACI curves have been revised based on more recent research by Emborg (2003). Comparisons of predicted and measured values of restraint are given in Appendix A5 and a spreadsheet calculator for external edge restraint is provided on the CD.

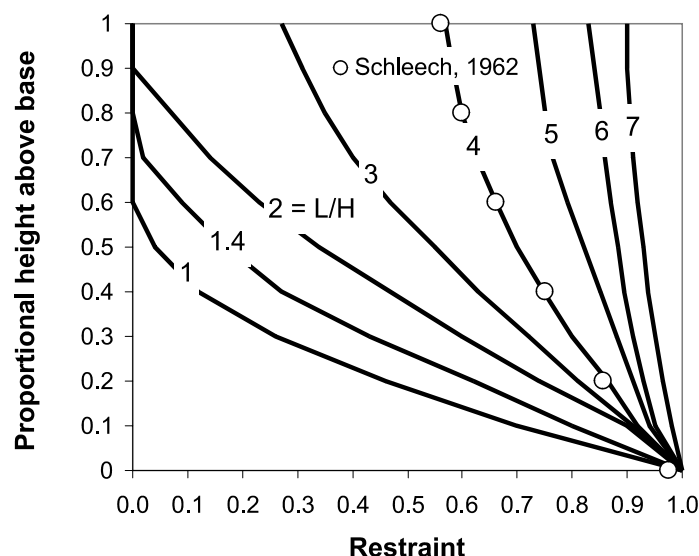


Figure 4.17 The relationship between restraint and distance from the joint (Emborg, 2003) including data for a wall with $L/H = 4$ (Schleech, 1962)

The relative areas of influence A_o and A_n may be difficult to define. For example, when a wall is cast onto a slab, what width of slab should be considered as providing effective restraint? In such circumstances it is recommended that the relative area is assumed to be in proportion to the relative thicknesses, h_n and h_o , of the wall and slab. The following simple rules may be applied:

- for a wall cast at the edge of a slab assume $A_n/A_o = h_n/h_o$
- for a wall cast remote from the edge of a slab assume $A_n/A_o = h_n/2h_o$
- for a slab cast against an existing slab assume $A_n/A_o = h_n/h_o$

CIRIA R135 (Bamforth and Price, 1997) recommends that when using the ACI approach to estimate restraint the ratio E_n/E_o is assumed to be in the range 0.7 to 0.8. The lower value should be used for conditions in which cool down is most rapid.

4.7.3

End and local restraint

It is important to recognise conditions of end restraint as the way in which cracking develops, and the resulting crack widths differ significantly from the condition of edge restraint (Beeby, 1990). This is acknowledged in EN1992-3 which provides different methods for calculating the design crack width. The essential difference is that when cracking occurs as a result of end restraint, the crack width is related specifically to the strength of the concrete and the steel ratio and each crack occurs to its full potential width before successive cracks occur. Under these conditions the restrained strain is only significant in relation to whether or not cracking occurs and how many cracks occur. It does not influence the crack width (Appendix A8 gives more detail of the mechanisms of cracking).

In general, when cracking occurs as a result of end restraint, cracks will be larger than those that occur due to edge restraint.

End restraint typically occurs in the following situations:

- ↖ suspended slab cast between rigid walls or columns

- ☞ ground slab cast on piles
- ☞ the top of an infill wall with a length/height ratio that is sufficiently low so that the base restraint is not effective at the top
- ☞ large area ground slabs cast onto membranes to achieve a low coefficient of friction, restrained locally, eg by columns, or by a build up of friction when the area is very large.

4.7.4 Internal restraint

Internal restraint is a result of differential temperature changes within an element. It may lead to both surface cracking and internal cracking that may not be observed from the surface. The development of cracking due to internal restraint is shown in Figure 4.18. As heating occurs, the surface is subject to tensile stresses as the centre of the pour gets hotter and expands to a greater extent. At elevated temperature and early-age, creep is high and the stresses generated are relieved, at least in part. As cooling occurs there is a stress reversal and the surface cracks generally reduce in width. At the same time tension is generated at the centre of the pour as it cools more than the surface and internal cracking may occur.

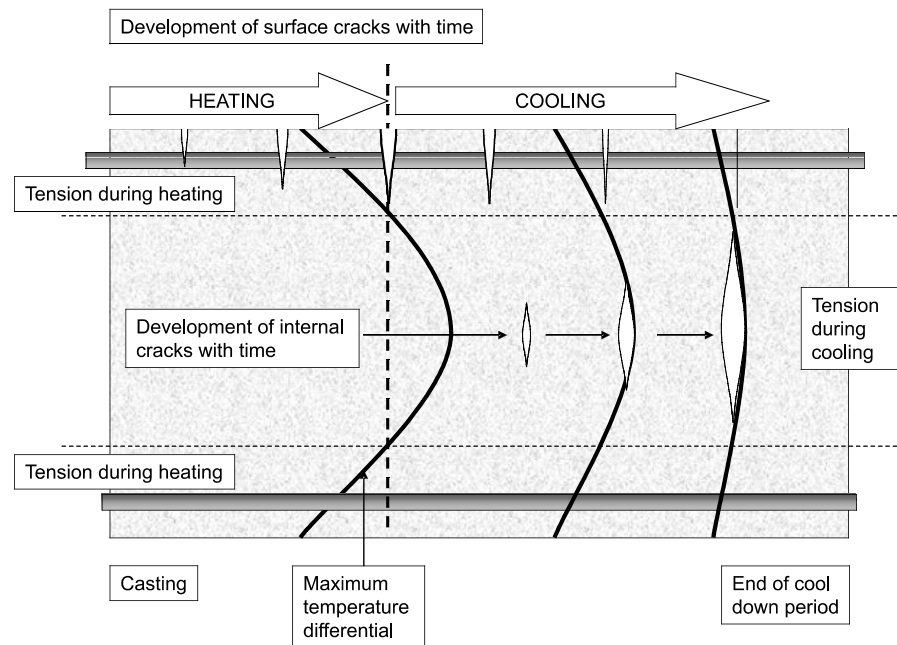


Figure 4.18 Schematic representation of the development of crack in a massive element due to temperature differentials assuming no external restraint (such cracking may occur in both the vertical and horizontal orientation)

Where property data are available for a particular mix, the limiting temperature differential, ΔT_{max} , ie the differential at which cracking may occur, can be calculated using the Equation 3.8 in which with the restraint factor $R = 0.42$ and assuming $K_1 = 0.65$ (for creep) and $K_2 = 0.8$ (for strength reduction due to sustained loading). In a previous investigation the value of R was determined to be 0.36 (Bamforth, 1982). This value was derived to match the recommended limiting temperature values with those observed in practice and based on property data available at the time. The adjustment in R has been made to maintain these limits with the application of property data from EN1992-1-1.

Guidelines on limiting temperature differentials are presented in Section 7, Table 7.1. It can be seen that the aggregate selection can have a significant impact.

4.7.5

Combined internal and external restraint

For internal restraint to cause cracking, differential movement must occur. During heating, as the core of a thick section heats up and expands more than the surface, tensile stresses can only be generated in the surface zone if the centre is free to expand. If the section is restrained externally and the full expansion of the core is prevented, then the magnitude of tensile strain developed at the surface will also be reduced and may be eliminated entirely hence the risk of surface cracking due to internal restraint will be reduced when external restraint exists.

At the centre of the section, however, the internal and external restraint will be additive, the core of the section now being restrained by both the surface zone and the external restraint. Hence the risk of internal cracking during cool-down will be increased, although such cracks may not propagate to the surface.

In situations in which external restraint is effective in preventing deformation it may be appropriate to allow a relaxation of limiting temperature differentials given in Table 7.1 in proportion to the level of external restraint. However, care should be taken to ensure that the restraint exists in all directions before such a relaxation is permitted.

4.8

Tensile strain capacity, ε_{ctu}

The tensile strain capacity ε_{ctu} is the maximum strain that the concrete can withstand without a continuous crack forming. The tensile strain capacity may be measured directly or derived from measurements of the tensile strength and the elastic modulus of the concrete (see Appendix A6). In a comprehensive review of data Tasdemir *et al*, (1996) developed a simple linear relationship between the ε_{ctu} and the ratio of the tensile strength f_{ctm} to the elastic modulus E_{cm} as follows:

$$\varepsilon_{ctu} = 1.01(f_{ctm}/E_{cm}) \times 10^{-6} + 8.4 \text{ microstrain} \quad (4.7)$$

Simplifying this equation to $\varepsilon_{ctu} = f_{ctm}/E_{cm}$ has been shown to represent lower bound values (based on the data presented) and may therefore be used to provide a basis for design. Using this relationship, values of ε_{ctu} at 28 days have been derived from estimates given in EN1992-1-1 for tensile strength and elastic modulus for each strength class. EN1992-1-1 also provides age functions and limited guidance on the effect of aggregate type and these have been used to generate the three-day and 28 days values of ε_{ctu} given in Figure 4.19.

The values apply under conditions of short-term loading. During the early-age thermal cycle the stresses are sustained. This has two effects on ε_{ctu} . Firstly, as creep occurs, the strain capacity increases by a factor of $1/K_1$. But under sustained loading the failure stress is reduced. The coefficient for sustained loading $K_2 = 0.8$ (Section 4.9.2). The net effect is to increase ε_{ctu} by a factor of $K_2/K_1 = 1.23$ (Appendix A6). The values derived using EN1992-1-1 have therefore been increased by 23 per cent to account for the effects of sustained loading and the resulting values for strength class C30/37 are given in Table 4.7.

The values presented for concretes using aggregate types that are not covered specifically by EN1992-1-1 have been interpolated on the basis of the elastic modulus of the aggregate, as described in Appendix A6.

When there is no knowledge of the aggregate the values for concrete using quartzite aggregate should be used as these are the base values for EN1992-1-1.

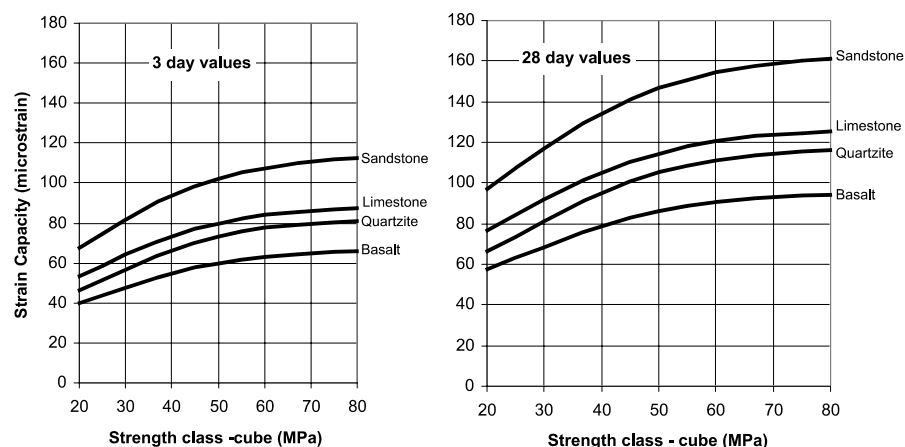


Figure 4.19 Values of tensile strain capacity at three and 28 days derived using concrete property estimates from EN1992-1-1

To estimate the strain capacity for other strength classes, the value obtained for class C30/37 should be multiplied by $0.63 + (f_{ck,cube}/100)$ for $f_{ck,cube}$ in the range from 20 to 60 MPa. For high strength concrete the value obtained for C50/60 should be used.

Table 4.11 Estimated values of ϵ_{ctu} for strength class C30/37 under sustained short term loading using different aggregate types

Aggregate type	Estimated ϵ_{ctu} under sustained loading for strength class C30/37	
	Early-age 3 days	Long-term 28 days
Basalt	63	90
Flint gravel	65	93
Quartzite	76	108
Granite, gabbro,	75	108
Limestone, dolomite	85	122
Sandstone	108	155
Lightweight aggregate (sintered fly ash) with natural sand	115	165

4.9

Coefficients and inherent safety factors

The time dependent nature of the processes leading to early thermal cracking requires that two effects are taken into account, the relaxation of stress due to creep and the reduction in the tensile strength under a sustained load. These effects are partially self cancelling when assessing the risk of cracking, with creep being beneficial in reducing stresses through relaxation but the influence of sustained loading being to reduce the level of tensile strength at which failure occurs.

4.9.1

Coefficient for creep, K_1

Creep has the effect of reducing the modulus to a lower “effective” value. Over the period of an early thermal cycle values of creep factor has been found to reduce stresses by up to 50 per cent (Altoubat and Lange, 2001) while a 35 per cent reduction may be more typical (Bamforth, 1982, Vitherana *et al*, 1995).

The creep coefficient K_1 used to modify the restrained strain is applied as a reduction factor, hence for a 35 per cent reduction in stress $K_1 = 0.65$. This applies to both the early-age and long-term stresses. At early-age the timescale is short but the concrete is immature and at elevated temperature, which accelerates creep. In the longer term, the rate of strain and stress development is much slower but occurs over a longer period of time.

It should be noted that the single coefficient of $K = 0.5$ used in the Simplified Method for estimating crack inducing strain (Equation 3.17) is used to take into account the effects of creep and the fact that the restraint factor is generally less than 1. Hence $K = K_1 R$. For the condition of continuous edge restraint to which the equation is applied R is in the range from 0.4 to 0.7, hence K would be expected to be in the range from 0.26 to 0.45. In most cases K will include a significant factor of safety.

4.9.2

Coefficient for sustained loading, K_2

Concrete that is maintained under a sustained tensile stress will fail at a load that is significantly lower than the load that may be sustained in a rapid load test. Under testing at constant load it has been demonstrated that when the stress exceeds about 80 per cent of the short-term tensile strength, failure may occur (Domone, 1974, Reinhardt & Rinder, 1998 van Breugel and Lokhorst, 2001) and some risk of failure is demonstrable at lower stress/strength ratios. Altoubat and Lange (2001) achieved failure in normal concretes at stress/strength ratios between 0.75 and 0.81 and Reinhardt & Rinder (1998) have reported data that show failure at a stress/strength ratio of as low as 0.6.

At early-age a value of $K_2 = 0.8$ is recommended.

4.9.3

Inherent safety factors

Due to the complexity of behaviour during the early life of concrete, and the theories describing early-age thermal cracking, a number of simplifying assumptions are made as follows:

- 1 The temperature change T_1 , is based on the mid-section temperature and not the peak temperature in the vicinity of the reinforcement. In relation to the risk of through cracking resulting from external restraint to contraction, it would be more appropriate to use the mean temperature through the section as this will determine the bulk contraction. Assuming that the temperature across a section is about parabolic, with a peak temperature T_1 and a surface temperature T_s the mean temperature T_m may be estimated using the equation:

$$T_m = T_1 - \frac{(T_1 - T_s)}{3} \quad (4.8)$$

Depending on the formwork/insulation applied the value of $T_1 - T_s$ will vary and may be difficult to predict (see, for example Figure 4.3). However, specifications may include limiting temperature differentials (commonly in the order of 20–30 °C with permissible values dependent on aggregate type as shown in Table 7,1), so the value

of T_m may be 7–10 °C below T_I . For a T_I value of, for example, 40 °C the bulk thermal contraction of the section may be over-estimated by as much as 20 per cent. Where plywood formwork is used this temperature differential may be much less than 20 °C (Table 4.3) and this effect will be less significant.

- 2 The previously cast element is assumed to remain at the mean ambient temperature. Some heat transfer will occur at the joint between the new and old concrete, causing the old concrete to expand and contract to a small extent and effectively reduce the restraint at the joint. This is taken into account by using the more rigorous method for estimating restraint, described in Section 4.7.2.
- 3 Tensile stresses can develop immediately when the concrete starts to cool (this is again conservative assumption). There is considerable evidence from stress rig measurements under laboratory conditions that compressive stresses (sometimes in excess of 1 MPa) may be generated and should be relieved before tensile stresses develop (Blundell and Bamforth, 1975, Kanstad *et al*, 2001, van Breugel and Lokhorst, 2001, van Beek *et al*, 2001, Pane and Hansen, 2002). A review of these data indicates that the temperature drop required to relieve the compressive stresses may vary between 10 and 30 per cent of the temperature drop T_I and is typically in the range of 2–6 °C.

Where these simplifications deviate significantly this leads to an overestimate of the magnitude of restrained thermal contraction, the risk of cracking, and the amount of reinforcement needed to control cracks that do occur. Combining the effects from 1 and 3 above, and taking into account the different temperature differentials achieved using plywood and steel formwork, **it is estimated that a margin of between 15–25 per cent is built into the estimate of restrained strain when using the full approach.**

4.10

Tensile strength of concrete, f_{ct}

With regard to the design of reinforcement, the time at which cracking occurs is important as it will influence the tensile strength of the concrete and the value of $A_{s,min}$. In outdoor conditions in the UK, early-age thermal movement is normally the dominant movement (Hughes, 1971); early-age concrete properties are the appropriate ones to select. Under indoor conditions, however, long-term shrinkage may be significant and in such cases the long-term values of the concrete properties should be used. Also, in hotter drier climates shrinkage is often the dominant movement (Base and Murray, 1978).

Observations have shown that early-age cracking is most likely to occur within three to six days (Alexander, 2006). An analysis of elements up to 1 m thick indicates that the time for the temperature to drop sufficiently to cause cracking under restrained conditions (15 °C in some concretes with 50 per cent restraint (Bamforth and Price, 1995) will be between one and four days, and in most sections less than 1 m thick, sufficient cooling will have occurred within three days (Appendix A10). The three-day value is proposed for early-age design purposes. For long-term cracking the 28-day value of mean tensile strength should be used. This has been shown to be a conservatively high value compared with the *in situ* strength, and takes account of any continued strength development beyond 28 days (Appendix A10).

EN1992-1-1 provides an expression relating to the 28-day mean tensile strength, f_{ctm} , to the compressive strength at 28 days and an age function which enables the estimation of the mean tensile strength $f_{ctm}(t)$ at time t in relation to the 28-day value (Appendix A10 on the CD). For the estimation of $A_{s,min}$, EN1992-1-1 recommends the use of the mean value of the tensile strength effective at the time that cracking is expected to occur, $f_{ct,eff}$.

$f_{c,eff} = f_{ctm}$ or lower, $f_{ctm}(t)$ if cracking is expected earlier than 28 days.

Values estimated using this approach have been given in Table 3.3 for CEM I. EN1992-1-1 notes that “*The development of tensile strength with time is strongly influenced by curing and drying conditions as well as the dimensions of the structural members*” and that where the development of tensile strength is important testing should be carried out. An assessment of the *in situ* tensile strength has been carried out using the method of EN1992-1-1 with modification factors to take account of the following:

- ⊗ a coefficient of variation of about 18 per cent in test specimens at 20 °C, in accordance with EN1992-1-1 (based on the 95 per cent fractile being 1.3 times the mean value)
- ⊗ *in situ* effects, including the peak temperature achieved during the early thermal cycle
- ⊗ a factor for sustained loading
- ⊗ a factor to account for the uncertainty of the time at which cracking occurs.

A probabilistic approach has been used which has indicated that the values estimated using the method of EN1992-1-1 represent values with less than a 1 per cent chance of being exceeded *in situ* (Appendix A10).

4.11 Estimating the minimum area of reinforcement $A_{s,min}$

4.11.1 Changes in surface zone

To ensure that cracking occurs in a controlled manner, the minimum area of steel, $A_{s,min}$ should be exceeded. In order to calculate $A_{s,min}$ a surface zone of influence is defined.

BS8007 specifies the surface zone of influence of the reinforcement. For walls <500mm thick, the gross section was used and for thicker sections a 250 mm surface zone was assumed. For ground slabs the same applied to the top face but the bottom face steel was reduced to 100 mm except in slabs <300 mm thick, where it was omitted. These surface zones were used in the calculation of both $A_{s,min}$ (formerly defined as ρ_{crit}) and the crack spacing and width.

EN1992-1-1 and EN1992-3 differ significantly from BS8007.

- ⊗ for the calculation of $A_{s,min}$, EN1992-1-1 defines the “surface zone” through the coefficients k_c and k and the area of concrete in tension, A_{ct} (Section 3.1). The surface zone depends on the form of restraint as discussed in Sections 4.11.2 and 4.11.3 for conditions of external and internal restraint respectively
- ⊗ for calculating crack spacing EN1992-1-1 defines the effective area of concrete in tension $A_{c,eff}$ around the reinforcement to a depth of $h_{c,ef}$, where $h_{c,ef}$ is $2.5(c+\phi/2)$ (Section 3.4). This applies regardless of the condition of restraint.

It is not clear how the mechanics of the system justifies the different values of steel ratio derived. However, it is assumed that in calibrating the crack spacing and crack width equations, these values have been used.

4.11.2

External restraint

The impact of the approach of EN1992-1-1 for calculating $A_{s,min}$ is most significant for sections thicker than 800 mm where a much larger “surface zone” is used. Figure 4.20 illustrates the effect of a surface zone as an “area reduction factor” to enable comparison with the surface zones used by BS8007. In sections up to 800 mm thick there is little difference but the EN1992-1-1 surface zone or “area of concrete in tension”, is significantly higher for thicker sections.

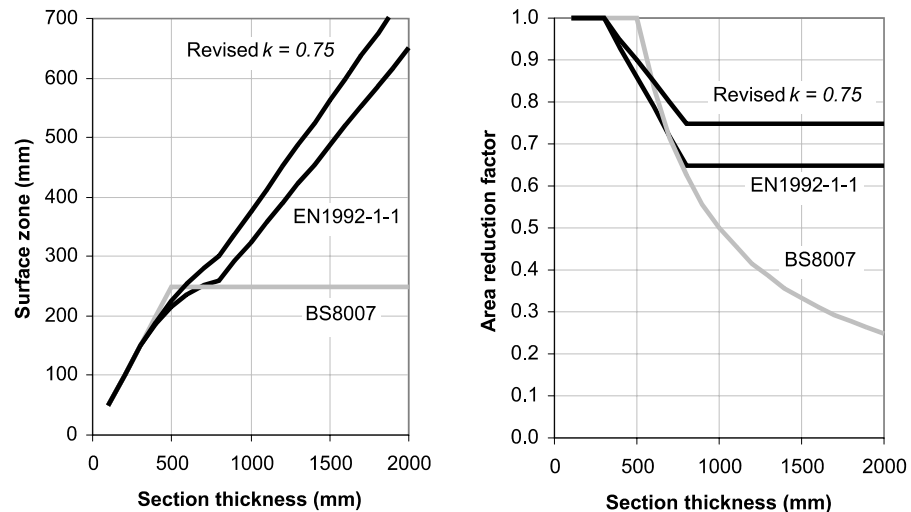


Figure 4.20 Surface zones of influence of reinforcement used to estimate the minimum reinforcement area, also presented as the area reduction factor, k

The difference is such that in a 1000 mm section, and all other factors being equal, the minimum amount of steel required by EN1992-1-1 is about 25 per cent more than that required by BS8007. In thicker sections the difference is even greater. This suggests that the use of guidelines in BS8007 may have led to insufficient reinforcement in thicker sections. This assumption is consistent with the authors experience in which crack widths in thick sections (500–1000 mm) have been in excess of those predicted using the 250 mm surface zone, even though the concrete has performed predictably in terms of temperature rise and thermal strain.

A review of the development of the approaches in both BS8007 and EN1992-1-1 has led to the conclusion that the underlying assumption used in developing the surface zones, namely that cracking is propagated from the surface, do not apply to thick sections subject to external restraint. Under these conditions cracking is more likely to propagate from the centre where the temperature rise and fall is greatest, as illustrated in Figure 4.21. However it may still be appropriate to use an “area reduction factor” to replace the values recommended by BS 8007 or EN1992-1-1 but one which more accurately reflects the nature of cracking under these conditions.

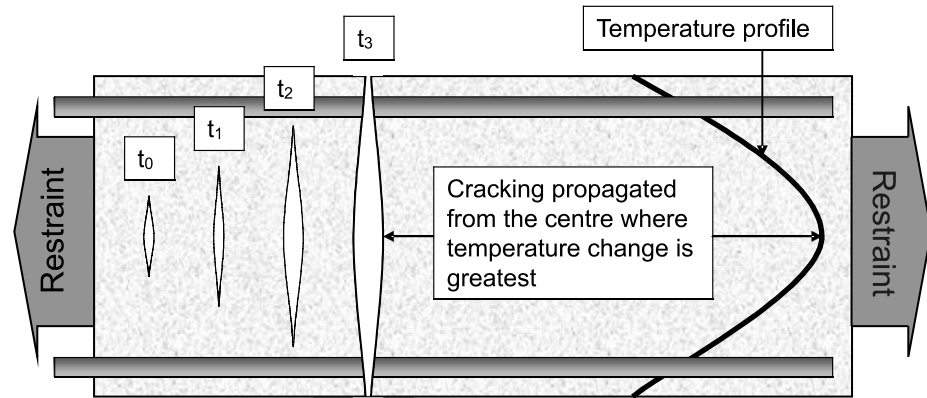


Figure 4.21 Development of cracking in an externally restrained, thick section during cooling

This is examined in more detail in Appendix A8 and a design value for k of 0.75 has been derived for sections thicker than 800 mm. This should replace the value of 0.65 given by EN1992-1-1 and be applied in the same way. Two factors were taken into account in deriving this revised value:

- ☞ the temperature varies through the section with the peak temperature T_I , used in the design, occurring only at the centre
- ☞ it is assumed that tensile stresses are developed as soon as cooling begins when, in fact, there is residual compression that needs to be relieved.

The effect of using the revised value of k for sections thicker than 800 mm is shown in Figure 4.20.

4.11.3

Internal restraint is dominant

When internal temperature differentials become the dominant form of restraint the stress distribution may be considered to be the same shape as the temperature profile through the section. Measurements (Bamforth, 1976) have shown that the temperature profile approximates to a parabola as shown in Figure 4.22.

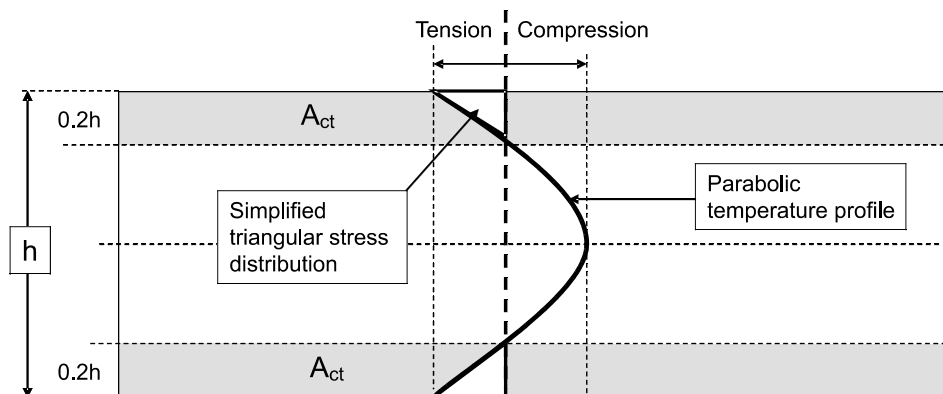


Figure 4.22 Simplified stress distribution used to determine the coefficient, k_c , for a member subjected to a temperature profile

In this stress condition, equilibrium requires that after cracking the tensile force in the concrete is carried by the reinforcement. The stress distribution in the tensile zone at the surface is approximately triangular and the coefficient k_c (which takes account of the stress distribution) may be taken as 0.5.

It would be sensible to adopt a conservative value of $k = 1$ as, in this case, the coefficient k_c has already taken account of the self-equilibrating stresses.

With the assumed parabolic distribution shown in Figure 4.22, the tensile zone at the surface may be about 20 per cent of the thickness ($= 0.2h$). On this basis, the surface zones are shown in Figure 4.23 for comparison with the previous requirements of BS8007. The surface zone (and the estimated value of $A_{s,min}$) is significantly lower when estimated using EN1992-1-1 for section thicknesses up to about 1250 mm. For thicker sections, EN1992-1-1 leads to higher values surface zone and $A_{s,min}$.

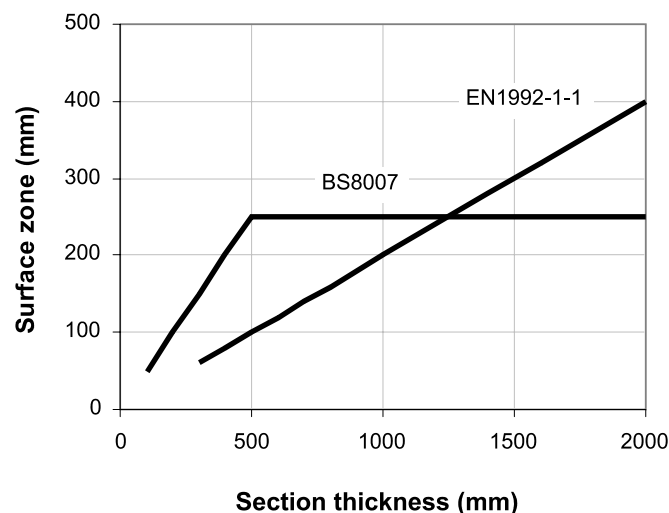


Figure 4.23 Surface zones used in estimating $A_{s,min}$ in sections that are dominated by internal restraint

4.12

The steel ratio used in calculating crack spacing, $\rho_{e,eff}$

The crack spacing predicted using EN1992-1-1 is generally in the order of 20–40 per cent lower than predicted using BS8007. This is due to the difference in the surface zones used in the calculation of the steel ratio. EN1992-1-1 derives $\rho_{p,eff}$ using the effective area of concrete in tension surrounding the reinforcement $A_{c,eff}$ based on the surface zone to a depth of $h_{e,ef} = 2.5(c + \phi/2)$, while the surface zone used by BS8007 is $h/2$ or 250 mm whichever is smaller. Consider a 500 mm thick wall. With a typical cover depth of 40 mm and using 20 mm diameter bars, $h_{e,ef} = 125$ mm, only half the value of 250 mm used by BS8007. As the value of $\rho_{p,eff}$ is inversely proportional to $h_{e,ef}$ the use of a lower value by EN1992-1-1 will result in the steel ratio $\rho_{p,eff}$ being double the value used by BS8007, thus halving the value of the second term in Equation 3.13. While this is partially offset by the first term which is related to cover, the effect is for values of early-age crack spacing estimated using EN1992-1-1 to be 20–40 per cent lower than values estimated using BS8007 and hence for the estimated crack width (see Section 3.5.2) to be lower also. With no other changes this would lead to a significant reduction in crack control reinforcement compared with that currently used.

Observations of early-age cracking suggest that the requirements of BS8007, while having been generally applicable, have occasionally led to crack spacing and crack widths in excess of those predicted and on this basis it would be unsafe to adopt a design that significantly reduces the current reinforcement requirements. Other factors have therefore been investigated to determine which factors may be most influential, in particular k_I (Section 4.13).

4.13

The ratio of tensile strength to bond strength f_{ct}/f_b

The steel ratio required to achieve a design crack width is directly proportional to the ratio of the tensile strength of the concrete to the steel concrete bond strength f_{ct}/f_b . In a study of the effect of reinforcement on cracking in high strength concrete (Sule, 2003) a range of strength classes were investigated at various ages. The results shown in Figure 4.24 have been derived for a bond slip of 0.05 mm. This would be consistent with the slip required to cause a 0.1 mm crack, assuming 0.05 mm deformation of the concrete on either side of the crack.

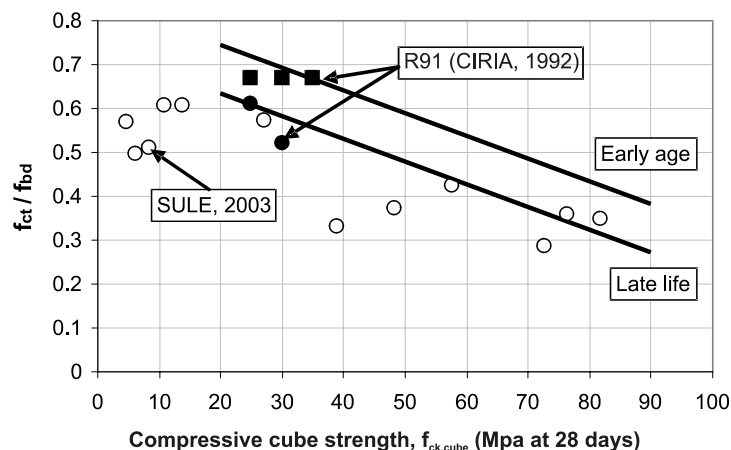


Figure 4.24 The ratio f_{ct}/f_b in relation to cube strength and age

EN1992-1-1 adopts a single value of $k_1 = 0.8$ for high bond bars. However, in reviewing the designers guide to EN1992-1-1 (Naryanan and Beeby, 2005) to understand the development of the expression in EN1992-1-1 for calculating the design crack spacing (Equation 3.13) it has become apparent that the factor k_1 not only accounts for the relationship between tensile strength and bond, but also the difference between the minimum and the mean crack spacing (Appendix A8) this being a factor of 1.33 (Beeby, 1990). On this basis it may be inferred that the ratio f_{ct}/f_b is $0.8/1.33 = 0.6$. This is lower than the value of 0.67 used in BS8007 but based on recent research data (Sule, 2003) shown in Figure 4.24, this value may be applied safely to all strength classes.

The results in Figure 4.24 indicates that f_{ct}/f_b reduces with an increase in strength while EN1992-1-1 assumes the same value for k_1 regardless of strength class and will provide an additional margin for safety in higher strength concretes.

This is an area where additional research is required. With confirmation of the results in Figure 4.24, the ratio of f_{ct}/f_b (and hence $k_1 = 1.33 f_{ct}/f_b$) may be reduced according to the following expressions:

$$k_1 = 0.8 - 0.0054 f_{ck,cube} \quad (4.9)$$

The above values all assume good bond around the full perimeter of the bar and data supporting these factors have been derived from laboratory specimens in which this may be achieved. However, in practice full bond is sometimes difficult to achieve. For example, a common occurrence is for bleed water to be trapped below the reinforcement reducing the effective bond over the lower part of the bar. If good bond cannot be guaranteed, EN1992-1-1 proposes a reduction factor of 0.7.

With regard to the appropriate value of k_1 for use in design to control early-age thermal cracking, observations indicate that the proposed value of 0.8, when used in combination with the effective increase in steel ratio (Section 4.12), may lead to insufficient reinforcement to achieve target crack widths. It is therefore proposed that k_1 should be increased to $0.8/0.7 = 1.14$ until sufficient experience has been gained with the application of the approach of EN1992-1-1 to early-age thermal cracking to enable this value to be reduced.

5

Application of the design process using worked examples

There are three particular conditions that are dealt with through the design process:

- ⌘ a member subject to continuous (external) edge restraint
- ⌘ a member subject to (external) end restraint
- ⌘ a member subject to (internal) restraint due to temperature differentials within the member.

A worked example is provided for each of these conditions which follows the design process described in Chapter 3 and is illustrated in Figure 3.2. The full method is used, with default values being applied when specific data are unavailable.

The process begins with a clear definition of the total allowable crack width and the amount that will be acceptable as a result of early-age effects and long-term effects. The likelihood and extent of cracking is then assessed both at early-age and at late life and the reinforcement is checked or selected to ensure that there is sufficient steel to control cracking and to achieve acceptable crack widths.

As discussed in Section 2.2, while long-term temperature changes and shrinkage may result in an increase in crack width, **it is not common practice to add early-age crack widths to those arising from structural loading, with no apparent detriment to structural performance.**

5.1

Example 1: Retaining wall on a rigid foundation (continuous edge restraint)

The retaining wall is 4 m high × 0.5m thick cast onto a rigid foundation 0.8 m deep and 2.85 m wide. The wall is cast in 12 m lengths. The specified strength class is C30/37. A binder containing 30 per cent fly ash (CEM IIB) is specified. The pressure gradient across the lower part of the wall is 4/0.5 = 8 the permissible crack width is 0.18 mm (Figure 2.2). The cover is 40 mm. The construction programme is unknown and summer concreting is assumed. Also no limits are placed on pour sequence, type of formwork or insulation/cooling measures.

Parameter	Value	Equations and assumptions		Source
Early-age				
Temperature drop T_1	27 °C	Binder content = 365 kg/m ³ for C30/37 and 30% fly ash		Table 4.2
		500 mm section cast using 18 mm plywood formwork (worst case)		Figure 4.7
Coefficient of thermal expansion α_c	12 $\mu\epsilon/^\circ\text{C}$	No information on aggregate. Default value used		Section 4.5
Autogenous shrinkage	15 $\mu\epsilon$	3-day value for C30/37		Section 4.6.1
Restraint at the joint	0.62	$R_j = \frac{I}{I + \frac{A_n E_n}{A_o E_o}}$	$A_o = 2.85 \times 0.8 = 2.26^2$ $A_n = 0.5 \times 4 = 2 \text{ m}^2$ $E_n/E_o = 0.7$	Section 4.7.2 Equation 4.6
Restraint at the top	0.18	$L/H = 3$ hence R at top of wall is 0.3 R_j		Figure 4.17
Creep coefficient, K_1	0.65			Section 4.9.1
Early-age restrained strain, ϵ_r	136 $\mu\epsilon$	$\epsilon_r = K_1[\alpha_c T_1 + \epsilon_{ca}]R$ $= 0.65[(12 \times 27 + 15)]0.62$		Section 3.2.1
Tensile strain capacity, ϵ_{ctu}	76 $\mu\epsilon$	No information on aggregate type. Assume quartzite		Section 4.8
Test for early-age crackng		$\epsilon_r > \epsilon_{ctu}$	Cracking predicted	Section 3.2.1
Early-age crack-inducing strain, ϵ_{cr}	99 $\mu\epsilon$	$\epsilon_{cr} = \epsilon_r - 0.5 \epsilon_{ctu} = 136 - 0.5 \times 76$		Equation 3.5
Minimum area of reinforcement per face, $A_{s,min}$	780 mm ²	Equation 3.12	$k_c = 0.9$	Table 3.1
		$A_{s,min} = k_c k_{Act} \frac{f_{ctm}(t)}{f_{ky}}$	$k = 1$ $A_{ct} = \text{area to depth } h/2 = 250 \text{ mm}$ $f_{ctm}(t) = 1.73 \text{ MPa}$ $f_{ky} = 500 \text{ MPa}$ $\rho_{crit} = 0.00347$	Table 3.1 Table 3.1 Table 3.2
Select steel required to achieve $A_{s,min}$ or structural steel, whichever is greater		16 mm bars at 225 mm centres provides $A_{s,min} = 894 \text{ mm}^2$		

Crack spacing	1177 mm	Equation 3.13	$c = 40 \text{ mm}$ $k_1 = 1.14$ $\phi = 16 \text{ mm}$ $\rho_{p,eff} = A_s/A_{c,eff}$ $A_{c,eff} = \text{area to depth of}$ $h_{e,ef} = 2.5 (c + \phi/2) = 120 \text{ mm}$	Specified Section 4.13 Specified Section 3.4 Section 3.4
Early-age crack width	0.12 mm	$W_k = s_{r,max} \epsilon_{cr}$ $= 1177 \times 99 \times 10^{-6} \text{ mm}$		
Long-term The element is subject to continuous edge restraint and the crack pattern is assumed to form at early-age. The long-term restrained contraction will cause the crack widths to increase.				
Long-term temperature change, T_2	20 °C	The foundation is buried and will respond to ambient conditions, but slower than wall. T_2 will be assumed as 20-10 °C for summer casting		Section 4.3
Autogenous shrinkage	33 $\mu\epsilon$	28-day value for C30/37		Section 4.6.1
Drying shrinkage	100 $\mu\epsilon$	Strength class C30/37. Assumed mean relative humidity = 90% (85% relative humidity on the exposed face and 100% rh on the wet face).		Section 4.6.2
Tensile strain capacity, ϵ_{ctu}	109 $\mu\epsilon$	No information on aggregate type. Assume quartzite		Section 4.8
Total crack-inducing strain	227 $\mu\epsilon$	$\epsilon_{cr} = K_1 \{ \alpha_c T_1 + \epsilon_{ca} \} R_1 + \alpha_c T_2 R_2 + \epsilon_{cd} R_3 \} - 0.5 \epsilon_{ctu}$ $= \{ 0.65 (12 \times 27 + 33) 0.62 + 12 \times 20 \times 0.62 + 100 \times 0.62 \} - 0.5 \times 109$		Section 3.2.1
Long-term crack width	0.27 mm	$W_k = s_{r,max} \epsilon_{cr}$ $= 1177 \times 227 \times 10^{-6} \text{ mm}$	As the cracks will have formed at early-age, the same crack spacing will apply	
In this case there is insufficient steel to achieve the design crack of 0.18 mm in the long-term. To achieve this requires 20 mm bars at 175 mm centres with an area of 1795 mm ² . This also exceeds the requirement for $A_{s,min} = 1303 \text{ mm}^2$ for new cracks which may form in the long-term based on $f_{ctm}(28) = 2.9 \text{ MPa}$.				

5.2

Example 2: Suspended slab cast between core wall and columns (end restraint)

The slab is 300 mm thick and spans between columns and a core wall. The specified strength class is C30/37. The service environment will be benign (XC0) as the slab will be in a controlled internal environment. However, the soffit of the slab will be visible in some areas. The specified cover to the reinforcement in the direction of restraint is 30 mm and the design crack width is 0.3 mm. The soffit formwork is plywood. The construction programme is unknown and summer concreting is assumed.

For the condition of end restraint, while the magnitude of restrained strain will determine whether or not cracking occurs, the crack width is determined by the tensile strength of the concrete immediately prior to cracking and the resulting stress transferred to the reinforcement.

Parameter	Value	Equations and Assumptions		Source
EARLY-AGE				
Temperature drop T_1	23 °C	CEM I is assumed The default cement content is 340 kg/m³ for strength class C30/37		Table 4.2
		The surface will be un-insulated. T_1 is estimated by applying a factor of 1.3 to the thickness of wall and assuming steel formwork, hence $300 \times 1.3 = 390$ mm.		Figure 4.5
Coefficient of thermal expansion α_c	12 $\mu\epsilon/^\circ\text{C}$	No information on aggregate. Default value used		Section 4.5
Autogenous shrinkage	15 $\mu\epsilon$	3-day value for C30/37		Section 4.6.1
Restraint	0.4	Assumed to be the upper end of the range for suspended slabs		Table 4.10
Creep coefficient, K_1	0.65			Section 4.9.1
Early-age restrained strain, ϵ_r	76 $\mu\epsilon$	$\epsilon_r = K_1\{[\alpha_c T_1 + \epsilon_{ca}]R\}$ $= 0.65\{[12 \times 23 + 15]\}0.4$		Section 3.2.1
Tensile strain capacity, ϵ_{ctu}	76 $\mu\epsilon$	No information on aggregate type. Assume quartzite		Section 4.8
Test for early-age cracking		$\epsilon_r = \epsilon_{ctu}$	The estimated restrained strain is about equal to the strain capacity and cracking is possible.	Section 3.2.1
Minimum area of reinforcement per face, $A_{s,min}$	635 mm²	Equation 3.12 $A_{s,min} = k_c k_{Act} \frac{f_{ct,m}(t)}{f_{ky}}$	$k_c = 1$ $k = 1$ $A_{ct} = \text{area to depth } h/2 = 150 \text{ mm}$ $f_{ctm}(t) = 1.73 \text{ MPa}$ $f_{ky} = 500 \text{ MPa}$	Table 3.1 Table 3.1 Table 3.1 Table 3.2
If the minimum area of steel consistent with $A_{s,min}$ is used, the stress in the steel after cracking would be expected to be close to the yield stress, $f_{ky} = 500$ MPa. It is not normal practice to design the reinforcement to operate at this high level of stress as this would lead to very wide cracks. In this case A_s would be expected to be significantly higher than $A_{s,min}$.				
Area of reinforcement per m on each face, A_s	1149 mm²	$A_s > A_{s,min}$ hence cracking controlled	16 mm bars 175 mm centres	

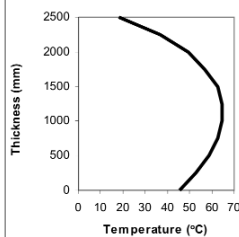
Crack spacing	552 mm	Equation 3.13 $s_{r,max} = 3.4c + 0.425 \frac{k_1 \phi}{\rho_{p,eff}}$ (Note: This crack spacing only applies when the crack pattern is fully developed)	$c = 30 \text{ mm}$ $k_1 = 1.14$ $\phi = 16 \text{ mm}$ $\rho_{p,eff} = A_s/A_{c,eff}$ $A_{c,eff} = \text{area to depth of}$ $h_{e,ef} = 2.5(c + \phi/2) = 95 \text{ mm}$	Specified Section 4.13 Specified Section 3.4 Section 3.4
Crack inducing strain, ϵ_{cr}	596 $\mu\epsilon$	Equation 3.16 $\epsilon_{cr} = \frac{0.5\alpha_e k_c k_s f_{ctm(t)}}{E_s} \left(1 + \frac{1}{\alpha_{ep}} \right)$	$k_c = 1$ $k = 1$ $f_{ctm(3)} = 1.73 \text{ MPa}$ $E_s = 200 \text{ MPa}$ $\alpha_e = 7.1$ $\rho = A_s/A_{ct}$ $A_{ct} = \text{area to depth } h/2 = 150 \text{ mm}$	Table 3.1 Table 3.1 Table 3.2
Early-age crack width	0.44 mm	$W_k = s_{r,max} \epsilon_{cr}$		
LONG-TERM				
<p>The concrete is in an internal environment at relatively low relative humidity (60 per cent). Assuming that the slab can dry from the soffit only, being sealed on the top surface by flooring material, the long-term shrinkage is estimated to be about 290 microstrain and cracking may be expected in the long-term. The element is subject to end restraint and the cracks will develop progressively. As the crack width is related to the tensile strength of the concrete, cracks that occur in the long-term will be wider than early age cracks.</p>				
Crack inducing strain, ϵ_{cr}	1208 $\mu\epsilon$	Equation 3.16 $\epsilon_{cr} = \frac{0.5\alpha_e k_c k_s f_{ctm(t)}}{E_s} \left(1 + \frac{1}{\alpha_{ep}} \right)$	$k_c = 1$ $k = 1$ $f_{ctm(28)} = 2.9 \text{ MPa}$ $E_s = 200 \text{ MPa}$ $\alpha_e = 6.1$ $\rho = A_s/A_{ct}$ $A_{ct} = \text{area to depth } h/2 = 150 \text{ mm}$	Table 3.1 Table 3.1 Table 3.2
Long-term crack width	0.74 mm	$W_k = s_{r,max} \epsilon_{cr}$		
<p>The crack width of 0.44 mm is significantly higher than specified even if cracking occurs at early-age when the tensile strength is low. Cracks occurring in the long-term would be more than double the allowable crack width.</p> <p>In this case taking measures to reduce the restrained strain will only be effective if cracking is avoided altogether. Any cracks that occur will achieve the width calculated.</p> <p>If cracking cannot be avoided then the steel would have to be increased to 20 mm bars at 150 mm centres. This is a substantial increase from 1149 mm² per face/m to 2094 mm² per face/m to 2094 mm² per face/m. This will lead to estimated crack widths of 0.19 mm at early-age and 0.32 mm in the long-term.</p> <p>In this case it would be most appropriate to plan the construction of the slab to avoid significant end restraints. It should be noted that the assumed level of restraint is unlikely to be achieved in practice. However, this example demonstrates the significant difference in crack width that may occur under conditions of end restraint, and the importance of recognising the restraint condition that exists when designing crack control steel.</p>				

5.3

Example 3: Massive raft foundation (internal restraint)

The raft is 2.5 m thick and 30 m square. The specified strength class is C30/37 and 65 per cent ggbs (CEM is specified to reduce early temperature rise). The specified cover is 50 mm. The raft is cast directly onto blinding. The limiting crack width is 0.3 mm. The construction programme requires early access to the surface of the slab and insulation to reduce temperature differentials may be impractical.

In this case the principal concern is with cracking caused by temperature differentials. The raft is sufficiently thick that external restraint is unlikely to be sufficient to restrain the bulk expansion and contraction of the massive slab.

Parameter	Value	Equations and Assumptions		Source
EARLY-AGE ONLY				
Temperature differential	46 °C	 <p>The binder content for the C30/37 concrete using 65 % ggbs is assumed to be 385 kg/m³</p> <p>Thermal model used to estimate temperature rise and maximum temperature differential. The wind speed assumed to be 4 m/s.</p>		Table 4.2 Appendix A2
Coefficient of thermal expansion, α_c	12 $\mu\epsilon/^\circ\text{C}$	No information on aggregate. Default value used		Section 4.5
Autogenous shrinkage	0	Autogenous shrinkage may be ignored as it will occur uniformly through the section and will not contribute to strain differentials.		Section 4.6.1
Early-age restrained strain, ϵ_r	151 $\mu\epsilon$	Equation 3.7 $\epsilon_r = K_1 \Delta T \alpha_c R$	$R = 0.42$ $K_1 = 0.65$	Section 4.7.4 Section 4.9.1
Tensile strain capacity, ϵ_{ctu}	76 $\mu\epsilon$	No information on aggregate type. Assume value for quartzite aggregate.		Section 4.8
Test for early-age cracking		$\epsilon_r > \epsilon_{ctu}$	Cracking predicted	Section 3.2.1
Crack inducing strain, ϵ_{cr}	113 $\mu\epsilon$	$\epsilon_{cr} = \epsilon_r - 0.5 \epsilon_{ctu}$		
Minimum area of reinforcement per face, $A_{s,min}$	866 mm²	Equation 3.12 $A_{s,min} = k_c k A_{ct} \frac{f_{ctm}(t)}{f_{ky}}$	$k_c = 0.5$ $k = 1$ $A_{ct} = \text{area to depth } 0.2h = 500 \text{ mm}$ $f_{ctm}(t) = 1.73 \text{ MPa}$ $f_{ky} = 500 \text{ MPa}$	Table 3.1 Table 3.1 Table 3.1 Table 3.2
Select steel required to achieve, $A_{s,min}$ or structural steel, whichever is greater		16 mm bars at 225 mm centres provides $A_s = 894 \text{ mm}^2$		

Crack spacing	1053 mm	Equation 3.13	$c = 50 \text{ mm}$ $k_{\perp} = 1.14$ $\phi = 16 \text{ mm}$ $\rho_{p,eff} = A_s/A_{c,eff}$ $A_{c,eff} = \text{area to depth } h_{e,ef}$ $= 2.5 (c + \phi/2) = 145 \text{ mm}$	Specified Section 4.13 Specified Section 3.4 Section 3.4
Early-age crack width	0.16 mm	$W_k = S_{r,max} \epsilon_{cr}$		
The crack width is below the specified value and would be expected to close as the section cools.				

6

Measures to mitigate cracking and minimise crack widths

6.1

Planning pour sizes and construction sequence

The reduction of restraint is one of the most economic methods of reducing the risk of early-age thermal cracking and this can be achieved through the sequence and timing of the construction. This applies not only to the sequence of casting the bays or slabs (“alternate bay” or “sequential” construction) but also to the timing of successive bays or lifts. For example, by always ensuring a free end, “sequential” construction produces less restraint than “alternate bay” construction. However, if the joints at the ends of the bay being cast are full movement joints, the order of construction makes no practical difference to the restraint.

With regard to the delay between adjacent bays or lifts, the following general rules apply:

- 1 The time between adjacent strips or lifts should be minimised as the principal restraint acts along the direction of the joint (Figure 6.1a). If the previous pour is still warm, the temperature (and the strain) differentials between new and old concrete will be minimised as the two pours contract together. If insulation is being used, maintaining the insulation for as long as is practically possible on previously cast concrete is advantageous. There is some limited evidence to show that in massive wall construction, casting a kicker about 1.5 m high within 24 hours of casting the base is of help. As this kicker is less rigid than the base, restraint is reduced. By insulating this kicker when the wall is cast, the heat which has flowed into the kicker is retained, and the temperature difference between the sections is reduced. However the cost of this extra operation casts doubt on whether it is a cost-effective solution.
- 2 The time between end-on elements should be maximised as the principal restraint acts perpendicular to the joint. (Figure 6.1b). This eliminates contractions in the old pour prior to casting the new element.

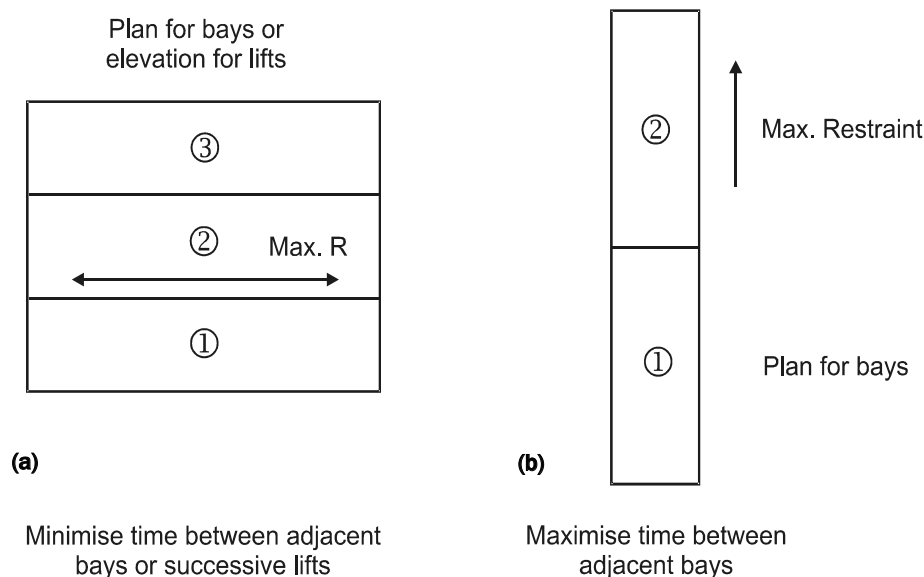


Figure 6.1 Pour configuration as it affects restraint and delay between casting adjacent bays

- 3 To avoid excessive restraint in either direction the preferred shape for a given volume of concrete is as close to square as possible.
- 4 If a source of local high restraint falls within the area of the proposed pour, it may be prudent to introduce a construction joint close to it. The gap, to be filled once the large pour has fully contracted, should be as small as practically possible.

In relation to restraint, it is also important to recognise the following:

- ☞ in very thick sections, external restraint is likely to be much less significant, as large forces can be generated even though the concrete may be relatively young. In this case, cracking is more likely to result from internal restraints caused by temperature differentials, and the use of insulation is most effective in these circumstances
- ☞ in sections which are relatively thin, and cast against existing mature concrete, external restraint will be predominant. The influence of internal restraints are diminished as the external restraint prevents differential internal strains developing. A relaxation of limits on temperature differentials may be achieved when external restraint is high.

In practice both internal and external restraint exist simultaneously, although in many cases one is predominant. Where combined restraints exist, the effects are superimposed (Bamforth and Grace, 1988) as shown in Figure 6.2 for a thick wall cast onto a rigid foundation. This demonstrates the difficulty in predicting restraints, and the level of simplification which has been adopted by BS8007, R91 (CIRIA, 1992) and EN1992-3. It is recommended that where external restraint exists, the need to minimise differential temperature using insulation should be carefully considered as such action may increase the risk of through cracking.

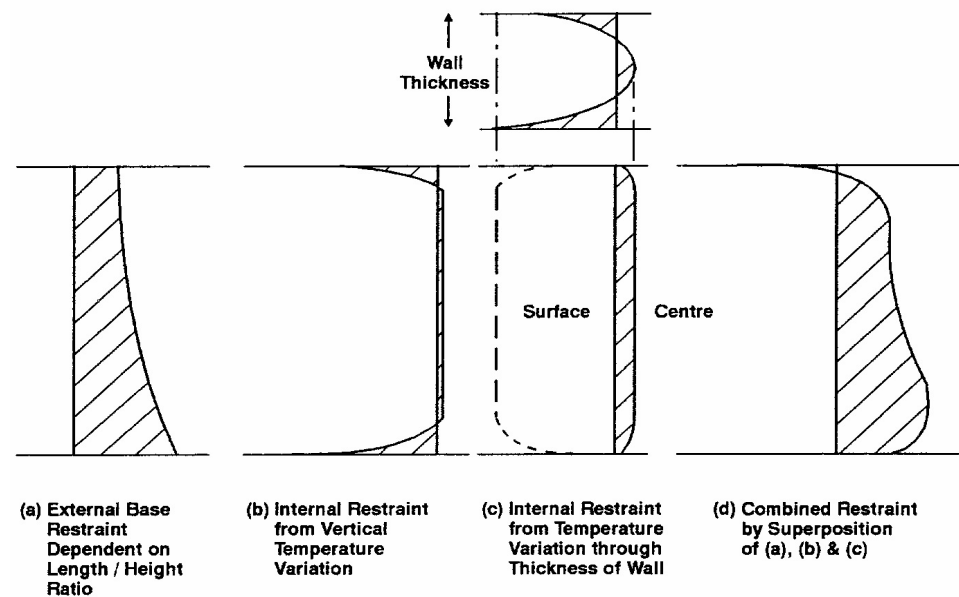


Figure 6.2 The superposition of internal and external restraint (Bamforth and Grace, 1988)

Each case should be considered separately, because of the inherent complexity of the problem. However, the following guidelines may be followed:

- 1 For elements of large cross-section, where external restraint is low, steps should be taken to limit temperature differentials as defined in Table 7.1.

- 2 For thin elements (<500 mm) subject to high external restraint, temperature differential limits in excess of those given in Table 7.1 may be tolerated, subject to an analysis of the likelihood and/or extent of cracking.

6.2 Movement joints

With regard to the provision of movement joints in liquid retaining structures, EN1992-3 recommends their use when “*effective and economic means cannot otherwise be taken to limit cracking*”. These will have the effect of reducing restraints. Annex N of EN1993-2 offers two options for control:

- ☞ design for full restraint with no movement joints
- ☞ design for free movement to achieve minimum restraint.

On this basis it would appear that the option for partial contraction joints has been excluded. For minimum restraint EN1992-3 recommends that free contraction joints are spaced at 5 m or 1.5 times the wall height, whichever is greater. This is similar to the natural crack spacing of a wall which has less steel than $A_{s,min}$, for which EN1992-1-1 gives a value of 1.3 times the height.

Movement joints may require maintenance and any initial savings on reinforcement have to be balanced against possible increased maintenance costs. EN1993-2 highlights the fact that sealants used in joints may have a considerably shorter life than that expected of the structures and joints should be constructed so that the sealant can be inspected and repaired or renewed if necessary.

There are two basic types of movement joints: expansion joints (which allow both expansion and contraction), and contraction joints (which only allow contraction). Contraction joints subdivide into free contraction joints and partial contraction joints (BS8007). The restraint at expansion joints and free contraction joints is zero, as required by EN1992-3, but at partial contraction joints the continuity of some or all of the reinforcement results in some restraint at the joint. An expansion joint (Figure 6.3) includes a compressible layer between the concrete sections. The reinforcement is not continuous through the joint and, where necessary, the joint is sealed to prevent leakage or seepage.

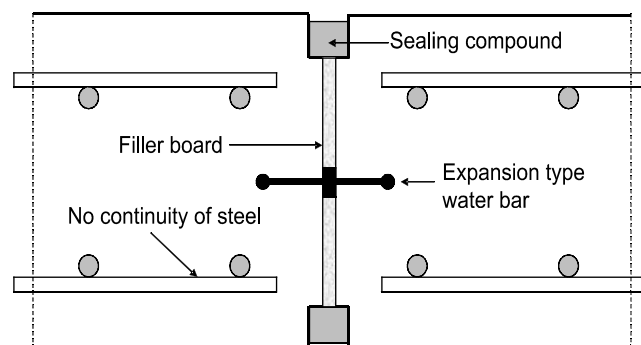


Figure 6.3 Expansion joint detail

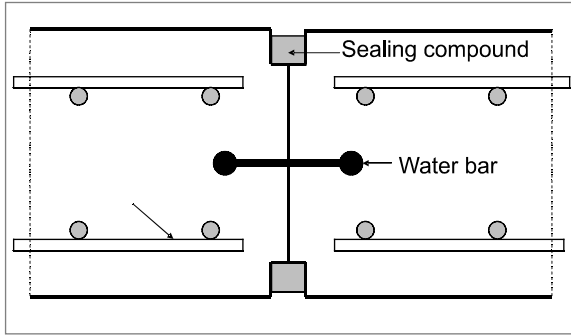
Both full and partial contraction joints can be formed against stop-ends or induced within a section (Figure 6.4). A full contraction joint has no continuity of reinforcement through the joint and, as its name implies, is used in situations where free contraction of the concrete is required. Of the two methods of forming a free contraction joint, the induced technique has the major advantage of giving the contractor more scope for efficient construction so that a number of successive bays can be cast in one operation.

With full steel continuity, and assuming that the current crack control theory for thermal cracks is correct, the crack widths at the partial contraction joint with full continuity of steel would be expected to be no wider than elsewhere in the section. Some site data confirm this deduction (Redhead, 1979). While movement is limited it is beneficial to control where the cracks occur so that appropriate measures to seal them can be made. However, if this approach is adopted the steel should be at a level such that the crack spacing is consistent with the joint spacing, otherwise cracks may occur between the joints.

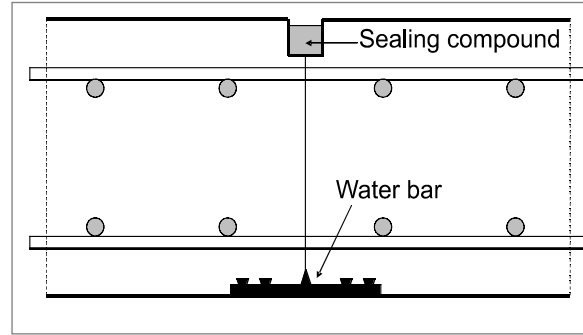
A partial contraction joint with some steel continuity but with the area of steel ratio less than $A_{s,min}$ would be expected to give an uncontrolled crack (see Section 3.3). The reinforcement in this uncontrolled crack depends on the sealing compound for its corrosion protection and experience with joints casts doubt on the adequacy of this protection (ACI, 1980). As shear transfer can be achieved by filling the crack inducing pipes in a full contraction joint, or with corrosion resistant dowel bars, there may be little need to have any continuity of reinforcement across the joint, except where the joint is required to resist tensile forces. Tests have shown that the technique of inducing cracks to form partial contraction joints is successful, even with full continuity of reinforcement (Base and Murray, 1978).

EN1992-3 states *“a moderate amount of reinforcement is provided sufficient to transmit any movements to the adjacent joint”*, hence the use of continuity with less than $A_{s,min}$ is still permitted”, the use of continuity with less than $A_{s,min}$ is still permitted. However, the example in Figure 5.1 of BS 8007 shows a 50 per cent continuity. If partial contraction joints are used, it is recommended that the joint has a reinforcement level of at least $A_{s,min}$ but significantly less than full continuity.

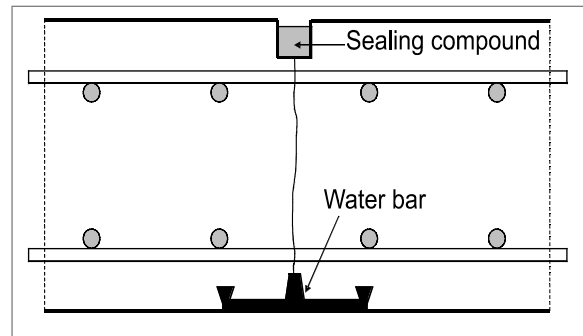
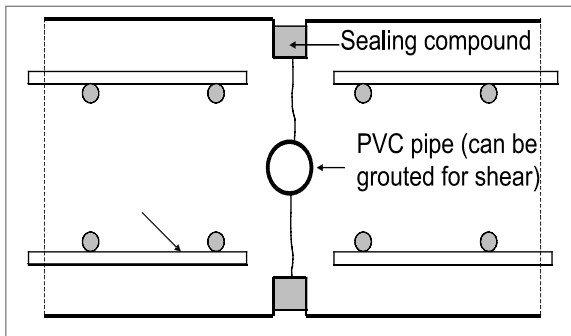
Full contraction joint, no steel continuity



Partial contraction joint, some continuity of reinforcement



Formed against a stop-end and requiring little joint preparation



Cracks induced using water bars, separator plates or PVC pipes. The latter may be grouted to provide a shear key

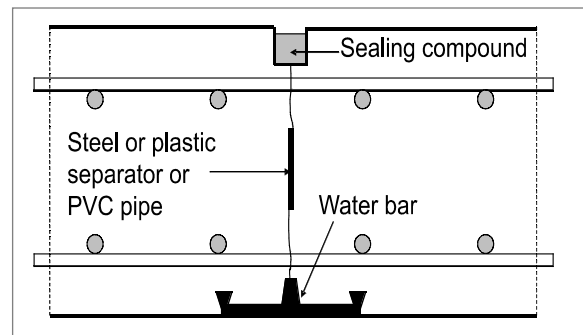
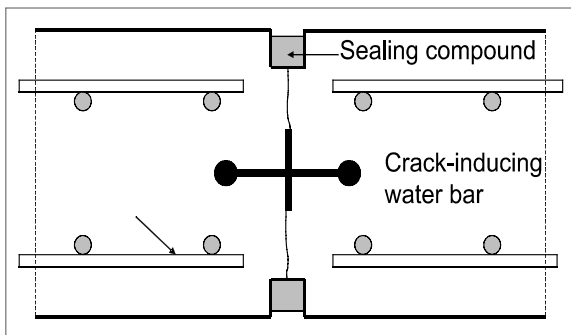


Figure 6.4 Full and partial contraction joint details

To determine the theoretical restraint factor in walls with full continuity of reinforcement, it is prudent to ignore the existence of the partial contraction joints and to use the distance between full contraction joints in determining the length/height ratio (Section 4.7.2).

In a few structures such as nuclear plants or radiation shields, cracks are highly undesirable. The French nuclear industry, as a cost-effective alternative to post-cooling, developed a system whereby grouting ducts were cast into the thick wall units at positions where cracks were likely to occur and where they were likely to be widest. These grout pipes act as crack inducers to ensure that the cracks occur at defined locations and when the crack has occurred it is relatively easy to grout the ducts.

6.3

Additional measures to cool the concrete

Opinions differ on the need to reduce or restrict the concrete placing temperature. With regard to the risk of early thermal cracking, it is recognised that a lower placing temperature is beneficial (Section 4.2.1). The most obvious benefit is the direct reduction in T_f but other advantages include:

- ☞ a slower rate of workability loss
- ☞ longer stiffening time
- ☞ a slower rate of heat generation and a reduced temperature rise as shown in all but very thick sections.

There are various methods available for achieving a reduced mix temperature, including reductions in the temperature of the mix constituents, the use of ice in the mix water and the use of liquid nitrogen to cool the mix immediately prior to placing. Spraying the formwork with water before commencing concrete placement or commencing concreting in the late afternoon are also beneficial.

The concrete may also be cooled *in situ* by the use of embedded cooling pipes.

6.3.1

Pre-cooling the constituent materials

The most common method for cooling the mix involves cooling one or all of the individual mix constituents. This can be achieved with relatively simple and cheap techniques including:

- ☞ shading the aggregate stockpiles from the direct rays of the sun
- ☞ controlled sprinkling of the aggregate stockpiles
- ☞ burying water supply pipes
- ☞ painting all exposed pipes and tanks white
- ☞ cooling the mix water using ice
- ☞ cooling the aggregate using liquid nitrogen (LN₂). This process has been used in Japan (Kurita *et al*, 1990) to cool sand to -140 °C and achieve a reduction in mix temperature of about 10 °C.

As the aggregate comprises the largest single component of the mix, cooling the aggregate will have the greatest effect on the concrete mix (except where ice is used).

Other more extreme measures include immersion in tanks of chilled water, spraying chilled water on aggregate on a slow moving belt, or blowing chilled air through the stockpiles (ACI, 1984). When the aggregates are cooled with water, this water should be taken into account during batching, by adjustment to the added mix water.

While the aggregate constitutes the greatest mass in the mix, the water has the greatest heat capacity, and hence cooling efficiency. The specific heat of water is about five times that of the aggregate and cement (4.18 kJ/kgK compared with 0.8 kJ/kgK respectively). In addition, water is much easier to cool and the temperature can be controlled more accurately. As it is practical to cool water to about 2 °C this is a very effective method of cooling the mix.

For very effective cooling, ice can be used. The latent heat of ice is 334 kJ/kg, and the heat absorbed by 1 kg of melting ice is equivalent to cooling 1 kg of water through about 80 °C or 1 kg of aggregate through 445 °C. Hence, a relatively small volume of

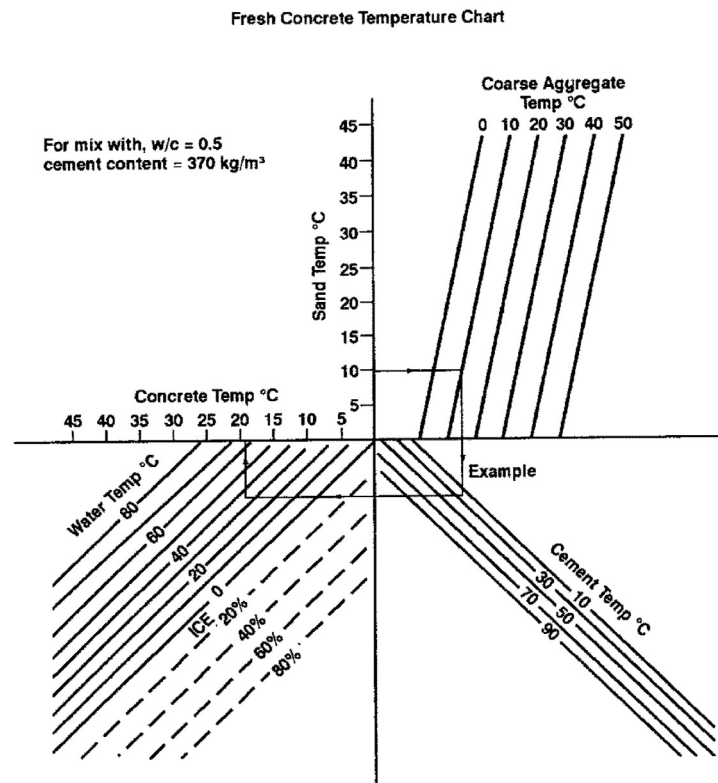
ice can have a significant cooling effect. Ice is usually added to the mix in the form of crushed or shaved ice as it is important to avoid incorporating larger fragments of ice that melt slowly leading to the formation of voids in the hardened concrete. To obtain an indication of the requirements for cooling the individual mix constituents, the following general rules may be applied (Nambiar *et al* 1984). To cool the concrete by 1 °C requires that:

- 1 The aggregate is cooled by 3 °C.
- 2 The mixing water is cooled by 7 °C.
- 3 7kgs of mixing water is replaced by ice.

A nomogram illustrating the effect of cooling the various mix constituents is given in Figure 6.5. This has been developed for a specific mix to provide a rapid means for identifying what steps are needed in specific cases. The nomogram is based on the simple method of mixture as follows:

$$\text{Concrete temperature} = \frac{0.75(T_c M_c + T_a M_a) + 4.18 T_w M_w - 334 M_i}{0.75(M_c + M_a) + 4.18(M_w + M_i)} \quad (6.1)$$

where T is temperature, °C and M is mass, kg/m³ and the subscripts c, a, w and i represent cement, aggregate, water and ice.



Where greater accuracy is required for a mix of different proportions, Equation 6.1 can be used.

One of the major considerations in using techniques to control the mix constituents is that much of the benefit may be lost if there is a long transportation time or delays in placing the concrete. It is the temperature of the concrete when placed that is important in determining the rate of heat generation and peak temperature rise, not the temperature at mixing. In selecting measures to achieve a particular placing temperature, the increase in temperature between mixing and placing should be noted.

6.3.2

Cooling of the fresh concrete before placing

Developments with the use of liquid nitrogen (LN₂) now enable the mixed concrete to be cooled on site. The method involves spraying a mist of LN₂ (which has a boiling point of 77 K (-196 °C)) into the mixer at a controlled rate. This is achieved with a customised lance which is inserted into a mixer truck (Figure 6.6).



Figure 6.6 *The use of liquid nitrogen to cool concrete on site immediately before placing*

The latent heat of boiling of the LN₂ is 199 kJ/kg, about 60 per cent of that of melting ice. With 100 per cent efficiency (and ignoring the subsequent heating of the gas which escapes rapidly to the atmosphere) about 12 kg of LN₂ is needed to cool 1 m³ of concrete by 1 °C. In practice, the efficiency is not much less than 100 per cent. During construction of an X-Ray facility for Maidstone Hospital (Robbins, 1991) about 1 tonne of LN₂ was used to cool a 6 m³ mixer load through about 13 °C. This is equivalent to about 13 kg of LN₂ per °C change in temperature per m³ of concrete (or 16 litres/°C/m³). A similar rate of consumption of 15 litres/°C/m³ was recorded during construction of the Faro Bridges in Denmark (Henriksen, 1983). As the cooling is achieved immediately prior to placing the concrete, concerns about the concrete warming up during transportation are avoided.

6.3.3

In situ cooling

There are two approaches to the cooling of placed concrete: casting a network of cooling pipes within the core of the pour, or attempting to reduce the core temperature rise by surface cooling with water. Either method may be appropriate when the specification prevents the use of concrete with low heat generating characteristics.

An embedded cooling system has the advantage that it can be designed to accommodate any mix type but the system needs to be an integral part of the design. Pumping chilled water or air through these pipes absorbs the heat of hydration of the binder materials and thereby reduces the temperature rise. The system should be designed to remove heat at the required rate without inducing excessive internal temperature differentials. For this reason, plastic pipes may be preferred to metal pipes as the heat flow into the coolant is limited by the conductivity of the pipe itself.

A method for designing a cooling system is given in ACI Report 207.IR-35 (1984). Typical pipe spacings are likely to be of the order of 1 m in large volume pours with relatively low heat generating capacity. In elements cast using high grade structural concrete, closer spacing, of the order of 400-500 mm may be necessary.

The location of internal cooling pipes is unlikely to coincide with the reinforcement, as the latter is usually concentrated near the surface. However, there may need to be some collaboration between the designer and the contractor when this approach is adopted. This technique is often used to construct water retaining structures. For example, in Germany, a rain water reservoir was cast as a single element using this technique to control the thermal stresses (Anon, 1982). The 2 m thick base (plan area 27.4×28.2 m) and the 1.2 m thick 12 m high walls were continuously cast (1100 m³ of concrete) over a 32 hour period, to avoid joints which were prohibited by the specification.

Due to the costs involved (pipes, pumps, refrigeration plant and labour etc), this system should not be applied without giving careful thought to alternative methods. It is also necessary to consider any potential durability problems with the embedded pipes.

The virtues or otherwise of cooling the surface of a concrete pour or the formwork with either ponded or continuously sprayed water depend on the formwork type, section thickness and the source of restraint. Obviously, it makes little sense to spray the back of formwork which effectively insulates the section. Spraying is normally used in conjunction with a formwork material that has poor insulation qualities. Keeping the surface cool can reduce the temperature rise of the core, but as the section thickness increases to more than about 500 mm the core temperature is unaffected, and internal restraint may be developed.

6.3.4 Application of cooling techniques

These practices to cool the fresh concrete are more commonly used in climates that are hotter than the UK. In the UK very few producers have installed the equipment needed for these techniques and in most cases, they are unlikely to be cost-effective. However, there are situations where it may be needed technically or as a cost-effective option on a large project. In these situations, it is better to specify the maximum concrete placing temperature required (with a note reminding the producer that this is likely to require the application of special techniques) than to specify the method. One should also check the producer's proposals for achieving the specification and make arrangements for checking the temperature of concrete at delivery.

7

Specification, testing and monitoring

7.1

Specification

Limiting crack widths is a routine part of the specification for reinforced concrete. To control the width of early-age thermal cracking it is also common to specify allowable limits on the centreline peak temperature, T_p , and on temperature differentials ΔT_{max} during the post construction period. Typical limits may be specified as follows:

- ☞ the max temperature at any point within the pour shall not exceed [.....] (commonly 70 °C)
- ☞ the max temperature differential within a single pour shall not exceed [.....] (commonly 20 °C)
- ☞ the max value of mean temperatures between adjacent elements cast at the same time shall not exceed [.....] (commonly 20 °C)
- ☞ the max value of mean temperatures between adjacent element cast at different times shall not exceed [.....] (commonly 15 °C).

This is a simplistic approach, as the object is to limit restrained thermal strain, ϵ_r , and the associated stresses that may lead to cracking. Temperature measurements are relatively easy to obtain and to interpret, while strain measurements are much more complex in both respects. As the acceptable temperature limits are used to imply limits on strain, they should be variable according to the assumed coefficient of thermal expansion of the concrete, α_c , and the restraint to thermal movement, R . Table 7.1 provides estimates of temperature differentials applicable for a variety of conditions of external restraint and for internal restraint due to temperature gradients.

Table 7.1 Limiting temperature drop $T_{1,max}$ and temperature differentials ΔT_{max} to avoid early-age cracking, based on assumed typical values of α_c (Table 4.4) and ϵ_{ctu} (Table 4.11) as affected by aggregate type (for $K_1 = 0.65$ and $\epsilon_{ca} = 15\mu\epsilon$)

Aggregate type	Gravel	Granite	Limestone	LWAC with natural sand
Thermal expansion coefficient ($\mu\epsilon/^\circ\text{C}$)	13	10	9	9
Tensile strain capacity ($\mu\epsilon$) under sustained loading	65	75	85	115
Limiting temperature change in °C for different external restraint factors:				
1.00	6	9	12	20
0.80	8	12	16	25
0.70	9	14	18	29
0.60	11	17	22	34
0.50	14	21	27	42
0.40	18	27	34	53
0.30	24	36	46	71
Limiting temperature differential (°C) for internal restraint $R = 0.42$	20	28	35	53

An example specification is given in Table 7.2. Such a specification was used for the BP Harding gravity base, constructed using class LC 40/45 lightweight aggregate concrete (LWAC) shown in Figure 7.1. The selection of LWAC enabled the structure to be built entirely in dry-dock, and enhanced the properties of the concrete by minimising the risk of early thermal cracking. The LWAC exhibited a very low thermal expansion coefficient of $6 \mu\epsilon/^\circ\text{C}$ and a very high strain capacity of $160 \mu\epsilon$.

The temperature difference within a pour was limited to 50°C and the maximum allowable temperature was 80°C . This high value was acceptable because of the presence of fly ash in the mix, reducing the risk of delayed ettringite formation.

A trial slab was cast to validate the temperature limits. No thermal curing was applied and no cracking was observed. In addition, cores were extracted from the slab and while the cube strength at 28 days was about 50 MPa, cores exhibited strengths of about 55 MPa. This enhanced *in situ* strength was attributed to the use of fly ash and is consistent with other results using fly ash (Appendix A9).

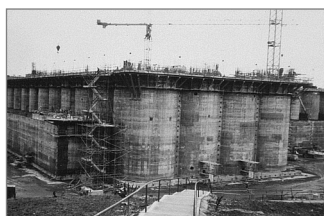


Figure 7.1
BP Harding gravity base
constructed using lightweight
aggregate concrete

Table 7.2 Example specification – control of concrete temperatures during hardening

<p>To control cracking as a result of early thermal movement, the contractor shall take measures to ensure that the following requirements are satisfied. The contractor shall describe in a method statement to be submitted to the engineer for his approval, before concrete operations are commenced.</p>	
A	<p>The maximum temperature of the concrete during its early-age heat cycle shall not exceed [... °C] unless it can be demonstrated by test that the compressive strength, after [...] days, of concrete heated to a higher temperature, exceeds the required design strength by a margin to be agreed with the engineer.</p>
B	<p>In elements, or parts of elements, which are not restrained by existing concrete, the difference between the maximum temperature and the surface temperature (measured within 10 mm of the surface) shall not exceed [... °C] unless it can be demonstrate by test that greater differentials can be tolerated without cracking.</p>
C	<p>When a new pour is cast against existing concrete of the same thickness, eg adjacent pours, the difference between the mean temperatures in the existing and the newly cast sections shall not exceed [... °C]. The mean temperature shall be determined at a distance of 1 m from the interface between old and new concrete and shall be calculated using the equation:</p> $T_m = 1/6(4 T_p + T_{s1} + T_{s2})$ <p>Where</p> <p>T_m is the mean temperature T_p is the peak temperature at the centre of the section T_{s1}, T_{s2} are the surface temperatures on opposite faces.</p>
D	<p>When a new pour is cast against existing concrete of a different thickness, account shall be taken of the difference in the restraint exercised by the old section on the new, when deriving the mean temperature differentials. The contractor shall include in his method statement, the temperature limits for the elements to be cast, together with the calculations supporting the limits, for approval by the engineer before concreting operations are started.</p>
E	<p>The assumptions made in the design process are provided in the attached table (Table 4.1). If measurements demonstrate that values are different from those assumed then the proposed limits may be revised accordingly. The results from site trials may also be used to revise the proposed limits. However, trials should be of sufficient scale to ensure that the levels of restraint are the same as those that occur during construction.</p>
F	<p>Results from <i>in situ</i> monitoring can provide values of actual concrete temperature and strain. By comparison with thermal strain in unrestrained blocks, actual <i>in situ</i> restraint may be calculated. Such data may be used to support changes in bay size and layout as construction proceeds.</p>

7.2

Test methods for obtaining relevant concrete properties

7.2.1

Heat generation and temperature rise

There are numerous tests that may be used to measure the heat generating capacity of a cement type or concrete and the type of test that is employed will depend upon how the results are used.

Two European Standard tests are available for the classification of cement. BS EN 196-8 describes the heat of solution method which involves dissolving hydrated cement in a solution of acids and recording the temperature rise in an insulated container. The method adopted by the UK cement manufacturers is the semi-adiabatic test to BS EN196-9:2003. This test is carried out on a mortar sample comprising 360 g binder, 1080 g sand and 180 g water. This scales up to a mix with a binder content of 505 kg/m³ with a w/b of 0.5 and is representative of a high cement content concrete. The sample is placed in a calorimeter and the temperature rise, typically between 10 and 50 °C, is measured and compared with an inert control sample. The temperature rise is converted to heat generated per unit weight of cement (kJ/kg) based on the mass and specific heat of the sample and calorimeter. Based on the properties of the individual constituents given in EN 196-9, the specific heat of the mortar may be calculated to be 1.13 kJ/kg (Wadsö, 2003). Some typical results obtained using the semi-adiabatic test are illustrated in Figure 7.2 for a range of cement combinations (Dhir *et al*, 2006).

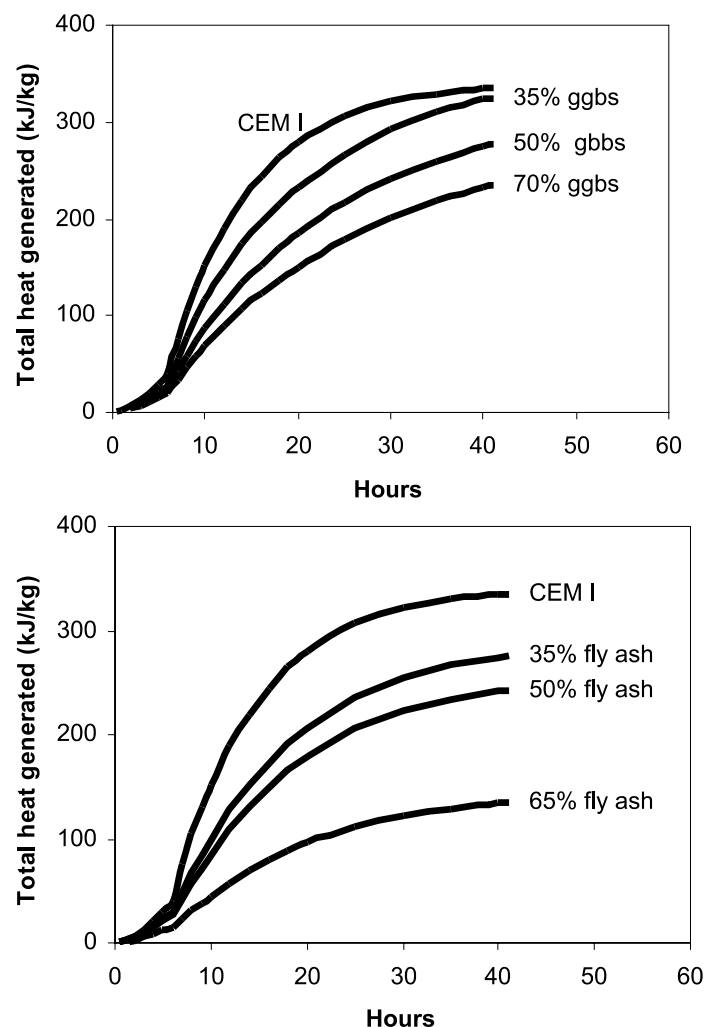


Figure 7.2 Semi adiabatic test results for concretes containing ggbs and fly ash (Dhir *et al*, 2006)

Isothermal testing of cement is also used to determine the heat generating characteristics of cement. These tests involve keeping the test sample at a constant temperature and measuring the amount of heat that should be removed to maintain this condition. By testing at different temperatures the relationship between temperature, rate of heat generation and ultimate heat output may be derived. In order to use such data to make temperature predictions, tests are carried out at different temperatures and used to derive parameters for input to a model (Dhir *et al*, 2006).

These standard tests are useful for categorising different cements and deriving relative performance in relation to heat generation. However to enable the results to be used in predictive models, information is needed on the density and specific heat of both the test materials and the materials to be used in the structure.

When generating data to make predictions of temperature rise, the most reliable approach is to test concrete using constituents and proportions that are the same as, or at least representative of, the mix to be used in practice. While it may be difficult to do this at design stage, it is advisable, where thermal cracking is critical, to undertake testing as soon as the concrete mixes have been established. On very large contracts trial pours may be required and this provides an opportunity to obtain representative *in situ* data (Bamforth and Grace, 1988). Under conditions where a high temperature rise is expected, (ie thick sections, mixes with a high cement content, or when placing at high temperature) a hot-box test is appropriate to provide information on temperature rise. This involves casting a cube, commonly 1 m³, which is insulated on all faces with 50 mm polystyrene. A typical output is shown in Figure 7.3 together with an adiabatic curve derived from the results.

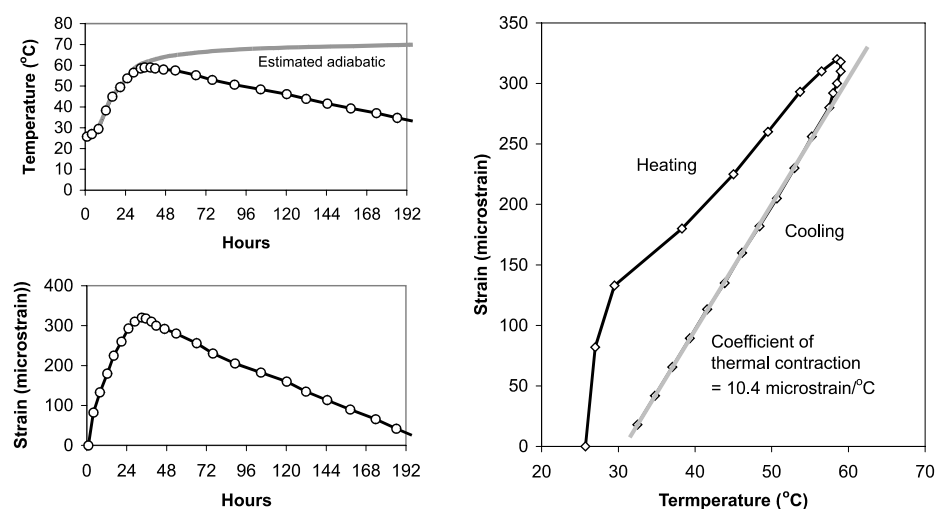


Figure 7.3 Results from a 1 m³ hot-box test where the placing temperature was 25 °C. The value of α_c is determined during cooling (Bamforth and Grace, 1988)

7.2.2

Coefficient of thermal expansion

The coefficient of thermal expansion α_c is a measure of the strain change per unit temperature change. Tests methods involve subjecting concrete specimens (usually cylinders or prisms) to a change in temperature and measuring the deformation. BS EN 1770 describes the Standard Method in Europe.

It is recognised that α_c changes with age and with moisture content (Sellevold, 2006). Values most relevant to early thermal cracking should be derived at an appropriate age

(within the first few days) and moisture condition (saturated). It is particularly important to ensure that, when using small specimens, drying does not occur to avoid additional strains associated with drying shrinkage.

Where tests are undertaken on site to measure temperature rise, α_c may also be determined by measurement of strain during the temperature cycle. An example of strain measurement in a hot-box is also shown in Figure 7.3. Strain was measured using a vibrating wire gauge (VWG). The relationship between temperature and strain during the cooling arm of the heat cycle is used to derive α_c as it is the restrained contraction that causes cracking. In the example shown a granite aggregate was used resulting in concrete with a thermal “contraction” coefficient of $10.4 \mu\epsilon/^\circ\text{C}$.

7.2.3 Tensile strain capacity

Direct measurement

The most direct way of measuring tensile strain capacity ϵ_{ctu} is to subject prisms to direct tensile loading and to measure the strain up to failure (Swaddiwudhipong, 2001). Direct measurement may also be achieved by creating conditions within a test specimen that are similar to those which lead to early thermal cracking. For example, stress rig tests subject a dog-bone shaped specimen to a thermal cycle. During heating the concrete is allowed to expand freely but it is restrained during contraction. When the concrete cracks, the release of strain defined by the crack width is used to derive the strain at failure. This may be compared with the measurement of the temperature change and, with a knowledge of α_c , the restrained thermal contraction required to cause failure may be calculated.

Other tests have involved subjecting specimens to temperature differentials and the measurement of the associated strain differentials up to the time of cracking (Hunt, 1972).

Indirect measurement

Direct measurement of ϵ_{ctu} often requires a large test rig and relatively sophisticated monitoring equipment. An alternative approach is to derive ϵ_{ctu} from measurements of tensile strength f_{ctm} and elastic modulus E_{cm} (Tasdemir *et al*, 1996). In a comprehensive review of test data a linear relationship was established of the form;

$$\epsilon_{ctu} = 1.01(f_{ctm}/E_{cm}) \times 10^6 + 8.4 \text{ microstrain} \quad (7.1)$$

As discussed in Section 4.8, this may be simplified to the relationship to provide a value for use in design:

$$\epsilon_{ctu} = (f_{ctm}/E_{cm}) \times 10^6 \text{ microstrain} \quad (7.2)$$

7.3 Measurement and assessment of *in situ* temperature and strain

7.3.1 Measuring temperature differentials

Temperature monitoring is required in order to demonstrate compliance with specified temperature limits. The simplest and most cost effective method is to use embedded thermocouples which are easy to install and monitor. The output can be monitored with simple manual devices or with automatic logging systems. In its simplest form,

temperature monitoring will involve thermocouples at the centre of a section and close to the surface. The maximum value at the centre and the difference between the centre and the surface will then be assessed against specified limits

The proposed locations for thermocouples in a thick slab are shown in Figure 7.4.

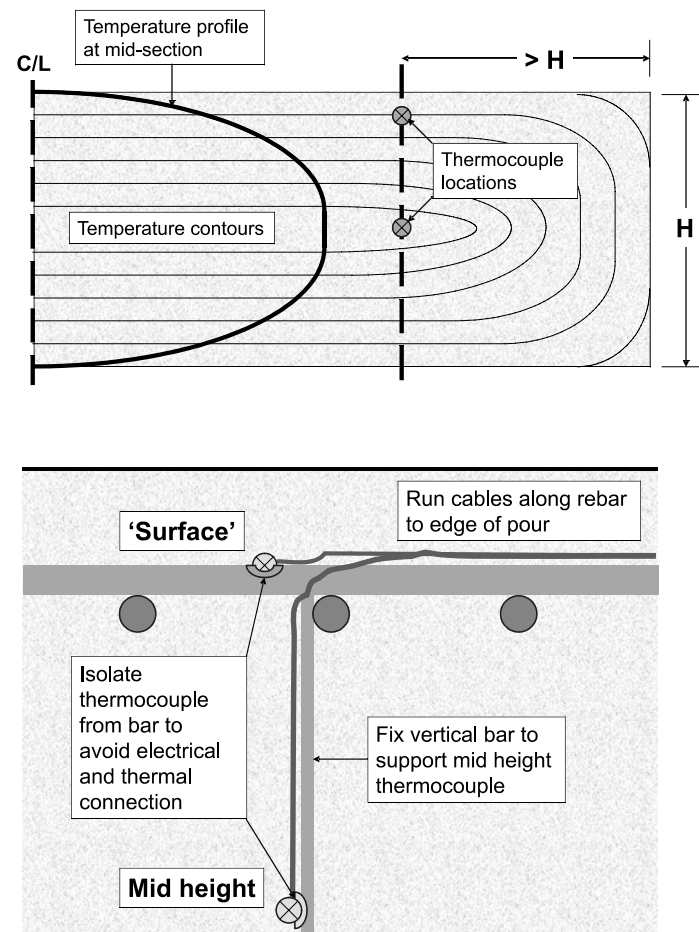


Figure 7.4 Proposed location and fixing of thermocouple to monitor temperature variation

In most slabs, the temperature profile through the depth will be similar over most of the width, so for practical purposes install thermocouple as close to the edge as possible to minimise cable runs. The same principle will apply to walls, the profile through the thickness being the same over most of the height and width.

It is common to fix the “surface” thermocouple to the top mat reinforcement. While there will be a temperature difference between the reinforcement and the concrete surface this will be small in situations where there is control of the temperature differential. Figure 7.5 gives estimates of the temperature difference between the outer rebar and the surface for different cover depths and for different peak to surface temperature differentials. The calculations have been made for a 2 m deep slab using concrete with 350 kg/m³ CEM I. When the maximum temperature differential is controlled to 20 °C, the temperature difference between the rebar and the surface is unlikely to be much greater than 2 °C, even with 50 mm cover. If thought to be significant, 1 or 2 °C may be subtracted from the limiting temperature differential to take account of the fact that the “surface” temperature is measured at rebar depth.

As shown in Figure 7.5, the rebar to surface temperature difference only becomes significant in situations in which the maximum temperature differential exceeds normally accepted levels.

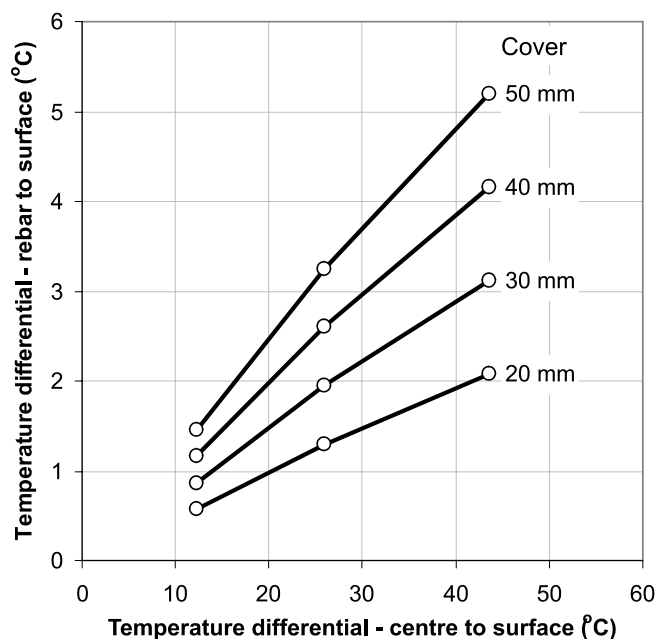


Figure 7.5 *Estimated temperature difference between the reinforcement and the surface as affected by cover depth and the maximum centre-surface differential*

When the specification is more complex, for example by limiting differences between the mean values in the new and the old concrete, the designer should specify how the mean is determined. This involves defining how many locations through a section will be monitored, where the thermocouples will be located, and how the results will be analysed. The temperature distribution through a section is usually close to parabolic and measurements at the surface and the centre are often sufficient to enable a reasonable approximation of the mean, determined using the expression:

$$T_m = 1/6(4T_p + T_{s1} + T_{s2}) \quad (7.3)$$

where

T_m is the mean temperature

T_p is the peak temperature at the centre of the section

T_{s1}, T_{s2} are the surface temperatures on opposite faces.

Again, when the “surface” temperature is measured at the depth of reinforcement, appropriate adjustments may be made (Figure 7.5) to the values of T_{s1} and T_{s2} . Where contracts specify the need to meet temperature limits, the contractor should obtain specific details from the designer on how compliance is to be demonstrated in relation to the location and number of monitoring points and how the results obtained will be interpreted.

Full scale mock-ups are very useful for providing data on temperature profiles and for identifying the precautions needed in terms of insulation. Computer models are also being used more often.

If the pour is a one-off, or if it is the first of many, pairs of thermocouples should be installed at critical locations to provide support in the event of a failure.

7.3.2 Deriving restraint factors

It is sometimes useful, on very large contracts with repetitive pour, to determine restraint factors by monitoring the first few pours. This may enable relaxation of costly procedures to minimise thermal cracking, or permit savings by enabling pour sizes to be increased and the construction sequence to be modified to achieve a reduction in the programme.

To determine restraint factors both the actual strain and the free strain, ie α_c , should be measured. The restraint factor is determined simply by comparing the observed strain in the element with the free strain that would have occurred with no restraint. If α_c represents the free strain, derived from a hot-box test, and α_r is the *in situ* (restrained) coefficient of expansion, then R is calculated as follows;

$$R = \frac{(\alpha_c - \alpha_r)}{\alpha_c} \quad (7.4)$$

Some typical stress-strain curves recorded in a slab with different levels of restraint in the longitudinal and transverse directions are shown in Figure 7.6. In this case the free strain was determined by installing vertical gauges that were subject to zero restraint and indicated a thermal expansion coefficient of $10.2 \mu\epsilon/^\circ\text{C}$. The stress-strain curves in the longitudinal and transverse directions yielded equivalent values of $6.3 \mu\epsilon/^\circ\text{C}$ and $1.2 \mu\epsilon/^\circ\text{C}$ respectively. Using Equation 7.4 restraint factors were calculated to be 0.38 and 0.88, representing moderate and very high restraint.

An interesting observation was the occurrence of cracking at one gauge location, caused by the highest level of restraint. It can be seen that the strain rapidly increased when the temperature had dropped by about 14°C from its peak value.

Having determined the true values of restraint at critical locations within a pour, comparison with the assumed values may allow cost effective changes to be made in a rational and safe manner.

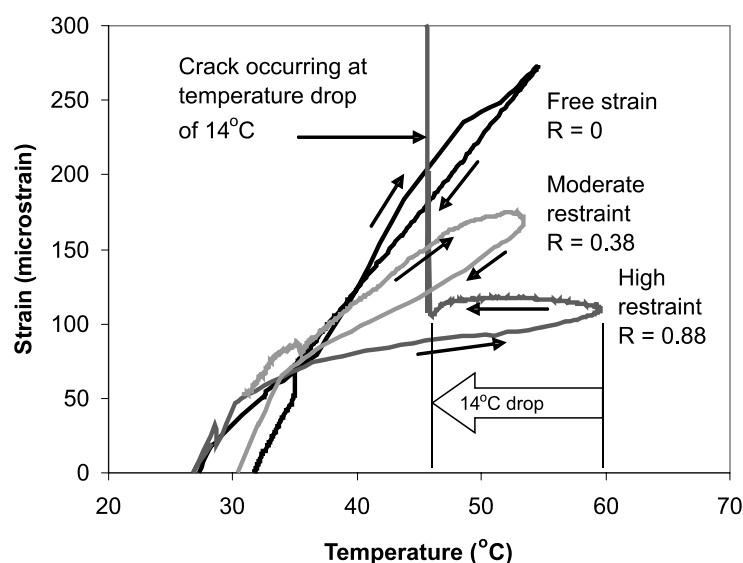


Figure 7.6 *In situ* stress-strain curves used to derive restraint factors

7.4

Measurement of crack width

For most practical purposes it is sufficient to measure the surface crack width. For spot measurements this may be achieved using either a simple crack comparator (Figure 7.7) or, for more precise measurements, a crack microscope. The latter may have a magnification of about 35 times with divisions down to 0.02 mm. To measure crack movement, either spot measurements may be taken periodically, or strain gauges may be installed on the surface. The latter do not measure crack width directly but enable the change in strain to be measured and converted to a change in crack width.

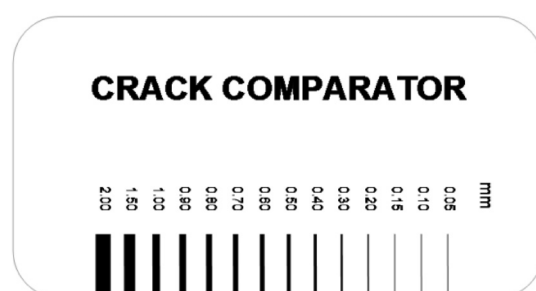


Figure 7.7 Crack comparator

In accordance with EN1992-1-1, allowable crack widths are characteristic values at the 95 per cent level, so it can be expected that some cracks may exceed this limit. This sounds relatively straightforward and would be easy to interpret if each individual crack was of uniform width over its entire length. Under conditions of normal loading this may be the case in some circumstances. For example, on the soffit of a beam, while crack widths may differ, each crack would be about uniform width across the width of the soffit. When cracking occurs due to early thermal contraction it is more common for each crack to vary in width, normally with the widest at a point close to the location of restraint. Situations may arise, where a crack may exceed the allowable value over only part of its length, with the remainder of the crack being within the acceptable limit. In considering compliance the characteristic value should represent:

- ⌘ the number of cracks within part of the crack which exceeds the allowable limit
- ⌘ the proportion of the total length of cracking that exceeds the allowable limit.

Within the design process, the worst case has been considered at each location, and each crack should be defined by the maximum crack width recorded within its length. To achieve compliance on this basis, no more than 1 in 20 cracks should exhibit a maximum crack width greater than the allowable value.

The issue of compliance and the need for repair should also be considered. While cracking may be designed and assessed based on characteristic values this does not mean that cracks in excess of the allowable value do not need to be repaired and this should be taken into account in the contract. If a structure is designed such that 1 in 20 cracks may exceed the allowable limit and if such cracks need to be repaired, then the contractor should be made aware of this and include appropriate costs in the tender.

Actions in the event of non compliance

Sufficient data are available to enable the concrete mix and site procedures to be established and temperature limits to be met. However, contingency plans should be defined which can be implemented when the results exceed “action levels”. For example if the allowable temperature differential is being approached, and is likely to be exceeded, additional insulation may be applied.

If the maximum allowable temperature is approaching its limit, no actions can be taken, except perhaps the removal of formwork in thin sections. However, little can be done in thick sections unless embedded cooling pipes are being used. This value is much easier to predict based either on the mix constituents and the mix temperature or if available, from test results for temperature rise.

If allowable limits on temperature differential are exceeded the following action can be taken:

- ⌘ inspect the surface for cracks after the pour has cooled back to ambient. As the purpose of limiting the temperature differential is to minimise the risk of cracking, if cracks widths are within allowable limits then no further action need be taken
- ⌘ if the cracks widths exceed the allowable limits initiate remedial measures. If cracks are to be repaired, the method used will depend on whether the cracks are “dead” or “alive”, and on the serviceability requirements of the structure. In a massive raft for example, surface cracks are unlikely to increase after the element has cooled and sealing will be primarily for durability. In this case injection grouting is most common, using an epoxy resin when the cracks are less than about 1 mm width. For cracks which are likely to continue moving, it is usual to make provision for further movement to continue after repair. Procedures are defined in Allen and Edwards (1987)
- ⌘ consider the consequences of internal cracking – it is possible that internal cracking may occur even if there is no evidence of surface cracking. In this case, it is difficult to establish the extent of cracking without extensive coring and even this is unlikely to indicate crack widths. The value in carrying out a detailed investigation to find cracks which do not propagate to the surface is still doubtful, except in circumstances where such cracks are clearly detrimental to the performance and safety of the structure.

The allowable maximum temperature is applied to limit the detrimental effect of temperature on the strength of concrete and sometimes to prevent delayed ettringite formation. If this value is exceeded, core testing will provide evidence of whether the deterioration in strength is excessive. BS6089:1981 provides guidance on the interpretation of *in situ* strength, and it is advisable that the parties involved agree the acceptance level of core strength before results are obtained.

8

Conclusions and recommendations

Despite considerable advances in this area of technology there are still a number of issues that could benefit from further research.

- 1 The effect of cement type on autogenous shrinkage which appears to play a more significant role in early-age cracking than previously considered.
- 2 The relationship between the tensile strength of the concrete and the bond strength to reinforcement, and the influencing factors.
- 3 The surface zone affected by the reinforcement.
- 4 Field data on levels of restraint.
- 5 Crack formation and the addition of early-age and long-term effects under different conditions of restraint and loading.
- 6 The influence of different forms of restraint on crack formation and crack width.
- 7 The impact of the early thermal cycle on durability.
- 8 The influence on crack width on reinforcement corrosion.

Most importantly, field data are needed to validate or modify the input parameters and the models used in the design process. Structured field data needs to be collected to provide feedback on the reliability of proposed methods for design. This should include information on the concrete constituents and mix design, the design of reinforcement, temperature rise and thermal strain, and crack pattern and width.

9. References

ACI Committee 207 (1980)
Cooling and insulating systems for mass concrete
Concrete International Report ACI, 207.4R.80, May 1980, pp 45-64, Detroit, Michigan

ACI
Cooling and insulating systems for mass concrete
ACI Manual of Concrete Practice, 207.4R-80, Detroit, Michigan

ACI COMMITTEE 207 (1990)
“Effect of restraint, volume change and reinforcement on cracking of mass concrete”
ACI Materials Journal, **87** (No.3), Detroit, Michigan

Alexander, S J (2006)
“Why does our concrete still crack and leak”
The Structural Engineer, 5 December 2006, pp 40-43, London

Ed Allen, R T L and Edwards, S C (1987)
Repair of concrete structures
Blackie and Son Ltd, Glasgow, ISBN 0 2169 2006X

Altoubat, S A and Lange, D A (2001a)
“Creep, shrinkage and cracking of restrained concrete at early-age”
ACI Materials Journal, July/August 2001, **98** (No.4), pp 323-331

ANON
“West Germany – Sub surface rainwater reservoir”
Construction Industry International, Aug 1982, pp 17-18

Arya, D and Ofori-Darko, F K (1996)
“Influence of crack width frequency on reinforcement corrosion in concrete”
Cement and COPncrete Research, Elsevier Science, **26** (No. 3), pp 345-353

Bamforth, P B (1976)
“Temperature prediction and it’s significance”
In: *Proc seminar Carry on casting*, Cement and Concrete Association, Fulmer Grange, Slough, February 1976

Bamforth, P B (1978)
Advantages from temperature studies
In: Proc paper presented at symposium *How hot is your concrete and does it matter?*
Cement and Concrete Association, June 1978, C&CA Wexham Springs, now BCA, Camberley, Surrey

Bamforth, P B (1980)
“In situ measurement of the effects of partial Portland cement replacement using either fly ash or ground granulated slag on the performance of mass concrete”
Proc. Instn. Civ. Engrs. **69**, Part 2, Sept 1980, pp 777-800

Bamforth, P B (1982)
Early-age thermal cracking in concrete
Institute of Concrete Technology, Technical Note TN/2, Slough

Bamforth, P B and Price, W F (1995)
Concreting deep lifts and large volume pours
Report 135, CIRIA, London

Bamforth, P B (1984)
Mass concrete
Concrete Society, Digest No.2, 1984, Camberley, Surrey
<<http://products.ihs.com/cis/Doc.aspx?AuthCode=&DocNum=50470>>

Bamforth P B and GRACE W R (1988)
“Early-age thermal cracking in large sections – towards a design approach”
In: *Proc conf Asia Pacific, Roads, highways and bridges*, Institute for International Research, Hong Kong, 1988, 29 pp

Bamforth, P B (2004)
Enhancing reinforced concrete durability – Guidance on selecting measures for minimising the risk of corrosion of reinforcement in concrete
Concrete Society Technical Report 61, Camberley, Surrey, ISBN 1 90448 211 2

Bamforth, P B and Price, W F (1995)
Concreting deep lifts and large volume pours
Report 135, CIRIA, London

Barnett, S J, Soutsos, M N, Bungey, J H and Millard, S G (2005)
“The effect of ground granulated blastfurnace slag on the strength development and adiabatic temperature rise of concrete mixes”
In: Dhir R K, Harrison, T A and Newlands, M D (eds), *Proc Int Conf Cement combinations for durability*, University of Dundee, 5-7 July, Thomas Telford, pp 165-172

Base, G D and Murray, M H (1978)
Thermal and shrinkage cracking in reinforced concrete
Australian Engineering and Building Industries Research Association Ltd

Beeby, A W (1978a)
“Corrosion of reinforcing steel in concrete and its relation to cracking”
The Structural Engineer, March 1978, **56A** (No. 3), pp 77-82

Beeby, A W (1978b)
“Cracking and corrosion”
Concrete in the Oceans Technical Report 1 CIRIA/Cement and Concrete Association/
Department of Energy, 1978, Concrete in the Oceans Research Programme

Beeby, W and FORTH, J P (2005)
“Control of cracking walls restrained along their base against early thermal movements”
In: *Proc 6th Int. Cong. on Global construction, ultimate concrete opportunities*, Dundee University, July 2005, pp 123-132. Published by Thomas Telford, London, ISBN 0 72773 387 7

Beeby, W (1990)
Fixings in cracked concrete – The probability of coincident occurrence and likely crack width
TN136, CIRIA, London

Van Beek, A, Baetens, B E J and Schlangen, E (2001)
“Numerical model for prediction of cracks in concrete structures”
In: *Proc RILEM PRO 23, Early-age cracking in cementitious systems*, **5**, Haifa, Israel, pp 39-48

Berwanger, C and Sarkar, A F (1976)
“Thermal expansion of concrete and reinforced concrete”

J. Am. Concr. Inst. November 1976, **73**, 618-621

Blundell, R and Bamforth, P B (1975)
“Humber tests prove Cemsave heat effect”
New Civil Engineer, 24 July 1975, 25-25

van Breugle, K and Lokhorst, S J (2001)
“The role of microstructural development on creep and relaxation of hardened concrete”
In: *Proc RILEM PRO 23, Early-age cracking in cementitious systems*, **1**, Haifa, Israel, pp 3-10

Browne, R D (1972)
“Thermal movement in concrete”
Concrete, November 1972, **6**, pp 51-53

Campbell-Allen, D (1979)
“*The reduction of cracking in concrete*”
The University of Sydney, May 1979

Clear, C (1985)
The effects of autogenous healing upon the leakage of water through cracks in concrete
Cement and Concrete Association, Technical Report 559, May 1985, BCA, Camberley, Surrey

Concrete Society (2004)
In situ strength of concrete – An investigation into the relationship between core strength and the standard cube strength
Working party of the Concrete Society, Project Report No 3, BCA, Camberley, Surrey, ISBN 0 94669 186 X

Dhir, R, Paine, K A and Zheng, L (2006)
Design data for use where low heat cements are used
DTI Research Contract No. 39/680, CC2257, University of Dundee, Report No CTU2704

Domone, P L J (1974)
Uniaxial tensile creep and failure of concrete
Magazine of Concrete Research, **26** (No 88), Sept 1974, pp 144-152

Emborg, M (1989)
Thermal stresses in concrete structures at early ages
Doctoral Thesis 1989:73D, Division of Structural Engineering, University of Technology, Sweden

Gerard, B Reinhardt, H W and Breysse D (1997)
“Measured transport in cracked concrete”
In: H W Reinhardt (ed), *Penetration and permeability of concrete – Barriers to organic and contaminating liquids*, RILEM Report 16, Chapter 8, E&F Spon, pp 265-324

Harrison, T (1992)
Early-age thermal crack control in concrete
R91, CIRIA, London

Henriksen, K R (1983)
“Avoidance of cracking at construction joints and between solid sections”
Nordisk Betong 1, 1983, pp17-27

- Highways Agency (1989)
 “Early thermal cracking of concrete”
Design manual for roads and bridges, Vol 1 Highways structures: Approval procedures and general design, Section 3: General design, HA BD 28/87, Incorporating Amendment No1, HMSO
- Houston, J T, Atimtay, E and Refguson, P M (1972)
Corrosion of reinforcing steel embedded in structural concrete
 Research Report 112-1F, Project 3-5-68-112, Centre for Highway Research, The University of Texas, Austin, March 1972
- Hunt, J G (1972)
Temperature changes and thermal cracking in concrete pavements at early-age
 Cement and Concrete Association (now BCA), Technical Report 42, 460, April 1972, Camberley, Surrey
- HUGHES, B (1971)
 “Control of early-age thermal and shrinkage cracking in restrained reinforced concrete walls”
 TN21, CIRIA, London
- Kandstad, T, Bjøntegaard, Ø, Sellevold, E and Hammer, T A (2001)
 “Crack sensitivity of bridge concretes with variable silica fume content”
Improved performance of Advanced Concrete Structures – IPACS, Report BE96-3843/2001:48-6, 2001, Selmer Skanska, Trondheim, Norway, ISBN 9 18958 077 X
- Khushefati W H A (2004)
 “Healing of cracks in concrete” PhD thesis, Imperial College, Department of Civil and Environmental Engineering, University of London
- Kurita, M, Goto, S, Minehishi, K, Negami, Y and Kuwuhara, T (1990)
 “Precooling concrete using frozen sand”
Concrete International, June 1990, pp 60-65, Detroit, Michigan
- MET OFFICE (2006)
 <<http://www.metoffice.gov.uk/>>
- Nambiar, O N N and Krishnamurthy, V (1984)
 “Control of temperature in mass concrete pours”
Indian Concrete Journal, March 1984, pp 67-73
- Narayanan, R S and Beeby, A W (2005)
 “Designers’ Guide to EN 1992-1-1 and EN 1992-1-2 Eurocode 2: Design of Concrete Structures. General rules and rules for buildings and structural fire design”
 Thomas Telford, London ISBN 0 72773 105 X
- Ohno, Y, Praparntanatorn, S and Suzuki, K, (1966)
 “Influence of cracking and water cement ration macrocell corrosion of steel in concrete”
 In: Page C L, Bamforth P B and Figg J W (eds), *Corrosion of reinforcement in concrete*, The Royal Society of Chemistry, pp 24-36 1996, Cambridge, ISBN 0 85404 731 X
- Pane, I and Hansen, W (2002)
 “Concrete Hydration and Mechanical Properties under Nonisothermal Conditions”
ACI Materials Journal, **99** (No 6), November/December 2002, 24–33pp, Detroit, Michigan
- Papworth, F (1996)
 “Low heat concrete”
 In: Proc Concrete Institute of Australia Seminar, Perth, September 1996

Pigeon, M, Bissonnette, B, Marchand, J, Boliy, D and Barcelo, L (2005)
“Stress relaxation of concrete under autogenous early-age restrained shrinkage”
ACI, Special Publication, SP-227-16, Detroit, Michigan

Raupach, M (1966)
“Corrosion of steel in the area of cracks in concrete – Labotaroty test and calculations using a transmission line model”
In: Corrosion of Reinforcement in Concrete, (Ed. Page, Bamforth and Figg), The Royal Society of Chemistry, pp 13-23. 1996

Redhead, A A (1979)
The Ladbroke Report – An investigation into the effects of early thermal movements
Chartered Institution of Water and Environmental Management, London (formerly Institution of Water Engineers and Scientists), October 1979

Reinhardt, H W and Rinder, T (1998)
“High strength concrete under sustained tensile loading”
Ototo-Graf-Journal, **9**, pp 123-134
<www.mpa.unistuttgart.de/publikationen/otto_graf_journal/ogj_1998/beitrag_reinhardt_rinder.pdf>

Robbins, J (1991)
“Cool Customer”
New Civil Engineer, 12 Sept 1991, 18–19 pp

Sato, S, Hattori, K and Ogata, H (2001)
“Mechanical properties in massive concrete specimens with different initial curing conditions” In: Banthai, N, Satai, K and Gjørsv, O E (eds) *Proc 3rd Int. Conf. Concrete under severe conditions, CONSEC '01*, University of British Columbia, Vancouver, Canada, 18-20 June 2001, 1554-1561

Schleech, W (1962)
“Die Zwangspannungen in eiseitig festgehaltenen Wand shceiben” (The positive strains in one way restrained EALLS)
Beton und Stahlbetonbau, March 1962, **57**, (No.3), pp 63-72

Sellevoid, E J and Bjøntegaerd, Ø (2006)
“Coefficient of thermal expansion of cement paste and concrete”
Materials and Structures, July 2006, **39**, 809-813, University of British Columbia, Vancouver, Canada

Swaddiwudhipong, S, LU, H R and Lee, T H (2001)
“Probabilistic model for tensile strain capacity of concrete”
In: Banthai, N, Satai, K and Gjørsv, O E (eds) *Proc 3rd Int. Conf. Concrete under severe conditions, CONSEC '01*, University of British Columbia, Vancouver, Canada, 18-20 June 2001, 1602-1609

Sugiyama, H, Masuda, Y and Abe, M (2000)
“Strength development of concrete cured under high temperature conditions at early-age”
In: *Proc 5th Int. Conf. Durability of concrete*, Spain, 2000, ACI SP 192-59, 965-982

Sule, M (2003)
Effect of reinforcement on early-age cracking in high strength concrete
Delft University Press, Netherlands, May 2003, ISBN 9 040723 915 E

Tasdemir, M A, Lydon, F D and Barr. B I G (1996)
“The tensile strain capacity of concrete”
Magazine of Concrete Research, Sept 1996, **48**, (No. 176) pp 211-218

Vitharana, V and Sakai, K (1995)
“Early-age behaviour of concrete sections under strain induced loadings”
In: Satai, K, Banthai, N, and Gjorv, O E (eds) *Proc 2nd Int. Conf. Concrete under severe conditions CONSEC '95*, Sapporo, Japan, 2-4 August 1995, 1571-1581

Wadso J (2003)
An experimental comparison between isothermal calorimetry, semi-adiabatic calorimetry and solution calorimetry for the study of cement hydration
Technical Report 533, Nordtest Project No. 1534-01, March 2003, Nordtest,
Tekniikantie 12, FIN-02150 Espoo, Finland

Witte, H J G (2001)
“Geothermal response test: The design and engineering of geothermal energy systems”
Europäischer Workshop über Geothermische Response Tests, EPFL, Lausanne, 26-27 October 2001

British Standards

BS 6089:1981 *Guide to assessment of concrete strength in existing*

BS8500-1:2000 *Concrete – Complementary British Standard to BS EN206-1 – Part 1: Method of specifying and guidance for the specifier*

BS8500-2:2002 *Concrete – Complementary British Standard to BS EN206-1 – Part 2: Specification for constituent materials for concrete*

BS8110-2: 1985 *Structural use of concrete – Part 2, Code of practice for special circumstances*

BS8500-1:2000 *Concrete – Part 1: Complementary British Standard to BS EN206-1 – Part 1: Method of specifying and guidance for the specifier*

BS8500-2:2002 *Concrete – Part 2: Complementary British Standard to BS EN206-1 – Part 2: Specification for constituent materials for concrete*

BS EN 206-1:2000 *Concrete – Part 1: Specification, performance, production and conformity*

BS 8007:1987 *Design of concrete structures fo retaining aqueous liquids*

Eurocodes

EN1770: 1998 *Products and systems for the protection and repair of concrete structures. Test methods. Determination of the coefficient of thermal expansion*

EN196-8: 2003 *Methods of testing cement. Heat of hydration. Solution method*

EN196-9: 2003 *Methods of testing cement. Heat of hydration. Semi-adiabatic method*

EN1992-1-1:2004 *Eurocode 2. Design of concrete structures. General rules and rules for buildings*

EN1992-3:2006 *Eurocode 2: Design of concrete structures – Part 3: Liquid retaining and containment structures*

National Annex to BS EN 1992-1-1:2004

Appendices

These are on the CD which accompanies this publication:

- A1 Heat generation, temperature rise and temperature differentials
- A2 A model for predicting the temperature rise and temperature differentials using adiabatic temperature data
- A3 Estimating drying shrinkage using the method of EN1992-1-1
- A4 Estimating autogenous shrinkage
- A5 Estimating restraint
- A6 Estimating tensile strain capacity
- A7 Evaluating risk/extent of cracking using a strain based approach
- A8 Reinforcement design to control crack widths
- A9 The effect of peak temperature on the *in situ* strength
- A10 Assessment of the *in situ* tensile strength of concrete

Spreadsheet calculators

Model for prediction of temperature rise and thermal gradients

EN1992-1-1 drying shrinkage calculator

EN1992-1-1 autogenous shrinkage calculator

Restraint calculator based on the ACI method for wall

Crack width calculator for edge restraint, end restraint and internal restraint

A1 Heat generation, temperature rise and temperature differentials

A1.1 Influencing factors

For the control of early-age thermal cracking, there are two important temperature considerations:

- the temperature rise above that of the adjoining concrete or substrate (eg hard rock). This depends on the location of the point being considered and is applicable to conditions of external restraint (eg casting a wall onto a rigid mature base)
- the maximum temperature differential and the thermal gradient within the section. This is the condition of internal restraint.

In the calculation of restrained early-age temperature movements in concrete, it is necessary to define the basis upon which the temperature drop from the peak temperature is calculated. This requires a definition of the placing temperature of the concrete, the maximum temperature rise and the temperature to which the element will return after cool down.

The **placing temperature** is as defined, the temperature of the concrete when placed into the forms. This may differ from the temperature at the mixing plant. As a general rule it has been assumed that the mixing temperature of the concrete will be 5°C above the **mean ambient temperature** as a result of the energy input during the mixing process. A review of published data (Concrete Society 2004, Anson *et al*, 1988) yielded mean values of 4.7 °C for winter concreting and 6.3 °C for summer concreting, with an overall mean of 5.5 °C although in each case there was a wide range of values as shown in Figure A1.1. Hence, while it may, in general, be appropriate to use a single design value of 5 °C, and this has been assumed in the presentation of T_l values, in circumstances where a greater value may be expected (eg in winter conditions when materials are heated or when there is a long haulage time) the margin should be adjusted accordingly.

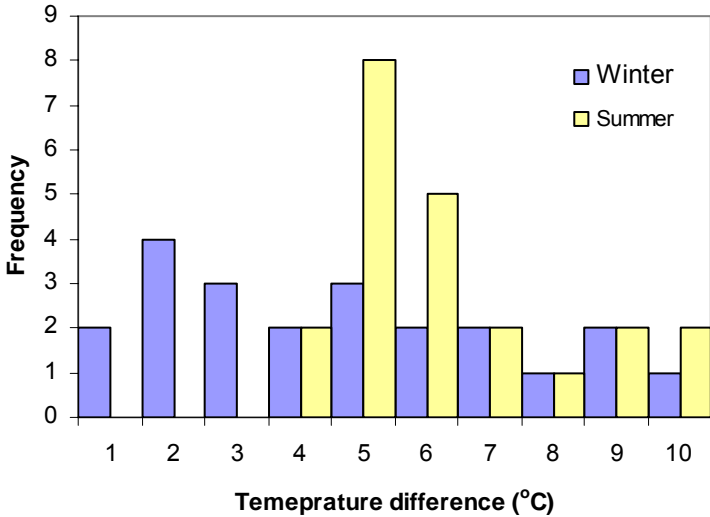


Figure A1.1 Measured values of the temperature difference between the concrete placing temperature and the mean ambient temperature during winter and summer concreting (Concrete Society, 2004; Anson *et al*, 1988)

Within the design equations, the **temperature rise** is assumed to be the difference between the placing temperature and the maximum temperature achieved during the early thermal cycle. However, some of the heat generated by the fresh concrete is transferred to adjoining concrete and its temperature rises also. For calculating the risk of cracking and the amount of crack control reinforcement, the temperature rise should be the peak

Licensed copy: HALCROW GROUP LTD, 16/03/2007, Uncontrolled Copy, © CIRIA

temperature in the new element less the temperature of the adjoining concrete occurring at the same time. To determine the extent to which heat is transferred across the joint would require a detailed thermal analysis for each situation. Hence, for practical purposes, and recognising that it is a conservative assumption, this heat transfer is ignored and the adjoining concrete is assumed to remain at the mean ambient temperature. This design assumption is offset when restraint factors are derived from observations on completed structures as these values will have taken this heat transfer effect into account.

In addition, uniaxial heat flow is assumed and the peak temperature at mid-section is normally used in the calculations. Again this is a conservative assumption as the bulk contraction will be determined by the mean temperature through the section. Depending on the allowable temperature differential, the mean value may, typically, be 5 to 10°C below the maximum value at the centre of the section.

The temperature rise depends upon the rate at which the heat is evolved, the total heat output and the rate of cooling. The heat generating characteristics are influenced by both the binder chemistry and its fineness. In thin sections, the rate of heat evolution is dominant in determining the temperature rise. In massive sections, where the heat loss is relatively slow compared with the heat being generated, the temperature rise is more dependent on the total heat evolved. The main variables influencing the temperature rise are:

- binder content
- types and sources of cementitious material
- other concrete constituents and mix proportions that influence the thermal properties of the concrete
- concrete placing temperature
- section thickness
- formwork and insulation and its time of removal
- ambient conditions
- active forms of temperature control such as internal cooling pipes.

It is important to appreciate that the best way to estimate the likely temperature rise is from measurement of the heat generating characteristics of the particular concrete, using the same cement or combination, aggregate type and mix proportions. This avoids errors that may occur in the assumptions regarding the thermal properties of the concrete (ie thermal conductivity, specific heat). However, at the design stage this is rarely possible and this Appendix (A1) provides estimates of the temperature rise likely to occur for a range of combinations of cement content, cement type, section thickness and formwork type.

The **temperature drop**, T_f , which determines the thermal contraction during cool down, is defined as the difference between the peak temperature and the mean ambient temperature.

A1.2 Binder content

As only the binder produces heat of hydration, the higher the binder content, the greater the heat evolved per unit volume and the greater the temperature rise. Along with the cement, combination and addition types (Sections A1.3 and A1.4) the binder content has a major effect on the temperature rise. However, because the temperature rise in thinner section is determined largely by the rate at which heat is generated, there is not direct proportionality between temperature rise and binder content in thinner sections, as shown in Figure A1.2 for concretes with CEM I contents ranging from 220 kg/m³ to 460 kg/m³. For this reason, for elements with a thickness of less than about 1.0 m there is no simple formula linking temperature rise to unit cement weight.

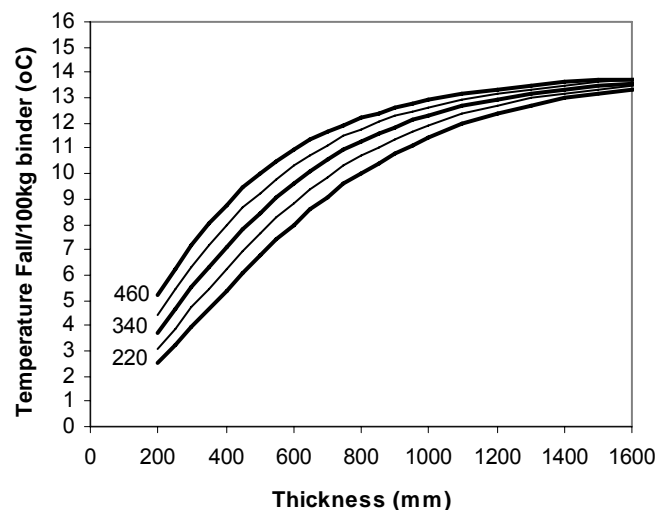


Figure A1.2 Relationship between unit temperature rise (per 100 kg binder) and section thickness (derived from data from University of Dundee) (Dhir et al, 2006)

A1.3 Cements and combinations

In Europe and the UK the most readily available cements are specified to the British and European Standard BS EN 197-1: 2000 Cement, composition, specification and conformity criteria for common cements (amended in July 2004). This standard covers 27 different types of cement available across Europe but only a proportion of these are likely to be available in any particular European country.

In the UK cement is often available as a combination, that is a combination of Portland cement (CEM I) with either ground granulated blastfurnace slag (ggbs), fly ash (also known as pulverized-fuel ash, pfa), or limestone fines. Strength class and other requirements equivalent to that set out in EN 197-1 are confirmed using the procedures and guidance set out in BS 8500-2 *Concrete – Complementary British Standard to BS EN 206-1 - Part 2: Specification for constituent materials and concrete*.

Also available in the UK is cement to the British Standard BS 4027 *Sulfate resisting Portland cement (SRPC)*. BS EN 197-4 is the British and European Standard for *Cement – Composition, specifications and conformity criteria for low early strength blastfurnace cements* and covers blastfurnace cements not covered by BS EN 197-1. Another European cement standard, BS EN 14216: 2004 *Cement – Composition, specifications and conformity criteria for low heat special cements* was published in 2004. BS 4027 and BS EN 14126 special cements are not going to be as readily available as EN 197-1 cements or BS 8500 combinations and so where these materials are required then it is prudent to confirm availability.

Table A1.1 lists cement types and combinations along with their designations and major constituents. Except for SRPC all cements listed may contain 0-5 of a minor additional constituent (mac).

Depending on the particular type of cement it may come in a range of strength classes, where each strength class is classified by a minimum early-age strength at either two or seven days, and by a strength range at 28 days. A summary of the strength classes is shown in Table A1.2 together with the requirements for initial setting time. In general the lower the strength class the lower the reactivity of the cement and hence the likelihood that the heat of hydration will also be lower. For example the strength class for Very Low Heat Special Cements to BS EN 14126 is the lowest class of 22.5, and this type of cement is considered particularly suitable for dams and similarly massive construction.

With respect to early-age thermal cracking it is worth noting that EN 197-1 includes a low heat classification for common cement, defined as cements with a heat of hydration that does not exceed the characteristic value of 270 kJ/kg, determined in accordance with either BS EN 196-8 at 7 days or in accordance with BE EN 196-9 at 41

hours. Similarly for Very low Heat Special Cement they are defined as a cement with a heat of hydration that does not exceed the characteristic value of 220 kJ/kg.

Such low heat is commonly obtained using combinations or additions using fly ash or ggbs. In a comprehensive study at the University of Dundee (Dhir *et al*, 2006) using a variety of combinations, limits were derived for the addition content required to achieve Low Heat and Very Low Heat classes as shown in Table A1.3. Two sources of ggbs and fly ash were combined with a single source of CEM1. The additions were differentiated by fineness and it can be seen that in each case the higher reactivity associated with higher fineness required that a higher proportion of addition was needed to achieve each heat class. It is also apparent that fly ash is almost twice as effective as ggbs in reducing heat output. However, when designing concrete of equal strength class, in either case some of the benefit may be offset by the need for a higher binder content.

Unfortunately, because of the complex nature of hydration reactions, there is no direct relationship between standard heat of hydration limits, such as the EN 197-1 CEM cement Low Heat (LH) and Very Low Heat (VLH) limits, and the temperature generated within large concrete sections. Furthermore, it should be appreciated that the heat of hydration test for cement is not what most designers are interested in and it is more effective to specify directly the performance limits for the concrete. However, where the heat of hydration information is available it should help select the most appropriate source and type of cement to help minimize the early-age temperature rise.

Prior to April 1989, when standard strength classes were introduced, Portland cement was classified as either: ordinary Portland cement, OPC, or rapid hardening Portland cement, RHPC. The terms Ordinary, "OP" or "OPC" and "RHPC" remain in colloquial use although the correct identification is CEM I, or Portland cement. The RHPC classification has been replaced by the rapid early-age strength classes denoted "R".

Some example standard cement and combination designations are shown in Table A1.4, but the manufacturer will normally require reasonable notice to confirm the availability of any Low Heat or Very Low Heat properties of cements and combinations.

The cement chemistry and fineness determine the rate of heat evolution and the total heat output. As standards specify only minimum requirements, the heat generating characteristics may vary within a particular cement type. For example, values of heat generated by seven UK CEM I cements are shown in Table A1.5. Values vary by about ± 10 per cent from the mean value. A similar range was reported by Dhir *et al* (2006) with 41 hour values ranging from 327 to 372 kJ/kg from nine cements tested. For critical structures, it may be appropriate to obtain results for the cement or combination to be used.

A1.4 Additions

The greatest difference to heat generation achieved through material selection is by the use of mineral additions such as ground granulated blast-furnace slag (ggbs) and fly ash. It has been recognized for many years that significant benefits in terms of reduced temperature rise may be achieved with these materials.

A1.4.1 Ground granulated blast-furnace slag

Ground granulated blast-furnace slag (ggbs) is a latent hydraulic material, but in practice it needs to be blended with a proportion of CEM I to give an adequate rate of strength development. Within the context of European Standards (see Table A1.1) the proportion of slag in a cement or combination may vary from 6 to 95 per cent but in practice it is most commonly used in the range from 30 to 70 per cent.

Where slag cements or combinations are used as an alternative to CEM I, the proportion of slag is typically in the range 40 to 50 per cent. At this level it is normally possible to achieve a specified strength class with similar binder contents and similar w/b ratios to those in a CEM I concrete.

Table A1.1 *Nomenclature and composition for cements and combinations*

Cement type	Cement		Designation of Combination ^a	Constituents of cement or combination					
	Standard	Designation		% clinker or CEM I	% fly ash ^b	% ggbs	% lime-stone	% silica fume	% meta-kaolin
Sulfate-resisting Portland	BS 4027	SRPC	—	100	—	—	—	—	—
Portland	BS EN 197-1	CEM I	—	95-100	—	—	—	—	—
Portland-fly ash	BS EN 197-1	CEM I CEMENTII/A-V	CIIA-V	80-94	6-20	—	—	—	—
		CEM I CEMENTII/B-V	CIIB-V	65-79	21-35	—	—	—	—
Portland slag	BS EN 197-1	CEM I CEMENTII/A-S	CII-S	80-96	—	6-20	—	—	—
		CEM I CEMENTII/B-S		65-79	—	21-35	—	—	—
Portland limestone	BS EN 197-1	CEM I CEMENTII/A-L	CIIA-L	80-94	—	—	6-20 ^c	—	—
		CEM I CEMENTII/A-LL	CIIA-LL	80-94	—	—	6-20 ^d	—	—
Portland silica fume	BS EN 197-1	CEM I CEMENTII/A-D	^h	90-94	—	—	—	6-10	—
Portland pozzolana	BS EN 197-1	CEM I CEMENTII/A-Q ^f		80-94	—	—	—	—	6-20
Blastfurnace	BS EN 197-1	CEM I CEMENTIII/A	CIIIA	35-74	—	36-65	—	—	—
	&	CEM I CEMENTIII/B	CIIB	20-34	—	66-80	—	—	—
	BS EN 197-4	CEM I CEMENTIII/C	—	43-58	—	81-95	—	—	—
Pozzolanic	BS EN 197-1	CEM I CEMENTV/A (V)	—	65-89	11-35	—	—	—	—
		CEM I CEMENTV/B (V)	CIVB (V)	45-64	36-55	—	—	—	—
Composite	BS EN 197-1	CEM V/A	—	40-64	18-30	18-30	—	—	—
		CEM V/B (*)	—	20-30	31-50	31-50	—	—	—
Very Low Heat Blastfurnace	BS EN 14216	VLH III/B	—	20-34	—	66-80	—	—	—
		VLH III/C	—	5.19	—	81-95	—	—	—
Very Low Heat Pozzolanic	BS EN 14216	VLH IV/A (V)	—	65-89	11-35	—	—	—	—
		VLH IV/B (V)	—	45-64	36-65	—	—	—	—
Very low heat Composite	BS EN 14216	VLH IV/A (*)	—	45-64	36-55	—	—	—	—
		VLH IV/B (*)	—	20-30	31-50	31-50	—	—	—

Notes to Table

Where the cement and combinations is identified by the shaded area of the table then it is prudent to confirm availability.

a Combinations of CEM I CEMENT with either fly ash, ggbs or limestone fines conforming to BS 8500-2

b Siliceous fly ash only in the UK

c Maximum total organic carbon content of limestone 0.50% by mass

d Maximum total organic carbon content of limestone 0.20% by mass

e These combinations are not currently covered by BS 8500-2: 2002, Annex A. However silica fume can be used in accordance with Clause 5.2.5 of BS EN 206-1: 2000. Until BS EN 13263 is published, the silica fume should conform to an appropriate Agrément certificate.

f Metakaolin only

* The components other than clinker to be declared, that is V for siliceous fly ash, S for ggbs,

Table A1.2 *Cement strength classes*

Strength class	Standard	Compressive strength, MPa				Initial setting time
		Early Strength		Standard strength		
		2 day	7 day	28 days		min
22,5	BS EN 14216	-	-	≥ 22,5	≤ 42,5	≥ 75
32,5 L	BS EN 197-4	-	≥ 12,0	≥ 32,5	≤ 52,5	
32,5 N	BS EN 197-1	-	≥ 16,0			
32,5 R	BS EN 197-1	≥ 10,0	-			
42,5 L	BS EN 197-4	-	≥ 16,0	≥ 42,5	≤ 62,5	≥ 60
42,5 N	BS EN 197-1	≥ 10,0	-			
42,5 R	BS EN 197-1	≥ 20,0	-			
52,5 L	BS EN 197-4	≥ 10,0	-	≥ 52,5	-	≥ 45
52,5 N	BS EN 197-1	≥ 20,0	-			
52,5 R	BS EN 197-1	≥ 30,0	-			

SRPC to BS 4027 may be supplied in strength class 32,5N, 32,5R, 42,5N, 42,5R and 52,5N where the early and standards strengths are as set out above. The initial setting time of SRPC to BS 4027 is not less than 60 min for 32,5N, 32,5R, 42,5N, 42,5R strength classes and not less than 45 min for the 52,5N strength class.

Table A1.3 *Minimum limits of addition content to achieve low heat and very low heat classes*

Heat Class	GGBS A	GGBS B	Fly Ash A	Fly Ash B
Fineness	602 m ² /kg	466 m ² /kg	7.2% retained on 45 µm sieve	35 % retained on 45 µm sieve
Low heat	56%	39%	25%	20%
Very low heat	69%	58%	42%	36%

Table A1.4 *Example standard cement and combination designations*

Example	Definition	EN designation	BS8500-2
1	Portland cement conforming to EN 197-1 of strength class 42,5 with a high early strength	Portland cement EN 197-1 CEM I CEMENT 42,5 R	
2	Portland-fly ash cement containing between 21 and 35% by mass of fly ash of strength class 42,5 with an ordinary early strength	Portland-fly ash cement EN 197-1 - CEM I CEMENTII/B V 42,5 N	Combination of similar composition is identified by CIIB-V
3	Blastfurnace cement conforming to EN 197-1 containing between 66% and 80% by mass of granulated blastfurnace slag of strength class 32,5 with an ordinary early strength and a low heat of hydration	Blastfurnace cement EN 197-1 - CEM I CEMENTII/B 32,5 - LH	Combination of similar composition is identified by the designation CIIB
4	Very Low heat special pozzolanic cement conforming to BS EN 14216 containing between 36% and 55% siliceous fly ash (V) of strength class 22,5 and a very low heat of hydration	Very low heat special pozzolanic cement EN 14216 - VLH IV/B (V) 22,5	Combination of similar composition is identified by CIVB (V)

Table A1.5 *Examples of heat of hydration for seven CEM I materials (W F Price, 2006) obtained using the semi-adiabatic method of EN197-9:2001*

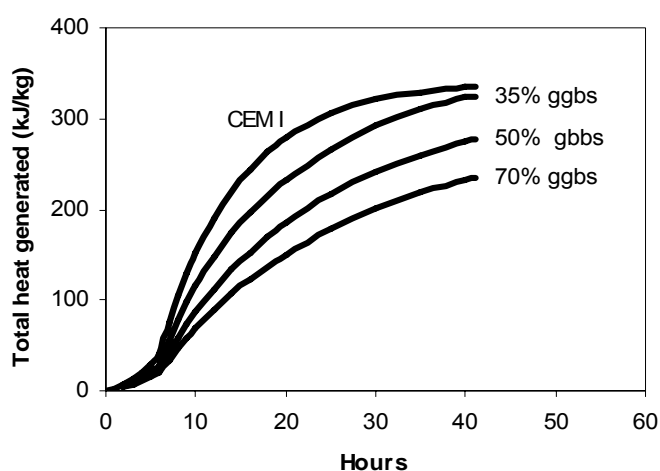
Time	Total heat of hydration (kJ/kg)						
12h	244.2	235.1	251.5	250.9	302.1	281.4	302.7
24 h	309.9	302.1	318.5	325.4	366.2	357.8	382.7
41 h	321.1	341.0	339.7	339.6	374.6	375.7	395.5
48 h	323.7	348.5	342.5	342.0	375.3	374.4	396.5
72 h	329.8	356.5	344.5	349.9	377.8	380.0	307.3
120 h	347.0	347.0	351.1	356.2	378.0	381.2	401.2

At higher slag levels, required for example for sulphate resistance or to achieve LH or VLH cement (Table A1.3), equality of strength may not be achieved at 28-days and some increase in the binder content or reduction in the w/b ratio is likely to be needed to achieve the strength class. Any increase in binder content will partially offset the benefit of lower heat. In such cases the extent to which the binder content has to be increased may be minimised by extending the time allowed to achieve the specified strength to 56 days or longer. This may be justified by the fact that the 28-day strength of ggbs concrete is less adversely affected by temperature than CEM I concrete, thus achieving a higher *in situ* strength for a comparable strength class (see Appendix A9).

An example of the effect of increasing the proportion of ggbs on the rate of heat generation is shown in Figure A1.3 (Dhir *et al*, 2006).

CIRIA R135 (Bamforth and Price, 1995) provided an indication of the likely temperature rise in large volume pours in relation to pour thickness, cement/addition combination and unit temperature rise (Figure A1.4). These curves were derived empirically from measurements in large pours (Bamforth, 1980). Revised curves have been developed using the model described in Appendix A2 based on adiabatic temperature rise for materials currently available (Dhir *et al*, 2006). It is apparent that the heat generation of cements has increased since these curves were originally developed. However, the use of ggbs still enables a significant reduction in temperature rise per unit weight of binder.

The position in the UK at the time of publishing is that the current production of slag cements and ggbs will, in general, give a reduction in the peak temperature for a particular strength class. In the future, changes in grinding technology and practice may alter this position and it is recommended that data are sought from the suppliers of ggbs on the applicability of Figures A1.3 and A1.4 to their specific materials.

**Figure A1.3** *The results of semi-adiabatic tests on mortar with different levels of ggbs (Dhir *et al*, 2006)*

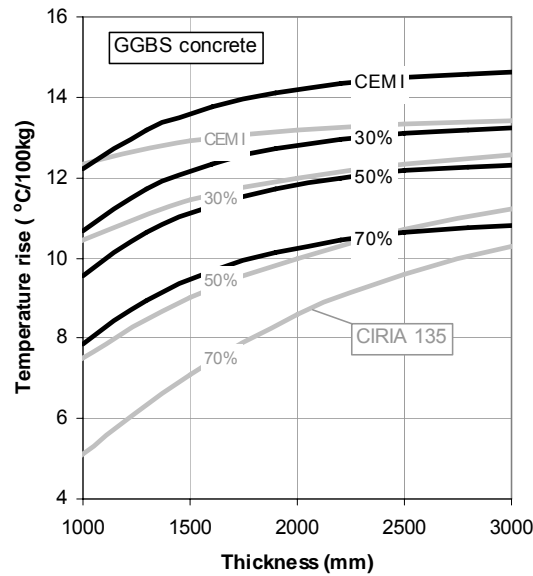


Figure A1.4 Unit temperature rise in relation to section thickness for concretes containing ggbs (Bamforth and Price, 1995). To obtain T_1 values 5°C should be added to the calculated temperature rise

At normal concrete placing temperatures, both the rate of heat evolution and the total heat evolved of CEM I /ggbs blends is lower than in the plain CEM I. The reactivity of ggbs is more sensitive to temperature than CEM I, increasing more rapidly with increasing temperature, and decreasing more rapidly with decreasing temperatures, particularly as the proportion of ggbs in the binder increases. At higher placing temperatures and with low levels of ggbs, the temperature rise per unit weight of binder may exceed that of CEM I

In practice, however, the temperature rises is normally lower when CEM I /ggbs concretes are used. The time taken for the peak temperature to occur is longer than for the plain CEM I concrete. This peak temperature occurs in the form of a plateau value which can last for around 20 h, depending on the section thickness.

A1.4.2 Fly ash

This report concerns itself mainly with the use and application of fly ash from coal fired power stations complying with BS EN450-1:2005 Category S or Category N fly ash for use as a Type II addition in structural concrete or the equivalent fly ash based cements such as CEM II B-V or CEM IV B-V. Fly ash to the quality and specification for Category S, is very restrictive and is a high quality fly ash product. The application of the procedures given in this guide should give safe solutions when using Category N fly ash.

In the context of European Standards (see Table A1.1) the proportion of fly ash in a cement or combination may vary from 6 to 65 per cent but in practice it is most commonly used in the range from 20 to 40 per cent.

As the strength development for concrete cured at 20°C is slower for fly ash based mixtures, these concretes generally require a lower w/b ratio than CEM I concrete of the same strength class. Some reduction in w/b may be achieved by the use of the fly ash itself and an additional reduction may be achieved through the use of admixtures. However, it is likely an increase in the binder content will be needed compared with CEM I concrete to achieve a particular strength class and this needs to be taken into account when estimating the temperature rise. In general, this will only partially offset the benefit of reduced heat generation and the use of fly ash will, in most cases, be beneficial with regard to the lowering of temperature rise.

The extent to which the binder content has to be increased compared with CEM I concrete of the same strength class may be minimised by extending the time allowed to achieve the specified strength to 56 days or longer. This may be justified by the fact that the 28-day strength of fly ash concrete is less adversely affected by temperature than CEM I concrete, thus achieving a higher *in situ* strength for a comparable strength class (see Appendix A9).

High lime fly ashes are not presently available in the UK. These vary considerably in their performance, particularly if “free lime” is available. No guidance is given in this guide on the use of such materials. Fly ash produced from semibituminous and lignite coals are influenced by the burning temperature. Burning temperatures above 1250 °C can produce fly ashes with similar morphology to granulated slag. No guidance is given in this Report on the use of these materials.

The research at the University of Dundee (Dhir *et al*, 2006) tested two sources of fly ash at levels up to 65 per cent of binder. Some typical results obtained in the semi-adiabatic test for are shown in Figure A1.5.

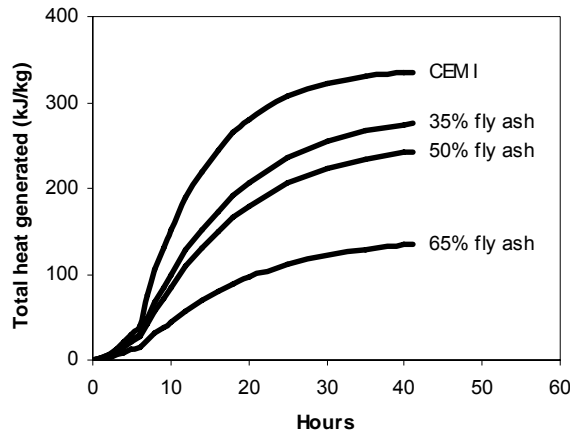


Figure A1.5 The results of semi-adiabatic tests with different levels of fly ash (Dhir *et al*, 2006)

CIRIA R135 (Bamforth and Price, 1995) provided an indication of the likely temperature rise in large volume pours in relation to pour thickness, cement/addition combination and unit temperature rise (Figure A1.6). Revised curves have been developed using the model described in Appendix A2 based on adiabatic temperature rise for materials currently available (Dhir *et al*, 2006). It is apparent that the heat generation of has increased since these curves were originally developed. However, the use of fly ash still enables a significant reduction in temperature rise per unit weight of binder.

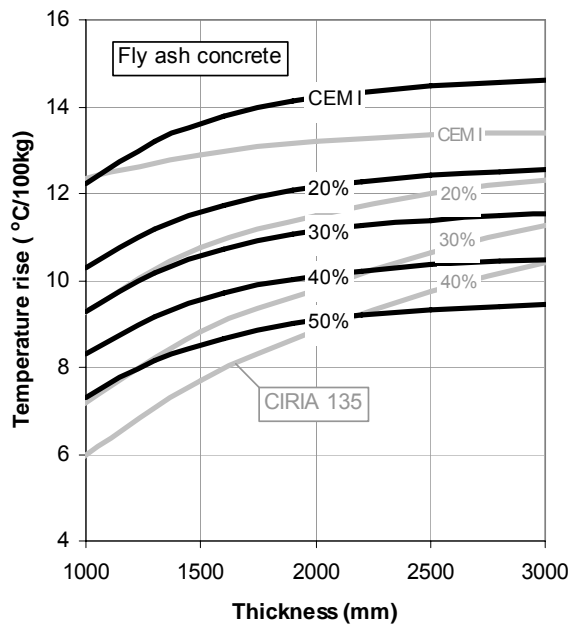


Figure A1.6 Unit temperature rise in relation to section thickness for concretes containing ggbs (Bamforth and Price, 1995). To obtain T_1 values 5 °C should be added to the calculated temperature rise.

A1.4.3 Silica fume

Silica fume is a by product extracted from the exhaust gases from silicon, ferrosilicon and other metal alloy smelting furnaces and is covered by the European Standard, EN 13263:1998. In the context of European Standards, addition rates are normally in the range 6 to 10 per cent wt of cement. The cementing efficiency is much higher than that of CEM I, and silica fume is most commonly used to produce very high strength concretes. It may also be used to achieve normal grades of structural concrete with a reduced binder content but this is less common. It is generally recognised that the heat generated by silica fume concrete is similar to that of CEM I at the same binder content (FIP, 1988) and more recent measurements have supported this (Kanstad *et al*, 2001). Hence any benefit in terms of temperature can only be achieved through a change in the binder content.

A1.4.4 Metakaolin

Metakaolin is a manufactured product formed by controlled thermal activation of clays with a high proportion of the mineral kaolinite (>90 per cent). Metakaolins that are commercially available in the UK are ground to fineness much greater than that of Portland cement. The primary constituents are similar to those of CEM I, but in different proportions, with predominantly silica and alumina. Metakaolin reacts only very slowly with water, but when mixed with cement in concrete, it reacts very rapidly (Lewis *et al*, 2003).

Metakaolin may be used either in partial replacement of, or in addition to, the CEM I in concrete, usually at levels of up to 20 per cent (by weight) depending on application. Typically, however, 8 to 15 per cent replacements are used. There are, as yet, no British, or European Standards specifically covering the specification and use of metakaolin in concrete. However, if covered by an Agrément certificate, the use of metakaolin is permitted by BS8500 for use in concrete.

With regard to heat generation, metakaolin is similar to silica fume in that, for a given binder content, there is not a significant difference compared with CEM I. However, benefits may be achieved by enabling the strength to be maintained while lowering the binder content.

A1.4.5 Limestone

Limestone fillers are permitted in cements or as mixer additions. Portland limestone cement contains 6 to 20 per cent limestone. As the limestone acts primarily as a filler, the heat of hydration is reduced but so is the strength and lower w/b, higher binder content mixes are needed to achieve the same strength class compared with CEM I concrete. This should be taken into account in assessing any low heat benefits when using limestone.

Measurements of semi-adiabatic temperature rise (Troli *et al*, 2003) resulted in a temperature rise of about 19 °C for a self-compacting concrete with 152 kg/m³ of CEM I 52.5R cement and 381 kg/m³ ground limestone. The temperature rise was consistent with the heat output from the CEM I alone. In terms of generating heat limestone filler may be assumed to be inert.

A1.5 Other mix parameters affecting temperature rise

Admixtures, which increase workability or retard the set of the concrete, have little direct effect on the peak temperature rise but may alter the time-scale of the temperature curve. However, their use is normally accompanied by a mix adjustment which can affect the temperature rise. For example, a water reducing admixture will normally result in lower binder content than a plain mix of the same strength class. It is this lower binder content, rather than the admixture, which results in a lower temperature rise. Provided durability is not impaired, workability aids can be effectively used to reduce the binder content and early-age thermal cracking. Accelerators are used mainly in cold weather, and as the calculation of temperature rise is normally based on warm weather placing, any increase in temperature rise as a result of using an accelerator is unlikely to exceed the design value.

The aggregate type and the concrete mix proportions influence both the thermal conductivity of the concrete and its specific heat capacity. These two properties are influential in determining temperature rise, the former determining the rate of heat flow and the latter the amount of heat required to generate a specific increase in temperature. Hence, if the temperature rise is to be modelled, data are needed on each of these properties.

Further detail on values of specific heat and thermal conductivity are given in Appendix A2 in relation to the prediction of temperature rise.

A1.6 Other factor affecting temperature rise

In addition to the concrete mix constituents and their proportions, a number of other factors are influential in determining the temperature rise. These include the concrete placing temperature, the section thickness, the formwork type and the time of removal, ambient conditions. These factors are all covered in Appendix A2 in relation to the model for predicting temperature rise.

A1.7 Estimating temperature rise and T_1 values

The design process requires the T_1 value as an input. In CIRIA R91 (Harrison, 1992), T_1 values were presented in tabular form for concretes with specific cement contents and for elements of specific thickness and for each condition a range of values was provided. In many cases, interpolation was required. In this report, as there are many more cement combinations considered, T_1 values are presented graphically. The values provided in CIRIA R91 (Harrison, 1992) had been initially derived and presented in CIRIA R91 (Harrison, 1992), and since that time the performance of cement has changed. A comparison of measured temperatures and the design values in CIRIA R91 (Harrison, 1992) indicates that the latter tends to underestimate the temperature rise that currently occurs. Figure A1.7 shows a comparison between measured values (Concrete Society, 2004, Anson *et al*, 1988) and values predicted for current cements using the upper values from the ranges provided in CIRIA R91 (Harrison, 1992). Data are presented for concrete cast in both summer and winter conditions.

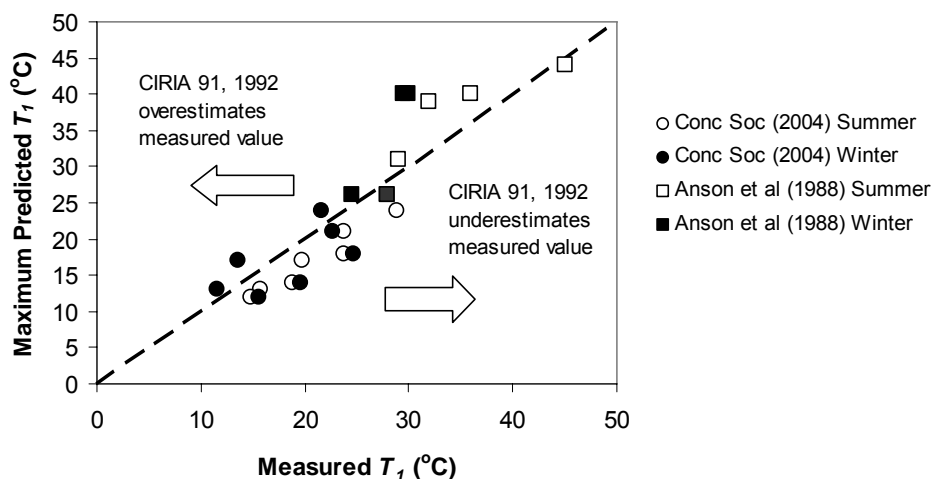


Figure A1.7 Comparison between T_1 values from CIRIA R91 (1992) and measured values

It may be deduced from Figure A1.7 that, in many cases, the prediction (even though based on the maximum value within the range) has significantly underestimated the measured value of T_1 , thus leading to unsafe design assumptions. The T_1 values should be modified to reflect the performance of modern cements.

At the University of Dundee (Dhir *et al*, 2006) a comprehensive investigation of the heat generating capacity of cements was carried out to provide additional information to support a modification to T_1 . These results have also indicated that the previously used T_1 values are no longer representative for all conditions. The difference is most significant for CEM I concrete cast into steel formwork (Table A1.6). In this case the revised T_1 values are generally increased to the extent that the lowest values current reported are approximately equal to the mid range of the values proposed by CIRIA R91 (Harrison, 1992). The difference is less significant for CEM I concretes cast into plywood formwork. These findings suggest that the total heat generated is not significantly different but that the rate of heat generation is initially higher.

Table A1.6 *Predicted T_I values for CEM I (Dhir et al, 2006) compared with the values given in CIRIA R91 (Harrison, 1992) (the lower values in italics are the CIRIA R91 values)*

SECTION THICKNESS (mm)	STEEL FORMWORK				18 MM PLYWOOD FORMWORK			
	Cement content (kg/m ³)				Cement content (kg/m ³)			
	220	290	360	400	220	290	360	400
300	6 - 9	8 - 13	11 - 17	12 - 20	10 - 15	14 - 21	18 - 28	21 - 33
	<i>5 - 7</i>	<i>7 - 10</i>	<i>9 - 13</i>	<i>10 - 15</i>	<i>10 - 14</i>	<i>14 - 19</i>	<i>18 - 26</i>	<i>21 - 31</i>
500	11 - 16	15 - 22	20 - 30	23 - 36	15 - 21	21 - 30	27 - 40	31 - 46
	<i>9 - 13</i>	<i>13 - 17</i>	<i>16 - 23</i>	<i>19 - 27</i>	<i>15 - 19</i>	<i>20 - 27</i>	<i>27 - 36</i>	<i>31 - 43</i>
700	15 - 22	21 - 30	27 - 40	32 - 47	19 - 26	26 - 36	33 - 47	38 - 54
	<i>13 - 17</i>	<i>18 - 24</i>	<i>23 - 33</i>	<i>27 - 39</i>	<i>18 - 23</i>	<i>25 - 32</i>	<i>34 - 43</i>	<i>40 - 49</i>
1000	20 - 28	28 - 38	36 - 50	41 - 57	23 - 30	31 - 42	40 - 54	45 - 61
	<i>18 - 23</i>	<i>24 - 32</i>	<i>33 - 43</i>	<i>39 - 49</i>	<i>22 - 27</i>	<i>31 - 37</i>	<i>42 - 48</i>	<i>47 - 56</i>

The study at the University of Dundee has also provided extensive information, previously unavailable, on combinations of CEM I with fly ash and ground granulated blast-furnace slag (ggbs): see for example Figures A1.3 and A1.5. Predicted values of T_I are given in Table A1.7 for concrete containing 50 per cent ggbs. In this case there is less difference between the predicted values and those estimated from the data in CIRIA R91 (Harrison, 1992).

Table A1.7 *Predicted T_I values for concrete with 50 per cent ggbs (Dhir et al, 2006) compared with the values given in CIRIA R91 (Harrison, 1992) (the lower values in italics are the CIRIA R91 values)*

SECTION THICKNESS (mm)	STEEL FORMWORK				18 MM PLYWOOD FORMWORK			
	Cement content (kg/m ³)				Cement content (kg/m ³)			
	220	290	360	400	220	290	360	400
300	5 - 6	5 - 8	6 - 10	7 - 11	7 - 10	9 - 13	11 - 16	13 - 18
	<i>5 - 6</i>	<i>6 - 8</i>	<i>7 - 10</i>	<i>8 - 11</i>	<i>9 - 11</i>	<i>12 - 15</i>	<i>15 - 19</i>	<i>17 - 22</i>
500	7 - 10	10 - 14	12 - 17	14 - 20	10 - 14	14 - 18	18 - 23	20 - 27
	<i>8 - 10</i>	<i>11 - 14</i>	<i>14 - 18</i>	<i>15 - 20</i>	<i>12 - 15</i>	<i>16 - 20</i>	<i>21 - 27</i>	<i>23 - 31</i>
700	10 - 14	14 - 18	18 - 24	20 - 27	13 - 17	18 - 23	23 - 30	27 - 35
	<i>11 - 14</i>	<i>15 - 18</i>	<i>19 - 23</i>	<i>21 - 27</i>	<i>15 - 18</i>	<i>19 - 25</i>	<i>25 - 33</i>	<i>28 - 38</i>
1000	14 - 18	19 - 25	26 - 33	30 - 39	17 - 21	23 - 29	31 - 38	36 - 44
	<i>15 - 18</i>	<i>19 - 24</i>	<i>24 - 32</i>	<i>28 - 37</i>	<i>17 - 22</i>	<i>23 - 30</i>	<i>30 - 40</i>	<i>34 - 45</i>

Dhir et al (2006) have compared the results from their model with published results and concluded that the model appears to underestimate T_I in sections < 500mm while overestimating T_I in thicker sections. An alternative method for deriving T_I has been used. The model uses adiabatic temperature rise data as the input and is described in detail in Appendix A2. Semi-adiabatic testing as part of the study at the University of Dundee (Dhir et al, 2006) has provided data for a variety of combinations of CEM I with ggbs and fly ash (Figures A1.3 and A1.5) and this been used to provide the input data to the model. A comparison of predicted and measured

results (Concrete Society 2004, Anson *et al*, 1988, Fan *et al*, 2004) has demonstrated that the model provides a reasonable prediction of temperature rise over a range of concrete mix types and mix temperatures, as shown in Figure A1.8. On this basis the model has been used to predict T_f values.

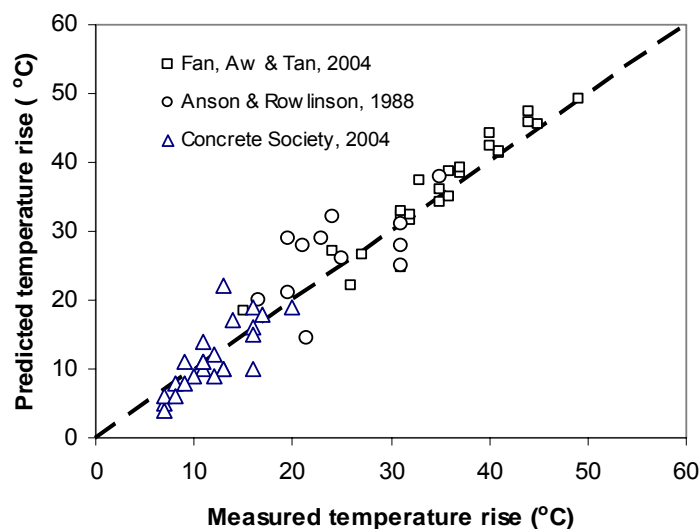


Figure A1.8 Comparison between measured temperature rise and values predicted using the adiabatic mode (see Appendix A2)

Values of T_f for CEM1 in relation to section thickness and cement content are given in Figure A1.9 Values for combinations with 35, 50 and 70 per cent ggbs are given in Figure A1.10 and combinations with 20, 35 and 50 per cent fly ash, are given in Figure A1.11. These values have been derived assuming CEM I with an ultimate heat output of 380 kJ/kg (about 15.8 °C/100kg in concrete with a specific heat of 1 kJ/kg°C and a density of 2400 kg/m³) and represent values with only a 10 per cent chance of being exceeded.

Table A1.8 Design values of T_f for CEM I predicted using the adiabatic model compared with the values given in CIRIA R91 (Harrison, 1992) (the lower values in italics are the CIRIA R91 values)

SECTION THICKNESS (mm)	STEEL FORMWORK				18 MM PLYWOOD FORMWORK			
	Cement content (kg/m ³)				Cement content (kg/m ³)			
	220	290	360	400	220	290	360	400
300	12	16	19	21	19	24	29	32
	<i>5 - 7</i>	<i>7 - 10</i>	<i>9 - 13</i>	<i>10 - 15</i>	<i>10 - 14</i>	<i>14 - 19</i>	<i>18 - 26</i>	<i>21 - 31</i>
500	19	24	29	32	24	31	37	41
	<i>9 - 13</i>	<i>13 - 17</i>	<i>16 - 23</i>	<i>19 - 27</i>	<i>15 - 19</i>	<i>20 - 27</i>	<i>27 - 36</i>	<i>31 - 43</i>
700	24	31	37	41	28	36	44	48
	<i>13 - 17</i>	<i>18 - 24</i>	<i>23 - 33</i>	<i>27 - 39</i>	<i>18 - 23</i>	<i>25 - 32</i>	<i>34 - 43</i>	<i>40 - 49</i>
1000	29	38	46	50	32	41	50	55
	<i>18 - 23</i>	<i>24 - 32</i>	<i>33 - 43</i>	<i>39 - 49</i>	<i>22 - 27</i>	<i>31 - 37</i>	<i>42 - 48</i>	<i>47 - 56</i>

The biggest differences are noted for thinner sections and this is consistent with the initial assessment of the CIRIA R91 (Harrison, 1992) in which values were found to underestimate T_f by up to about 5 °C, even when compared with the upper end of the range.

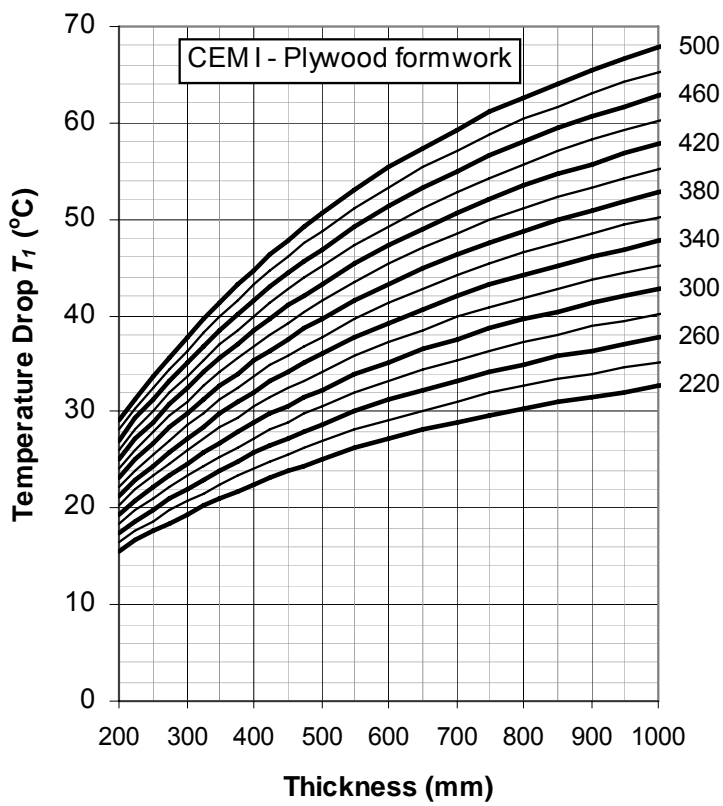
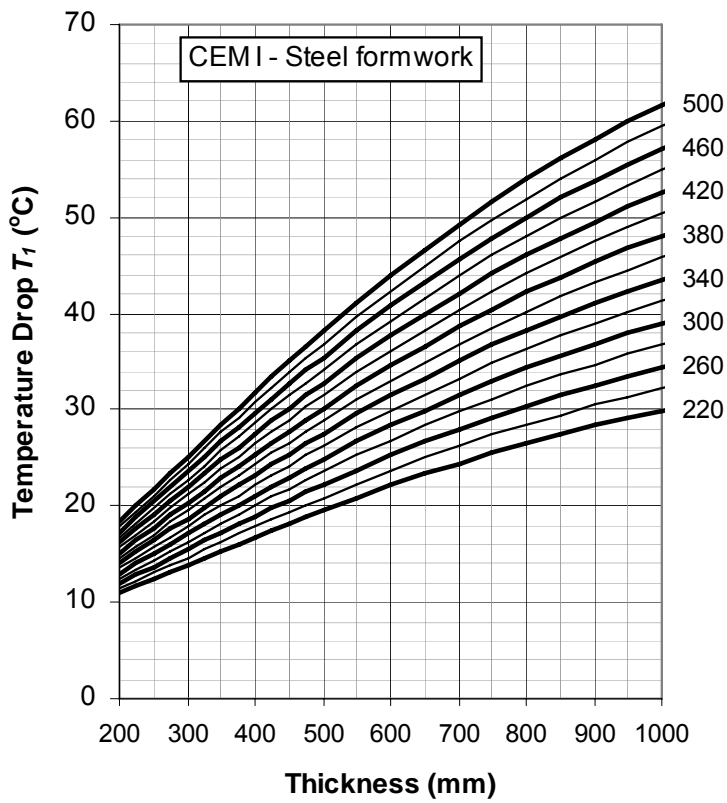


Figure A1.9 T_1 values for CEM I in walls

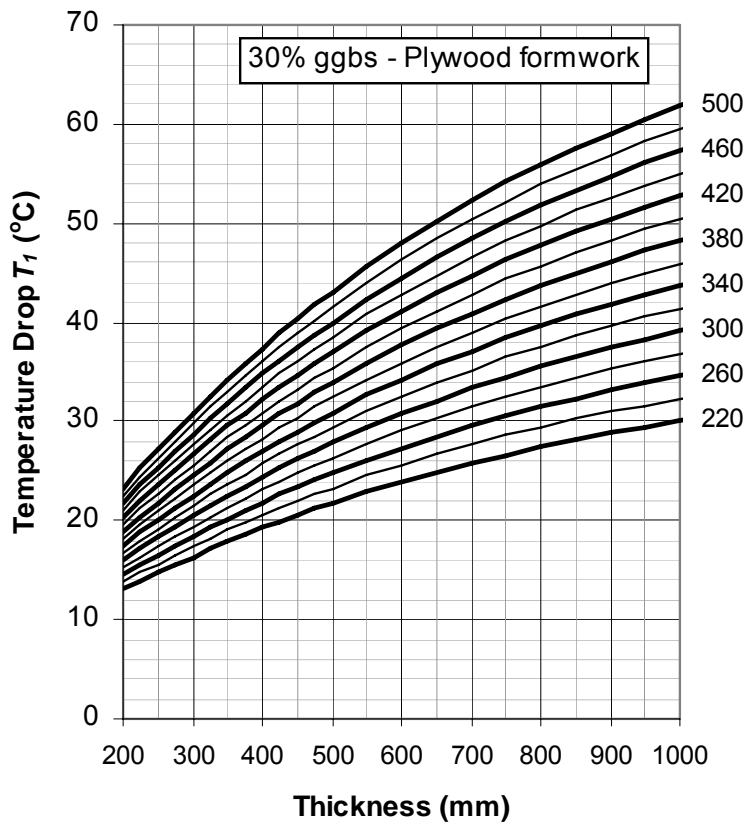
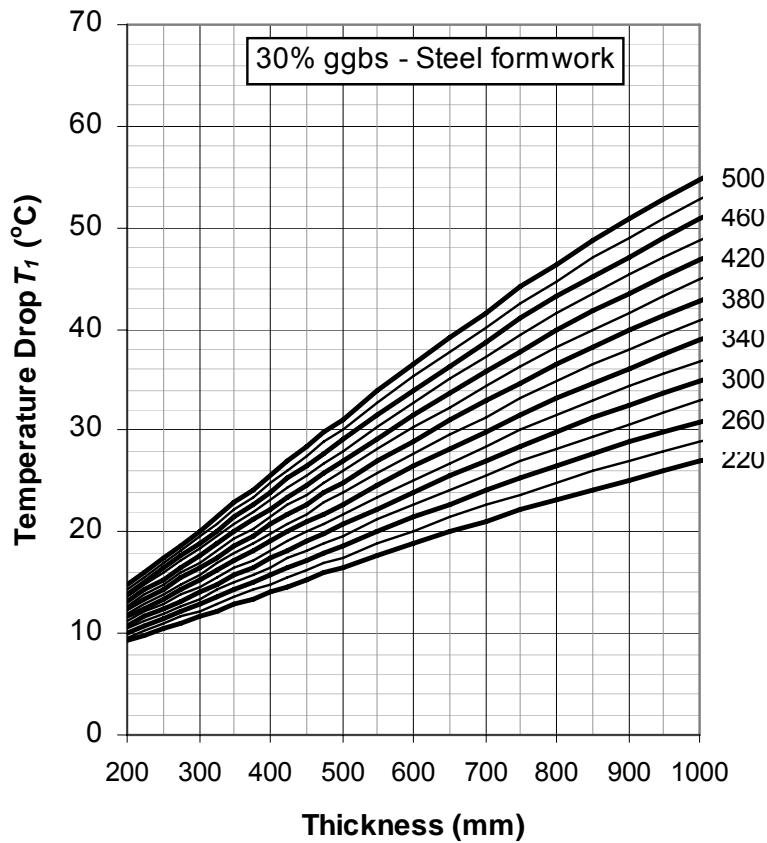


Figure A1.10 T_1 values for concretes containing 30 per cent ggbs

Licensed copy:HALCROW GROUP LTD, 16/03/2007, Uncontrolled Copy, © CIRIA

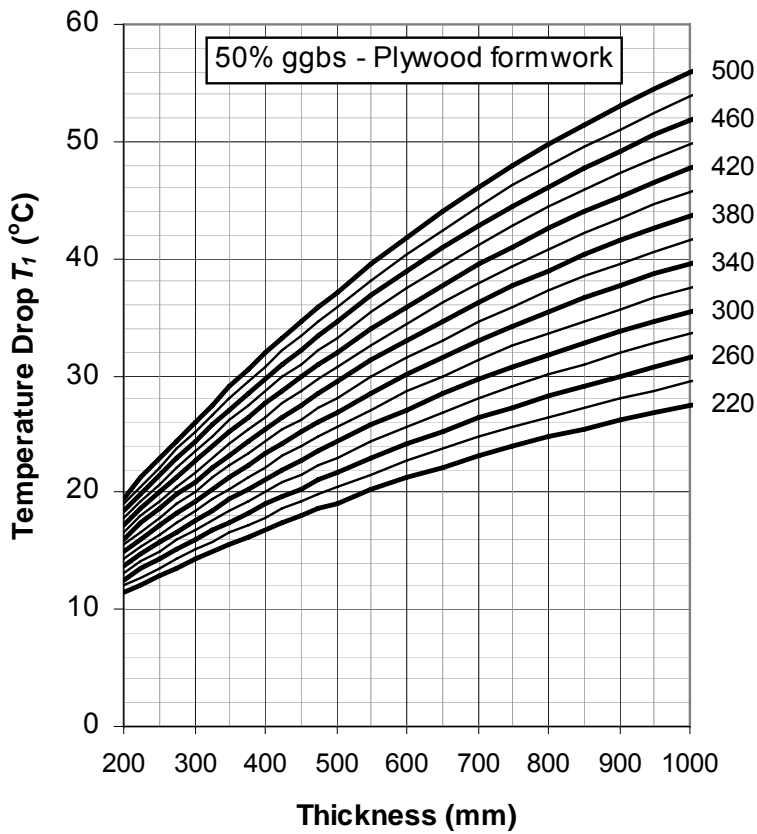
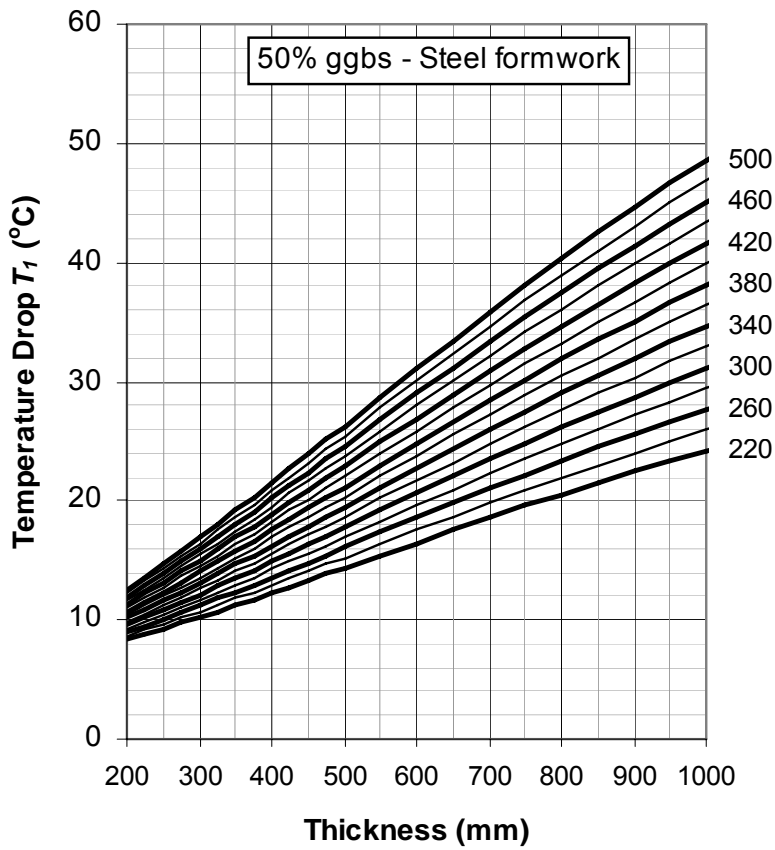


Figure A1.10 (contd) T_1 values for concretes containing 50 per cent ggbs

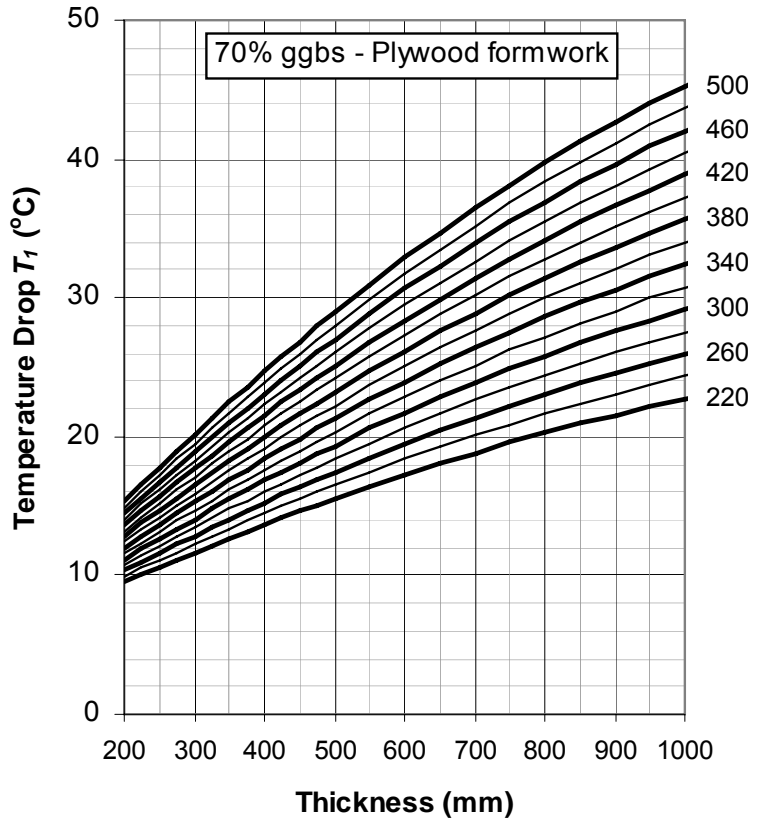
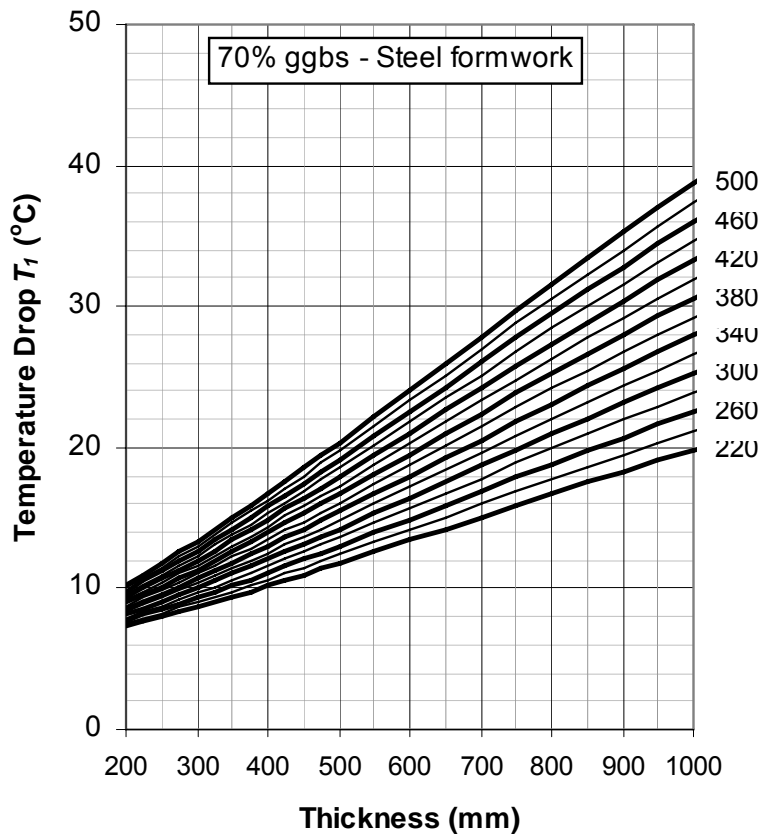


Figure A1.10 (contd) *T₁ values for concretes containing 70 per cent ggbs in walls*

Licensed copy:HALCROW GROUP LTD, 16/03/2007, Uncontrolled Copy, © CIRIA

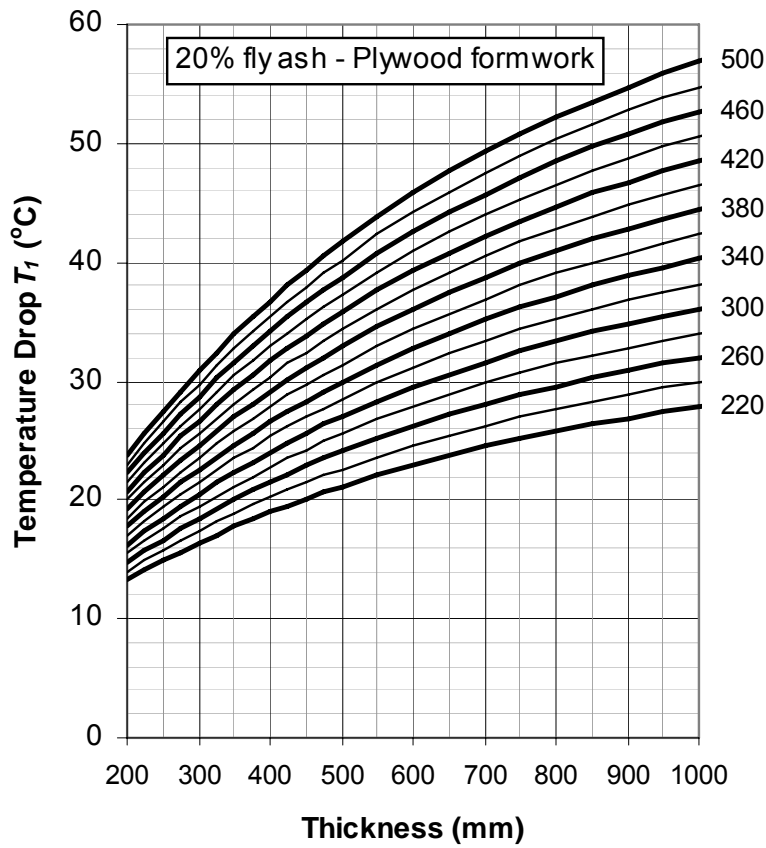
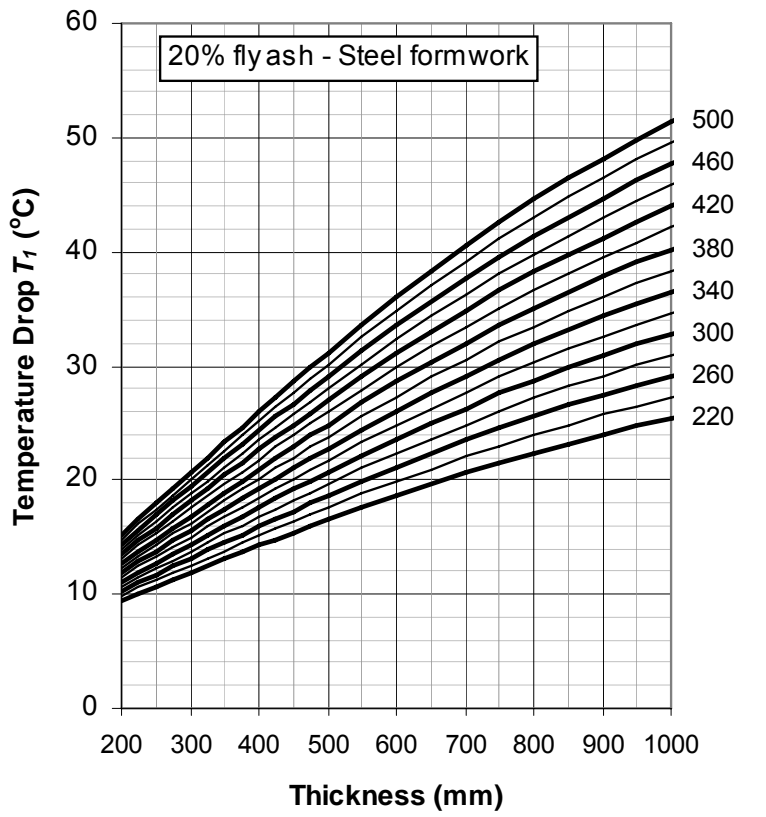


Figure A1.11 *T₁ values for concretes containing 20 per cent fly ash in walls*

Licensed copy:HALCROW GROUP LTD, 16/03/2007, Uncontrolled Copy, © CIRIA

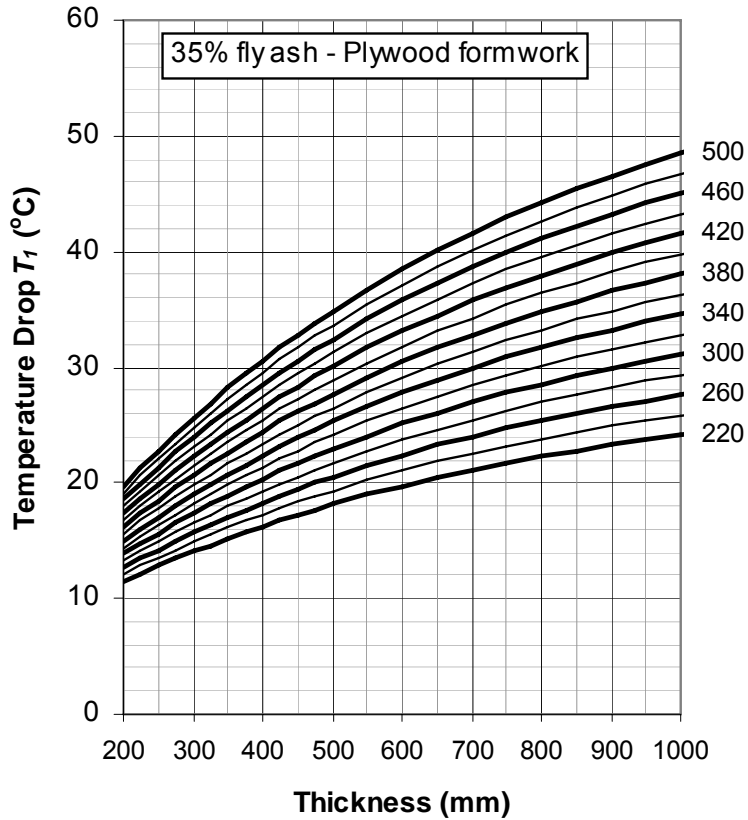
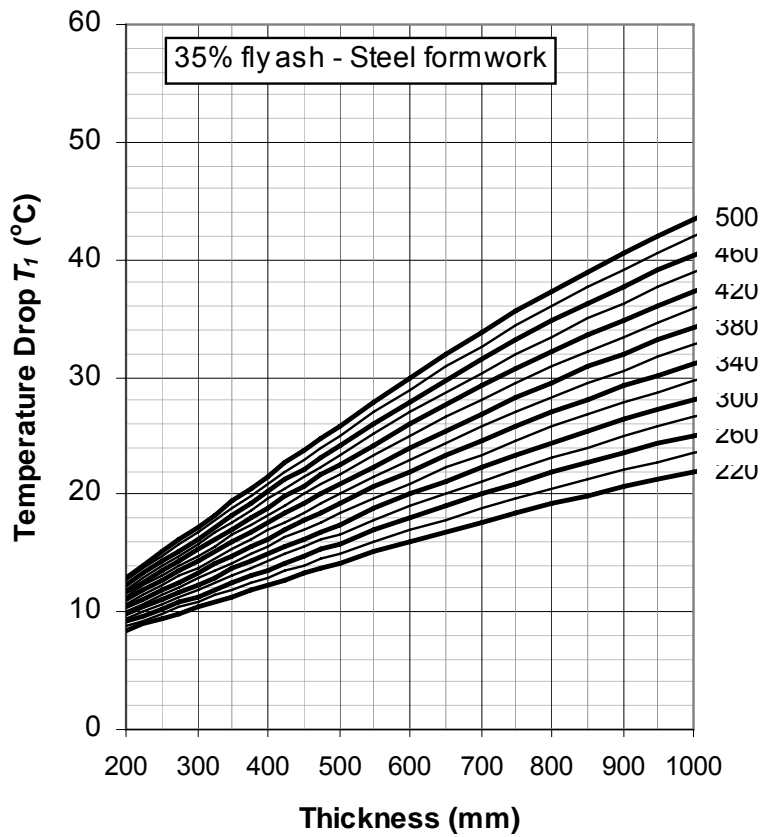


Figure A1.11 (contd) *T₁ values for concretes containing 35 per cent fly ash in walls*

Licensed copy:HALCROW GROUP LTD, 16/03/2007, Uncontrolled Copy, © CIRIA

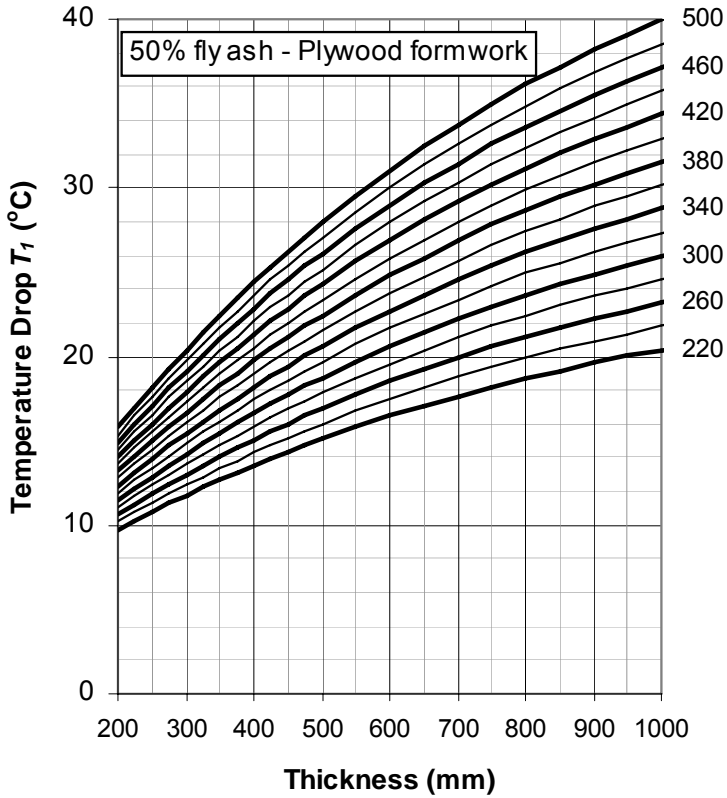
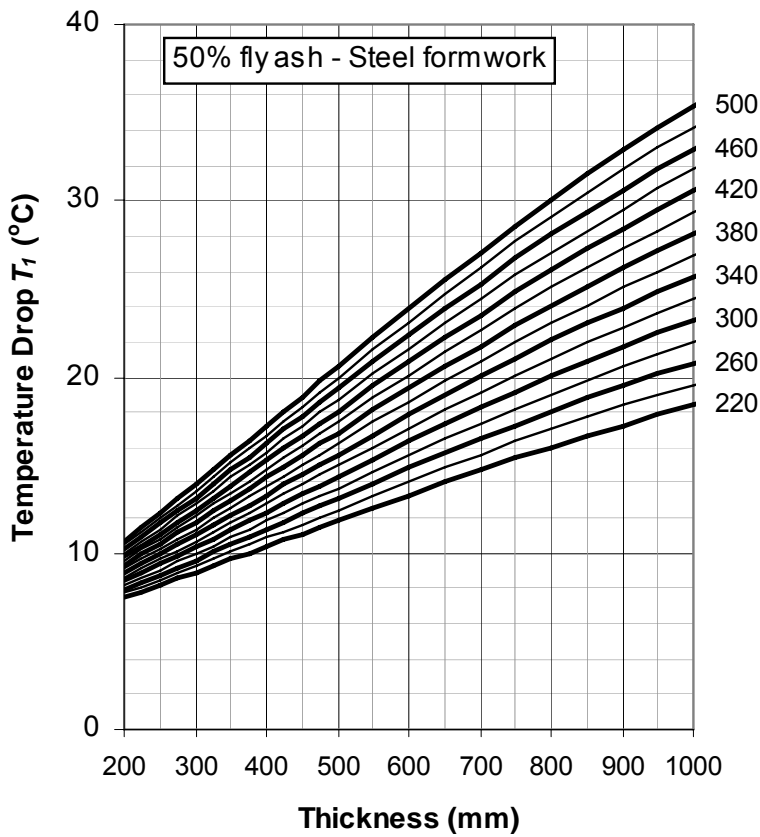


Figure A1.11 (contd) T_1 values for concretes containing 50 per cent fly ash in walls

A1.8 Effect of placing temperature

The T_f values given in Figures A1.9, A1.10 and A1.11 have been derived assuming a concrete placing temperature of 20 °C and a mean temperature of 15 °C. Where there is significant deviation from these values then T_f should be adjusted accordingly. The model described in Appendix A2 (and included on the CD) enables the mix temperature and the ambient temperature to be adjusted. Using the model, adjustments for placing temperature have been derived and are given in Figure A1.12 related to section thickness. However, as a general rule, to avoid errors that may arise is adjusting for mix temperature, when very high or very low placing temperatures are expected, temperature rise tests should be measured at a start temperature close to that likely to be achieved in practice.

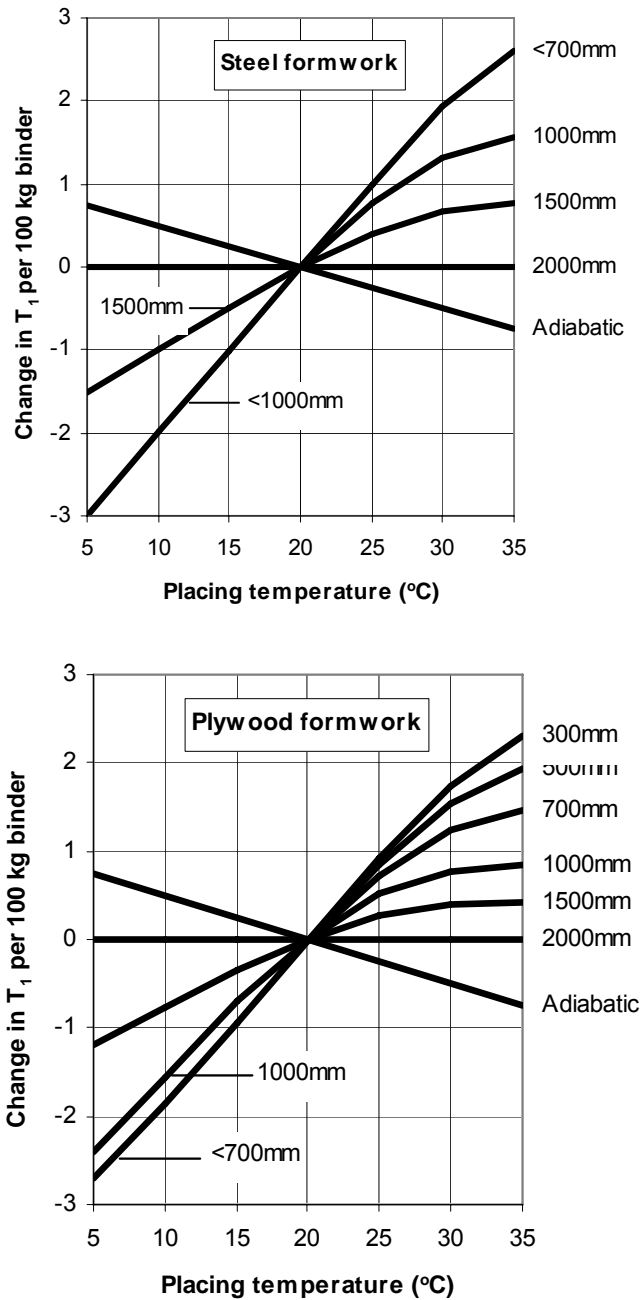


Figure A1.12 The estimated change in T_1 (per 100 kg/m³ CEM I) with placing temperatures for elements of varying thickness

A1.9 Temperature differentials, ΔT

In order to estimate the likely temperature differentials that will occur, it is necessary to undertake thermal modelling. Some indicative values are provided however, in Table A1.9. These values have been obtained using the model described in Appendix A2 and provided on the CD which can be used to undertake comparative assessments.

Section thickness (mm)	Steel formwork				18 mm plywood formwork			
	Cement content (kg/m ³)				Cement content (kg/m ³)			
	280	320	360	400	280	320	360	400
300	8	9	10	11	4	5	5	6
500	14	15	17	19	7	8	9	10
700	18	20	22	25	10	12	13	14
1000	23	26	29	31	15	17	19	21
1500	31	35	39	41	20	22	25	27
2000	35	39	44	48	24	27	30	33

Figure A1.9 *Estimated values of temperature differential in walls assuming a placing temperature of 20 °C and a mean ambient temperature of 15 °C (assuming thermal conductance values of 18.9 and 5.2 W/m²K for steel and plywood formwork respectively with a wind speed of about 3.5m/s. Solar gain has not been included)*

The temperature differential will be highly dependent on the thermal diffusivity of the concrete; the surface conditions, in particular the type of formwork and the time at which it is removed; and the environmental conditions such as wind speed and effects of solar gain. While the values in Table A1.9 provide an indication of temperature differentials for a particular concrete under a specific set of conditions, they may not be applicable when different conditions apply. Where limiting the temperature differential is critical to the design, thermal modelling is required. Commercial software is available for this purpose and the simple spreadsheet model is described in Appendix A2 and provided on the CD.

A1.9 Conclusions

1. Values of temperature rise and the temperature drop T_f have been estimated for a range of concrete mixes. These values have been derived using a predictive model which uses adiabatic temperature rise data as input data. Comparison with published *in situ* temperature measurements indicates that the model, despite its limitations, provides a reasonable prediction of T_f .
2. The design values are higher than those recommended in CIRIA R91 (Harrison, 1992) which, when compared with measurements over a wide range of concretes, were found to be low, even at the high end of the range.
3. Guidance on likely temperature differentials are given but thermal modelling is required to determine a reliable value which takes account of the formwork type and exposure conditions.

A1.10 References

- Anson, M and Rowlinson, P M (1988)
 “Early-age strain and temperature measurements in concrete tank walls”
Magazine of Concrete Research, Vol. 40, No. 145, December 1988
- Bamforth, P B (1980)
 “*In situ* measurement of the effects of partial Portland cement replacement using either fly ash or ground granulated slag on the performance of mass concrete”
Proc. Instn. Civ. Engrs. **69**, Part 2, Sept 1980, pp 777-800
- Bamforth, P B and Price, W F (1995)
Concreting deep lifts and large volume pours
 R135, CIRIA, London
- Concrete Society (2004)
 “*In situ* strength of concrete – An investigation into the relationship between core strength and the standard cube strength”
Working party of the Concrete Society, Project Report No 3, BCA, Camberley, Surrey, ISBN 0 94669 186 X
- Dhir, R, Paine, K A and Zheng, L (2006)
Design data for use where low heat cements are used
 DTI Research Contract No. 39/680, CC2257, University of Dundee, Report No CTU2704
- Fan, S C, Aw, K M and Tan Y M (2004)
 “Peak temperature rise for early-age concrete under tropical climate condition”
Journal of the Institution of Engineers, Singapore, Vol. 44, 1, pp 1-10
- FIP (1988)
 “Condensed silica fume in concrete”
State of the Art Report, ISBN 978 0 72770 361 3
- Harrison, T (1992)
Early-age thermal crack control in concrete
 R91, CIRIA, London
- Kandstad, T, Bjøntegaard, Ø, Sellevold, E and Hammer, T A (2001)
 “Crack sensitivity of bridge concretes with variable silica fume content”
Improved performance of Advanced Concrete Structures – IPACS, Report BE96-3843/2001:48-6, 2001, Selmer Skanska, Trondheim, Norway, ISBN 9 18958 077 X
- Lewis, R Sear, L Wainwright P and Ryle, R (2003)
 “Cementitious additions”
Advanced Concrete Technology (ed Newman and Choo), *Constituent Materials*, Chapter 4, Elsevier Butterworth Heinemann
- Troli, R Ogoumah Olagot, J.J Monosi, S and Collepard, M (2003)
 “Low heat development in self-compacting concrete for massive structures”
 In Proc. 7th CANMET/ACI Int. Conf. *Superplasticizers and other chemical admixtures in concrete*, Berlin, Germany, 20-24 October 2003, pp. 103-112
- Price, W F (2006)
 Production data provided by Lafarge Cement
Lafarge Cement UK, Manor Court, Chilton, Oxon

A2 A model for predicting the temperature rise and temperature differentials using adiabatic temperature data

A2.1 The model

A numerical model for predicting the temperature rise in hardening concrete was developed by Ross and Bray (1949). The method is based on standard heat diffusion theory and employs an established numerical method described by Crank (1975). Numerical methods lend themselves very easily to spreadsheet calculations and the flexibility they offer. Engineers are also very familiar with spreadsheet applications. The method of calculation is shown in Figure A2.1. At a particular time increment, the temperature within a cell is calculated from the mean of the temperatures in the adjacent cells in the previous increment added to the increment of adiabatic temperature within the time increment. For this approach to work the time increment, dt , and the space increment, dx , should obey the formula:

$$dt = 0.5 * dx^2 / \text{Thermal diffusivity}$$

Calculating the temperature remote from the surface

Adiabatic temp increment	Ambient temp	Surface temp	Concrete temperature				
dAa	Aamb	A1	A2	A3	A4	A5	etc
dAb	Bamb	B1	B2	B3	B4	B5	etc
dAc	Camb	C1	C2	C3	C4	C5	etc
etc	etc	etc	etc	etc	etc	etc	etc

$$B3 = 0.5 * (A2 + A4) + dAb$$

Calculating the surface temperature

Adiabatic temp increment	Ambient temp	Surface temp	Concrete temperature				
dAa	Aamb	A1	A2	A3	A4	A5	etc
dAb	Bamb	B1	B2	B3	B4	B5	etc
dAc	Camb	C1	C2	C3	C4	C5	etc
etc	etc	etc	etc	etc	etc	etc	etc

$$B1 = dAb + \frac{k * (A2 - Aamb)}{k + (S * dx)}$$

Where A1, A2... B1, B2 etc represent the temperatures at defined locations
 dAa, dAb, etc represent the adiabatic temperature rise within the time increment
 Aamb, Bamb etc represent the ambient temperature at each time increment
 k = coefficient of thermal conductivity of the concrete
 S = surface conductance of the concrete
 dx = the depth increment used in the numerical calculation

Figure A2.1 Spreadsheet showing the equations used in the numerical calculation

A2.2 Heat generation data

A2.1.2 Modelling the adiabatic curve

As the model has, historically, been applied most frequently to thick sections, the input data is in the form of the adiabatic temperature rise (ie the temperature rise that occurs in a perfectly insulated condition). In large pours, the centre may be in an effectively adiabatic condition for several hours. Adiabatic data may be obtained from a test, or from historical measurements. Hence data obtained from the results of the

semi-adiabatic test to

EN 196-9, after correcting for heat loss, may be used.

A substantial test programme has been carried out at the Concrete Technology Unit of the University of Dundee (Dhir *et al*, 2006). Part of the programme involved semi-adiabatic tests in accordance with EN 196-9 to measure the heat generation of a variety of combinations of CEM I with fly ash and ggbs. An analysis of this data has been carried out to develop a predictive model for the adiabatic heat curve derived from the standard test. These data are then be used as input data to the diffusion model for the prediction of temperature rise and thermal gradients.

The shape of the heat generation curves indicates that an exponential equation should provide a reasonable fit. Figure A2.2 shows the test data obtained using a CEM I cement and a best fit exponential curve of the form:

$$Q = Q_{ult}[1 - \exp(-B.t^c)] \quad (\text{A2.1})$$

where Q is the total heat output after time t and Q_{ult} is the ultimate heat output.

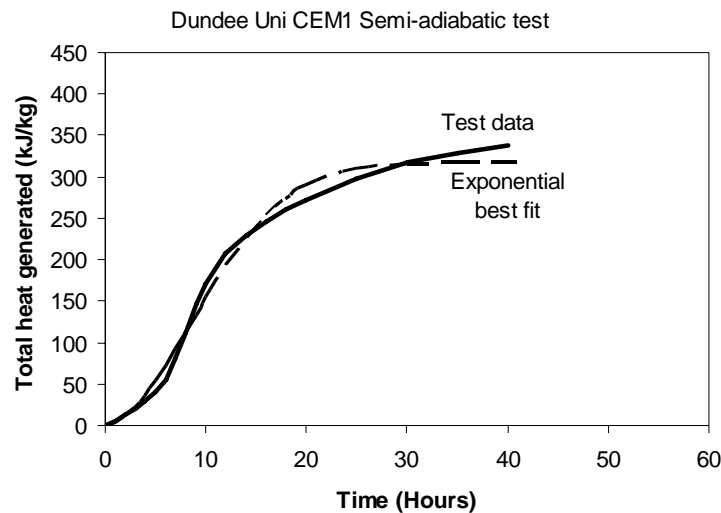


Figure A2.2 Heat output measured in the semi-adiabatic test and a best fit exponential curve

While the exponential curve provides a reasonable fit it tends to mismatch the rate of heat evolution at various stages. The difficulty arises in trying to match the early rate of heat development with the ultimate heat output. Observation of the heat generation curve indicates that a better fitted may be obtained using a two component curve with the first component, the exponential curve, starting at time zero, and the second component being delayed to start at time t_2 , as shown in Figure A2.3 The second component may be modelled by the an equation of the form:

$$Q_2 = Q_{ult} \frac{t - t_2}{t - t_2 + D} \quad (\text{A2.2})$$

A two part equation for heat generation has been developed on this basis of the form:

$$Q = Q_1 + Q_2 = \frac{Q_{ult}}{2} (1 - \exp(-B.t^c)) + \frac{Q_{ult}}{2} \cdot \frac{t - t_2}{t - t_2 + D} \quad \text{A2.3}$$

where the two components are given equal weighting.

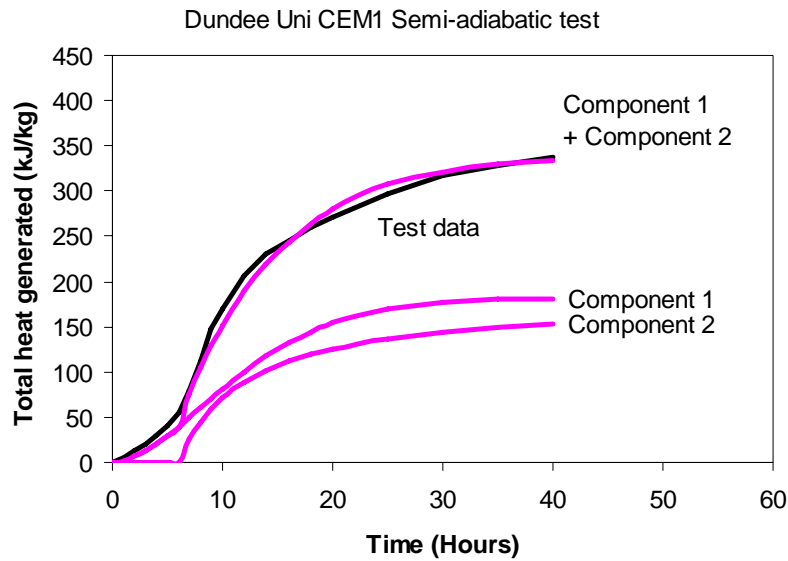


Figure A2.3 A comparison between measured semi-adiabatic test data and the two component model

In order to establish values for the coefficients, analysis has been carried out on semi-adiabatic test data from tests at University of Dundee (Dhir *et al*, 2006) for cement with a start temperature of 20 °C.

A2.1.2 Ultimate heat generation Q_{41}

Relationships between the proportion of addition and the heat generated after 41 hours are given in Figure A2.3 for both fly ash and ggbs. The relationships are defined by the following expressions. The value for CEM I is 338kJ/kg.

$$Q_{41(fly\ ash)} = Q_{41(CEM\ I)} - 2.989 (\% \text{ fly ash}) \tag{A2.4}$$

$$Q_{41(ggbs)} = Q_{41(CEM\ I)} - 60 \left(\frac{\%ggbs}{100 - \%ggbs} \right)^{0.6} \tag{A2.5}$$

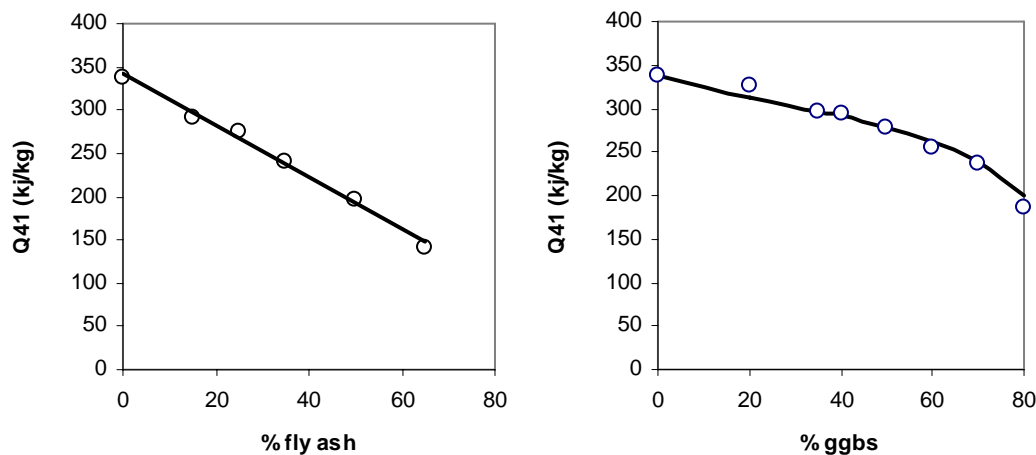


Figure A2.4 The relationship between the percent addition and the adiabatic heat at 41 hours

A2.1.3 Ultimate heat generation Q_{ult}

The value of Q_{ult} has been derived from the 41hr value derived from the standard test, Q_{41} , using the equations:

$$\text{For CEM I} \quad Q_{ult} = Q_{41} / 0.925 \quad (\text{A2.6})$$

$$\text{For fly ash} \quad Q_{ult} = Q_{41} / (0.00002(\% \text{ fly ash})^2 - 0.0034(\% \text{ fly ash}) + 0.925) \quad (\text{A2.7})$$

$$\text{For ggbs} \quad Q_{ult} = Q_{41} / (0.00003(\% \text{ ggbs})^2 - 0.0047(\% \text{ ggbs}) + 0.925) \quad (\text{A2.8})$$

These relationships are shown in Figure A2.5

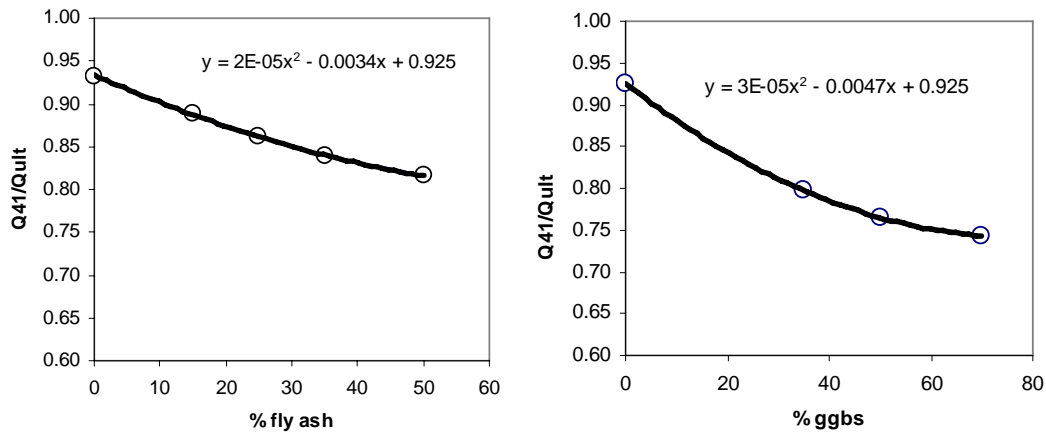


Figure A2.5 The relationship between the percent addition and the proportion of ultimate heat generated after 41 hours

A2.1.4 The coefficient B

The coefficient B is equal to 0.011724, regardless of the cement type.

A2.1.5 The coefficient C

The coefficient C varies with both the type of addition and the amount used. For CEM I, $C = 1.6$ and C reduces with an increase in additions as follows:

$$\text{For fly ash} \quad C = 1.6 - 0.001 (\% \text{ fly ash}) \quad (\text{A2.9})$$

$$\text{For ggbs} \quad C = 1.6 - 0.0072(\% \text{ ggbs}) - 0.00003(\% \text{ ggbs})^2 \quad (\text{A2.10})$$

The coefficient C is the dominant factor influencing the shape of the curve as show in Figure A2.6. A lower value of C is indicative of slower reacting cement, hence the relationships between C and the fly ash and ggbs content described by equations A2.9 and A2.10.

A2.1.6 The coefficient D

The coefficient D varies with both the type of addition and the amount used. For CEM I $D = 6.2$ and D increases with an increase in additions as follows:

$$\text{For fly ash} \quad D = 6.2 + 0.2131 (\% \text{ fly ash}) \quad (\text{A2.11})$$

$$\text{For ggbs} \quad D = 6.2 + 0.0848(\% \text{ ggbs}) - 0.0004(\% \text{ ggbs})^2 \quad (\text{A2.12})$$

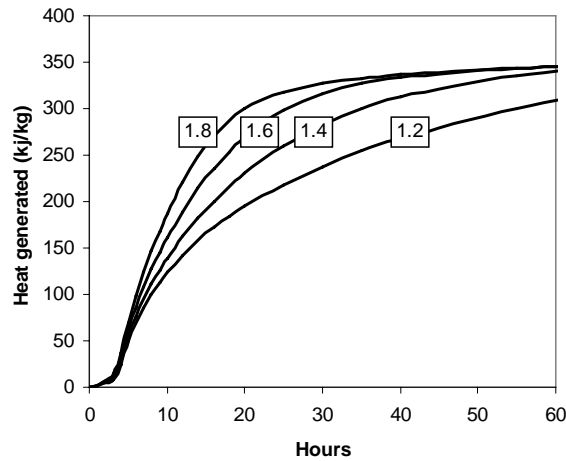


Figure A2.6 The influence of the coefficient C on the shape of the heat generation curves

A2.1.7 Activation time t_2 for component 2

The time at which component 2 of the heat generation curve becomes active is increased by the use of additions. For CEM I $t_2 = 3.5$ hours.

For fly ash $t_2 = 3.5 + 0.0236(\% \text{ fly ash})$ (A2.13)

For ggbs $t_2 = 3.5 + 0.0125(\% \text{ ggbs})$ (A2.14)

A2.1.8 Comparison of modelled heat generation with the measured values

Comparisons between test results and heat output curves generated using the two component model with the coefficient defined above are shown in Figures A2.7 and A2.8 for fly ash and ggbs concretes respectively. It can be seen that the two component model provides a good fit to the data.

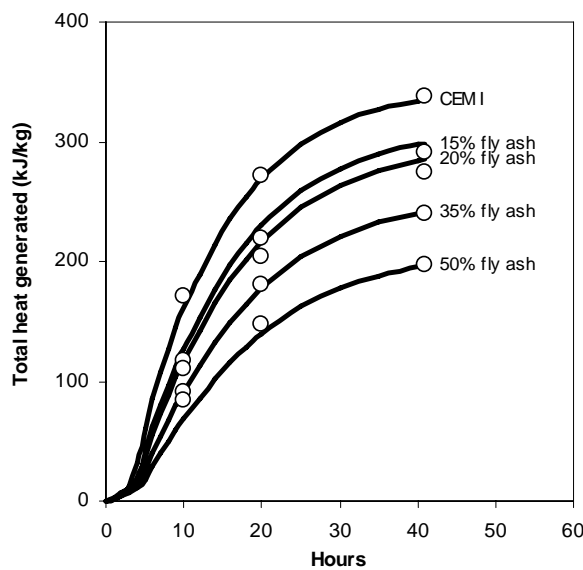


Figure A2.7 Comparison between the reported adiabatic heat output and the curves generated by the proposed model for cement combinations of CEM I and fly ash

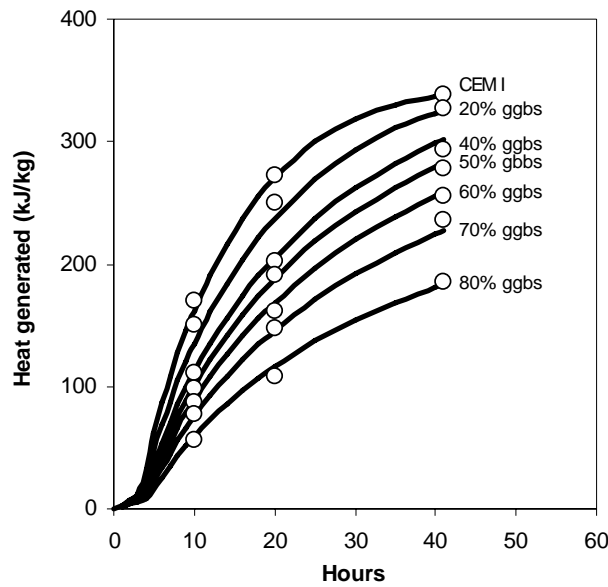


Figure A2.8 Comparison between the reported adiabatic heat output and the curves generated by the proposed model for cement combinations of CEM I and ggbs

A2.3 The effect of placing temperature

The model also modifies the adiabatic heat generation curve to take account of the mix temperature. The curve may be adjusted to take account of differences between the start temperature in the test and the start temperature in practice (Rastrup, 1954). This is achieved using the Rastrup function:

$$t_r = t_t \times 2^{[(\theta_t - \theta_p)/12]} \quad (\text{A2.15})$$

where

- t_r = predicted time to achieve a particular temperature
- t_t = recorded time to achieve a particular temperature in the test
- θ_t = start temperature in the test
- θ_p = start temperature for the prediction

This implies that a 12 °C increase in temperature will halve the time taken to achieve the same level of total heat generated. Thus a concrete placed at 22 °C initially evolves heat twice as quickly as a similar mix placed at 10 °C, and, if the heat loss conditions are the same, the concrete placed at the higher temperature has a higher temperature rise.

A validation of this equation based on site measurements is shown in Figure A2.9, which compares temperature rise curves from a range of concrete pours from 300 mm up to 3 m thick, all of which have been normalised to the same placing temperature using the above equation.

Further confirmation of this function was provided in a study of Japanese cements (Kishi and Maekawa, 1995), in which adiabatic tests were carried out at 10, 20 and 30 °C. The results, shown in Figure A2.10, indicate that the empirical Rastrup function gives an adequate estimation of the rate of heat evolved for normal UK conditions.

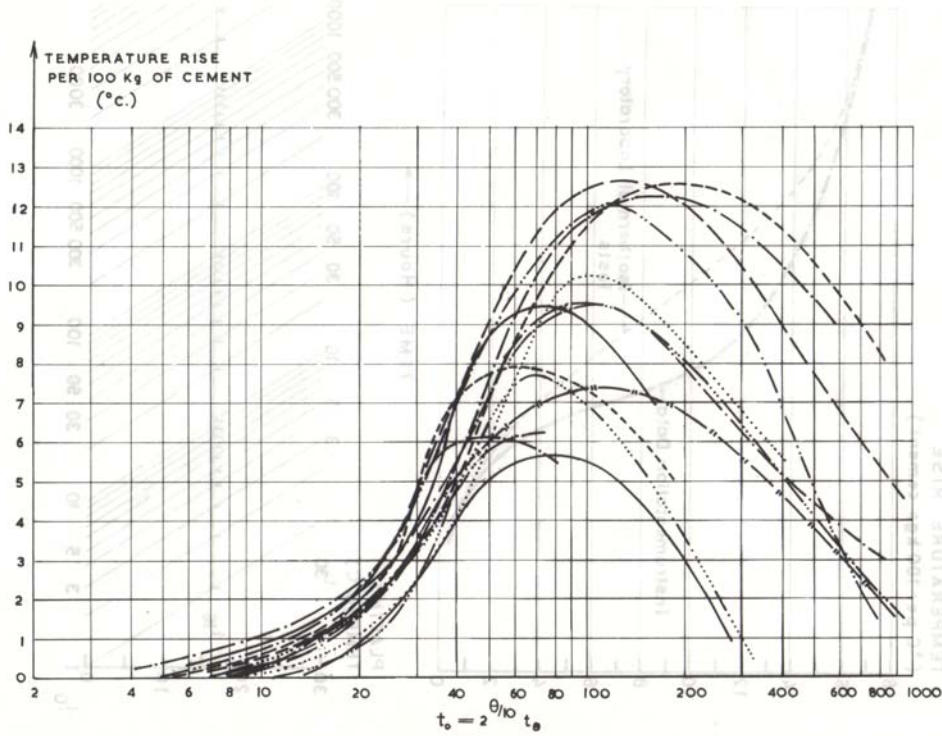


Figure A2.9 Normalised temperature rise curves for a range of pours (Bamforth, 1976)

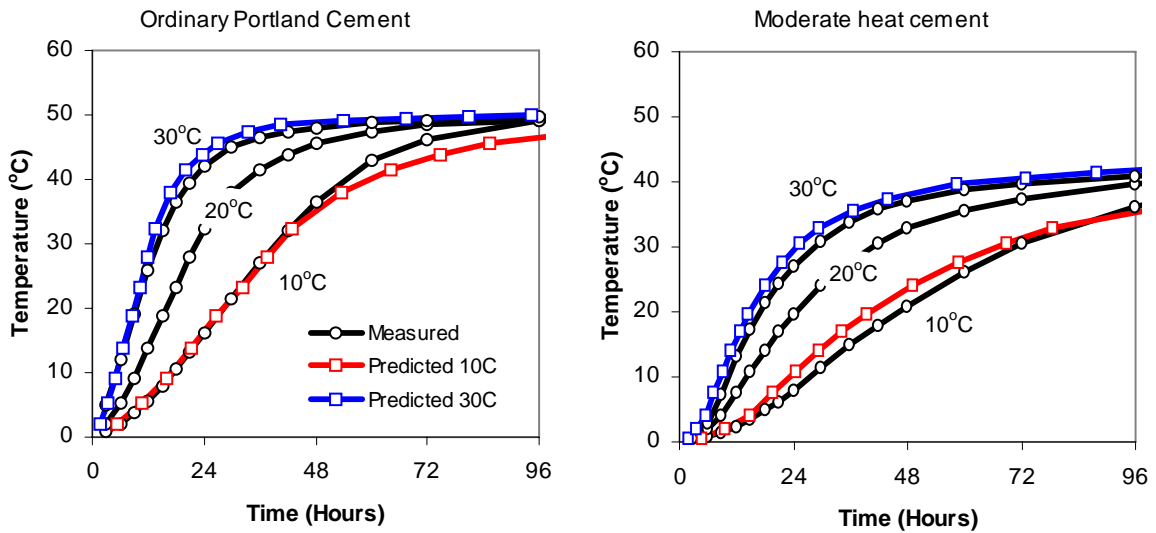


Figure A2.10 Adiabatic temperature rise for CEM I cement and moderate heat cements tested at mix temperatures of 10°C, 20°C and 30°C. Also shown are 10°C and 30°C curves derived from the 20°C curve using the Rastrup function (data from Kishi and Maekawa, 1995)

A2.4 Thermal properties of the concrete

A2.4.1 Thermal conductivity

The thermal conductivity of concrete, λ_c , determines the rate at which heat will be transported through it and hence the rate of heat loss. Two main factors influence the thermal conductivity of concrete, the aggregate type and the moisture content. Published values of thermal conductivity vary considerably but are typically within the range from 1.0 to 2.5 W/m.K. This range is due in part to the range of moisture conditions under which the tests have been conducted and in part to the variation of the aggregate properties (Clauser and Huenges, 1995).

With regard to the prediction of temperature rise in hydrating concrete it is only the moisture content within the first day or so that is important. During this period the volume of free water will be reducing as the cement hydrates and the thermal conductivity will reduce accordingly. It has been reported that the thermal conductivity of maturing concrete is about 33 per cent higher than that of hardened concrete (Ruiz *et al*, 2003). Based on this observation a relationship is proposed which relates the thermal conductivity at time t , λ_{ct} to the initial thermal conductivity λ_{ci} using the expression;

$$\lambda_{ct} = \frac{\lambda_{ci}}{(1.33 - 0.33[\alpha_t/\alpha_{ult}])} \quad (\text{A2.16})$$

where α_t is the degree of hydration at time t and α_{ult} is the ultimate hydration.

The initial thermal conductivity can be calculated using a multiphase model if the properties of the individual constituents are known. Various models have been used to predict concrete properties, the most common being the series model and the parallel model.

The series model is of the form

$$\frac{1}{\lambda_c} = \frac{v_a}{\lambda_a} + \frac{v_s}{\lambda_s} + \frac{v_{ce}}{\lambda_{ce}} + \frac{v_w}{\lambda_w} \quad (\text{A2.17})$$

where v is the volume fraction of each component and the subscripts a , s , ce and w represent aggregate, sand, cement and water respectively.

The parallel model is of the form

$$\lambda_c = v_a.\lambda_a + v_s.\lambda_s + v_{ce}.\lambda_{ce} + v_w.\lambda_w \quad (\text{A2.18})$$

It is generally assumed that the series and parallel represent the lower and upper bound values respectively. Concrete comprises discrete aggregate and sand particles within a continuous matrix and true model will lie somewhere between the two estimates. As the aggregate represents about 70 per cent of the volume and the cement paste about 30 per cent, the value of λ_{ci} has been estimated by taking a weighted average of the results from the series and parallel models in the ratio 70:30 and the results are given in Table A2.1. Both mean and lower 95 percentile values are given, the latter resulting in higher values of temperature rise when used in modelling and hence providing a safe design option. In addition, results have been derived for concretes in which both the sand and aggregate is from the same rock type and for combinations of the defined rock type with a siliceous sand, the latter being a common combination in the UK.

Table A2.1 *Estimated values of thermal conductivity at early age for concretes using different aggregate types. Aggregate data were obtained from Clauser and Huenges (1995)*

Rock type		Examples	Thermal conductivity, W/m.K						
			Aggregate			Concrete			
			Mean	SD	lower 95%	Aggregate and sand		Aggregate with siliceous sand	
Mean	Lower 95%	Mean				Lower 95%			
Metamorphic	High quartz content	Quartzite	5.80	0.40	5.14	3.20	2.91	3.20	2.91
	Low quartz content	Gneisses, hornfels, schist, slate	2.90	0.60	1.92	1.86	1.37	2.34	2.01
Plutonic	Low in feldspar	Granite, diorite, gabbro,	3.00	0.60	2.02	1.91	1.42	2.37	2.05
	High in feldspar	Syenite, grano-syenite, syenite porphyry	2.80	0.40	2.14	1.81	1.48	2.31	2.09
Volcanic	Low porosity	Basalt, rhyolite	2.90	0.70	1.75	1.86	1.28	2.34	1.95
Sedimentary	Chemical sediments	Limestone, dolomite, chert,	2.60	0.70	1.45	1.71	1.12	2.24	1.84
	Physical sediments	Sandstone	2.40	0.60	1.42	1.61	1.05	2.18	1.83

It can be seen that for many of the rock types a similar value of thermal conductivity is obtained, with the lower 95 percentile values being within the range from 1.0 to 1.5 W/m.K for concrete using sand and aggregate from the same rock type. The most notable exception is for quartzite, for which much higher values are obtained when using rocks with high quartz content. As it is common to use siliceous sand with various rock types, values have also been derived for such combinations. The effect is to increase the range of lower 95 percentile values to 1.8 to 2.1 W/m.K.

Based on the above data, proposed values for use in modelling of early age temperature rise are given in Table A2.2.

Table A2.2 *Proposed values of thermal conductivity of concrete for use in early age thermal modelling*

Aggregate type	Thermal conductivity of concrete (W/m.K)	
	Sand and aggregate from same rock type	Aggregate from defined rock type with siliceous sand
Quartzite and siliceous gravels with high quartz content	2.9	2.9
Granite, gabbros, hornfels	1.4	2.0
Dolerite, basalt	1.3	1.9
Limestone, sandstone, chert	1.0	1.8

A2.4.2 Specific heat

The specific heat of concrete is determined by the specific heat of the individual components and their relative proportions. It has been reported that the range for mass concrete may vary from 0.75 to 1.17 kJ/kg°C (USACE, 1997). This is a very significant variation, indicating that the temperature rise associated with a particular amount of heat generated by vary by as much as ± 20 per cent from a mean value of about 0.96 kJ/kg°C. It is important that a representative value is used in any model for temperature prediction.

Two factors in particular influence the specific heat of concrete, the aggregate type and the water content, the former because it constitutes the largest proportion of the mass and the latter because it is the component with the highest specific heat (greater than 4 times that of the other mix constituents). Reported values of specific heat for rocks range from 0.8 to 1.0 kJ/kg°C and for a typical structural concrete this change alone may result in values from 1.0 to 1.15 kJ/kg°C. Dealing with the water content is more complicated as the specific heat differs for free water (4.18 kJ/kg°C) and bound water (2.22 kJ/kg°C) in concrete. To calculate the specific heat for concrete it is necessary to know the relative amounts of free and bound water and this is determined by the degree of hydration. Hydration in concrete does not occur to 100 per cent. The ultimate degree of hydration α_{ult} is determined by both the w/c ratio and the type of cement. A relationship has been developed by Schindler and Folliard (2005) of the form

$$\alpha_{ult} = \frac{1.031.w/c}{0.194 + w/c} + 0.5pfa + 0.3ggbs \quad (A2.19)$$

For CEM I cement this indicates that the ultimate degree of hydration for concrete with w/c ratios from 0.4 to 0.7 varies from 0.7 to 0.8. However, during the early life of the concrete the degree of hydration will be significantly less than the value for mature concrete. Firstly, at the time at which the peak temperature is achieved, the degree of hydration will be less than the ultimate degree of hydration. As, in most cases, the peak temperature is achieved within 30 hours of casting, the proportion of ultimate heat Q_{ult} generated after 30 hours Q_{30} in the semi-adiabatic undertaken by University of Dundee (Dhir *et al*, 2006) has been used as a measure of the degree of hydration at this time. The value of Q_{30}/Q_{ult} varies with the cement type as shown in Figure A2.11.

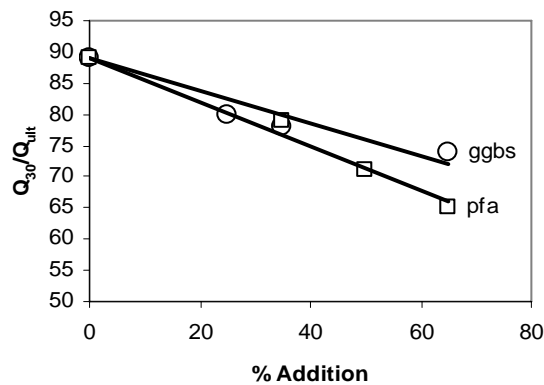


Figure A2.11 The relationship between Q_{30}/Q_{ult} and the percentage of mineral addition

Hence the degree of hydration after 30 hours, h_{30} , may be estimated as follows:

$$\alpha_{30} = \alpha_{ult} \cdot \frac{Q_{30}}{Q_{ult}} \quad (A2.20)$$

Having established a means for estimating the degree of hydration during the period up to achievement of the peak temperature, consideration must be given to the value to be applied to represent the average value during this period. It is clear that immediately after casting the concrete, the degree of hydration will be zero, with all of the water being in a free state. As hydration proceeds the amount of free water will progressively reduce until, at 30 hours, the degree of hydration has reduced to the value calculated using equ A2.20. Assuming that the degree of hydration is directly proportional to the heat generated during this period, the average degree of hydration will be equal to half the value achieved at 30 hours and it is this value that should be used in the thermal calculations.

Applying this principle to the mortar mix used in the semi-adiabatic test with a w/c of 0.5 leads to an estimated value of mean hydration of 0.33 and a mean specific heat value of 1.118 kJ/kg°C (Table A1.8). The latter is close to the value of 1.1 kJ/kg°C recommended by SP, the Swedish National Testing and Research Institute (Wadsö, 2003) for analysis of the semi-adiabatic test results.

Table A2.3 Estimate of specific heat capacity for test mortar in the semi-adiabatic test)

Material	Weight (kg)	Specific heat (kJ/kg.C)
Cement	3.60	0.87
Water - Free	1.20	4.18
Water - Bound	6.00	2.22
Sand	10.80	0.80
TOTAL	16.20	1.118

Calculated early age values for typical structural concretes using aggregate with an assumed specific heat of 0.8 kJ/kg.C are estimated to be in the range from 0.97 to 1.07 kJ/kg°C with ultimate values generally being 5 to 10 per cent lower, the difference being greatest for concretes with high levels of fly ash or ggbs. Figure A2.12 enables a rapid estimate of specific heat to be made based on the cement content and w/c ratio of the concrete. Where the specific heat of the aggregate is known to be greater than 0.8 kJ/kg°C, the values for concrete in Figure A2.12 should be increased by 0.8 times the change in the value for the aggregate. So for aggregate with a specific heat of 0.9 kJ/kg°C, concrete with a value of 1.01 would increase by $0.8 \cdot (0.9 - 0.8) = 0.08$ to 1.09 kJ/kg°C.

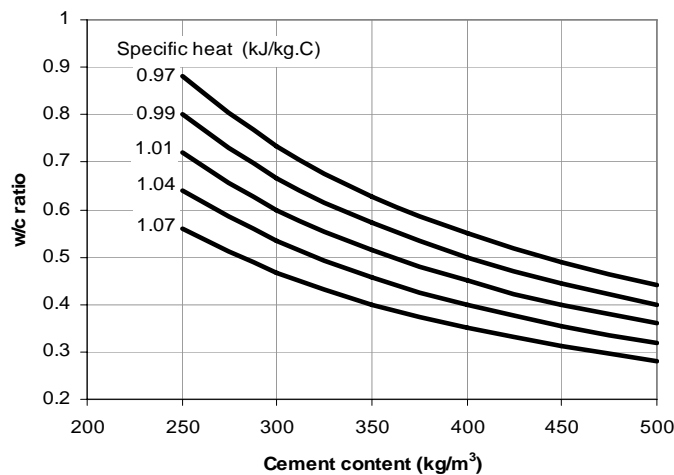


Figure A2.12 The relationship between cement content, w/c ratio and early-age specific heat (assuming the specific heat of the aggregate is 0.8 kJ/kg°C)

A2.5 Ambient temperature

Knowledge of the temperature variations at the site is needed for the calculation of the early-age thermal movement and the subsequent daily and seasonal movements. In the UK, the relevant information can be obtained from the climatology service of the Meteorological Office. Abroad, this information is not always so readily available. An assessment of the mean daily temperature during the period of construction is needed to predict the temperature rise. Knowing this mean daily temperature, the section thickness, type of formwork, and the cement type and content, the temperature rise can be predicted with adequate accuracy.

In order to predict thermal gradients, however, the daily temperature variation is needed. The ambient temperature can be modelled using a sinusoidal curve as shown in Figure A2.13. In this example, the modelled temperature varies between 10 °C and 22 °C. The effect of using a varying ambient temperature on a 300 mm thick wall using steel formwork is shown in Figure A2.14. As shown, even in a thin section with low insulation formwork the use of the mean daily temperature has little effect on the peak temperature.

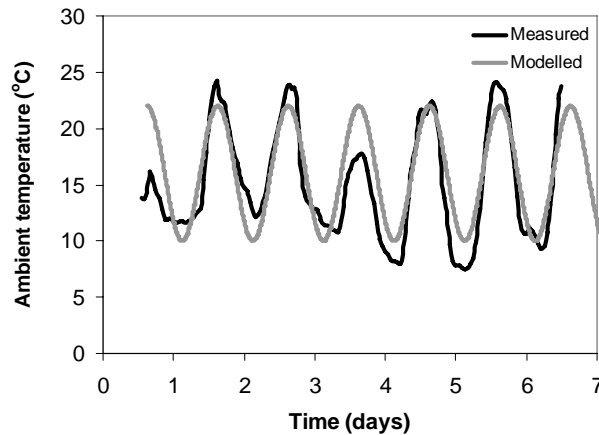


Figure A2.13 *Modelling the ambient temperature variation*

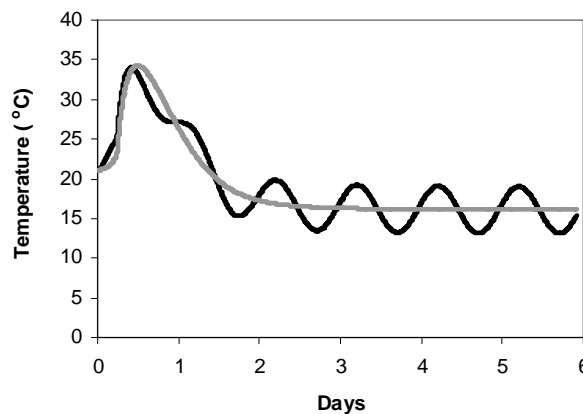


Figure A2.14 *The effect of ambient temperature variation on the temperature rise in a 300 mm wall using steel formwork*

While changes in the ambient temperature may have little impact on the concrete at the centre of a section, they will, of course, have a significant effect on the development of temperature differentials.

A2.6 Thermal conductance of the surface

The thermal conductance, G , has a significant impact on both the peak temperature and the temperature gradient as it determines the rate at which heat is lost from the surface. The value of G is determined by the nature of the formwork and by the wind speed, the latter having less impact on formwork with better insulating properties. Values of G were presented in CIRIA R67 (Harrison, 1978) and are given in Table A2.4.

Table A2.4 Values of thermal conductance for various formwork types and insulating materials

Form face and/or insulating material	Thermal conductance	
	W/m ² C	kcal/m ² .h.C
Exposed concrete	22.2	19.1
Formwork		
Up to 25mm steel	18.9	16.3
3mm glass fibre reinforced plastic	15.9	13.7
18mm plywood	5.2	4.5
37mm plywood	3.2	2.8
Precast planks		
50mm normal density concrete	13	11.2
100mm normal density concrete	10.1	8.7
150mm normal density concrete	8.3	7.1
Insulation		
Air space (20mm minimum)	4.5	3.9
50mm nominal (37mm actual) spruce	2.4	2.1
50mm wood wool	1.9	1.6
25mm glass wool	1.5	1.3
25mm dry sand	1.3	1.1
Mineral wool	1.3	1.1
Kapok quilt	1.3	1.1
Expanded polystyrene	1.3	1.1

The wind speed has a significant effect of the surface heat transfer. In a model developed by NIST (Bentz, 2000) using the FEMMASSE system (Schlangen, 2000) the following relationships were used;

$$G = 5.6 + 4.0 v_{\text{wind}} \quad \text{for } v_{\text{wind}} \leq 5 \text{ m/s} \quad (\text{A2.21})$$

$$G = 7.2 \times v_{\text{wind}}^{0.78} \quad \text{for } v_{\text{wind}} > 5 \text{ m/s} \quad (\text{A2.22})$$

Values used in FE analysis of early thermal behaviour by Bentz (2000) are summarised in Table A2.5 and included estimated using Equations A2.21 and A2.22.

Table A2.5 Values of thermal conductance used by the Bentz (2000)

Time span	Wind velocity km/h (m/s)	Surface heat transfer coefficient (W/m ² .K)				
		Wind velocity only	Estimated using equ. A2.22	Wind velocity and plywood	Wind velocity and insulation	Air, plywood and insulation
Nov-Apr	16 (4.44)	25.72	23.36	4.913	1.345	1.101
May-June	13 (3.61)	22.01	20.04	4.763	1.333	1.094
July-Sept	11 (3.06)	19.71	17.84	4.644	1.324	1.087
Oct	13 (3.61)	21.88	20.04	4.756	1.333	1.093

It is clear that the wind speed is far less significant when the surface is insulated. Within the model, Equations A2.21 and A2.22 have been used for exposed surfaces and the following equations have been used for formed surfaces:

$$\text{For steel formwork} \quad G = 5.3 + 3.3 v_{\text{wind}} \quad (\text{A2.23})$$

$$\text{For 18mm plywood formwork} \quad G = 4.4 + 0.2 v_{\text{wind}} \quad (\text{A2.24})$$

$$\text{For 37mm plywood formwork} \quad G = 2.4 + 0.2 v_{\text{wind}} \quad (\text{A2.25})$$

A2.7 Formwork striking times

The formwork striking time may influence T_1 but only if formwork is removed before the peak temperature is achieved. In some circumstances removing formwork the morning after casting can reduce the peak temperature. Figure A2.15 illustrates the effect of removing 18mm plywood formwork 15 hours after casting.

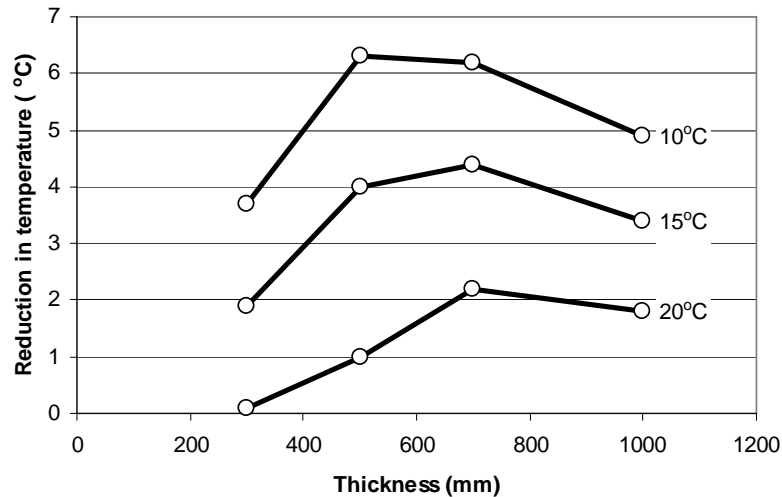


Figure A2.15 *The effect of removal of formwork after 15 hours on the peak temperature rise (for 350 kg CEM I, placing temperature 20 °C)*

For the example shown, it can be seen that the greatest reduction is achieved when the mix temperature is low and for sections with a thickness of about 500 to 700 mm although a reduction in T_1 of 5 °C may still be achieved in sections up to 1000 mm. The reduced benefit in thinner sections is because the peak temperature is achieved relatively early.

While it is clear that some benefit may be achieved under some circumstances, this reduced temperature rise does not form a safe basis for design as there are times when the formwork may be left in position for a longer period than planned (eg weekends). Even extending the striking time from 15 to 24 hours may largely negate any benefit. Nevertheless, contractors generally remove their formwork as soon as possible for economic reasons. In the assessment of formwork striking times, a number of factors need to be considered. For example, it should be noted that early removal of formwork will usually require additional efforts to adequately cure the young concrete.

While the peak temperature rise may be reduced, early removal of formwork will increase the temperature differential between the centre and the surface. An example of the effect of early striking of formwork is shown in Figure A2.16.

As the peak temperature is generally achieved at or close to about 24 hours, striking at this time may result in the most severe temperature differential. In the example shown, the removal of formwork results in a rapid drop in surface temperature, and a rapid increase in temperature differential of about 10 °C.

Where temperature differentials are considered to be a problem, most commonly in sections greater than about 500 mm, surfaces should remain insulated until the whole section has cooled to the extent that when the formwork is finally removed, the thermal strain associated with the rapid drop in the surface temperature does not exceed the tensile strain capacity of the concrete under rapid loading. This will depend on the aggregate type, being about 10 °C for flint gravel concretes and up to about 20 °C for limestone concretes. In thick sections this may require keeping the formwork and insulation in place for up to two weeks, and this is almost certainly the controlling striking criterion.

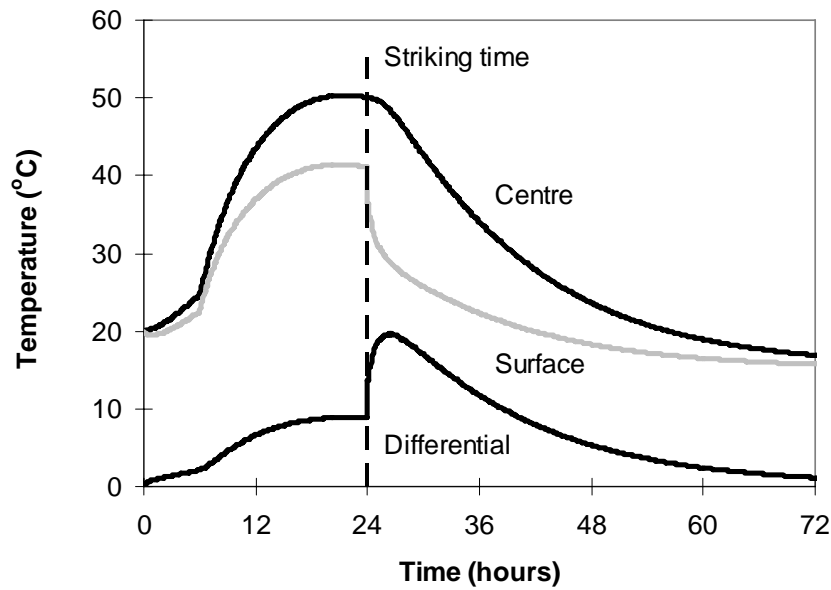


Figure A2.16 The effect of early removal of 18 mm plywood formwork on the temperature differential in a 500 mm thick wall (for 350 kg CEM I, placing temperature 20 °C)

When striking formwork, the thermal shock may be reduced by releasing the formwork and leaving it in place for a few hours to allow the surface to adjust more slowly to ambient conditions. It is also acceptable to replace formwork with insulation but care must be taken to ensure that the concrete is not exposed for too long a period while this process takes place. Table A2.6 gives estimates of temperature rise and temperature differential as affected by early formwork removal.

The arguments for the optimum choice of formwork materials closely follow those for surface cooling. Allowing the heat to escape from the surface of sections less than 500 mm thick reduces the core peak temperature without giving significant internal restraint. The best formwork materials for thin sections are the poor insulators (eg steel and GRP). However, for large isolated sections, the best solution is to insulate the section and let the temperature rise and fall as uniformly as possible. The optimum level of insulation with regard to the economics of construction is that which gives a temperature gradient just insufficient to cause cracking.

Table A2.6 Maximum temperature rise and temperature difference in a 500 mm thick wall section

Formwork type	Formwork left in place		Formwork removed after 15 hours	
	Temperature rise(°C)	Maximum temperature difference (°C)	Temperature rise(°C)	Maximum temperature difference (°C)
Steel	27	17	27	17
18 mm plywood	32	9	31	19
25 mm insulation on steel	42	4	37	22

cement content, 360 kg/m³ CEM I
 concrete placing temperature, 20 °C
 mean ambient temperature, 15 °C

A2.8 Running the model

The first page of the model – *Adiabatic temperature* – generates the adiabatic heat curve based on the model developed to represent the data generated in the study by University of Dundee (Dhir *et al*, 2006). Input data include:

- cement content (including any additions)
- cement type (CEM I, fly ash, ggbs)
- addition (as per cent of total CEM1 plus addition)
- density, δ , (kg/m³)
- specific heat, s , kJ/kg°C.

The details of the cement generate the reference adiabatic curve in terms of heat output, Q . This is then converted to an adiabatic temperature rise, $T_{ad(t)}$ for the proposed concrete using the equation:

$$T_{ad(t)} = \frac{Q(t)}{\partial \cdot s} \quad (\text{A2.26})$$

The results are generated and presented as curves as shown in Figure A2.17.

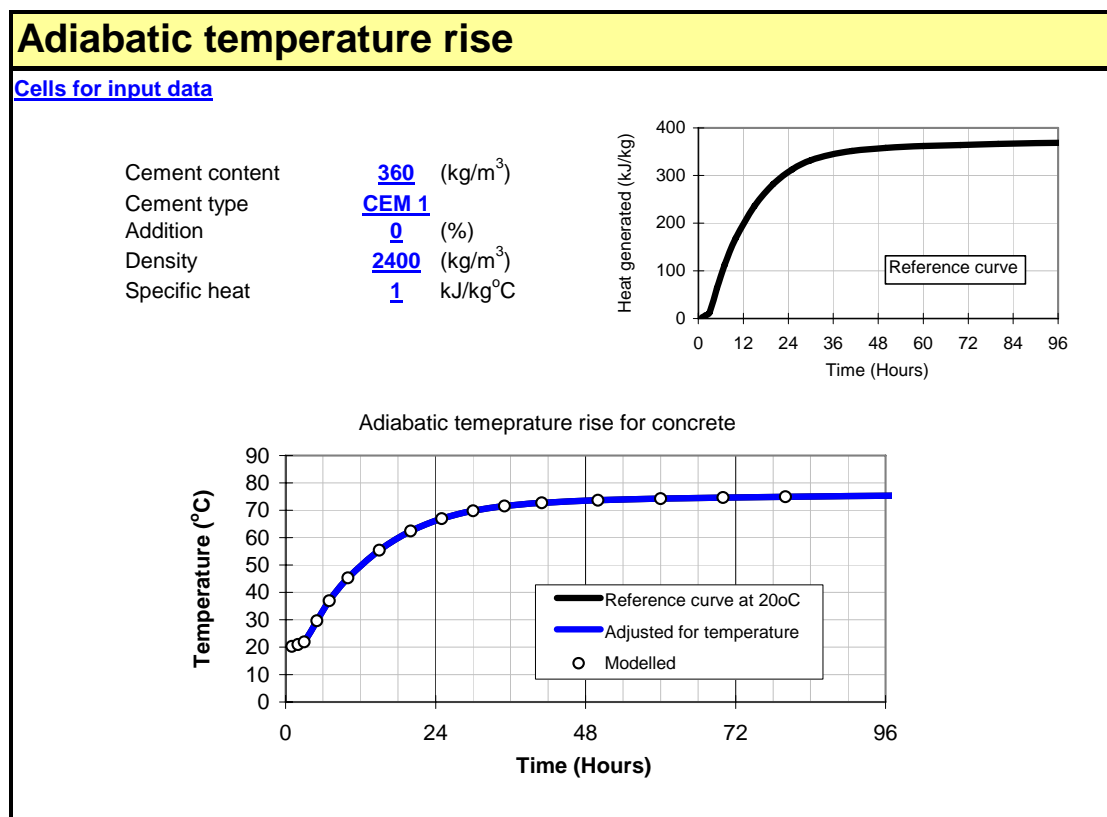


Figure 2.17 Page 1 of the spreadsheet model showing the adiabatic data generated for a particular cement type and concrete cast at 20 °C

Page two of the spreadsheet model – *Temperature calculations* – requires further input as follows:

- section thickness (mm)
- formwork type – selected from menu including:

- Up to 25 mm steel
 - 18 mm plywood
 - 37 mm plywood
- wind speed (m/s)
 - time of formwork removal (hours)
 - coefficient of thermal conductivity of the concrete (W/m.K)
 - placing temperature (°C)
 - minimum, MEAN and maximum ambient temperature (if no information is available on the range assume $\pm 5^\circ\text{C}$)
 - start time for concreting (using the 24 hour clock).

Outputs are then calculated as shown in Figure A2.18 and include:

- the maximum temperature and the time at which it is achieved
- the maximum differential and the time at which it is achieved
- T_f for use in the design process.

Also shown graphically are:

- the rate of change of the temperature differential between the centre and the surface
- the maximum temperature differential and the temperature differential at the time of the maximum temperature.

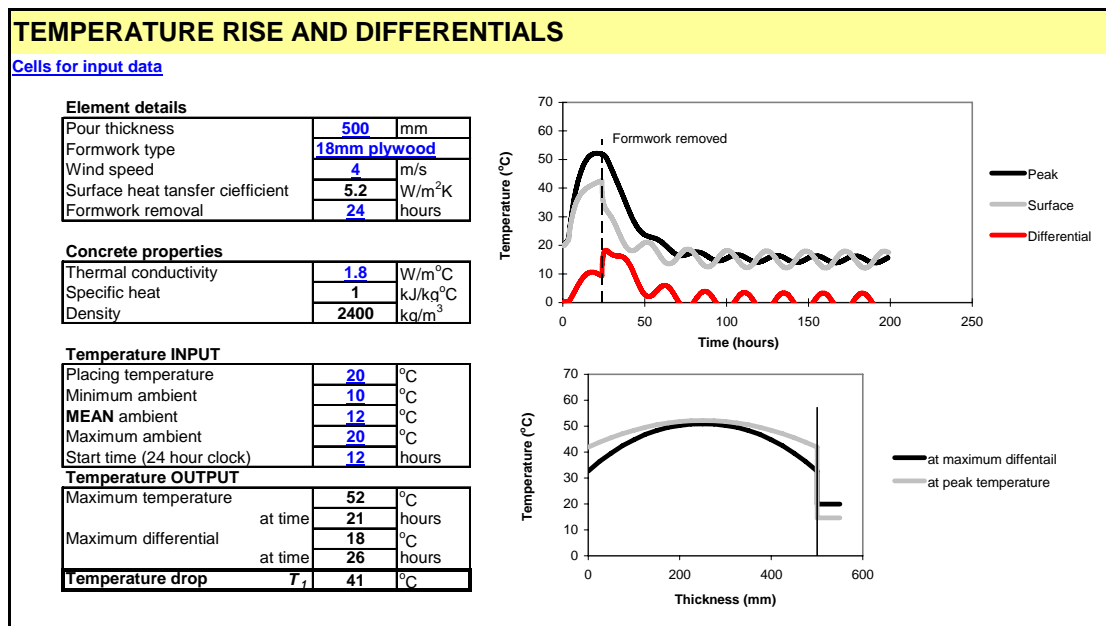


Figure A2.18 The temperature calculation page of the spreadsheet showing required *inputs* and calculated *outputs*

A2.9 Validation

In order to test the model comparisons have been made with published data in conditions where measurements have been obtained from structures or full size test specimens. Three sources have provided a significant quantity of data covering a range of cement types and casting conditions.

1 Study of temperature rise and restraint in walls (Anson and Rowlinson, 1988).

In this paper data are reported from 12 full size walls varying in thickness from 300 mm to 850 mm. Concretes varied in binder content from 290 kg/m³ to 360 kg/m³ and contained combinations with both fly ash and ggbs. Mix temperatures varied from 7 °C to 23 °C. Details are given in Table A2.7.

Table A2.7 Data reported by Anson and Rowlinson (1988) for concrete walls up to 850 mm thick

Thickness	Cement content (kg/m ³)	Cement type	Aggregate type	Temperature (°C)			
				Ambient (°C)	Placing (°C)	Rise above placing (°C)	T ₁
400-680 (assumed 623)	360	39% ggbs	Gravel	2.0	7.0	16.5	21.5
600	360	CEM I	Gravel	4.0	14.0	19.5	29.5
600	360	CEM I	Gravel	5.0	12.0	23.0	30.0
850	290	30% fly ash	Limestone	9.0	14.0	19.5	24.5
800	330	40% ggbs	Limestone	12.0	17.0	31.0	36.0
800	330	40% ggbs	Limestone	14.0	23.0	31.0	40.0
400-800 (assumed 720)	360	50% ggbs	Limestone	12.0	19.0	21.0	28.0
400	345	CEM I	Limestone	15.0	19.0	25.0	29.0
600	345	CEM I	Limestone	13.0	21.0	24.0	32.0
600	355	CEM I	Limestone	18.0	23.0	31.0	36.0
300	360	CEM I	Limestone	3.0	9.5	21.5	28.0
400-880 (assumed 784)	360	CEM I	Limestone	11.0	21.0	35.0	45.0

2 Study of *in situ* strength (Concrete Society 2004).

As part of the Concrete Society project to measure *in situ* strength, a series of large scale specimens were cast. These included 1.5 m cubes insulated on all but one face, 300 mm thick walls and 200 mm thick slabs. Sixteen concretes types were investigated, using two aggregate types each at two levels of strength and four cement types in a full factorial study. In addition, specimens were cast in the winter and the summer. Mix details and temperature measurements are given in Table A2.8.

3 Measurement of temperature rise under tropical conditions (Fan, Aw and Tan, 2004).

In Singapore, an extensive test programme was carried out to determine T_1 values in tropical conditions for concrete with a placing temperature of 34 °C. Tests were carried out on the range of element thickness covered by CIRIA R91 (Harrison, 1992) using CEM I cement at level of 315, 365 and 390 kg/m³. Both steel and plywood formwork were investigated. The results from these tests are shown in Table A2.9.

It can be seen that the combination of data from these three sources provided 54 data points covering a wide range of conditions, with variation in cement contents from 215 to 390 kg/m³, the inclusion of fly ash (30 per cent) and ggbs (from 39 to 50 per cent), section thicknesses from 300 to 1000 mm, and placing temperatures from 7 to 34 °C.

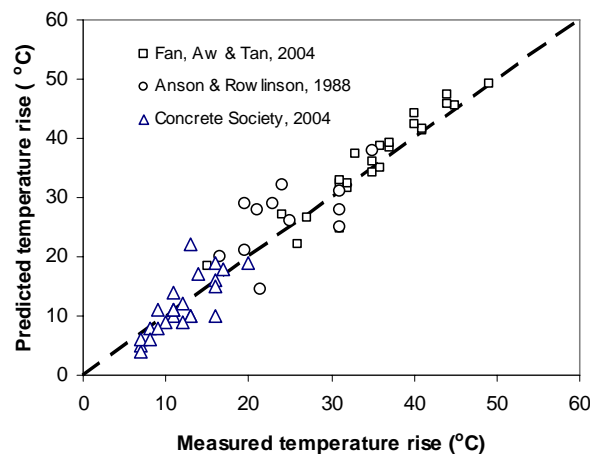
In order to test the model, a comparison was made between the predicted levels of temperature rise in each of the elements above the placing temperature. This eliminated any errors in the assumptions regarding the mean ambient temperature. The results are shown in Figure A2.17.

Table A2.8 Data reported by the Concrete Society (2004) for concrete walls 300 mm thick

Cement content (kg/m ³)	Cement type	Aggregate	Temperature (°C)							
			Winter casting				Summer casting			
			Amb.	Placing	Rise above placing	T _l	Amb.	Placing	Rise above placing	T _l
240	CEM I	gravel	7	12	10	15	11	21	11	21
345	CEM I	gravel	6	14	16	24	12	22	19	29
220	CEM I	limestone	10	14	14	18	13	19	12	18
310	CEM I	limestone	10	12	19	21	12	18	18	24
275	30% fly ash	gravel	7	12	8	13	11	20	8	17
385	30% fly ash	gravel	8	11	22	25	13	21	15	23
255	30% fly ash	limestone	10	13	11	14	13	17	10	14
365	30% fly ash	limestone	10	13	10	13	12	15	17	20
230	50% ggbs	gravel	7	10	5	8	11	19	6	14
330	50% ggbs	gravel	6	9	9	12	13	18	10	15
215	50% ggbs	limestone	10	14	4	8	13	18	6	11
305	50% ggbs	limestone	10	11	11	12	12	16	9	13

Table A2.9 Measured T_l values for concretes with a casting temperature of 34 °C and a mean ambient temperature of 29 °C (Fan et al, 2004)

Section thickness (mm)	Steel formwork			Plywood formwork		
	315 kg/m ³	365 kg/m ³	390 kg/m ³	315 kg/m ³	365 kg/m ³	390 kg/m ³
300	20	31	36	32	37	40
500	29	36	41	37	42	46
700	36	41	46	40	45	50
1000	38	45	49	42	49	54

**Figure A2.17** Comparison between measured temperature rise and values predicted using the adiabatic model

It is apparent from the results in Figure A2.15 that, although there is considerable scatter of the results, the model does, on average, provide a reasonable prediction of temperature rise over the range of conditions investigated. Indeed, it is to some extent surprising that that data from one source is able to lead to predictions which are as close as they are to a range of concretes using entirely different source materials, and recognising, in particular the heat generating capacity of different cements.

A2.10 Limitations

While the model, using a specific data source for heat generation of cements, has been shown to be able to predict temperature rise with a reasonable degree of accuracy, it is limited inasmuch as it is uniaxial only. This is not a significant problem in most pours where one dimension (eg the depth of a slab or the thickness of a wall) is generally much less than the other two dimensions.

It is recognised that such a model will be most reliable when predicting the temperature rise in thick sections. A comparison was made by Vithanara and Sakai (2001) using predictions of temperature rise in 200 mm and 2000 mm sections. The results demonstrated that higher temperatures were predicted using the adiabatic approach. As expected, the difference was greater in the thinner sections, being about 4 °C in the 200mm section, where the temperature rise was only predicted to be in the order of 10°C. It is apparent that the errors are most significant under conditions of low temperature rise where the risk of thermal cracking is lowest and that the error reduces as the level of risk increases.

It is also recognised that the Rastrup function must be adjusted to take account of the different activation energy of different cements and combinations, in particular when using ggbs. Within the model, there is scope to revise the factor of 12 currently used in the Rastrup equation for different cement types but currently the same value is applied to all cements and combinations. For this reason the error is likely to increase when large adjustments are made from the mix temperature at which the reference data was obtained. This may be overcome, however, by carrying out the test at a mix temperature which is closer to the expected placing temperature.

Hence, while the method has its limitations, it is useful in that it tends to predict values of temperature rise that are conservatively, but not excessively high and offers the flexibility to undertake scoping studies to investigate the effects of varying the mix, the boundary conditions (formwork or insulation) and environmental conditions. It also enables temperature differentials to be estimated, helping to inform decisions regarding appropriate types of formwork and insulation and when they may be removed.

A2.11 Conclusions

1. A model has been developed which enables a prediction to be made of the temperature rise in concrete elements. The input data are adiabatic curves derived from extensive testing at the University of Dundee (Dhir *et al*, 2006). The model is able to take account of variations in the following factors
 - cement content
 - the use of fly ash or ggbs in different proportions
 - mix temperature
 - ambient temperature and its daily variation
 - section thickness
 - formwork type
 - time of formwork removal.
2. Reasonable correlation has been obtained between predictions of temperature rise using the model and independent published data on temperature rise for a variety of concrete mixes, element sizes and mix temperatures.

A2.12 References

- Anson, M and Rowlinson, P M (1988)
 “Early-age strain and temperature measurements in concrete tank walls”
Magazine of Concrete Research, Vol. 40, No. 145, December 1988
- Bamforth, P B (1976)
 “Temperature prediction and it’s significance”
 In: Proc seminar *Carry on casting*, Cement and Concrete Association, Fulmer Grange, Slough, February 1976
- BAMFORTH, P B (1979)
 “The Early Age Behaviour of a Massive Reinforced Concrete Suspended Slab”
 In: Proc Int. Conf. on *Concrete slabs*, University of Dundee, 3-6 April 1979
- Bamforth, P B (1980)
 “*In situ* measurement of the effects of partial Portland cement replacement using either fly ash or ground granulated slag on the performance of mass concrete”
Proc. Instn. Civ. Engrs. 69, Part 2, Sept 1980, pp 777-800
- Bamforth, P B (1984)
Mass concrete
 Concrete Society, Digest No.2, 1984, Camberley, Surrey
 <<http://products.ihs.com/cis/Doc.aspx?AuthCode=&DocNum=50470>>
- Bamforth, P B (1984b)
 “Heat of Hydration of Pfa Concrete and its Effect on Strength Development”
 In: Proc 2nd Int. Conf. on *Ash technology and marketing* (ASHTECH '84) London, September 1984
- Bamforth, P B and Price, W F (1995)
Concreting deep lifts and large volume pours
 R135, CIRIA, London
- Bamforth, P B, (2003)
 “Concreting large-volume (mass) pours”
Advanced Concrete Technology, (eds: J Newman and B S Choo), Processes, **13**, Elsevier, Butterworth, Heinemann
- Bentz D P (2000)
 “A computer model to predict the surface temperature and time-of-wetness of concrete pavements and bridge decks”
 United States Department of Commerce, Technology Administration, National Institute of Standards and Technology, NISTIR 6551, 2000
- Clauser, C and Huenges, E (1995)
 “Thermal conductivity of rocks and minerals”
Rock physics and phase relations – A handbook of physical constants (ed: T J Ahrens), American Geophysical Union, pp 105-126
- Concrete Society (2004)
In situ strength of concrete – An investigation into the relationship between core strength and the standard cube strength
Working party of the Concrete Society, Project Report No 3, BCA, Camberley, Surrey,
 ISBN 0 94669 186 X
- Crank, J, (1975)
The mathematics of diffusion
 Second Edition, Oxford Science Publications, **8**, Numerical methods

- Dhir, R, Paine, K A and Zheng, L (2006)
Design data for use where low heat cements are used
 DTI Research Contract No. 39/680, CC2257, University of Dundee, Report No CTU2704
- Fan, S C Aw, K M and Tan, Y M (2004)
 “Peak temperature-rise for early-age concrete under tropical climatic conditions”
Journal of the Institution of Engineers, Singapore, Vol.44, Issue 1
- Harrison, T (1978)
Tables of minimum striking times for soffit and vertical formwork
 R67, CIRIA, London
- Harrison, T (1992)
Early-age thermal crack control in concrete
 R91, CIRIA, London
- Kishi, T and Maekawa, K (1995)
 “Multi-component model for hydration heating of Portland cement”
 Translation from *Proc. JSCE, No. 526, V-29, November 1995*
- Rastrup, E (1954)
 “Heat of hydration in concrete”
Magazine of Concrete Research, September 1954, pp 79-92
- Ross, A D and Bray, J W (1949)
 “The prediction of temperatures in mass concrete by numerical calculation”
Magazine of Concrete Research, January 1949, pp 9-17
- Ruiz, J M, Schindler, A K, Rasmussen, R O and Johnson, T (2003)
 “Prediction of heat transport in concrete made with blast-furnace slag aggregate”
Advances in Cement and Concrete IX, Volume Changes, Cracking and Durability, Colorado
- Schindler K and Folliard, K J (2005)
 “Heat of hydration models for cementitious materials”
ACI materials journal Vol. 102, No. 1, 2005, pp 24-33
- Schlangen, E (2000)
Online Help/Manual module HEAT of FEMMASSE, 1990-2000
 FEMMASSE b.v. The Netherlands, 2000
- USACE (1995)
 “Temperature control of mass concrete”
Engineering Manual EM1110-2-2200, 6, June 1995
- Vitharana, V and Sakai, K (1995)
 “Early-age behaviour of concrete sections under strain induced loadings”
 In: Proc 2nd Int. Conf. on *Concrete under severe conditions CONSEC '95*, (eds: Satai, K, Banthai, N, and Gjorv, O E) Sapporo, Japan, 2-4 August 1995, pp 1571-1581
- Wadso J (2003)
An experimental comparison between isothermal calorimetry, semi-adiabatic calorimetry and solution calorimetry for the study of cement hydration
 Technical Report 533, Nordtest Project No. 1534-01, March 2003, Nordtest, Tekniikantie 12, FIN-02150 Espoo, Finland

A3 Estimating drying shrinkage using the method of EN1992-1-1

EN1992-1-1 provides a method for estimating drying shrinkage. It is based on the strength class of the concrete, the average ambient relative humidity and the dimensions of the element under consideration. The process starts by estimating the nominal unrestrained drying shrinkage value, $\varepsilon_{cd,0}$ based on the strength class of the concrete and the average ambient humidity. This is derived using the equations

$$\varepsilon_{cd,0} = 0.85 \left[(220 + 110 \cdot \alpha_{ds1}) \cdot \exp\left(-\alpha_{ds2} \cdot \frac{f_{cm}}{f_{cmo}}\right) \right] 10^{-6} \beta_{RH} \quad (\text{A3.1})$$

and

$$\beta_{RH} = 1.55 \left[1 - \left(\frac{RH}{RH_0} \right)^3 \right] \quad (\text{A3.2})$$

where:

- f_{cm} is the mean compressive strength (cylinder)
- $f_{cmo} = 10 \text{ MPa}$
- α_{ds1} is a coefficient which depends on the type of cement
 - = 3 for cement Class S
 - = 4 for cement Class N
 - = 6 for cement Class R
- α_{ds2} is a coefficient which depends on the type of cement
 - = 0.13 for cement Class S
 - = 0.12 for cement Class N
 - = 0.11 for cement Class R
- RH is the ambient relative humidity (%)
- $RH_0 = 100\%$.

Values of $\varepsilon_{cd,0}$ calculated using equations A3.1 and A3.2 are presented as Table 3.2 in EN1992-1-1 for different grades of concrete and levels of relative humidity. The data is illustrated in Figure A3.1.

To take account of the fact that the ultimate shrinkage will be lower in larger sections, even when considered over very long timescales, a coefficient k_h is applied to the nominal unrestrained drying shrinkage. The coefficient k_h is related to the notional size of the cross-section h_0 according to the equation

$$h_0 = 2A_c/u, \quad (\text{A3.3})$$

where:

- A_c is the concrete cross-sectional area
- u is the perimeter of that part of the cross section which is exposed to drying.

For walls drying from both faces, h_0 approximates to the wall thickness h .

For walls or slabs drying from one face only, $h_0 = 2h$.

The relationship between k_h and h_0 is shown in Figure A3.2. This is a graphical representation of values given in Table 3.2 of EN1992-1-1 for concrete with CEM I.

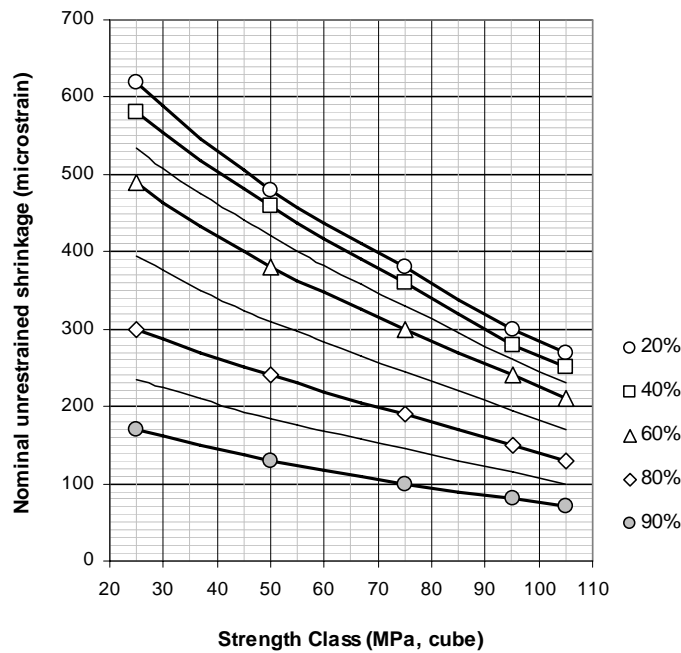


Figure A3.1 The relationship between unrestrained drying shrinkage, strength class and ambient humidity

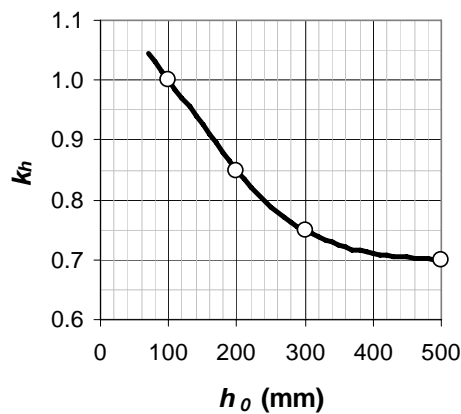


Figure A3.2 The relationship between the coefficient, k_h , and the notional size, h_0

Having established the maximum drying shrinkage for a specific element cast using a specific concrete, the rate at which the shrinkage occurs may be calculated using the equation,

$$\epsilon_{cd}(t) = \beta_{ds}(t, t_s) \cdot k_h \cdot \epsilon_{cd,0} \tag{A3.4}$$

where
$$\beta_{ds}(t, t_s) = (t - t_s) / \{ (t - t_s) + 0.04 \sqrt{h_0^3} \} \tag{A3.5}$$

and t is the age of the concrete at the time considered, in days
 t_s is the age of the concrete (days) at the beginning of drying, normally the end of the curing period.

Shrinkage curves estimated using this approach for a C30/37 concrete, cast into walls drying from both faces into ambient relative humidity's of 45 per cent (indoor conditions) and 85 per cent (typical UK outdoor conditions) are shown in Figure A3.3.

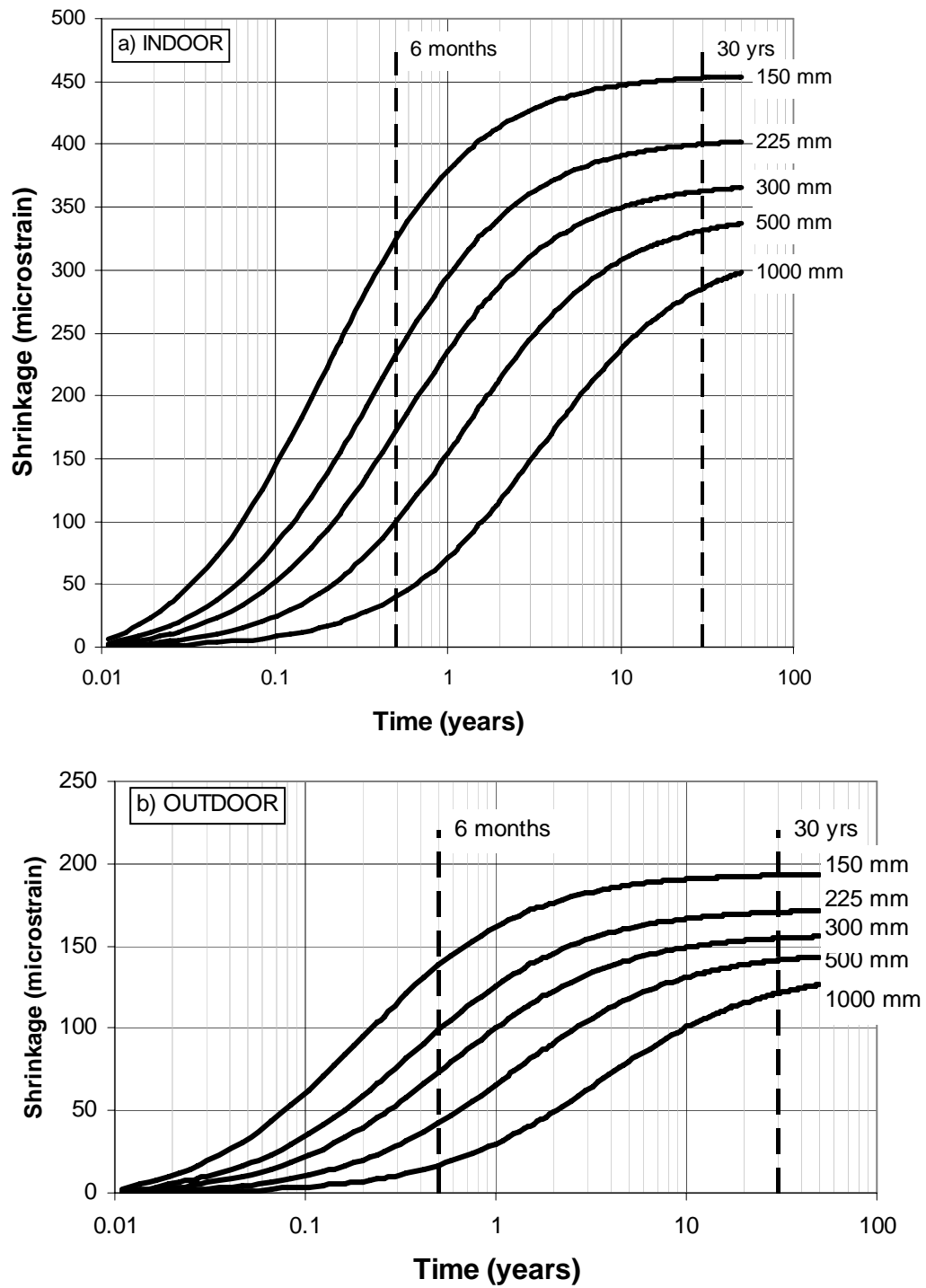


Figure A3.3 *Drying shrinkage curves estimated using the method of EN1992-1-1 for a) indoor conditions (45 per cent rh) and b) UK outdoor conditions (85 per cent rh)*

A4 Estimating autogenous shrinkage

A4.1 Introduction

While considerable research has been carried out to measure autogenous shrinkage and many of the influencing factors have been identified (most notably the water/binder ratio [w/b] and the binder composition) it is still recognised that the magnitude of autogenous shrinkage is difficult to predict. Nevertheless, EN1992-1-1 offers a method for estimating autogenous shrinkage based solely on the strength class of the concrete. This method is described and compared with published data. The influence of different cementing materials has also been investigated.

A4.2 The method of EN1992-1-1

The EN1992-1-1 method for estimating autogenous shrinkage is based solely on the strength class of the concrete according to the equation,

$$\varepsilon_{ca}(t) = \beta_{as}(t) \cdot \varepsilon_{ca}(\infty) \quad (\text{A4.1})$$

where:

$$\begin{aligned} \varepsilon_{ca}(t) & \text{ is the autogenous shrinkage at time } t \text{ days} \\ \varepsilon_{ca}(\infty) & \text{ is the ultimate autogenous shrinkage} = 2.5(f_{ck} - 10) \times 10^{-6} \end{aligned} \quad (\text{A4.2})$$

where

$$\begin{aligned} f_{ck} & \text{ is the characteristic cylinder strength} \\ \beta_{as}(t) & \text{ is a function defining the time dependent development of autogenous shrinkage} \\ \beta_{as}(t) & = 1 - \exp(-0.2 \cdot t^{0.5}) \end{aligned} \quad (\text{A4.3})$$

Using these equations a series of autogenous shrinkage curve have been developed for different strength classes as shown in Figure A4.1.

While it has previously been assumed that autogenous shrinkage will only occur in concretes with very low w/b ratios, typically below about 0.40 (Pigeon *et al*, 2005) EN1992-1-1 predicts that autogenous shrinkage will occur, to some degree, in all structural concretes. An investigation of published data has been carried out to support this supposition.

The results from tests on cement pastes over a range of w/b ratios are shown in Figure A4.2. It can be seen that in the short term the magnitude of autogenous shrinkage may be low when the w/b is of the order of 0.45 and at higher w/b ratios swelling may occur (Nawa and Horita, 2004). However, in the long-term, autogenous shrinkage may be significant (Baroghel-Bouny and Kheirbek, 2000) even when the w/b ratio is as high as 0.6. The magnitude of the values for concrete will, of course, be much lower than the values shown in Figure A4.2, as shown by the comparison with values estimated in accordance with EN1992-1-1.

Unfortunately, because of the assumption that autogenous shrinkage is only significant in high-performance, low w/b concrete, published data for concretes with w/b ratios above about 0.4 are both limited and variable. Saje *et al* (2001) reported autogenous shrinkage at 48 hours of 180 and 0 microstrain for concretes with w/b ratios of 0.40 and 0.52 respectively. These concretes had mean cube strengths of 67.4 and 48.4 MPa (representing class C50/60 and C33/40) with EN1992-1-1 predicting 48-hour values of autogenous shrinkage of 25 and 14 microstrain. For the higher strength concrete the measured value was significantly higher than predicted while for the lower strength class, EN1992-1-1 predicted higher shrinkage than reported.

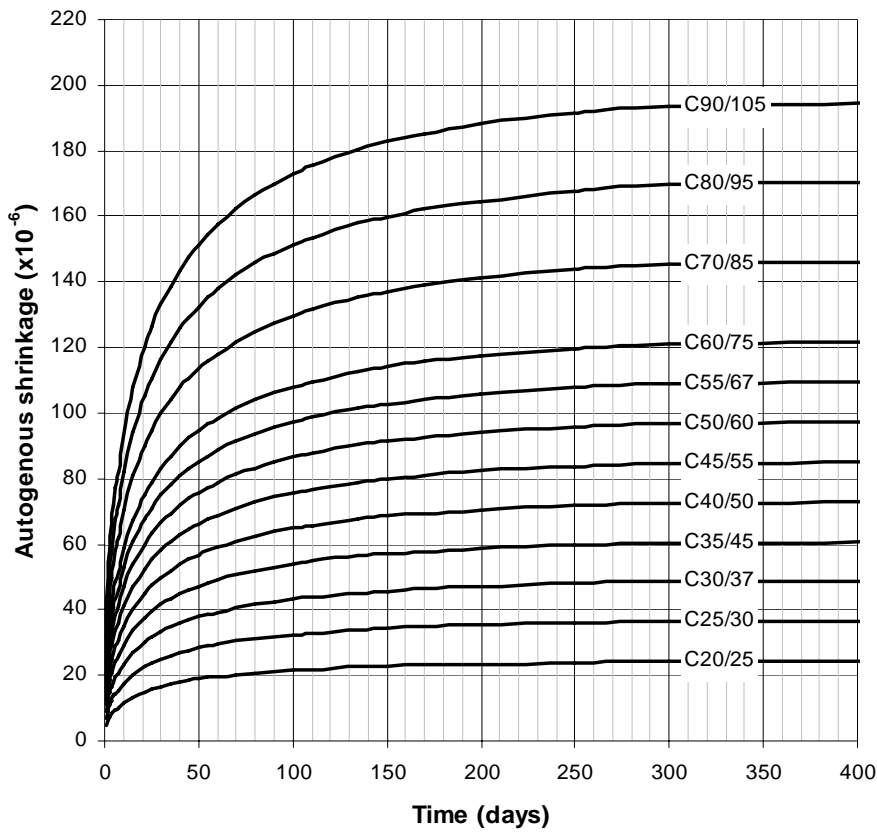


Figure A4.1 Autogenous shrinkage for different strength classes estimated using the method of EN1992-1-1

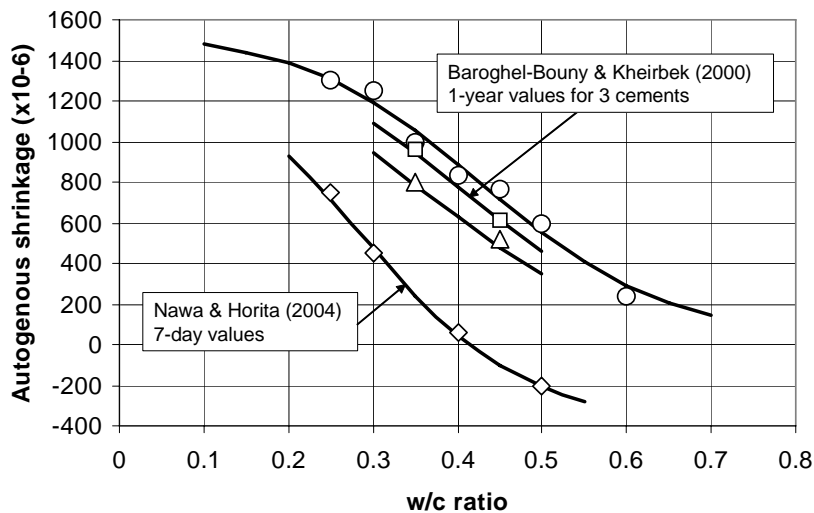


Figure A4.2 Reported values of autogenous shrinkage in cement pastes

Other comparisons with EN1992-1-1 can be made for concretes at lower w/b ratios. Pigeon *et al* (2005) tested 5 concretes, all with w/b =0.35 but with different binders and additives. Autogenous shrinkage was measured at 5 days and the results are shown in Figure A4.3 compared with the mean cylinder strength. Again, all measured values were in excess of values predicted by EN1992-1-1.

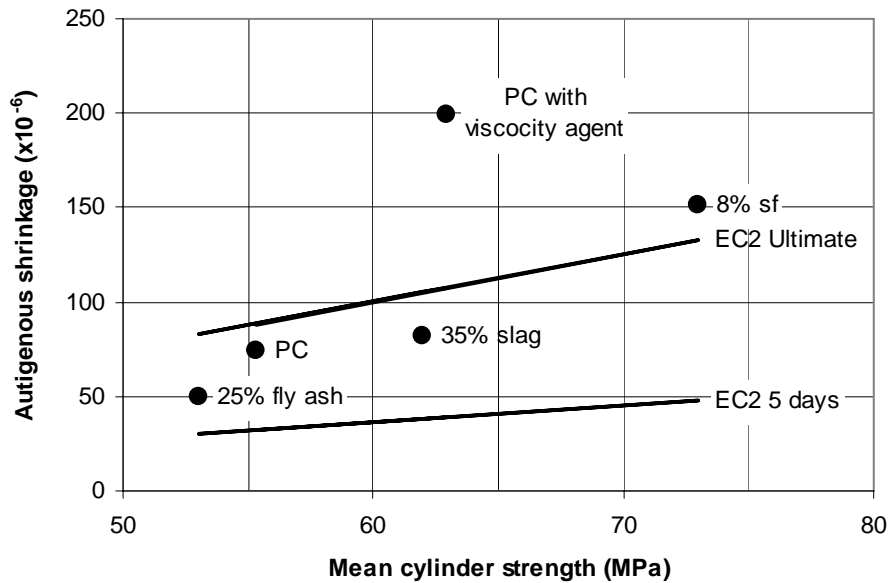


Figure A4.3 Measured (at 5 days) and predicted values of autogenous shrinkage for concretes using different binders and additives (Pigeon *et al*, 2005)

Scheißl *et al* (2000) tested high performance concretes, mostly with silica fume and again reported values of autogenous shrinkage that are appreciably higher than predicted by EN1992-1-1. After 21 days values typically in the range 300-400 microstrain were obtained while EN1992-1-1 predicts values which are only about 50 per cent of those reported.

In a review of work carried out by the JCI committee on autogenous shrinkage, Tazawa *et al* (2000) offers equations for ultimate autogenous shrinkage of the form:

$$\text{for } 0.2 \leq w/b \leq 0.5 \quad \varepsilon_{ca0} = 3070 \cdot \exp\{-7.2(w/b)\} \quad (\text{A4.4})$$

$$\text{for } w/b > 0.5 \quad \varepsilon_{ca0} = 80 \quad (\text{A4.5})$$

At a w/b ratio of 0.35, this predicts an ultimate autogenous shrinkage of about 250 microstrain compared with values of about half this magnitude predicted by EN1992-1-1 for concretes with a strength class associated with this w/b ratio.

The evidence suggests, therefore, that the approach of EN1992-1-1 will underestimate autogenous shrinkage for concretes of a high strength class, but may overestimate the magnitude for concretes of lower strength classes. The apparent underestimate for normal structural grades of concrete may be due to the fact that EN1992-1-1 only requires that autogenous shrinkage be considered when new concrete is cast against hardened concrete and that the values presented take into account a 50 per cent reduction for creep. This would seem to be a reasonable explanation and is discussed in more detail in Section A4.3.

A4.3 The critical w/b ratio

In order to determine whether a critical w/b exists, below which it may be assumed that autogenous shrinkage will not occur, and to derive a method of prediction which is more consistent with measurements, a detailed analysis has been carried using one of the most comprehensive studies undertaken on cement pastes with w/b ratios varying from 0.25 to 0.60 (Baroghel-Bouny and Kheirbeck, 2000). Recognising that shrinkage in concrete will be significantly less than in cement paste, the composite model developed by Hobbs (1974) has been applied to estimate values for concrete. This takes account of the relative volume of cement paste and aggregate and the relative stiffness of the two components. Calculations have been carried assuming an aggregate with an elastic modulus of 55 GPa.

The elastic modulus of the cement paste is based on a relationship with w/b ratio derived from the data of Nawa and Horita (2004). The Hobbs model predicts that the shrinkage in concrete will be between 20 and 30 per cent of that occurring in cement paste, with the higher percentage being achieved in the lower w/b mixes.

The results from this analysis are shown in Figure A4.4, presented as the time-dependent strain at different w/b ratios. Data were reported for a period of 12 months and the results have been shown for the full period and on an expanded scale for the first 28 days. The results indicate that short term autogenous shrinkage (ie within the first 7 days) is unlikely in concretes with values of w/b in excess of 0.45. Indeed, during this early period some swelling may be expected. However, even for these higher w/b concretes, autogenous shrinkage may need to be taken into account when assessing longer term strains.

The results shown in Figure A4.4 indicate that EN1992-1-1 may underestimate the magnitude of autogenous shrinkage for the lower w/b mixes, particularly within the period when it will have the greatest impact on early thermal cracking. Consider a concrete with a w/b ratio of 0.45. Using CEM I this might be expected to achieve a class C40/50 concrete with a mean cube strength of about 60 MPa. For this strength class, EN1992-1-1 predicts 30 microstrain autogenous shrinkage, while measurements suggest a 7-day value of 70 microstrain. The difference in the longer term strain is greater. At 1 year, while EN1992-1-1 predicts 75 microstrain, the value based on observations is closer to 200 microstrain.

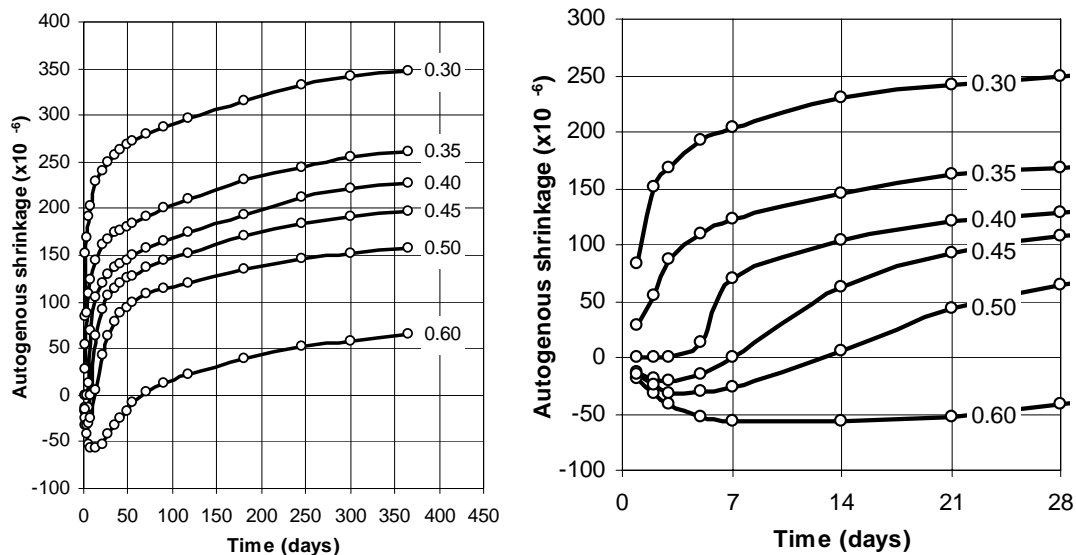


Figure A4.4 Estimated values for autogenous shrinkage of concretes using CEM I with w/b ratios from 0.3 to 0.6 (left – long-term; right – up to 28 days)

While for low w/b ratio concrete EN1992-1-1 would appear to underestimate the shrinkage, at higher w/b ratios EN1992-1-1 predicts higher values than indicated by measured results. At a w/b of 0.6, the results in Figure A4.4 suggest that autogenous shrinkage will not be apparent within the first three months, while EN1992-1-1 predicts that for a C25/30 concrete, the shrinkage within this period will be 20 microstrain.

Hence, while the method of EN1992-1-1 for predicting autogenous shrinkage is simple, it is likely that if these estimates are used in design, particularly for low w/b concrete, the magnitude of strain will be underestimated.

A4.3 Dealing with autogenous shrinkage in design

Many of the observations of autogenous shrinkage indicate that the biggest impact of w/b ratio is on the magnitude of shrinkage within the first few days. In studies on cement paste, Baroghel-Bouny and Kheirbeck, (2000) reported that for very low w/b mixes, more than 50 per cent of the 1-year shrinkage was achieved within the first 24 hours. It was also reported that for pastes with normal w/b ratios (0.45 and above) some swelling may occur during this early period. Others have observed this early swelling (Scheißl *et al*, 2000). The results also indicated beyond the first month or so after casting, w/b ratio had very little effect on the rate of shrinkage. For example, between 28 days and 360 days Baroghel-Bouny and Kheirbeck, (2000) reported an increase in autogenous shrinkage of about 400 ± 50 microstrain for pastes with w/b ratios from 0.25 to 0.60. Interestingly the trend was for the magnitude to be higher for the higher w/b mixes.

With regard to early-age cracking, however, it is the stress-inducing component of autogenous shrinkage that is important. In the study by Scheißl *et al* (2000) the stress development associated with autogenous shrinkage after 7 days was measured. It was concluded that tensile stresses could not be determined directly from autogenous shrinkage. Indeed, in some specimens tensile stresses were recorded even though there was a reported net swelling of the concrete. A closer inspection of these results suggests that, as assumed for early thermal stresses, much of the stress developed due to strain within the period immediately after setting is relieved by creep and may be ignored in relation to stress development. Where data are provided (Scheißl *et al*, 2000) it would appear that the stress at seven days may be related broadly to the strain that occurs between 1 and 7 days, indicating that strains within the first 24 hours, whether shrinkage or swelling, did not contribute to stress development. During the period from 1 to 7 days, shrinkage strains were of the order of 100 microstrain, leading to stresses of about 3 MPa. The estimated mean elastic modulus of these concretes derived from the stress and strain measurements is about 33 GP, this being consistent with high performance, low w/b concrete.

Assuming that the early autogenous shrinkage will not contribute to stress development, the data from Figure A4.4 have been normalised to show only the change in autogenous shrinkage beyond 24 hours. The curves are shown in Figure A4.5 and are compared with the estimates of EN1992-1-1.

When taking into account the uncertainties in generating the results for concrete from tests on cement paste may be concluded that the values estimated using the method of EN1992-1-1 are broadly consistent with the reported data over the long-term. The principal difference is at very early-age, the period of interest for this guide, where there is evidence of some early swelling in concretes with w/b ratios greater than about 0.45. These early values are shown in Figure A4.6 on an expanded timescale. The results have been used in considering an alternative set of design values for early-age autogenous shrinkage and these are given in Figure A4.7. Using this approach autogenous shrinkage may be expressed by the equation:

$$\epsilon_{ca} = 240t^{0.15} - 650(w/b) \quad (\text{A4.6})$$

where: t is the time in days.

These results are consistent with current practice in the UK which has assumed that autogenous shrinkage does not occur when $w/b < 0.45$. In view of the current uncertainties in predicting autogenous shrinkage it is proposed that swelling is not taken into account in the design process.

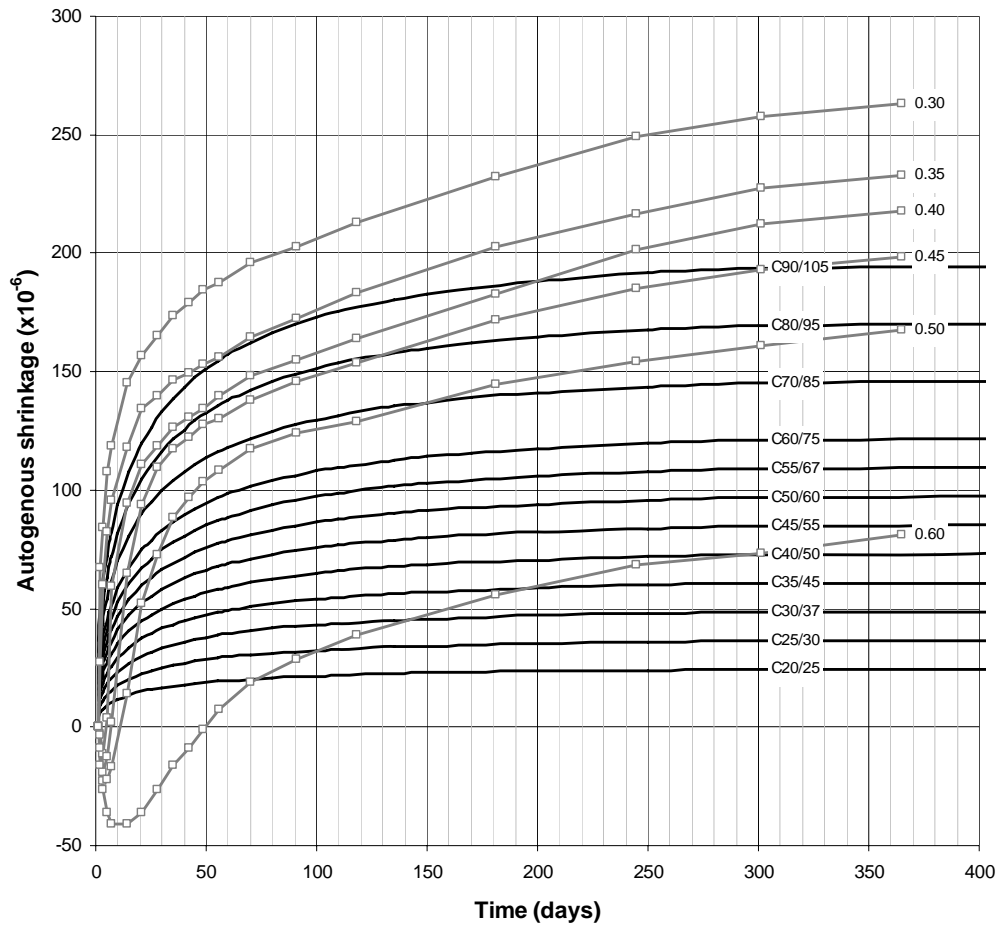


Figure A4.5 *A comparison between autogenous shrinkage estimated using the method of EN 1992-1-1 and values derived from the results of Baroghel-Bouny and Kheirbeck*

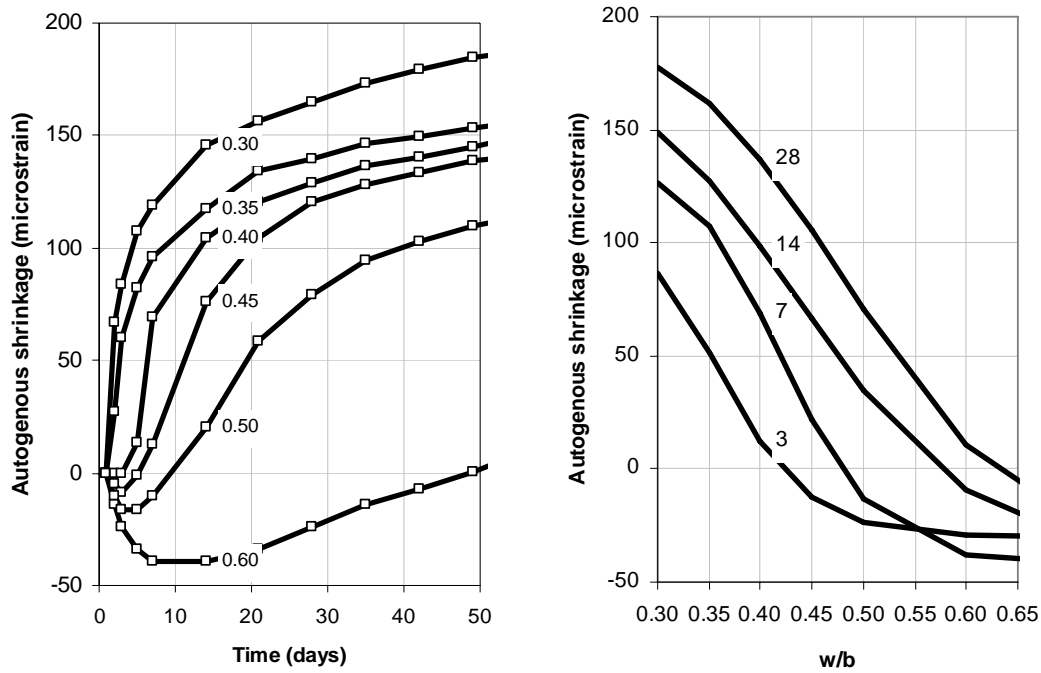


Figure A4.6 Data used as the basis for the development of alternative design values for early-age autogenous shrinkage related to time and w/b ratio

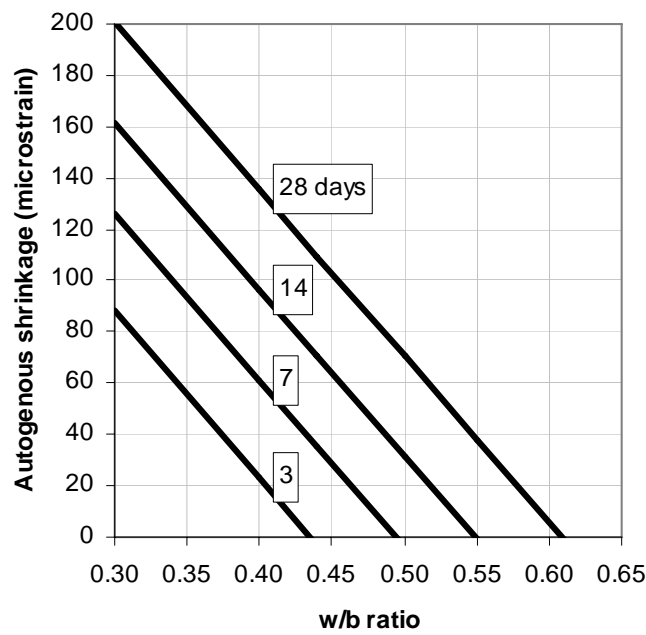


Figure A4.7 Alternative design values for autogenous shrinkage for CEM I concrete

A4.4 Influence of binder type

The above analysis has dealt with concretes containing CEM I. Limited data are available, however, on the influence of cement chemistry and binder type. It is apparent that the use of silica fume or ggbs will increase the magnitude of autogenous shrinkage at a given w/b ratio, while a reduction is achieved through the use fly ash. A summary of the data reviewed is given in Table A4.1.

Table A4.1 *The influence of mineral additions on autogenous shrinkage*

Source CP = cement paste C = concrete		w/b	Time days	% silica fume	% change	% fly ash	% change	% slag	% change
Baroghel-Bouny <i>et al</i> , (2000)	CP	0.25	28	5	37	-	-	-	-
		0.25	28	10	89	-	-	-	-
		0.35	28	5	46	-	-	-	-
		0.35	28	10	83	-	-	-	-
Pigeon <i>et al</i> , (2005)	C	0.35	5	8	50	25	-30	35	10
Scheißl <i>et al</i> , 2000	C	0.35	21	4	50	22	-10	-	-
		0.35	21	8	200	50	-50	-	-
Saje <i>et al</i> , (2001)	C	0.4	2	10	20	-	-	-	-
Igarashi <i>et al</i> , (2001)	CP	0.25	7	10	0	-	-	-	-
Poppe <i>et al</i> , (2001)	C	0.37	6	-	-	-	-	33-40	0
		0.37	6	-	-	-	-	66-80	70
Nawa and Horita, (2004)	CP	0.32	7	-	-	10	-19	10	27
		0.32	7	-	-	30	-53	30	51
		0.32	7	-	-	60	-79	60	63

A4.4.1 Silica fume

Much of the published data on autogenous shrinkage covers concrete with silica fume (sf) as is it typically used in low w/b, high strength concretes. However, the results are extremely variable. In work on cement pastes at a w/b of 0.25 and 0.35, Baroghel-Bouny *et al* (2000) reported an increase in autogenous shrinkage after 28 days of about 40 per cent with 5 per cent sf and 85 per cent with 10 per cent sf. In concretes with a w/b of 0.35 Pigeon *et al* (2005) reported a 50 per cent increase after 5 days over CEM I concrete with 8 per cent sf. Also using concretes at a w/b of 0.35, Schießl *et al* (2000) recorded significant increases in autogenous shrinkage after 21 days with the use of sf; about 50 per cent with 4 per cent sf, over 200 per cent at 8 per cent sf and over 400 per cent at 16 per cent sf. Saje *et al* (2001) also reported an increase in autogenous shrinkage in sf concretes at a w/b ratio of 0.4. After 48 hours the increase was about 20 per cent using 10 per cent sf. Based on these studies it would appear, therefore, that the use of silica fume will result in an increase in autogenous shrinkage by a significant extent although, in other studies the effect of silica fume has been found to be much less significant. For example, Igarashi *et al* (2001) reported little difference between CEM I and silica fume concrete at a w/b of 0.25. However, no data have been identified that show a reduction in autogenous shrinkage with the use of silica fume and no data have been identified for concretes at more commonly used w/b ratios.

Current evidence indicates that silica fume causes an increase in autogenous shrinkage and **that the values given in Figure A4.7 are increased by 10 per cent for every 1 per cent of silica fume expressed as weight of the total binder content (Figure A4.8).**

A4.4.2 Fly ash

Scheißl *et al* (2001) tested concrete at a w/b of 0.35 with fly ash levels of 22 per cent and 50 per cent and reported reductions after 21 days in the order of 10 per cent and 50 per cent respectively. These concretes also contained 8 per cent sf and it should be noted that the use of fly ash partially offset the increase caused by the silica fume. Pigeon *et al* (2005) investigated low w/b concrete with 25 per cent fly ash and observed a reduction after 5 days of about 30 per cent compared with CEM I concrete. Testing cement pastes with a w/b of 0.32, Nawa and Horita (2004) observed reductions in autogenous shrinkage after 7 days of 19, 53 and 79 per cent with fly ash contents of 10, 30 and 60 per cent. While the results are varied, it may be concluded from the evidence available that fly ash will reduce the extent of autogenous shrinkage.

The evidence available indicates that fly ash causes a reduction in autogenous shrinkage and **that the values given in Figure A4.7 are reduced in direct proportion to the weight percentage of fly ash used in the mix (Figure A4.8).**

A4.4.3 GGBS

In a study of self-compacting concrete with a w/b of 0.37, Poppe and Schutter (2001) reported an increase in autogenous shrinkage after 7 days of about 70 per cent when using CEM III/B42.5 (66 to 80 per cent blast furnace slag) when compared with identical concrete using CEM I 52.5R. Using a 50:50 blend of the two binders (ie with 33 to 40 per cent slag) achieved a result similar to that of the CEM I 52R concrete. Pigeon *et al* (2005) using 35 per cent slag, observed an increase at 5 days of about 10 per cent when compared with CEM I concrete at a w/b of 0.35. Using binder pastes at a w/b of 0.32, Nawa and Horita (2004) reported increases after 15 days of 27, 51 and 63 per cent with 10, 30 and 60 per cent slag respectively. While the results are varied, it may be concluded from the evidence available that blast furnace slag will increase the extent of autogenous shrinkage.

Current evidence indicates that ggbs causes an increase in autogenous shrinkage and **that the values given in Figure A4.7 are increased by 8 per cent for every 10 per cent of ggbs expressed as weight of the total binder content (Figure A4.8).**

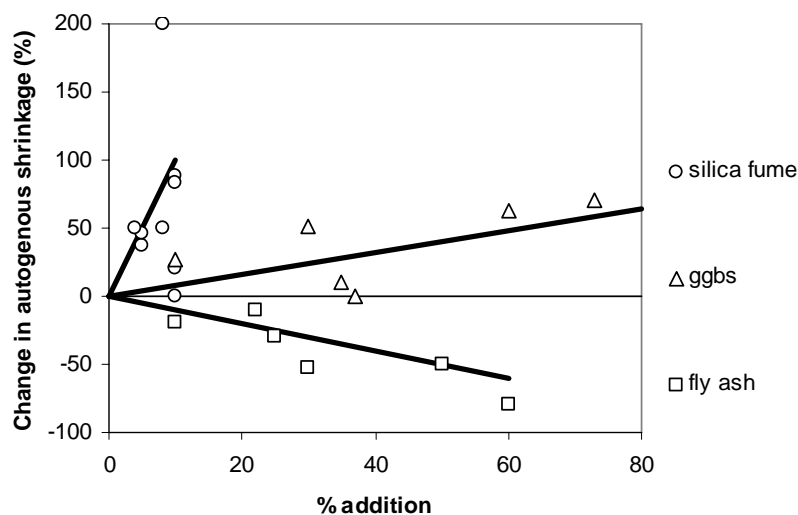


Figure A4.8 Adjustments to the design curves in relation to the use of silica fume, ggbs and fly ash

A4.5 Conclusions

1. A review of published data has indicated high degree of variability of results and a difficulty in predicting reliably the magnitude of autogenous shrinkage for use in design. EN1992-1-1 assumes that autogenous shrinkage occurs in all structural grades of concrete and the evidence available indicates broad agreement when considering the uncertainties involve in generating the data. A more comprehensive review of the available data and additional research would be needed to justify a change in the EN1992-1-1 method.
2. The magnitude of stress developed is not always in proportion to the magnitude of unrestrained autogenous shrinkage, with early creep playing a significant role. On this basis it would appear that deformation within the first 24 hours or so, whether shrinkage or expansion, has little direct effect on stress development. Comparing the values estimated using EN1992-1-1 with publish results indicates that this effect may have been taken into account.
3. There is evidence to suggest that the nature of mineral additions may also be influential in determining the magnitude of autogenous shrinkage, at least in concretes of low w/b ratio. Both silica fume and ggbs may result in an increase in autogenous shrinkage compared with CEM I, while a reduction may be achieved with the use of fly ash. Additional research on the effects of these materials at more realistic levels of w/b would be useful.

A4.6 References

- Baroghel-Bouny, V and Kheirbek, A (2000)
 “Effect of mix-parameters on autogenous deformations of cement pastes – microstructural interpretations”
 In: Proc Int. RILEM PRO17 workshop *Shrinkage of concrete – Concrete 2000*, Paris, France, 16-17 October 2000 (eds: V Baroghel-Bouny and P-C Aïtcin) Paper **8**, pp 115-142
- Hobbs, D W (1974)
 “Influence of aggregate restraint on the shrinkage of concrete,
Journal of ACI, Sept, 445-450, American Concrete Institute, Detroit, Michigan
- Igarashi, S and Kawamura, M (2001)
 “Effects of microstructure on restrained autogenous shrinkage behaviour in high strength concrete at early-ages”
 In: Proc Int. Conf. RILEM PRO 23 *Early-age cracking in cementitious systems – EAC’01*, Haifa, Israel, 12-14 March 2001 (eds K. Kovlerand, A. Bentur), RILEM Publications, Paper 13, 125-132
- Nawa, T and Horita, T (2004)
 “Autogenous shrinkage of high-performance concrete”
 In: Proc. Int. Workshop *Microstructure and durability to predict service life of concrete structures*, Sapporo, Japan, 2004
- Pigeon, M, Bissonnette, B, Marchand, J, Boliy, D and Barcelo, L (2005)
 “Stress relaxation of concrete under autogenous early-age restrained shrinkage”
ACI, Special Publication, SP-227-16, Detroit, Michigan
- Poppe, A-M and Deschutter G (2001)
 “Heat of hydration of self-compacting concrete”
 In: Proc Int. Conf. RILEM PRO 23 *Early-age cracking in cementitious systems – EAC’01*, Haifa, Israel, 12-14 March 2001 (eds K. Kovlerand, A. Bentur), RILEM Publications, **13**, pp 71-78
- Saje, D Saje, F and Kavčič, F (2001)
 “Autogenous shrinkage as a special property of HPC”
 In: Proc 3rd Int. Conf. *Concrete under severe conditions CONSEC ’01*, Vancouver, Canada, 18-20 June 2001 (eds N Banthai, K Satai and O E Gjorv), University of British Columbia, pp 1538-1545
- Scheibl, P, Plannerer, M and Brandes, C (2000)
 “Influence of binders and admixtures on autogenous shrinkage of high performance concretes”
 In: Proc Int. RILEM PRO17 workshop *Shrinkage of concrete – Concrete 2000*, Paris, France, 16-17 October 2000 (eds: V Baroghel-Bouny and P-C Aïtcin) Paper **12**, pp 179-190
- Tazawa, E SATO, R Sakai, E and Miyazawa, S (2000)
 “Work of JCI committee on autogenous shrinkage”
 In: Proc Int. RILEM PRO17 workshop *Shrinkage of concrete – Concrete 2000*, Paris, France, 16-17 October 2000 (eds: V Baroghel-Bouny and P-C Aïtcin) Paper **2**, pp 21-41

A5 Estimating restraint

A5.1 Introduction

As the magnitude of stress-inducing strain is directly proportional to the level of restraint it is important that in calculating the risk of early-age thermal cracking, the designer uses values of restraint that are likely to occur in practice. Getting it wrong may result in wasteful over-design, or under-design leading to unacceptable cracking. For example, a difference in restraint factor of 0.1 from, say, 0.5 to 0.6, will result in a 20 per cent increase in the estimated restrained strain and this could make the difference between no cracking and cracking, or acceptable and unacceptable crack widths. Quantifying the restrained proportion of the thermal movement is therefore essential for both the assessment of the risk of cracking and the economic design of reinforcement to control of crack widths.

With regard to the development of cracking, restraint to thermal movements can be grouped into two principal types: external restraint and internal restraint.

External restraint to a newly cast element can be subdivided into *continuous edge restraint*, *end restraint*, and *intermittent restraint*, and in many cases all three forms of restraint may act together. These are illustrated in Figure A5.1.

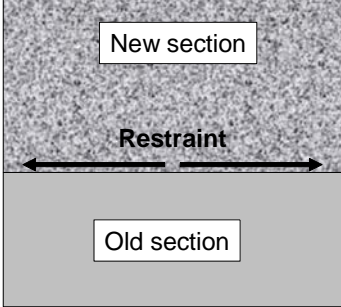
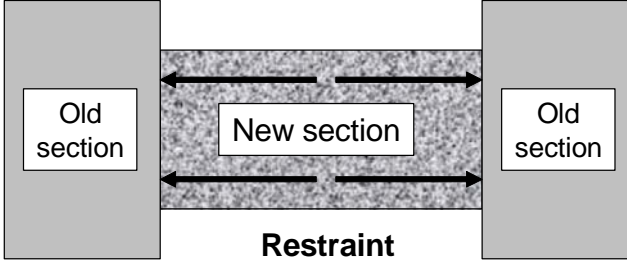
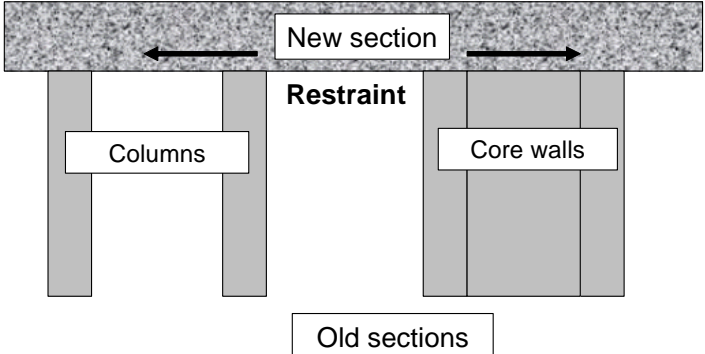
<p>Edge restraint</p>		<p>Walls cast onto rigid foundations, adjacent sections of slabs, tunnel linings</p>
<p>End restraint</p>		<p>Walls or slabs cast as infills. Large area ground slabs</p>
<p>Intermittent restraint</p>		<p>Slabs on piles, suspended slabs cast on columns and core walls</p>

Figure A5.1 *Forms of external restraint*

Cracking resulting from external restraint occurs as the concrete is cooling and the cracks which develop may reduce in width over time due to the self-equilibrating nature of the stresses leading to cracking.

The type of restraint has a significant influence on both the way in which the cracks develop and the crack width. The crack spacing, and hence the crack width, for a member subject end restraint only (ie with no edge restraint) is generally significantly greater than that occurring for a member subject to edge restraint, being determined by the tensile strength of the concrete rather than the magnitude of restrained strain. The difference is due to the fact that with the edge restraint, the restraint itself acts to limit the deformation at each crack location. With end restraint, when a crack develops the deformation at the crack is limited only by the reinforcement and the stress that is transferred to it from the concrete.

It is important that the nature of the external restraint is properly defined as it has a significant effect on the development of cracking, the crack spacing and the crack width.

Internal restraint arises when one part of the freshly placed section expands or contracts differentially to another part of the same section (Figure A5.2). Cracking resulting from internal restraint occurs either during the heating phase, as the core of the section achieves a much higher temperature and expansion and causes tension to developed at the surface; or if formwork or insulation is removed too early and too quickly, resulting in a sudden cooling of the surface. Such cracks may close, at least partially, as the core of the concrete cools and ultimately reaches the same temperature as the surface.

In thin sections, external restraint is generally dominant, while internal restraint is dominant in thick (massive) sections. For intermediate sections a combination of internal and external restraint may occur.

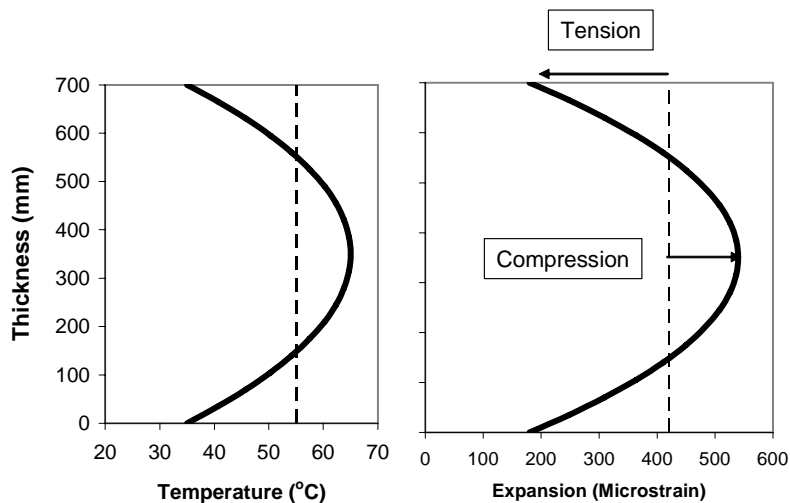


Figure A5.2 Development of internal restraint through the thickness of a 700 mm wall

In most conditions, the restraint will be less than 1. There are two principal reasons for this. Firstly, heat is transferred from the new concrete to the old, resulting in some degree of compatibility of thermal movement. In addition, the new concrete does not have some inherent stiffness, particularly by the time that cool down commences. This has been estimated to be about 70 per cent of that of mature concrete over the duration of a cooling cycle, and the movement is not, therefore, entirely dominated by the concrete against which it is cast.

A5.2 Industry guidance on the magnitude of restraint and acceptable temperature changes and differentials

Various industry documents provide guidance on restraint and a review of values for different restraint conditions is given in Table A5.1. However, care has to be taken in the interpretation of the values as the way in which they are applied varies also.

The values provided in BS 8110 Part 2:1985 and HA BD 28/87 represent observed restraints and are used in the context of a predictive equation which applies a separate modification factor, K , for sustained loading and creep, having adopted the approach proposed in ACT Technical Note No 2 (Bamforth, 1982).

BS 8007; 1987 and now EN 1992-3; 2006 have adopted a simpler approach with $R = 0.5$ and this includes the factor for creep.

CIRIA R91 (Harrison, 1992), presented the restraint values as 1, with the recommendation of a modification factor of 0.5 to take account of the simplifying assumptions. The outcome is similar to that of BS8007.

Table A5.1 Restraint values for different conditions

Restraint condition	BS 8110 Part 2	HA BD 28/87	CIRIA 91 1992 [1]	BS 8007 [2]	EN 1992-3 [2]
Wall cast on to a massive base –at the joint	0.6 to 0.8	0.6	1.0	0.5	0.5
Wall cast on to a massive base – at the top	0.1 to 0.2		0 to 1.0	0 to 0.5	0 to 0.5
Edge restraint in box type deck cast in stages		0.5			
Edge element cast onto a slab		0.8			
Massive pour cast onto blinding	0.1 to 0.2	0.2			
Massive pour cast onto existing mass concrete	0.3 to 0.4 at base				
Suspended slabs	0.2 to 0.4				
Infill bays, eg rigid restraint	0.8 to 1.0	1.0	1.0	0.5	0.5

[1] CIRIA 91 recommends that a modification factor of 0.5 be applied to take account of simplifying assumptions and notes that this factor is applied in BS 8007 by modifying the restraint factor from 1 to 0.5.

[2] These values represent effective restraint which takes into account sustained loading and creep.

It is apparent that for walls cast onto rigid bases, for which both BS 8110 Part 3;1985 and HA BD 28/87 assume a restraint value of 0.6 and a creep factor of 0.8m the value of $K.R$ is $0.8 \times 0.6 = 0.48$, being very close to the value of 0.5 proposed in CIRIA R91 (1992), BS 8007;1987 and EN1992-3;2006. However, in other situations this value may differ significantly.

Since the production of CIRIA R91, considerable research has been carried out both on the magnitude of restraint that occurs in practice, particularly in relation to edge restraint, and on the magnitude of the modification factors, enabling more reliable estimates to be made.

The acceptable temperature drop T_l or temperature differential ΔT is affected by the magnitude of restraint and some guidance was given in BS 8110; Part 2. This has been modified in this report to take account of more information that is available on the properties of concrete, including the guidance in EN1992-1-1 for estimating the tensile strain capacity of the concrete. Proposed values are given in Table A5.2.

Table A5.2 *Limiting temperature changes and differentials to avoid cracking for different levels of restraint based on assumed typical values of coefficient of thermal expansion and tensile strain capacity as affected by aggregate type (this is an update of values provided in Mass Concrete Digest 2, 1982 and BS 8110; Part 2 to take account of the concrete properties using the methods of EN1992-1-1)*

Aggregate Type	Gravel	Granite	Limestone	LWAC with natural sand
Thermal Expansion Coefficient ($\mu\epsilon/^\circ\text{C}$)	13	10	9	9
Tensile Strain Capacity ($\mu\epsilon$) under sustained loading	65	75	85	115
Limiting Temperature Change in $^\circ\text{C}$ for Different External Restraint Factors:				
1.00	6	9	12	20
0.80	8	12	16	25
0.70	9	14	18	29
0.60	11	17	22	34
0.50	14	21	27	42
0.40	18	27	34	53
0.30	24	36	46	71
Limiting Temperature Differential ($^\circ\text{C}$) for Internal restraint $R = 0.42$	20	28	35	53

A5.3 External restraint

A5.3.1 Continuous edge restraint

The most recognisable form of edge restraint occurs when a wall is cast on a rigid foundation. A typical example is shown in Figure A5.3 for the walls of a box-section tunnel. The classic crack pattern can be observed.

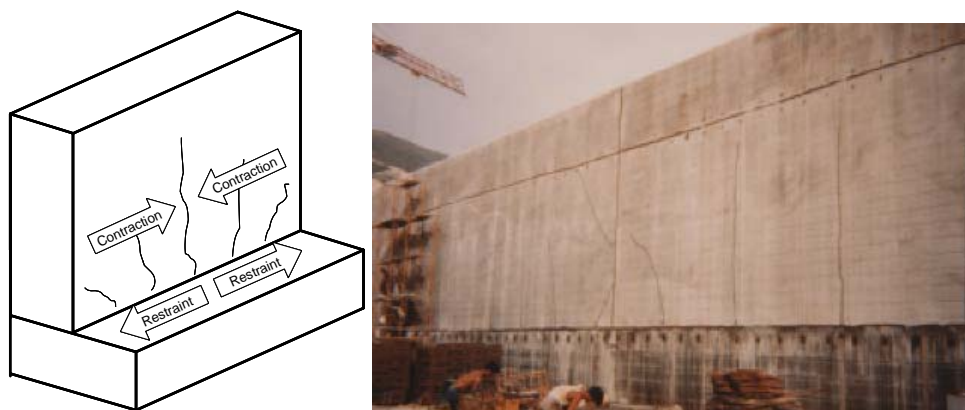
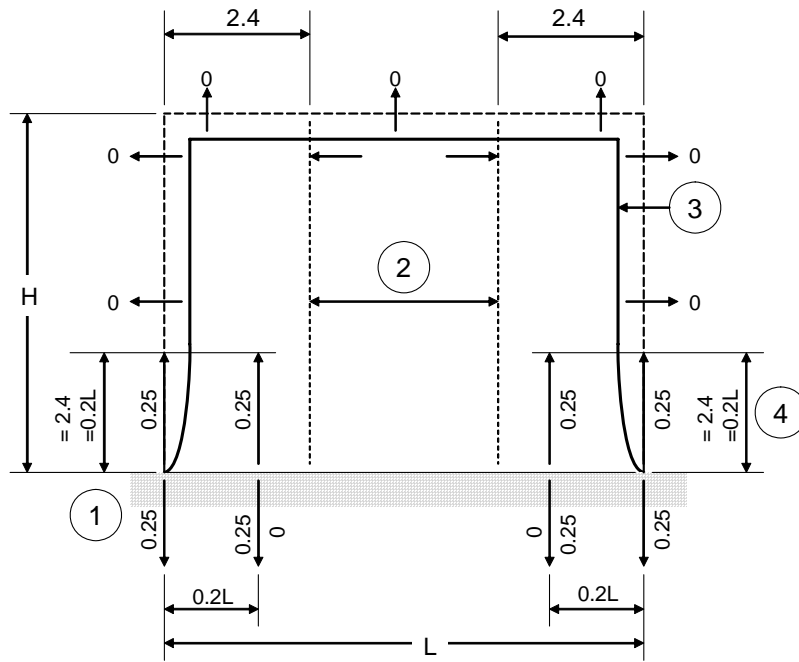
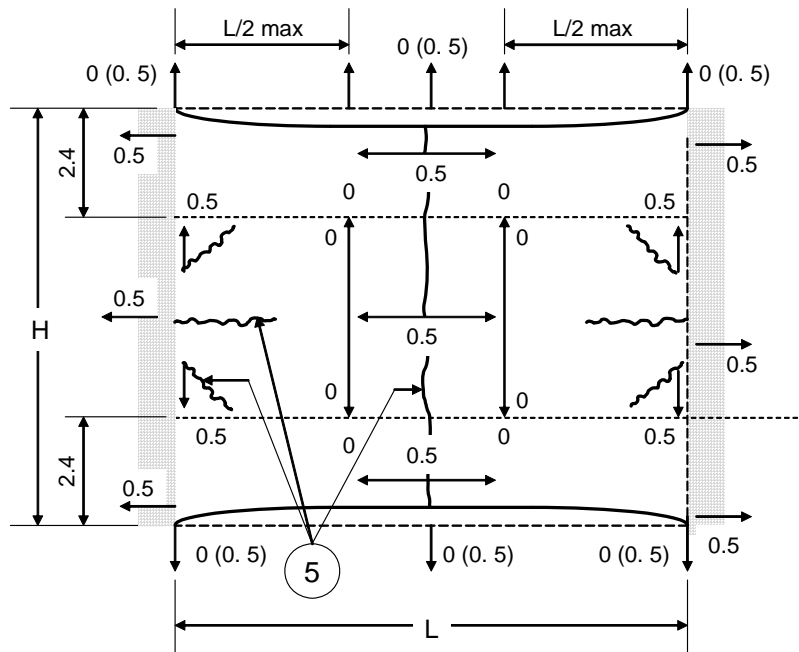


Figure A5.3 *Early thermal cracking in the walls of a box-section tunnel wall*

Under these conditions, values of restraint are typically in the range from 0.3 to 0.7 and it is tempting to assume an average value of 0.5 as previously proposed by CIRIA R91 and BS8007 and now by EN 1992-3. (Figure A5.4).



(a) Wall on a base



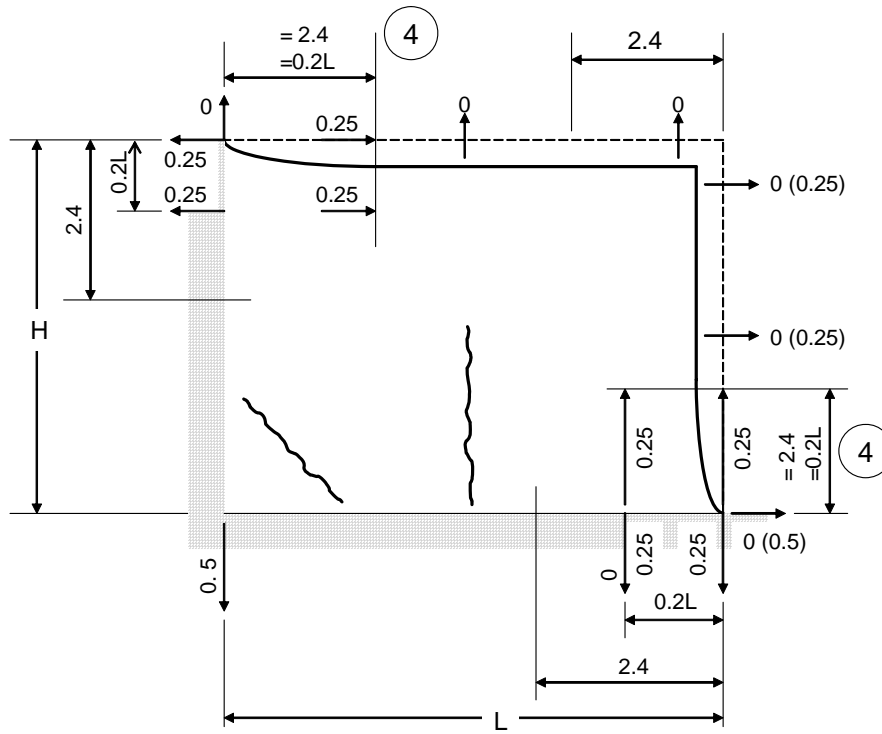
(b) Horizontal restraint between rigid restraint

KEY

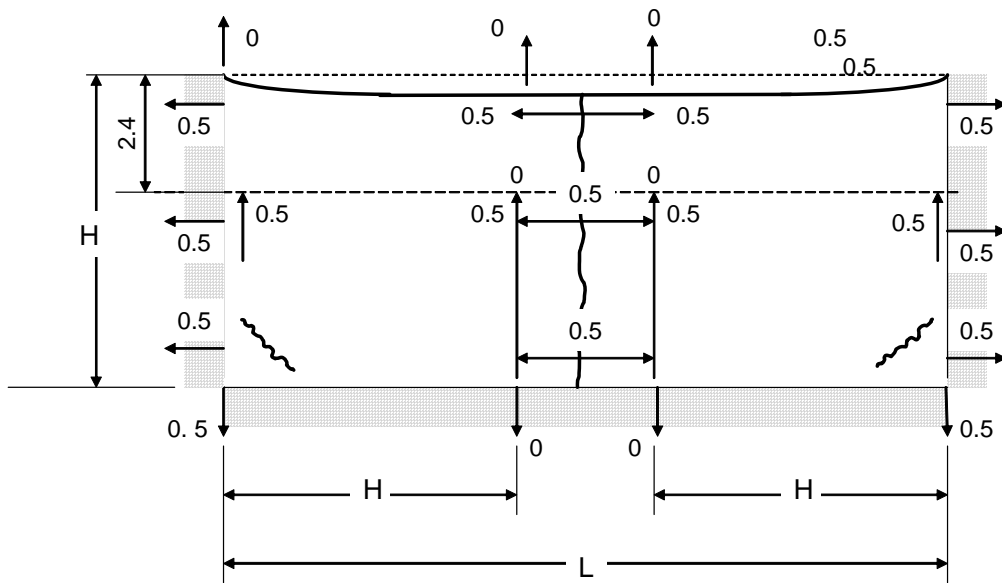
- 1 Vertical restraint factors
- 2 Horizontal restraint factor
- 3 Expansion or free contraction joints
- 4 Whichever value is greater
- 5 Potential primary cracks

Restraint factors for central zone of walls		
Ratio L/H	R at base	R at top
1	0.5	0
2	0.5	0
3	0.5	0.05
4	0.5	0.5
>8	0.5	0.5

Figure A5.4 Recommended values of restraint given in EN 1992-3



(c) Sequential bay wall construction (with construction joints)



(d) Alternate bay wall construction (with construction joints)

KEY

- 1 Vertical restraint factors
- 2 Horizontal restraint factor
- 3 Expansion or free contraction joints
- 4 Whichever value is greater
- 5 Potential primary cracks

Restraint factors for central zone of walls		
Ratio L/H	R at base	R at top
1	0.5	0
2	0.5	0
3	0.5	0.05
4	0.5	0.5
>8	0.5	0.5

Figure A5.4 (contd) Recommended values of restraint given in EN 1992-3

However, a difference in restraint of 0.1 from this mean value will affect the level of restrained strain by 20 per cent and for elements with a relatively simple geometry it is recommended that a more rigorous assessment of the restraint is undertaken. EN 1992-3 provides the option to calculate restraint factors from knowledge of the stiffness of the element considered and the elements attached to it.

Consider the example of a wall cast onto a rigid foundation. Without restraint the wall would freely contract, maintaining its rectangular shape. However, because the wall should remain compatible with its base, the actual finished shape is as indicated in Figures A5.5 a) and b), depending on whether the base is rigid or flexible. The forces needed to stretch the freely contracted shape into the actual shape indicate the directions of the main stresses set up in the concrete and hence the likely crack pattern. For example, in Figure A5.5a a horizontal force is necessary to maintain compatibility of length, but this tends to warp the wall, so that an additional vertical tensile force is needed to maintain vertical compatibility. In this case, the potential primary cracking pattern is vertical cracks at mid-span and splayed cracks towards the ends of the walls. At the ends of the wall, it is also possible for a horizontal crack to form at the joint between the wall and base.

When the base is flexible, the wall is allowed to warp and both the horizontal and vertical stresses are thus reduced. While cracking may still occur, in this case the cracks will be shorter and less wide. The end cracks are less splayed and there is less chance of a horizontal crack appearing at the joint. These primary crack patterns are completely independent of the reinforcement and are due solely to the restraint. When the level of reinforcement in these walls is sufficiently high, the width of these primary cracks is controlled by the reinforcement, and secondary cracks are induced. The distribution of these secondary cracks are dependent on the distribution of the reinforcement. All these cracks extend completely through the section, and they could therefore result in leakage or seepage.

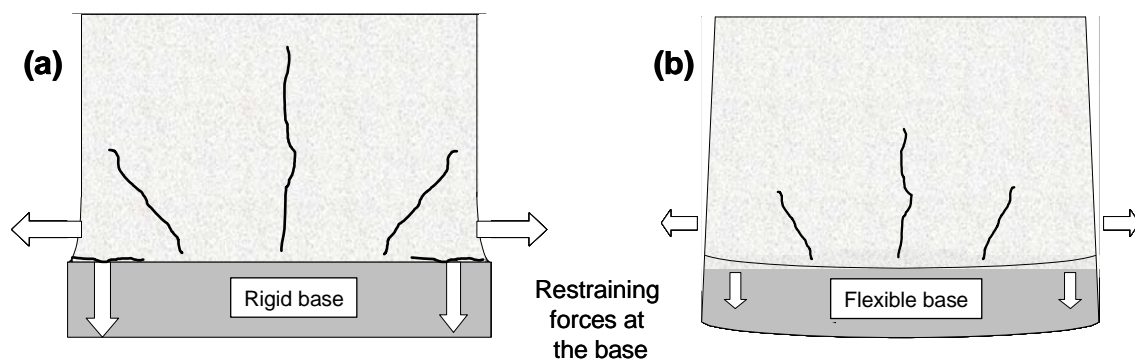


Figure 5.5 Restraining forces and cracking in a wall cast onto a base

As cracking resulting from edge restraint is a common occurrence considerable research has been undertaken to enable restraints to be predicted and therefore to provide a more reliable estimate of the risk and extent of cracking.

It is apparent that the restraint offered by “old” concrete against which a new element is cast should be influenced the relative size and stiffness of the new element and the old. The stiffness of an element is defined by its elastic modulus.

For new elements cast against existing concrete with continuous restraint along one edge, ACI 207.2R-73 provides a method for estimating restraint based on the relative cross-sectional areas and elastic moduli of the new and old elements and the distance from the joint. This has been described in CIRIA R135 (Bamforth and Price, 1995). The restraint at the joint R_j is estimated using the equation A5.1 and the variation in restraint away from the joint is derived using Figure A5.6.

Restraint at the joint,
$$R_j = \frac{I}{I + \frac{A_n E_n}{A_o E_o}} \tag{A5.1}$$

where:

- A_n = cross sectional area (c.s.a) of the new (restrained) pour
- A_o = c.s.a. of the old (restraining) concrete
- E_n = modulus of elasticity of the new pour concrete
- E_o = modulus of elasticity of the old concrete.

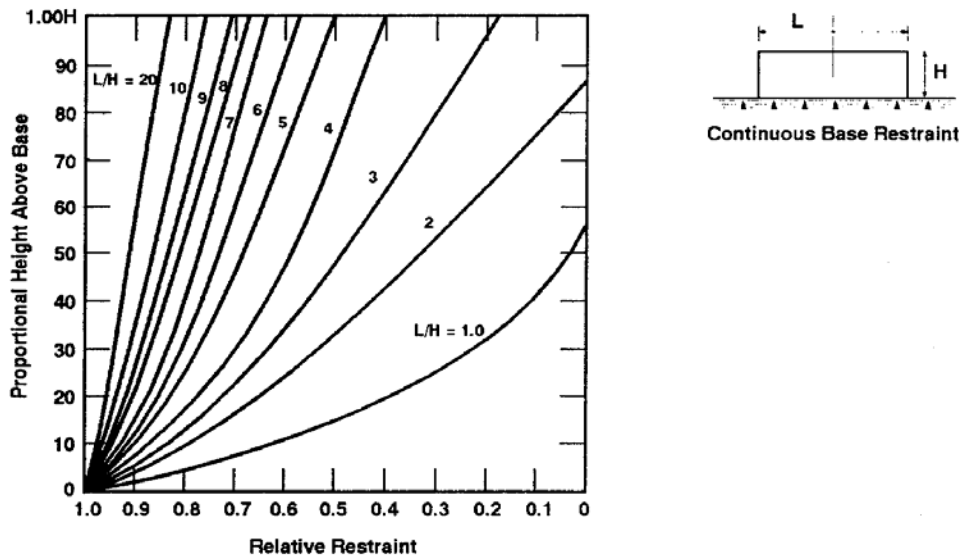


Figure A5.6 Restraint factors for elements with continuous base restraint

While the size and geometry remain constant for both new and old concrete, the same does not apply to the elastic modulus. For the “old” concrete it is unlikely that the modulus E_o will change significantly during the period of an early age heat cycle of concrete cast against it and it is reasonable, therefore, to assume that E_o remains constant in any calculations. However, the elastic modulus of the new section will be changing rapidly over the first few days and this will therefore influence the degree to which deformation is restrained by the older and stiffer concrete.

Figure A5.7 illustrates the influence of the change in elastic modulus during an early age heat cycle (Browne and Blundell, 1973) and its influence on the ratio E_o/E_n and the restraint. Immediately after casting, when the new concrete is relatively “soft”, the ratio of E_o/E_n is low and hence the restraint is high. As the elastic modulus increases, the ratio of E_o/E_n increases and the restraint reduces. CIRIA R135 recommends that when using the ACI approach to estimate restraint the ratio E_o/E_n is assumed to be in the range 0.7 to 0.8. As shown in the example in Figure A5.7, this represents the value from about 48 hours, after which time the restraint is approaching a value of about 0.55.

Recognising the change in restraint with time it is appropriate that this is taken into account when undertaking calculations of the risk of early thermal cracking (predictive models that use estimated, time-dependent properties for the new and old concrete will automatically take this into account).

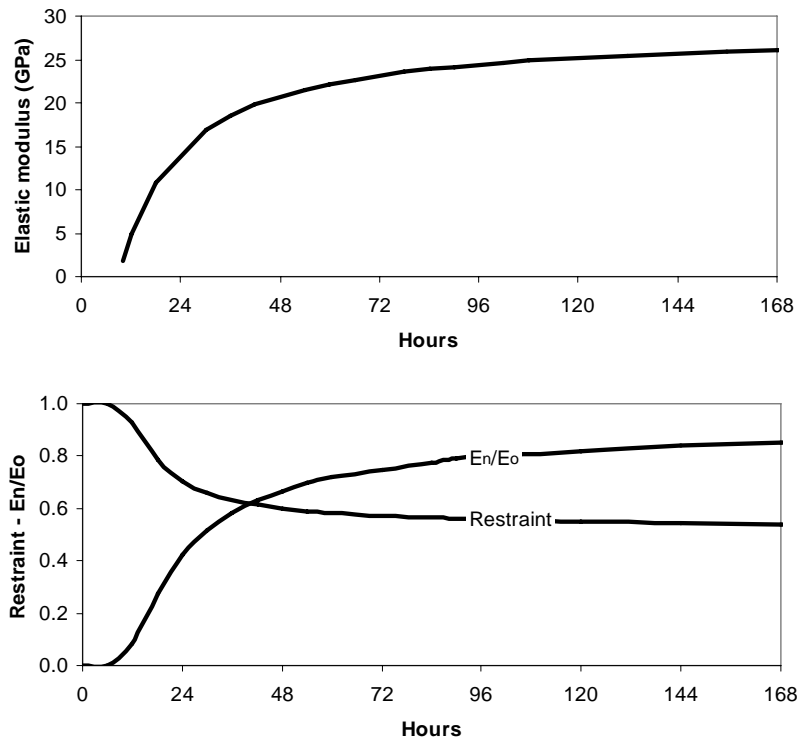


Figure A5.7 The variation in elastic modulus at early age and the influence on the ratio of E_n/E_o and the restraint derived using equation A5.1 (it is assumed in this example that the ratio $A_n/A_o = 1$)

The value of restraint calculated using equation A5.1 is the value at the joint between the new and the old concrete but, depending on the pour geometry, and in particular the length/height ratio of the element, the restraint will reduce with distance from the joint to varying degrees as shown in Figure A5.6. Since the development of the ACI data, further investigations have been carried out into restraint and Emborg (2003) has proposed revised estimates of restraint for elements of different L/H ratio. These revised values are shown in Figure A5.8 compared with the original ACI curves. For elements with low L/H ratios, the values are very similar, but there are significant differences for pours with high L/H ratios.

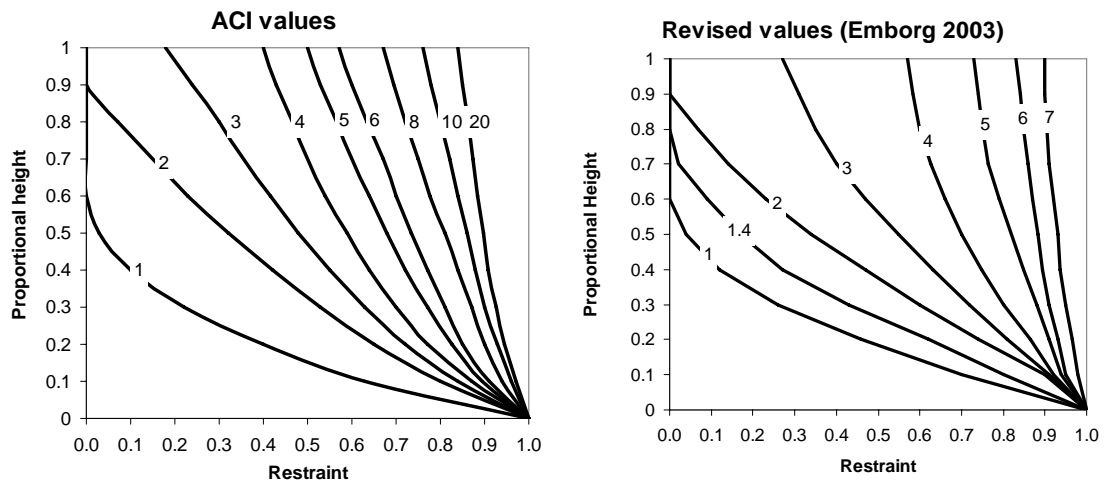


Figure A5.8 A comparison of restraint values from ACI 207 and Emborg (2003)

To establish which set of curves are most representative, comparisons have been made between estimated and measured restraint, as shown in Figure A5.9. To calculate the restraint at the joint, a value of E_o/E_n of 0.7 has been used. Unfortunately data are only available for walls with low L/H ratios for which both methods predict similar restraint values. It is apparent however that restraint calculated using the revised Emborg approach is marginally closer to the observed values.

To develop a simple spreadsheet calculator for deriving the restraint for a wall cast onto a rigid foundation, the curves developed by Emborg have been expressed mathematically using the equation:

$$R = R_j \cdot [(1.372 (h/L)^2 - 2.543 (h/L) + 1) + 0.044 ((L/H) - 1.969) (h/H)^{1.349}] \quad (A5.2)$$

where:

- R_j is the restraint at the joint calculated using equation 1
- h is the distance from the joint in m
- H is the height of the pour in m
- L is the length of the pour in m.

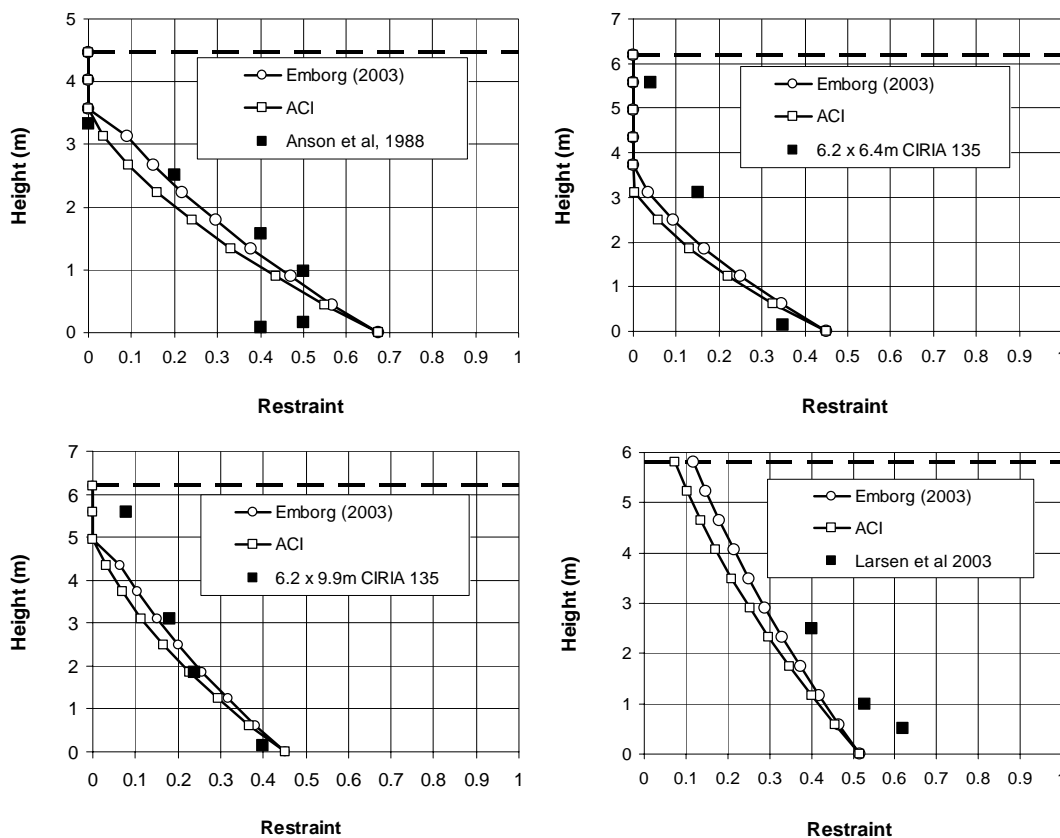


Figure A5.9 Comparison of estimated and measured restraints using the ACI approach and the revised Emborg model ($E_n/E_o = 0.7$)

A comparison between the curves proposed by Emborg (2003) and the curves derived using equation A5.2 is shown in Figure A5.10. The reducing restraint towards the top free surface indicates that the percentage of steel may be reduced with height for early age thermal crack control purposes.

In some cases, the relative areas of influence A_o and A_n may be difficult to define. For example, when a wall is cast onto a slab, what width of slab should be considered as providing effective restraint? In such circumstances it is recommended that the relative area is assumed to be in proportion to the relative thicknesses, h_n and h_o , of the wall and slab. The following simple rules may be applied.

- for a wall cast at the edge of a slab assume $A_n/A_o = h_n/h_o$
- for a wall cast remote from the edge of a slab assume $A_n/A_o = h_n/2h_o$
- for a slab cast against an existing slab assume $A_n/A_o = h_n/h_o$.

More complex geometries may require more detailed analysis.

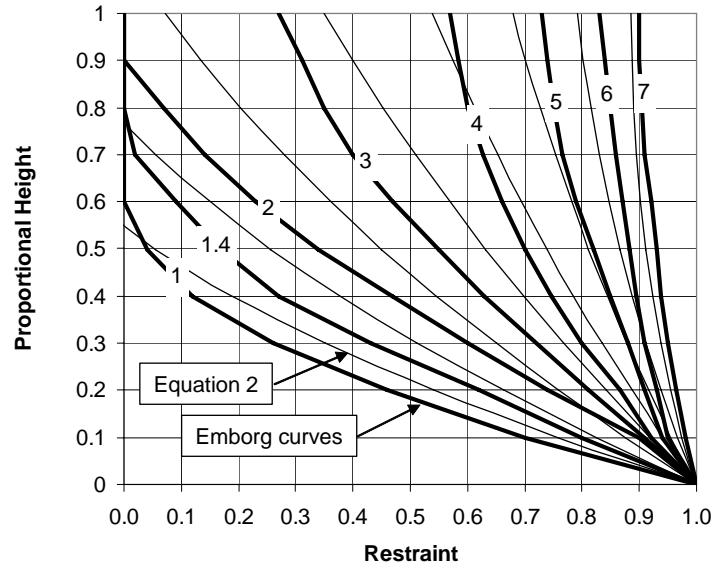


Figure A5.10 A comparison between the restraint curves proposed by Emborg (2003) and curves defined by Equation A5.2

As well as varying with distance from the joint, the restraint will also vary along the joint. Figure A5.11 shows that, except for a strip at the kicker level, the horizontal restraint reduces towards the ends of a wall and is at a maximum at the centreline.

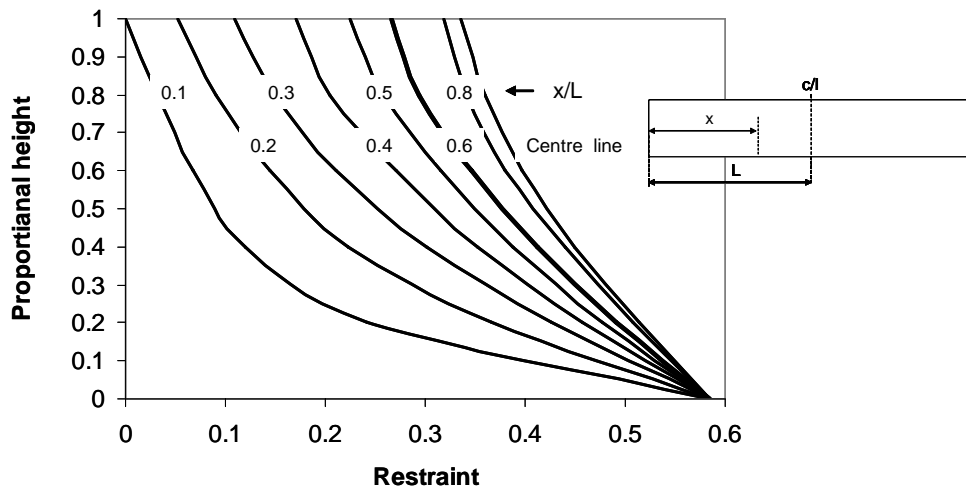


Figure A5.11 Restraint factors for an uncracked wall (length/height ratio = 4) on a rigid base (Schleech, 1962)

In general, the restraint perpendicular to the joint is low except close to the ends of the joint where warping tries to open the joint. The vertical restraint is apparent in the formation of cracks close to the ends of a wall that run diagonally across the corner of the section, as shown in Figures A5.4 and A5.5

In practice, the theoretical crack pattern is modified by any stress inducers or planes of weakness. Stress inducers known to have modified the cracking pattern are weepholes, box outs and through pipes. Planes of weakness can occur at horizontal or vertical construction joints or where a large proportion of the reinforcement is terminated (ie where laps are not staggered). Planes of weakness are often deliberately constructed to induce the concrete to crack in predetermined planes.

The example given of a wall cast onto a base is just one of a range of situations in which continuous edge restraint can occur. Other examples are successive lifts of a wall or adjoining strips of a slab.

Cylindrical structures in which the walls are cast in complete rings are further complicated by the fact that the diameter of the ring attempts to reduce as the concrete cools down to the ambient temperature. In theory, this could result in a horizontal crack between the new and old sections in addition to any vertical cracks, but such cracks are rarely seen in practice.

As restraint reduces towards the ends of a wall, there should be some joint spacing which reduces restraint sufficiently to give a low probability of cracking or to limit the cracking to one central crack equal to, or less than, the permitted maximum crack width. Observation of structures built in the UK with wall heights exceeding 4 m showed that there was no cracking within 2.4 m of a free movement joint (Deacon, 1978). Deacon (1978) used this observation to show that for bay lengths of 5-6 m, only one crack equal to or less than the permitted width will form. At this bay length, the crack does not rely on reinforcement for its control. However, the observation is, strictly, only related to lift heights greater than 4 m and observations from lower walls indicate that cracks may form, even though the joints are at closer than about 5m. EN1992-1-1 suggests that the crack spacing should be assumed to be $1.3 \times$ height, hence for, say, a 3 m high wall cracking might be expected to occur at about 3.9 m centres.

A5.3.2 End restraint and intermittent restraint

It is important to recognise conditions of end restraint as both the way in which cracking develops, and the resulting cracks widths, differ significantly from the condition of edge restraint. This is acknowledged in EN1992-3 which provides different methods for calculating the design crack width. The essential difference is that when cracking occurs as a result of end restraint, the crack width is related specifically to the strength of the concrete and the steel ratio and each crack occurs to its full potential width before successive cracks occur. Under these conditions the restrained strain is only significant in relation to whether or not cracking occurs and how many cracks occur. It does not influence the crack width. (Appendix A8 gives more detail of the mechanisms of cracking).

In general, when cracking occurs as a result of end restraint, cracks will be larger than those that occur due to edge restraint.

End restraint typically occurs in the following situations:

- suspended slab cast between rigid walls or columns
- ground slab cast on piles
- the top of an infill wall with a length/height ratio that is sufficiently low that the base restraint is not effective at the top
- large area ground slabs cast onto membranes to achieve a low coefficient of friction, restrained locally, eg by columns, or by a build up of friction when the area is very large
- the top high infill bays.

An example of the early behaviour of a suspended slab was reported by Bamforth (1980). Temperature and strain measurements were taken in 1m deep transfer beams forming the third floor of Queen Anne's Mansions in London. Restraint values arising from the columns onto which the slab was cast were reported to be in the range from 0.13 to 0.20. Had the slab been thinner, generating less force on expansion and contraction in relation to the restraining forces from resistance to bending of the columns, the restraint would have been expected to be higher.

The restraint under these conditions may be calculated using a process of deformation compatibility at the slab/wall joint. An example is shown in Figure A5.12 for a 300 mm thick slab spanning 15 m between

2.5 m high \times 0.6m thick walls. It is assumed that $T_l = 25^\circ\text{C}$ and $\alpha_c = 12 \mu\text{E}/^\circ\text{C}$ resulting in free contraction at each end of the slab of 2.25 mm. As a much greater force is required to restrain the slab than can be achieved by resistance to bending in the wall, the restraint in this example is low ($R = 0.14$).

Calculations may be undertaken using the same principal when there are several local restraints, eg slabs cast on columns or piles.

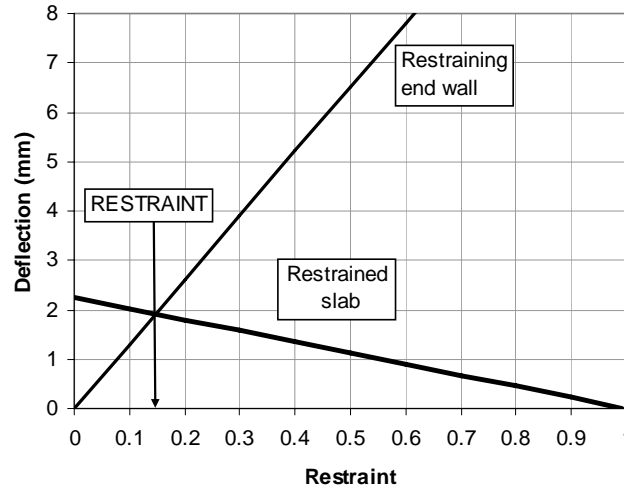


Figure A5.12 Using deformation compatibility to estimate restraint in a suspended slab

Large area pours, often with lightweight aggregate concrete (LWAC), have become a common feature of fast track construction. This does not appear to increase the incidence of early-age thermal cracking. This is not surprising in view of the low coefficient of thermal expansion and high tensile strain capacity associated with LWAC (Bamforth, 2006).

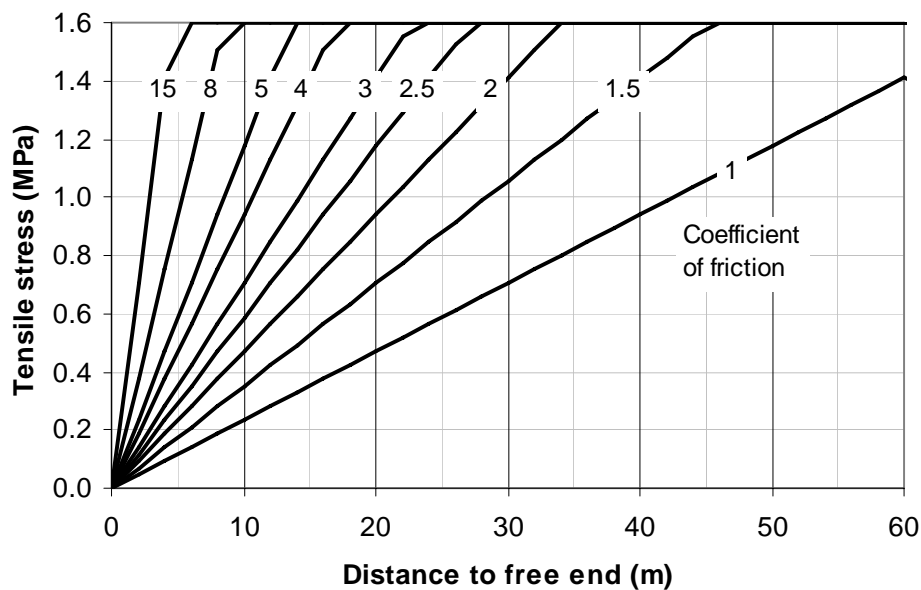
Pile caps or piles are examples of intermittent points of restraint. Large piles in stiff soils can be assumed to provide a number of rigid points restraining the movement of any connecting concrete member. At the other extreme, practical experience has shown that piles over water or tidal mud flats provide little restraint to thermal movements, and long sections of jetty have been constructed without movement joints or additional reinforcement. Piles in soft ground probably fall between these extremes and provide some intermediate level of restraint.

Another important type of partial restraint is that resulting from the friction between, say, a slab or base and the ground. Some typical coefficients of friction for various types of substrate are given in Table A5.3. Using these values the length of slab required to generate sufficient tensile stress to cause cracking may be estimated as shown in Figure A5.13. With a low friction coefficient the required distance from a free end to develop the level of tensile strength developed at early-age is likely to exceed 50 m.

The important point to note here is that when a crack occurs the restraint local to the crack will reduce immediately, with the crack location acting as a free end. It will not, therefore, act in the same way as edge restraint to limit the crack width.

Table A5.3 *Coefficients of friction for various substrate condition (ACPA, 2002)*

<i>Subbase</i>	<i>Coefficient of Friction</i>
Polythene	0.5-0.9
Sand	0.7-1.0
Granular sub-base	0.9-1.7
Plastic soil	1.3-2.1
Lime treated clay soil	1.5
Bituminous surface treatment	3
Crushed stone	6
Asphalt stabilised (smooth)	6
Asphalt stabilised (rough)	15
Asphalt treated open graded	15
Cement treated open graded	15
Cement stabilised	15
Lean concrete	15

**Figure A5.13** *The relationship between the length of slab and the tensile stress developed as affected by the coefficient of friction (ignoring the effects of warping)*

Hunt (1972) describes two other types of restraint which occur in pavements. Warping restraint is caused when the strains associated with a temperature gradient across the slab is restrained by the self-weight of the concrete. Full restraint to warping in slabs occurs when the length is 30 m or greater. In 6 m slabs, the restraint to warping is still about 0.5. In practice, restrained warping is the cause of most early-age thermal cracking in pavements.

A5.3.3 Combined end and edge restraint (thin sections)

While as a general rule, infill bays are not recommended they are, on occasion, difficult to avoid. The final bay in a circular tank wall with a free-to-slide base is an example of pure end restraint. In theory, there is uniformly high horizontal restraint for the full height of the wall. As the wall contracts, uniform tension develops along its length. If the wall is low, vertical restraint could be ignored. When the restraining edge exceeds about 5 m in length (see Figure A5.4b for example), the contraction parallel to the rigid supports needs to be considered. There are no published data on the restraint factors for these situations, but a reasonable estimate could be obtained by using the centreline horizontal restraint factors given in Figure A5.4a. In this case, L is the length of the side parallel to the rigid support and H is half the span.

When both of the panel ends are fixed, the restraint will be uniformly high and fixing an additional edge does not increase the horizontal restraint, although it will modify the cracking pattern (compare Figures A5.4b and A5.4d). What is of more interest is the restraint induced when two adjacent edges are fixed (eg one end and the base of a wall) as this is a common situation during sequential construction. From Figure A5.4c, it can be seen that more of the thermal contraction is free than in Figure A5.4b. As only restrained movement causes cracking, sequential construction can result in less cracking or smaller crack widths than “alternate bay” construction. The exception to this general rule is when the infill bays in “alternate bay” construction are short.

There are few published data on the numerical values of restraint with sequential construction, but Figure A5.4 does give estimated values derived by superposition from simpler cases. Locally, high restraint factors do not necessarily cause cracking as crack widths are a function of the distance over which the restraint operates.

A5.4 Internal restraint caused by differential thermal strain

In the UK, internal restraint is normally only significant in large sections, but in climates with greater diurnal temperature variations, it can be significant in thin sections. Changes in the temperature profile across these sections can cause one part of the section to restrain the movement of another part of the same section. Figure A5.14 illustrates typical temperature profiles that develop through a 2 m thick section exposed to the environment and it can be seen that temperature differentials of up to about 35 °C have developed. Steeper gradients will occur if the formwork or insulation is removed from a deep section while the surface is still hot. The rapid cooling and contraction of the surface zone is restrained by the hot interior and the surface cracks. These cracks can penetrate deeper than the reinforcing bars, but, because of the nature of the restraint, cannot be continuous through the section. As the core cools, these surface cracks would be expected to close up and this has been observed in practice (Bamforth, 1980).

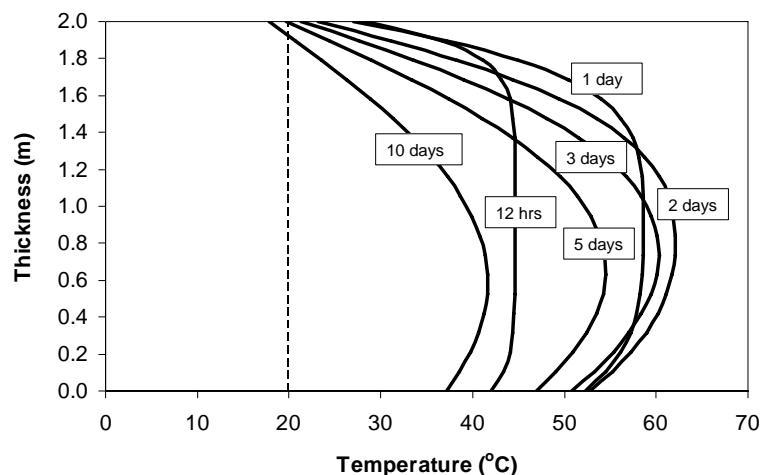


Figure A5.14 Temperature profiles in an uninsulated 2 m thick section

This particular type of cracking is avoidable by the use of insulation on otherwise exposed surfaces as shown in Figure A5.15. In this case results are estimated when an air gap created by the use of polythene sheets on batons. The effect was to reduce temperature differentials to about 20 °C. Avoiding exposure of “hot” surfaces to rapid cooling is also essential.

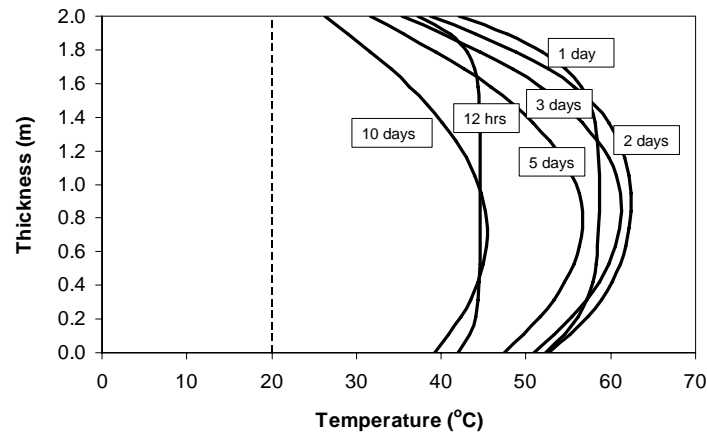


Figure A5.15 *Temperature profiles in a 2 m thick section insulated on the top surface using polythene sheet on batons to create a 25 mm air gap*

In addition to surface cracking, internal restraint may also result in internal cracks. These occur because the stress changes during cooling exceed the stress changes during heating (due to the increase in elastic modulus) hence the compressive stresses generated in the core of the section are more than offset when the core cools back to ambient. By the time the concrete has reached the ambient temperature, the surface cracks will have closed sufficiently to be able to transmit compressive stresses and in extreme cases, internal cracking occurs as a result of the tensile stresses in the core (Figure A5.16). In the area between the top and bottom mat reinforcement, the shape of the crack will broadly follow that of the peak temperature profile, being widest at the point where the temperature fall was greatest.

Some guidance on limiting values of temperature differential is given in Table A5.2.

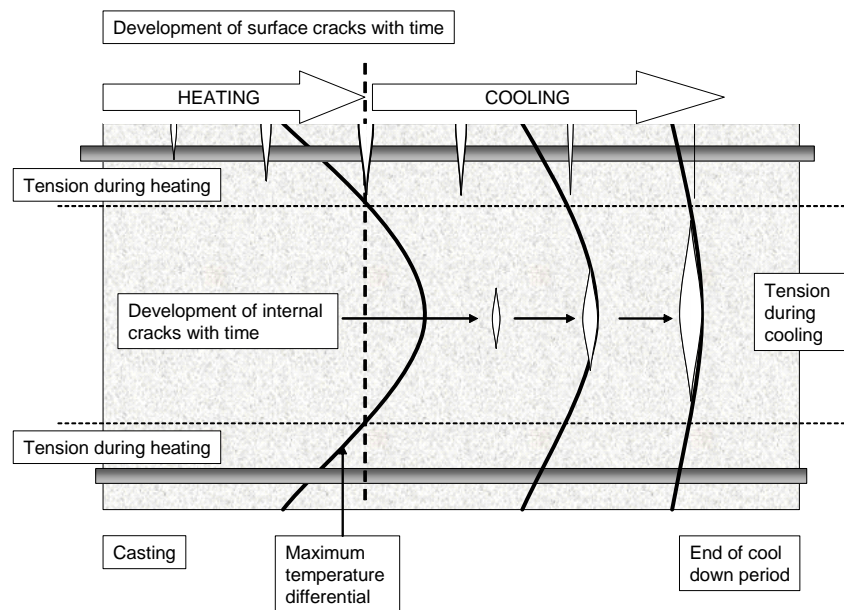


Figure A5.16 *Schematic representation of the development of crack in a massive element due to temperature differentials assuming no external restraint (such cracking may occur in both the vertical and horizontal orientation)*

A5.5 Combined internal and external restraint

For internal restraint to cause cracking, differential movement may occur. During heating, as the core of a thick section heats up and expands more than the surface, tensile stresses can only be generated in the surface zone if the centre is free to expand. If the section is restrained and the full expansion of the core is prevented, then the magnitude of tensile stress developed at the surface will be reduced also and may be eliminated entirely. Hence the risk of surface cracking due to internal restraint will be reduced when external restraint exists.

At the centre of the section, however, the internal and external restraint will be additive, the core of the section now being restrained by both the surface and zone and the external restraint. Hence the risk of internal cracking during cool down will be increased and any cracks that form would be expected to be larger, as shown in Figure A5.17.

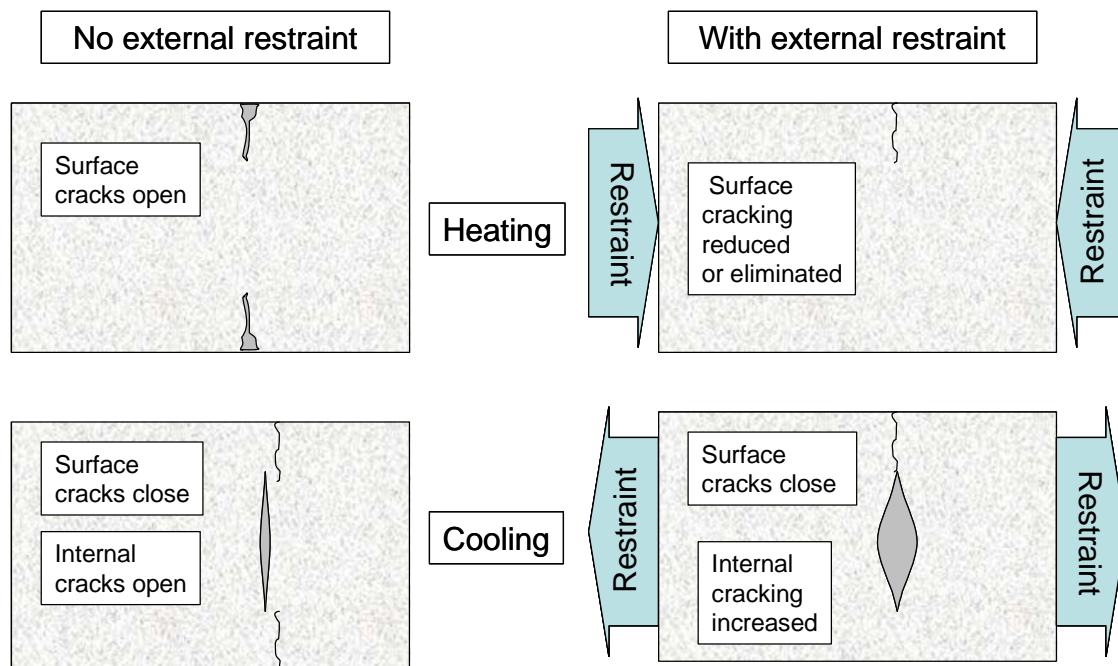


Figure A5.17 The effect of combined internal and external restraint on the risk and extent of cracking

A common case of combined internal and external restraint is in close to the joint in thick walls cast onto rigid foundations. Under these conditions, a question that frequently arises is whether such walls should be insulated to reduce internal restraint. At the base of the wall, where horizontal restraint is highest, the limiting temperature differential may be relaxed based on the level of restraint. For example, if the concrete is such that under conditions of zero restraint the limiting temperature differential is, say, 20 °C, then if the restraint close to the base is, say, 0.6 (ie only 40 per cent of the tensile thermal strain at the surface may develop, permitting the limiting temperature differential to be increased, at least in theory, to $20/(1-0.6) = 50$ °C. However, in such circumstance, the strains developed in the vertical direction, where restraint may be zero, may prevent such an approach. However, this approach may be applicable to infill bays which are restrained in each direction.

Permitting a higher temperature differential is beneficial in two respects. Firstly it avoids unnecessary and possibly costly precautions to insulate the surface and secondly it permits more heat loss, thus reducing the mean temperature through the section and the risk of through cracking due to external restraint.

A5.6 Performance of joints

Joint opening may be a problem in thick sections, even when using sequential construction. The mechanism of joint opening for a thick slab with base restraint is shown in Figure A5.18. The movement at a joint is compounded by the fact that the old concrete is heated by the new pour and expands locally, being stiffer than the newly placed concrete. During cool down, not only does the new pour contract, but the old pour returns to its original profile.

With sufficient levels of reinforcement continuity through the joint (exceeding $A_{s,min}$) controlled joint opening may be achieved.

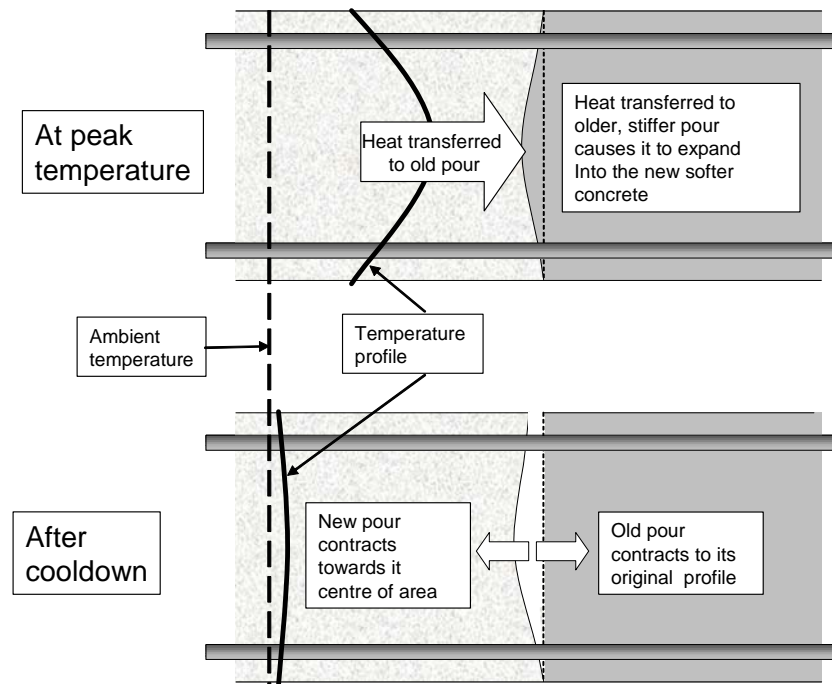


Figure A5.18 The mechanism of joint opening between adjacent thick sections

A5.7 Deriving restraint factors

It is sometimes useful, on very large contracts with repetitive pours, to determine restraint factors by monitoring the first few pours. This may enable relaxation of costly procedures to minimise thermal cracking, or permit savings by enabling pour sizes to be increased and the construction sequence to be modified to achieve a reduction in the programme.

To determine restraint factors both the *in situ* strain and the free strain should be measured. The restraint factor is determined by comparing the observed strain in the element with the free strain that would have occurred with no restraint. If α_c represents the free strain, derived from either a Hot Box test (an insulated, unrestrained specimen in which the temperature and strain change are measured) or a part of the structure that is unrestrained (ie the vertical direction in a wall), and α_r is the *in situ* (restrained) coefficient of expansion, then R is calculated as follows;

$$R = \frac{(\alpha_c - \alpha_r)}{\alpha_c} \quad (\text{A5.3})$$

Some typical stress-strain curves recorded in a slab with different levels of restraint in the longitudinal and transverse directions are shown in Figure A5.19. In this case the free strain was determined by installing vertical gauges that were subject to zero restraint and indicated a thermal expansion coefficient of $10.2 \mu\epsilon/^\circ\text{C}$. The stress-strain curves in the longitudinal and transverse directions yielded equivalent

values of $6.3 \mu\epsilon/^\circ\text{C}$ and $1.2 \mu\epsilon/^\circ\text{C}$ respectively. Using equation A5.3 restraint factors were calculated to be 0.38 and 0.88, representing moderate and very high restraint.

An interesting observation in this example was the occurrence of cracking at one gauge location, caused by the highest level of restraint. It can be seen that the strain rapidly increased when the temperature had dropped by about 14°C from its peak value. The concrete contained granite aggregate and, based on the recommendations in Table A5.2, had it been recognised that such a high level of restraint would occur, the limiting temperature drop to avoid cracking would be about 11°C . In this example, the recommendations would therefore have provided a margin of safety of about 25 per cent.

Having determined the true values of restraint at critical locations within a pour, comparison with the assumed (design) values may allow cost effective changes to be made in a rational and safe manner.

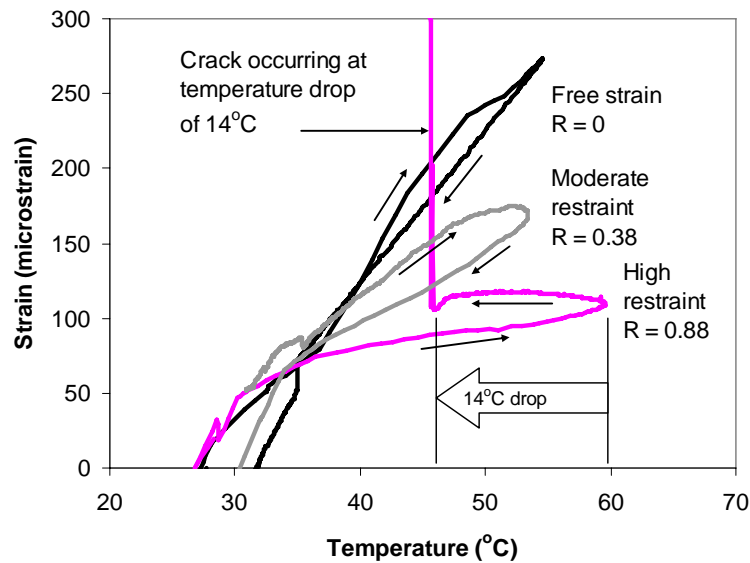


Figure A5.19 *In-situ stress-strain curves in a suspended slab cast between rigid restraints*

A5.8 Conclusions

1. The level of restraint is a critical factor in determining both the risk of early-age thermal cracking and the resulting crack width.
2. Values of restraint are available for a range of element types and vary significantly.
3. For elements with a simple geometry, eg wall on a rigid foundation, methods are available for estimating restraint based on the relative stiffness of the new element and the (old) element against which it is cast. A comparison with *in situ* measurements has indicated that such methods provide an estimate of restraint which is adequate for design purposes.
4. When the geometry is complex, restraint may be difficult to determine without complex analysis. In such cases, it would be prudent to adopt a conservatively high value.
5. The strain developed in structures during the early-age thermal cycle is rarely measured. While more complex (and expensive) than measuring temperature, the data obtained is of far greater value in relation to the impact that it may have on our understanding of early-age behaviour in concrete and hence the opportunity to optimise future design and construction procedures.

A5.9 References

ACPA (2002)

“Early cracking of concrete pavement – causes and repairs”

Concrete Paving technology, TB016P, American Concrete Paving Association, Skokie, Illinois

BAMFORTH, P B (1980)

“The early age behaviour of a massive reinforced concrete suspended slab”

Advances in concrete slab technology (eds Dhir and Munday), Pergamon Press, 1980

ACI (1984)

“Effect of restraint, volume change and reinforcement on cracking of mass concrete”

ACI Manual of Concrete Practice, 207.2R-73

Bamforth, P B and Price, W F (1995)

Concreting deep lifts and large volume pours

Report 135, CIRIA, London

Bamforth, P B (2006)

Guide to the use of lightweight aggregate concrete in bridges – A state-of-the-art report

Concrete Bridge Development Group, Report CCIP-015, Camberley, Surrey, ISBN 1 90448 227 9

Browne, R D and Blundell, R (1973)

“Early age behaviour of mass concrete pours”

Symposium on *Large pours for R C structures*, University of Birmingham, **6**, September 1973, pp 42-65

Emborg, M (1989)

Thermal stresses in concrete structures at early ages

Doctoral Thesis 1989:73D, Division of Structural Engineering, University of Technology, Lulea, Sweden

Hunt, J G (1972)

Temperature changes and thermal cracking in concrete pavements at early-age

Cement and Concrete Association (now BCA), Technical Report 42, 460, April 1972, Camberley, Surrey

Nilsson, M (2003)

Restraint factors and partial coefficients for crack risk analyses of early age concrete structures

Doctoral Thesis 2003:19, Lulea University of Technology, Sweden

Schleech, W (1962)

Die Zwangspannungen in eiseitig festgehaltenen Wand scheiben

(*The positive strains in one way restrained EALLS*) *Beton und Stahlbetonbau*, **57** (No.3), pp 63-72

A6 Tensile strain capacity

A6.1 Deriving values of tensile strain capacity

The tensile strain capacity, ε_{ctu} is the maximum strain that the concrete can withstand without a continuous crack forming. Values of ε_{ctu} are normally obtained by testing the concrete in flexure (Houk *et al*, 1970), in direct tension (Hughes *et al*, 1980, Dunstan, 1981) or by producing conditions of internal restraint which give tensile forces in the surface zones. However, flexural tests produce significantly higher values of ε_{ctu} than tests with more uniform tensile loading (Hunt, 1971), possibly because of the “weakest link” theory.

Care has to be taken when interpreting values of ε_{ctu} as the value will depend on the nature of the test, in particular the rate of loading. In the last version of CIRIA 91 values were presented from tests under slow rates of loading as shown in Table A6.1, with recommendation that for rapid cooling, these values should be halved. Values presented in ICT Technical Note No2 (Bamforth, 1982) and subsequently adopted by BS8110: Part 2 are also presented in Table A6.1. These represent values under short term loading and with the exception of the lightweight concrete are, in general, equal to about 50 per cent of the values for long-term loading.

Table A6.1 *Estimated values of concrete tensile strain capacity for slow rates of straining*

CIRIA R91, 1992		ICT TN/2, 1982 and BS 8110:Part 2, 1985	
Aggregate used in the concrete	Tensile strain capacity under slow loading	Aggregate used in the concrete	Tensile strain capacity under rapid loading
Gravel	130×10^{-6}	Gravel	70×10^{-6}
Crushed rock	180×10^{-6}	Granite	80×10^{-6}
		Limestone	90×10^{-6}
Lightweight	400×10^{-6}	Lightweight (Lytag with natural sand)	110×10^{-6}

The tensile strain capacity may also be derived from measurements of the tensile strength and the elastic modulus of the concrete. In a comprehensive review of data (Tasdemir *et al*, 1996) developed a simple linear relationship between ε_{ctu} and the ratio of the tensile strength f_{ctm} to elastic modulus E_{cm} as follows:

$$\varepsilon_{ctu} = 1.01(f_{ctm}/E_{cm}) \times 10^6 + 8.4 \text{ microstrain} \quad (\text{A6.1})$$

The data from which this relationship was derived are illustrated in Figure A6.1, together with the best fit relationship and a line representing direct proportionality between ε_{ctu} and f_{ctm}/E_{cm} . It is apparent that the line of proportionality represents a lower bound value for the data presented and may therefore be used to provide a basis for design.

A6.2 The influence of strength class and aggregate type

Tensile strain capacity ε_{ctu} depends on the concrete mix proportions, in particular on the shape, type and size of the aggregate. The differences are due to both the elastic modulus of the aggregate and the aggregate/cement paste bond. It is recognised, for example that crushed rock aggregates give a higher value than rounded aggregates. Concrete made with crushed quartzite has a reported tensile strain capacity of 120 microstrain compared to 75 microstrain for a similar mix with quartzite gravel (Houghton, 1976). Lightweight aggregate concretes have higher tensile strain capacities than normal concretes (Bamforth, 1982, Tasdemir *et al*, 1996). Concrete made with all Lytag aggregate has a tensile strain capacity (Hunt's method) of about 200 microstrain (Brooks *et al*, 1987). This value is higher than any concretes made with normal weight aggregates when tested under similar conditions.

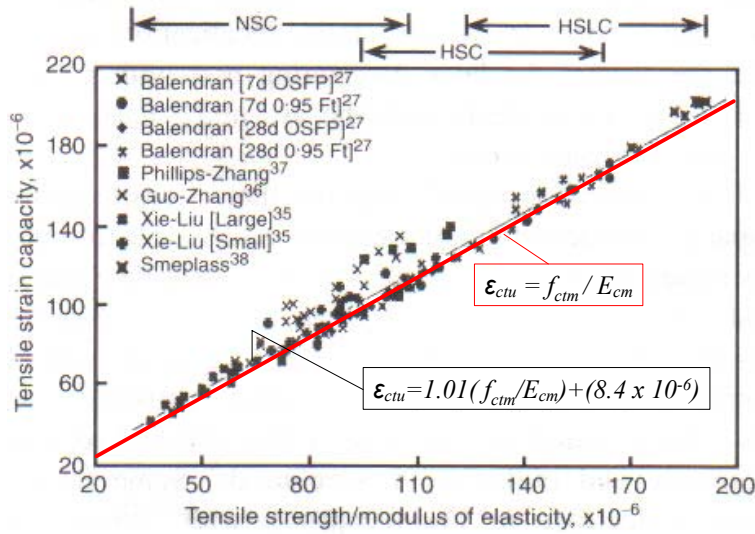


Figure A6.1 The relationship between tensile strain capacity and the ratio of tensile strength to elastic modulus (Tasdemir *et al*, 1996)

If it is accepted that ϵ_{ctu} may be derived from values of tensile strength and elastic modulus, values may be derived from values provided in EN1992-1-1 for different strength classes. Results obtained assuming $\epsilon_{ctu} = f_{ctm}/E_{cm}$ are shown in Figure A6.2, which indicates that ϵ_{ctu} changes not only with aggregate type but also with strength class. This is consistent with the findings of Tasdemir *et al*, (1996) in Figure A6.1, which shows higher values of ϵ_{ctu} for the high strength concrete.

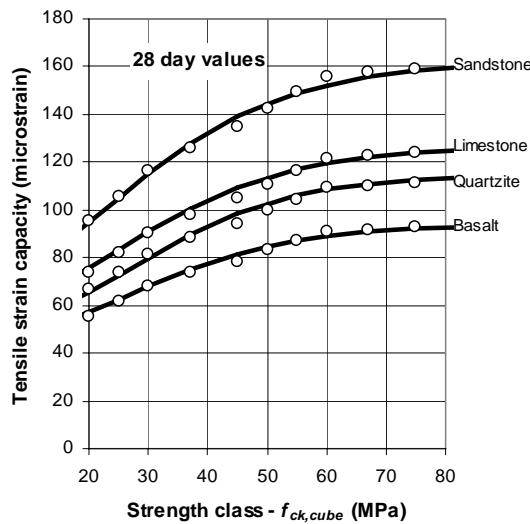


Figure A6.2 Values of tensile strain capacity at 28 days derived using concrete property estimates from EN1992-1-1

The values shown in Figure A6.2 were derived from 28 day property estimates but early-age thermal cracking generally occurs much earlier. It is necessary, therefore, to determine ϵ_{ctu} as it varies with age. This may be achieved using the age functions for tensile strength and elastic modulus provided in equations 3.4 and 3.5 of EN1992-1-1 for tensile strength and elastic modulus respectively. Using this approach the development of ϵ_{ctu} may be estimated and some results are shown in Figure A6.3.

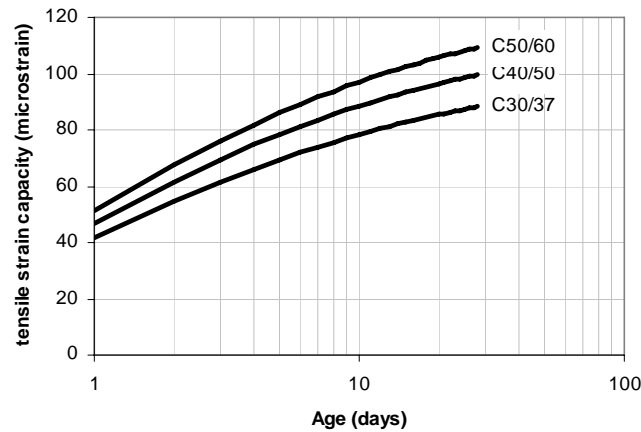


Figure A6.3 The development of tensile strain capacity with time derived using the age functions for tensile strength and elastic modulus given in EN1992-1-1 for concrete using quartzite aggregate

In each case the properties are related back to the mean compressive strength, hence, when using this approach the relative rate of development of ϵ_{ctm} is independent of the strength class and a general curve may be used as shown in Figure A6.4 which illustrates the rate of development of ϵ_{ctm} in relation to the value at 28 days. It can be seen that the three-day value is about 70 per cent of the 28-day value. The three-day values are shown in Figure A6.5.

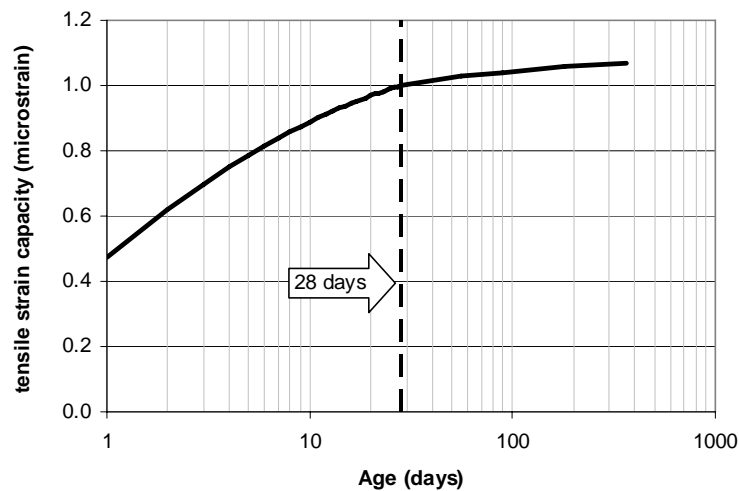


Figure A6.4 The development of tensile strain capacity with time relative to the 28-day value, derived using the age functions for tensile strength and elastic modulus given in EN1992-1-1

The information provided in EN1992-1-1 relates to standard properties at 20 °C and takes no account of the effect of the early-age heat cycle in accelerating the early strength and stiffness and using these relationships would, therefore, provide a safe, lower bound estimate for design purposes.

A study on the effects of silica fume on sensitivity to cracking (Kanstad *et al*, 2001) included measurements of both tensile strength and elastic modulus subject to simulated early heat cycle. The properties are related to maturity (equivalent time at 20 °C) as shown in Figure A6.6.

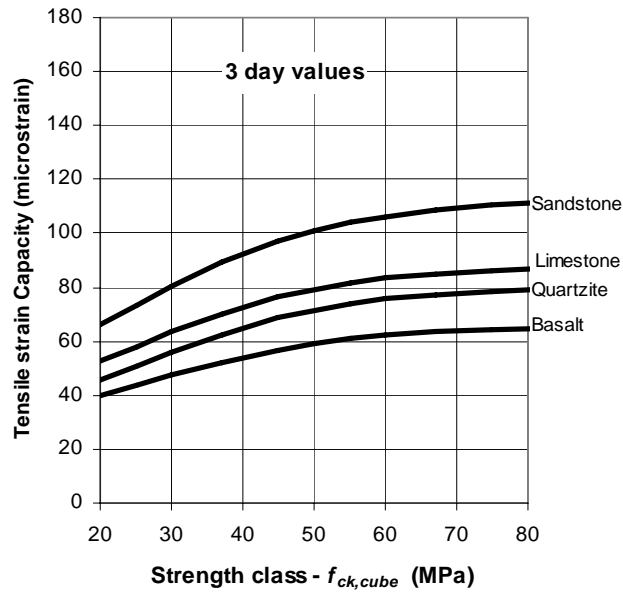


Figure A6.5 The tensile strain capacity at 3-days derived using the relationships from EN1992-1-1

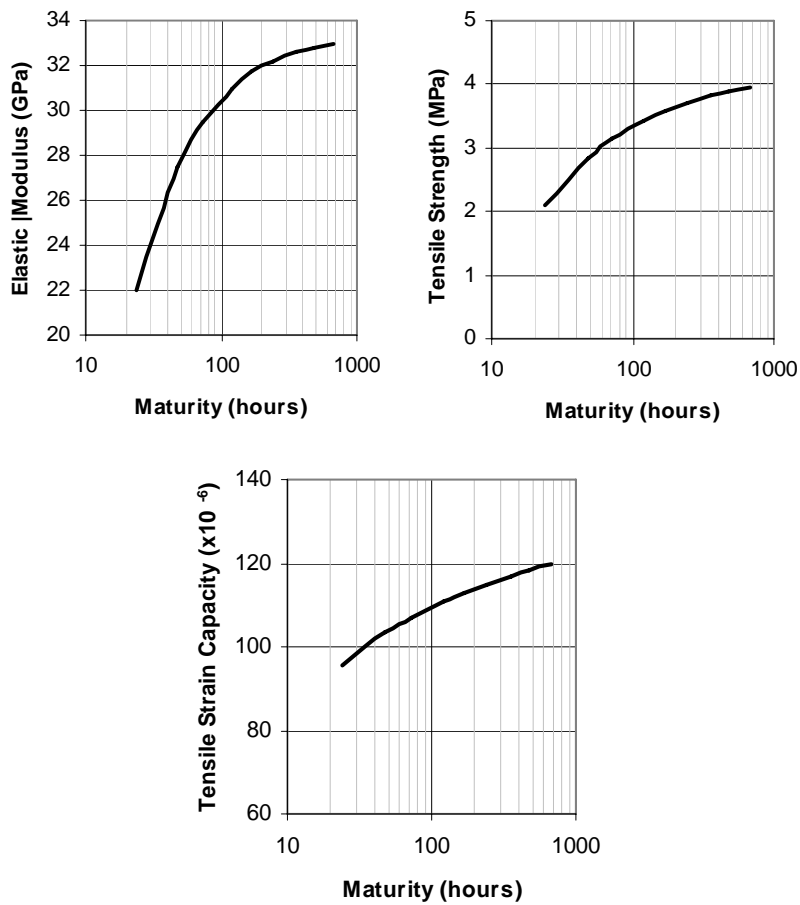


Figure A6.6 Measured development of elastic modulus and tensile strength with maturity (Kanstad et al, 2001) and the estimated development of strain capacity for concrete using CEM I cement and a $w/b = 0.4$

The estimated strain capacity at 28 days is about 120 microstrain for concrete with a compressive strength of 75 MPa. This is broadly consistent with the range of values estimated using EN1992-1-1 for high strength concrete shown in Figure A6.2. The results indicate that ε_{ctu} increases by about 20 per cent between 1 day and 28 days and that the increase is approximately log-linear. At 3 days ε_{ctu} is about 87 per cent of the 28 day value.

Studies in the US have also demonstrated the effect of age on ε_{ctu} (USACE, 1997). Under rapid loading conditions, ε_{ctu} at seven days was reported to be in the range 40-105 microstrain, increasing to a range from 73-139 microstrain at 90 days, an average increase of about 50 per cent. These results are broadly consistent with the results derived from EN1992-1-1 (Figure A6.2) with the seven day range representing concrete with strength in the order of 20-30 MPa and the 90 day range being consistent with a strength of about 50 MPa.

Other researchers have reported that ε_{ctu} is independent of both strength and age. In a study using granite aggregate in concretes with strengths ranging from 20 to 70MPa and tested at ages from 1 to 28 days (Swaddiwudhipong *et al.*, 2001) it was concluded that “the tensile strains at failure and at 90 per cent failure load are insignificantly affected by mix proportions, curing age and compressive strength”. A wide range of values were reported, however, from 80 to 140 $\mu\varepsilon$. The range of values was therefore consistent with the range of values shown in Figure A6.2.

The balance of evidence appears to support the conclusion that ε_{ctu} is related to strength and is hence age dependent. Hence the values derived from EN1992-1-1 may be applied with a reduction factor when estimating the crack risk at ages less than 28 days. Based on the results of Kandstad *et al.* (2001) a reduction of 13 per cent seems appropriate when cracking occurs within the first three days. On this basis, values for ε_{ctu} at early-age have been estimated and are given in Figure A6.7.

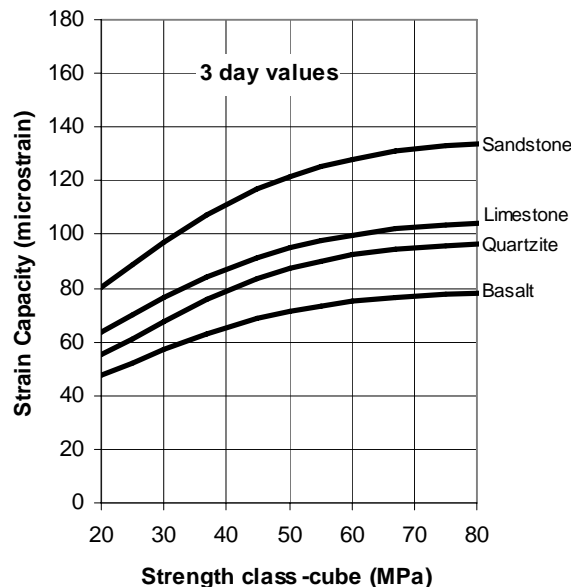


Figure A6.7 Values of tensile strain capacity at three days for concrete subjected to an early thermal cycle

The values given in Figure A6.7 are broadly consistent with previously published results give in Table A6.1 for rapid loading.

The aggregate modulus is a predominant factor in the determination of the tensile strain capacity. The curves shown in Figure A6.7 have been for the limited number of aggregate types for which EN1992-1-1 provides information, ie quartzite, basalt, limestone and sandstone. Published data on the elastic modulus of various aggregate types are given in Table A6.2 (Davidson, 1987, Aulia and Deutschmann, 1999).

Table A6.2 *The elastic modulus of aggregates*

Aggregate type	Elastic modulus of aggregate (GPa)	
	Davidson (1987)	Aulia & Deutschmann, (1999)
Basalt	82	90
Diabase	-	72
Flint gravel	69	-
Serpentine	-	62
Quartzite gravel	59	57
Gabbro	-	56
Granite	48	-
Dolomite	48	-
Limestone	55	39
Natural river gravel	42	-
Sandstone	21	-
Sintered pfa (lightweight)	8	-

Using mean values, the relationship between the ϵ_{ctu} at 3 days (for concrete with a mean cube strength of 45 MPa) and the aggregate modulus is shown in Figure A6.5. There appears to be a simple linear relationship as follows:

$$\epsilon_{ctu(3)} = 118 - 0.66 E_a \quad (\text{A6.2})$$

Using equation A6.2, values of ϵ_{ctu} for concretes containing other aggregate types have been derived and the results are given in Table A6.3. Having established the three days value for concrete with a mean strength of 45 MPa (C30/37) values for other strength classes may be determined by generating a curve through this point in Figure A6.4.

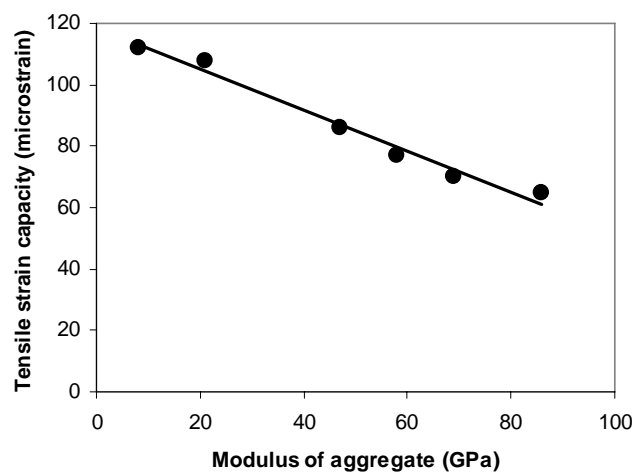


Figure A6.5 *The relationship between the tensile strain capacity at 3 days and the elastic modulus of the aggregate for concrete with a mean 28 day cube strength of 45 MPa*

A6.3 Period of loading

In addition to being influenced by age, the period of loading also has an impact on the strain at failure due to creep. In the US study (USACE, 1997) on mass concrete cooling over a very long period, specimens loaded at seven days and failing at about 90 days exhibited strain capacities in the range from 88-237 $\mu\epsilon$. Corresponding values obtained under rapid loading at seven days were in the range from 40 to 105 $\mu\epsilon$, while specimens loaded rapidly at 90 days achieved values in the range 73-136 $\mu\epsilon$. The increase of more than 100 per cent due to slow loading may therefore be assumed to be a combination of the change in concrete properties between seven and 90 days and the effects of creep. The former would appear to have contributed about 50 per cent to the increase and it may be inferred therefore that the remaining 50 per cent was due creep which occurs under the sustained load. This provides additional validation for the use of the creep factor $K_I = 0.65$ ($\approx 1/1.5$) used in the estimation of crack inducing strain.

A6.4 Other factors

The effects of admixtures on the concrete tensile strain capacity are variable. Hunt (1971) showed that air-entraining agents have little effect on the tensile strain capacity. Research into the effects of ggbs and fly ash on the tensile strain capacity is very limited. There are some field data (Bamforth, 1980) which indicate that the concrete tensile strain capacity with 70 per cent ggbs is lower than that of equivalent CEM I or CEM I /fly ash concretes. With sections over 2.5 m deep, Bamforth (1980) estimated that the reduced tensile strain capacity of the ggbs concrete may cancel out the benefit of the reduced temperature rise. However, in sections under 2.5 m deep the reduction in thermal contraction is greater than the reduction in tensile strain capacity.

The higher the cement content of the concrete, the higher the tensile strain capacity (Carlson *et al*, 1979). Unfortunately, higher cement contents also result in higher temperature rises and larger potential thermal contractions, so the benefit of increased tensile strain capacity is more than cancelled out by the increase in thermal contraction.

A6.5 Values for use in design

For a particular concrete, the tensile strain capacity used to assess the risk of cracking should be a value appropriate to the rate of straining and the thermal and moisture conditions obtaining during the period of cooling on site. All the normal methods of measuring the tensile strain capacity are at relatively rapid rates of straining compared with the straining rate produced during the period of the concrete cooling. As the body of evidence (Houk *et al*, 1970, Carlson *et al*, 1979, USACE, 1997) indicates that the rate of straining significantly affects the tensile strain capacity this has, therefore, to be taken into account in the design process.

Sustained loading has two effects on ϵ_{ctu} .

- as creep occurs, the strain capacity increases by a factor of $1/K_I$ where $K_I = 0.65$ (see Section 4.9.1 of the main guide)
- under sustained loading the tensile strength, and hence the strain at failure, is reduced. The coefficient for sustained loading $K_2 = 0.8$ (see of Section 4.9.2 of main guide).

The net effect is to increase ϵ_{ctu} by a factor of $K_2/K_I = 1.23$. The values derived using EN1992-1-1 have therefore been increased by 23 per cent to account for the effects of sustained loading and the resulting values for strength class C30/37 are given in Table A6.3. The values presented for concretes using aggregate types that are not covered specifically by EN1992-1-1 have been interpolated on the basis of the elastic modulus of the aggregate as shown in Table A6.2 and Figure A6.5.

To estimate the strain capacity for other strength classes, the value obtained for class C30/37 should be multiplied by $0.63 + (f_{ck,cube}/100)$ for $f_{ck,cube}$ in the range from 30 to 60 MPa. For high strength concrete the value obtained for C50/60 should be used. A comparison of 3-day values calculated on this basis with values derived from f_{ctm}/E_{cm} is shown in Figure A6.6.

Table A6.3 *Estimated values of ϵ_{ctu} for strength class C30/37 under sustained loading using different aggregate types*

Aggregate type	Estimated ϵ_{ctu} under sustained loading for strength class C30/37	
	Early-age 3 days	Long-term 28 days
Basalt	63	90
Flint gravel	65	93
Quartzite	76	108
Granite, gabbro,	75	108
Limestone, dolomite	85	122
Sandstone	108	155
Lightweight aggregate (sintered fly ash) with natural sand	115	165

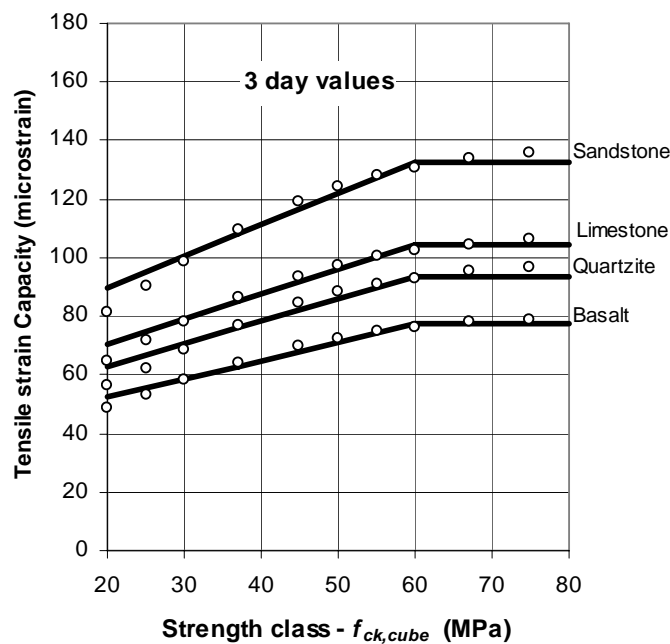


Figure A6.6 *Values of ϵ_{ctu} under sustained loading at 3 days. The symbols represent values estimated using property data derived from EN1992-1-1. The lines represent values obtained by factoring the values for C30/37 concrete*

It is recognised that the approach of EN1992-1-1 is based on property development at 20 °C and that the effect of the early heart cycle will increase the rate of strength development at early-age. However, to incorporate this effect into the design process would be complex as different concretes in different sizes of element would behave differently. Values based on data from EN1002-1-1 should be used, therefore, recognising that they may include an indeterminate factor of safety.

When there is no knowledge of the aggregate the values for concrete using quartzite aggregate should be used as these are the base values for EN1992-1-1.

A6.7 Conclusions

1. The tensile strain capacity of concrete ϵ_{ctu} is dependent on a number of factors including the strength class, the elastic modulus of the concrete (as affected by aggregate type) and the age.
2. Values for ϵ_{ctu} may be obtained from the ratio of the tensile strength of the concrete to the elastic modulus and this approach has been used to derive values for a range of concrete mixes based on property data provided by EN1992-1-1. These values represent ϵ_{ctu} under rapid loading.
3. The strain capacity is affected by sustained loading and it has been estimated that when the effect of both creep and the reduction in tensile strength are taken into account ϵ_{ctu} is increased by 23 per cent.
4. It is estimated that ϵ_{ctu} measured at 28 days and beyond is about 45 per cent higher than the three day value.
5. The combined effect of age and sustained loading is to increase ϵ_{ctu} by about 75 per cent compared to the three day value under rapid loading.
6. The effect of strength class is to increase ϵ_{ctu} by about 50 per cent from C16/20 to C50/60. Above strength class C50/60 there is a relatively small increase in ϵ_{ctu} and for such mixes it is proposed that the value for C50/60 be applied.

A6.8 References

- Aulia, T B and Deutschmann, K (1999)
Effect of mechanical properties of aggregate on the ductility of high performance concrete
 LACER, No.4, pp133-148, 1999
 <www.uni-leipzig.de/~massivb/institut/lacer/lacer04/104_15.pdf>
- Bamforth, P B (1982)
Early-age thermal cracking in concrete
 Institute of Concrete Technology, Technical Note TN/2, Slough
- Brooks, J J, Bennett, E W and Owens, P L (1987)
 "Influence of lightweight aggregates on thermal strain capacity of concrete"
Mag. of Conc. Res., Vol. 39, No. 139, June 1987, 60-72
- Carlson, R W, Houghton, D L and Polivka, M (1979)
 "Causes and control of cracking in unreinforced concrete"
J. Am. Concr. Inst. July 1979, **70**
- Davidson R J (1987)
Report on an investigation into the variability of the elastic modulus of concrete
 United Kingdom Atomic Energy Authority, Contract No. E/5A/CON/565/1524, Taylor Woodrow Wind Energy Group, Report No 014H/87/3241
- Dunstan, M R H (1981)
Rolled concrete for dams - a laboratory study of properties of high fly ash content concrete
 TN105, CIRIA, London
- Houghton, D L (1976)
 Determining tensile strain capacity in mass concrete
J. Am. Concr. Inst. December 1976, **67**, 691-700
- Houk, I E, Paxton, J A and Houghton, D L (1970)
 "Prediction of thermal stress and strain capacity of concrete by tests on small beams"
J. Am. Concr. Inst. March 1970, **67**, 253-261
- Hughes, B P and Chapman, C P (1980)
Direct tensile tests for concrete using modern adhesives
 RILEM Bulletin 26, March 1980, 70-80
- Hunt, J G (1971)
A laboratory study of early-age thermal cracking of concrete
 Cement and Concrete Association, Technical Report 42.457
- Kandstad, T, Bjøntegaard, Ø, Sellevold, E and Hammer, T A (2001)
 "Crack sensitivity of bridge concretes with variable silica fume content"
Improved performance of Advanced Concrete Structures – IPACS, Report BE96-3843/2001:48-6, 2001,
 Selmer Skanska, Trondheim, Norway, ISBN 9 18958 077 X
- Swaddiwudhipong, S, Lu, H R and Lee, T H (2001)
 "Probabilistic model for tensile strain capacity of concrete"
 In: Proc 3rd Int. Conf. *Concrete under severe conditions' CONSEC'01*, Vancouver, Canada, 18-20 June 2001 (eds N Banthai, K Satai and O E Gjorv), University of British Columbia, 1602-1609
- Tasdemir, M A, Lydon, F D and Barr, B I G (1996)
 "The tensile strain capacity of concrete"
Magazine of Concrete Research, 1996, **48**, No. 176, Sept., 211-218

USACE (1997)
Determination of tensile strain capacity
Appendix 1 of ETL 1110-2-542, 30 May 1997

A7 Using probabilistic analysis

A7.1 Description of the method

Concrete is recognised as a variable material and to accommodate this in the structural design process partial safety factors are applied to minimise the risk of failure.

In the process of estimating the risk of cracking, there are many factors, all of which are subject to both variability and uncertainty. However, the design method of CIRIA R91, (Harrison, 1992) and the approach adopted in this revised version is deterministic, with single values in and a single result out, although modification factors have been selected to provide “safe” solutions. However, without being able to quantify the variability of the input parameters it is impossible to determine the risk that is being accepted (ie the reliability) when adopting such an approach. Coupled with the fact that situations have arisen in which performance has not matched the design (eg when crack widths have exceeded design values) a more rigorous approach using probabilistic analysis had been adopted to determine the level of risk associated with the design method proposed.

Probabilistic analysis can be applied to each of the phases of the design process including the assessment of the risk of cracking; the risk of the steel ratio falling below the critical level; and the risk of exceeding the specified crack width.

Essentially, the probabilistic approach is very simple. The same basic equations are used to model the processes but instead of the input data for the various parameters being deterministic (ie single values) they are expressed as distributions that represent the range of values that may occur. Commercial software, in this case @RISK (although others are available, eg Crystal Ball) is then used to run a simulation of the range of possible outcomes when the input parameters are combined in different ways. To do this, @RISK uses Monte Carlo simulation and each simulation may involve up to 10 000 iterations.

A simple example of probabilistic analysis is shown in Figure A7.1 applied to the risk of cracking. Both the estimated restrained-strain and the assumed tensile strain capacity are represented by a distribution of values. In the example shown, the distributions begin to overlap and the degree of overlap is an indication of the risk of cracking. In this case, probabilistic analysis would consider the risk of cracking by determination of the likelihood of the ratio of the restrained strain to the tensile strain capacity exceeding 1.

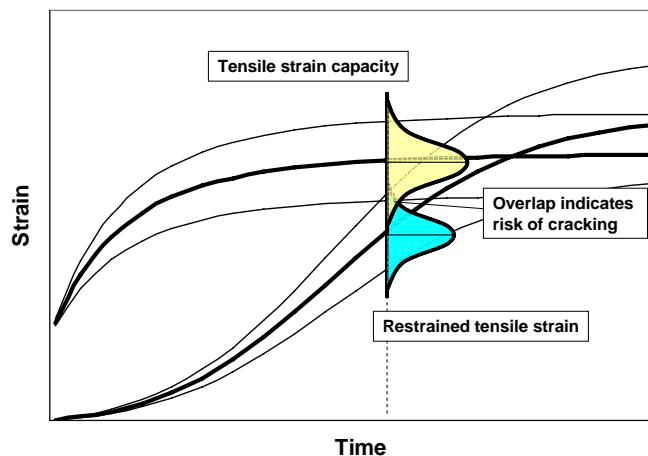


Figure A7.1 A representation of probabilistic analysis applied to early-age thermal cracking

The way in which this approach has been applied to the three design stages is described in the following sections.

A7.2 Estimating the restrained strain

A7.2.1 The equation for estimating the risk of cracking

The risk of cracking is determined by comparing the restrained strain, ε_r , with the tensile strain capacity ε_{ctu} of the concrete under sustained loading. The restrained strain is estimated using the equation:

$$\varepsilon_r = K_1 \left\{ \begin{array}{l} [\alpha_c T_1 + \varepsilon_{ca}] R_1 + \\ \text{Early thermal and Annual temperature} \end{array} \quad \begin{array}{l} \alpha_c T_2 R_2 + \varepsilon_{cd} R_3 \\ \text{Drying shrinkage} \end{array} \right\} \quad \text{Autogenous shrinkage} \quad (\text{A7.1})$$

T_1 is the peak temperature, T_p - mean ambient temperature T_a

α_c is the coefficient of thermal expansion of concrete

ε_{ca} is autogenous shrinkage

ε_{cd} is drying shrinkage

R is the restraint factor (which may vary with age)

K_1 is a coefficient for creep effects.

The risk of cracking is determined using the ratio of $\varepsilon_r/\varepsilon_{ctu}$ where ε_{ctu} is the tensile strain capacity under sustained loading. This is equal to the strain capacity under rapid loading multiplied by the factor K_2/K_1 (see Appendix A6).

where: K_2 is a coefficient for the effect of sustained loading on the tensile strength.

To undertake the probabilistic analysis, each of the parameters in equation A7.1 should be expressed as a distribution.

A7.2.2 Temperature drop, T_1

The likely variation in the temperature rise has been derived both by an evaluation of the results from standard semi-adiabatic tests and by comparing in-situ results with predicted results. Based on the results for a range of CEM I cements given in Table A7.1, it is apparent that the variation is about ± 10 per cent from the mean value, based on the standard 41 hour value. A similar variation might, therefore, be expected in the T_1 values. However, other factors also affect the reliability of predictions, most notably the ambient conditions which are difficult to predict. To estimate the errors associated with such uncertainties an analysis has been carried out in which predicted and measured values have been compared (see Appendix A2). The results are shown Figure A7.2.

It is apparent that while, on average, the model predicts the observed temperature rise reasonably well, there is considerable scatter of the results. Furthermore, the difference between the predicted and measured temperature does not appear to increase in proportion to the temperature rise, indicating that the errors are unlikely to be due solely to variation in the heat generating capacity of the cement.

Table A7.1 *Examples of heat of hydration for seven CEM I (W F Price, 2006) obtained using the semi-adiabatic method of EN197-9:2001*

Time	Total heat of hydration (kJ/kg)						
12h	244.2	235.1	251.5	250.9	302.1	281.4	302.7
24 h	309.9	302.1	318.5	325.4	366.2	357.8	382.7
41 h	321.1	341.0	339.7	339.6	374.6	375.7	395.5
48 h	323.7	348.5	342.5	342.0	375.3	374.4	396.5
72 h	329.8	356.5	344.5	349.9	377.8	380.0	307.3
120 h	347.0	347.0	351.1	356.2	378.0	381.2	401.2

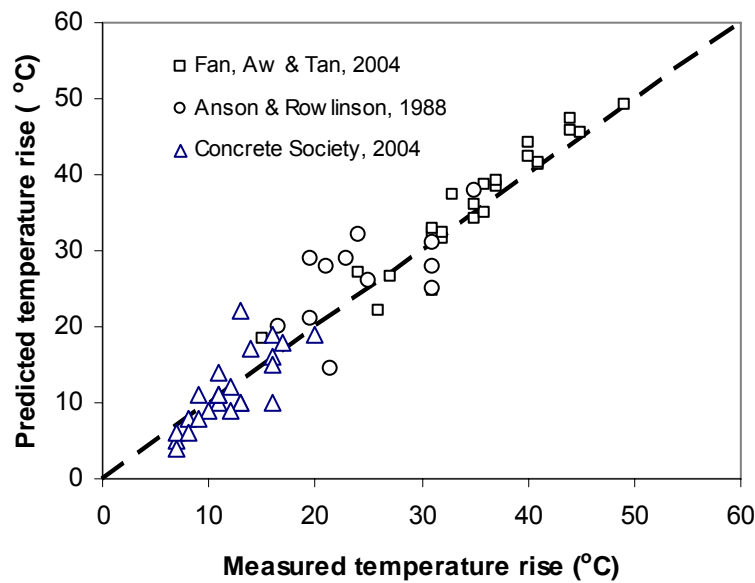


Figure A7.2 *Comparison between measured temperature rise and values predicted using the adiabatic model described in Appendix A2*

An analysis of the difference between the measured and the predicted values shown in Figure A7.2 indicates that, on average, the predicted temperature rise is marginally higher than the measured temperature rise (by 0.7 °C) but that the difference may vary between -7 °C to +9 °C. The estimated SD on the difference between measured and predicted temperature rise is 3.41 °C. Using this data in conjunction with the results of the cement tests, it will be assumed that the likely variation in T_I is independent of the temperature rise and may be calculated using the equation

$$T_I = T_{Ip} + \Delta T_I \tag{A7.2}$$

where ΔT_I has a mean value of -0.7 and a SD of 3.4.

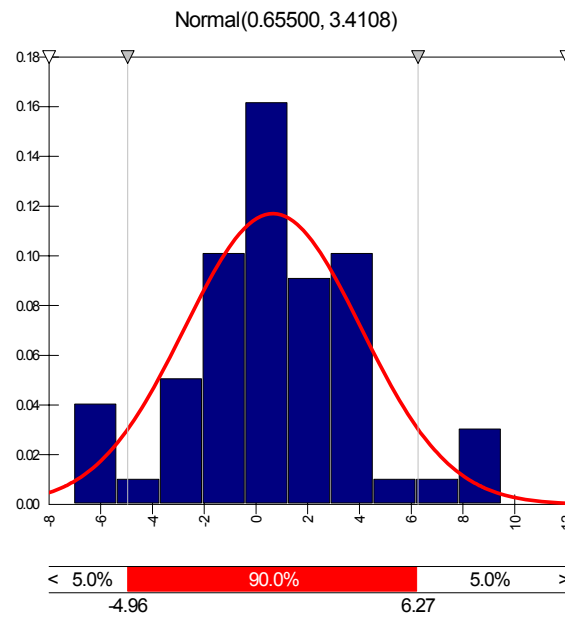


Figure A7.3 The distribution of the difference between measured and predicted values of temperature rise using data shown in Figure A7.2

A7.2.3 Coefficient of thermal expansion, α_c

Values of thermal expansion coefficient will vary according to the aggregate type and will typically be in the range from 8 to 14 $\mu\epsilon/^\circ\text{C}$, as shown in Table A7.2. If no information is available then it will be assumed that the most likely value is 10.5 $\mu\epsilon/^\circ\text{C}$ with a SD of 1 $\mu\epsilon/^\circ\text{C}$. The distribution associated with these parameters is shown in Figure A7.4

Table A7.2 Coefficients of thermal expansion

Coarse aggregate/rock group	Thermal expansion coefficient ($\times 10^{-6}/^\circ\text{C}$ (microstrain/ $^\circ\text{C}$))		
	Rock	Saturated concrete	Design value
Chert or flint	7.4 - 13.0	11.4 - 12.2	12
Quartzite	7.0 - 13.2	11.7 - 14.6	14
Sandstone	4.3 - 12.1	9.2 - 13.3	12.5
Marble	2.2 - 16.0	4.4 - 7.4	7
Siliceous limestone	3.6 - 9.7	8.1 - 11.0	10.5
Granite	1.8 - 11.9	8.1 - 10.3	10
Dolerite	4.5 - 8.5	Average 9.2	9.5
Basalt	4.0 - 9.7	7.9 - 10.4	10
Limestone	1.8 - 11.7	4.3 - 10.3	8
Glacial gravel	-	9.0 - 13.7	13
Lyttag (coarse and fine)	-	5.6	7
Lyttag coarse and natural aggregate fines	-	8.5 - 9.5	9

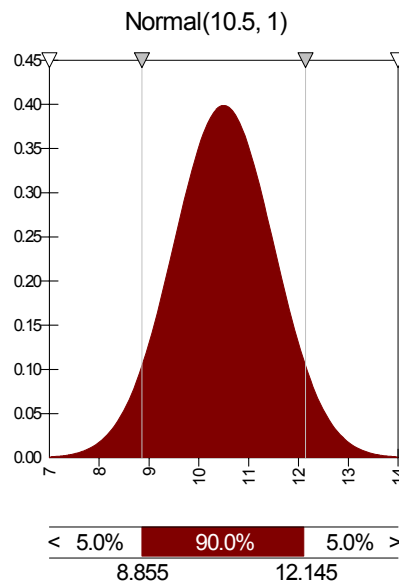


Figure A7.4 Probability distribution of coefficient of thermal expansion

A7.3.4 Autogenous shrinkage

Insufficient data are available to enable the distribution of values to be evaluated. It is therefore proposed that the same coefficient of variation be applied to autogenous shrinkage as applied by EN1992-1-1 to drying shrinkage, ie 30 per cent. Hence the SD = $0.3 \times \text{Mean}$, resulting in 5 and 95 per cent limits of Mean ($1 \pm (0.3 \times 1.64)$) $\approx 0.5 \times \text{Mean}$ and $1.5 \times \text{Mean}$ respectively.

A7.3.5 Restraint

Data on the variability of restraint is limited. However, an estimate may be obtained by consideration of the way that restraint is calculated. Consider the case of a wall on a rigid foundation. In this case the restraint at the joint R_j is estimated using the equation

$$R_j = \frac{I}{I + \frac{A_n E_n}{A_o E_o}} \quad (\text{A7.3})$$

where:

- A_n = cross sectional area (c.s.a) of the new (restrained) pour
- A_o = c.s.a. of the old (restraining) concrete
- E_n = modulus of elasticity of the new pour concrete
- E_o = modulus of elasticity of the old concrete.

While the size and geometry remain constant for both new and old concrete, the same does not apply to the elastic modulus. For the “old” concrete it is unlikely that the modulus E_o will change significantly during the period of an early-age heat cycle of concrete cast against it and it is reasonable, therefore, to assume that E_o remains constant in any calculations. However, the elastic modulus of the new section will be changing rapidly over the first few days and this will influence the degree to which deformation is restrained by the older and stiffer concrete.

Figure A7.5 illustrates the influence of the change in elastic modulus during an early-age heat cycle (Browne and Blundell, 1973) and its influence on the ratio E_o/E_n and the restraint.

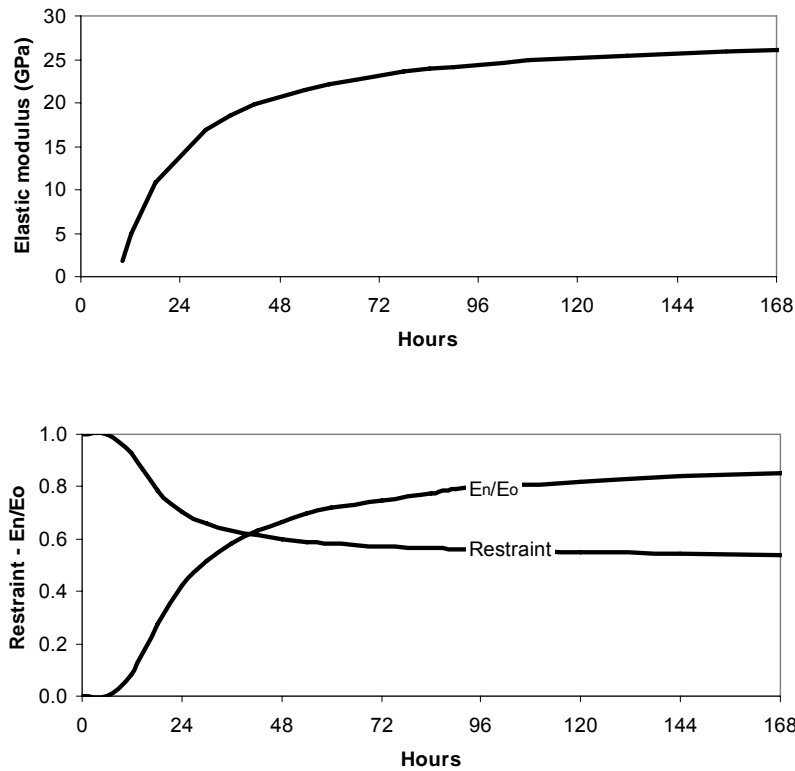


Figure A7.5 The variation in elastic modulus at early-age and the influence on the ratio of E_n/E_o and the restraint derived using equation A5.1 ($A_n/A_o = 1$)

Recognising the change in restraint with time it is appropriate that this is taken into account when undertaking calculations of the risk of early thermal cracking. Predictive models that use estimated, time-dependent properties for the new and old concrete will automatically take this into account. The assumed distribution of E_n/E_o and its effect on the distribution of R_j are shown in Figure A7.6a) and b) respectively. In this example (for $A_n/A_o = 1$) the effect of the change in E_n/E_o is relatively small, resulting in a mean value of 0.59 with a 90 per cent probability of the results falling within the range from 0.56 to 0.62. A change in the ratio of areas A_n/A_o is much more significant, as shown in Figure A7.7. However, the ratio A_n/A_o is determined by the designer and is therefore a deterministic value.

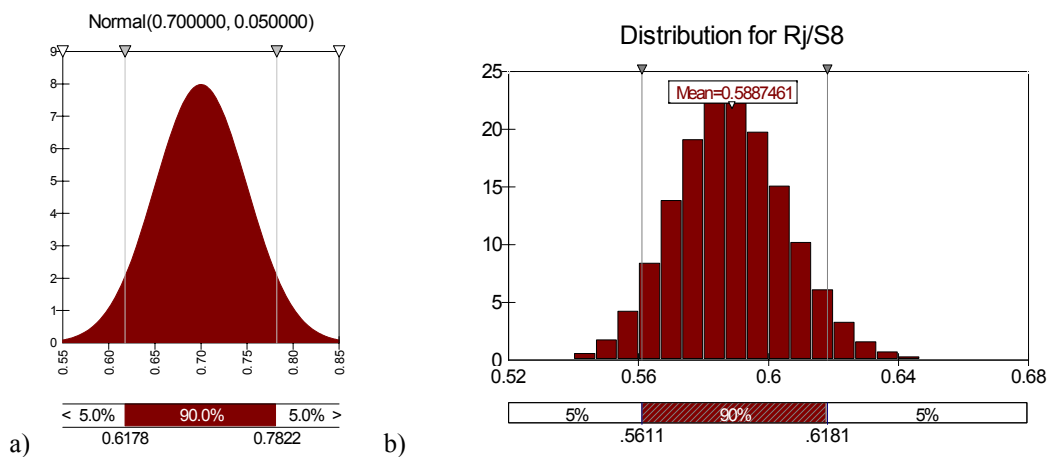


Figure A7.6 The assumed probability distribution of E_n/E_o and the resulting distribution of R_j (assuming that $A_n/A_o = 1$)

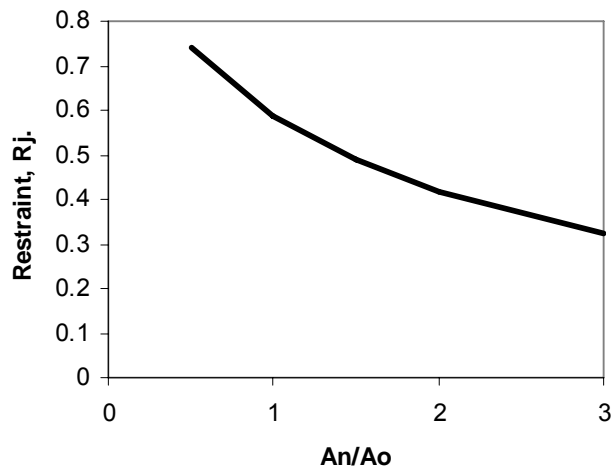


Figure A7.7 The relationship between An/Ao and the estimated restraint at the joint

A7.2.6 Coefficient for creep K_1

The creep factor K_1 has been estimated from limited tests undertaken to measure both the load-deformation behaviour of concrete at very early-age (Bamforth, 1982) and the relaxation that occurs under sustained load (Vitharana *et al*, 1995). Reported values typically fall within the range from 0.5 to about 0.65. It is assumed that K_1 is the same in relation to early-age and long-term stresses. During the early thermal cycle the concrete is relatively immature and at elevated temperature, with both factors contributing to higher creep. In the long-term relaxation may occur over a very long period in the order of months or years, rather than days.

The assumed distribution of K_1 is shown in Figure A7.8. It is represented by a PERT distribution with minimum, mean and maximum values of 0.5, 0.6 and 0.7. The upper 95 per cent value using this distribution is 0.66.

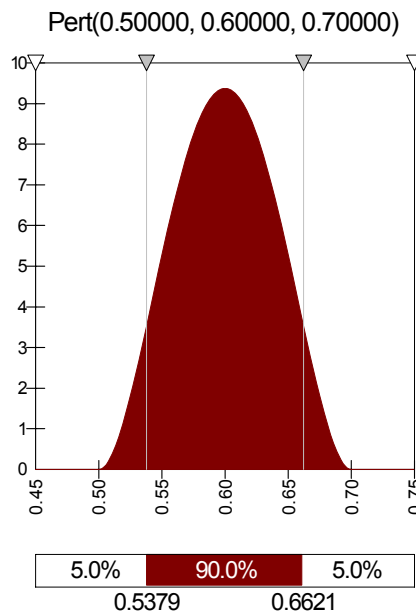


Figure A7.8 The probability distribution for the creep coefficient, K_1

A7.3.7 The coefficient for sustained loading K_2

Concrete that is maintained under a sustained tensile stress will fail at a load that is significantly lower than the load that may be sustained in a rapid load test. Under testing at constant load it has been demonstrated that when the stress exceeds about 80 per cent of the short term tensile strength, failure will almost certainly occur (Domone, 1974, Reinhardt and Rinder, 1998 van Breugel and Lokhorst, 2001) and some risk of failure is demonstrable at lower stress/strength ratios. Altoubat and Lange (2001) achieved failure in normal concretes at stress/strength ratios between 0.75 and 0.81 and Reinhardt and Rinder (1998) have reported data that shows failure at a stress/strength ratio of as low as 0.6. In probabilistic terms the risk of cracking in relation to the stress/strength ratio may be expressed as a PERT distribution with 0.6, 0.7 and 0.8 as minimum, mean and maximum values, shown in Figure A7.9. This represents no chance of cracking if the stress/strength ratio is below 0.6, a 50 per cent chance of cracking when the stress/strength ratio exceeds 0.7 and certainty of cracking if the stress/strength ratio exceeds 0.8.

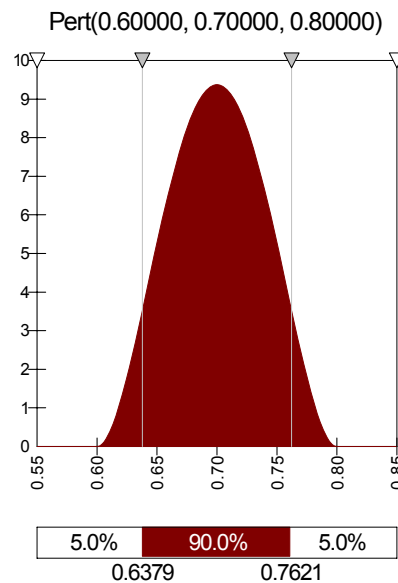


Figure A7.9 The probability of cracking in relation to the stress/strength ratio in tension

A7.3.8 Tensile strain capacity ϵ_{ctu}

The tensile strain capacity ϵ_{ctu} varies with the aggregate type, the strength grade and the age. At the design stage only the strength class may be known. Variations due to aggregate type and age (with the first six days) should be taken into account in the probabilistic analysis.

The estimated values of f_{ctm} and E_{cm} from which ϵ_{ctu} under rapid loading is derived are based on the use of quartzite aggregate. The aggregate type affects E_{cm} and where no knowledge of the aggregate is available this should be taken into account in the analysis. EN1992-1-1 indicates that stiffer aggregate (basalt) may exhibit an elastic modulus that is 10 per cent higher, while less stiff aggregate (sandstone) may exhibit a value that is 20 per cent lower. As ϵ_{ctu} is estimated from f_{ctm}/E_{cm} the variation in E_{cm} may result in values of ϵ_{ctu} that vary from $1/1.1 = 0.91$ to $1/0.8 = 1.25$ times the value for quartzite aggregate. This may be represented by the PERT distribution shown in Figure A7.10.

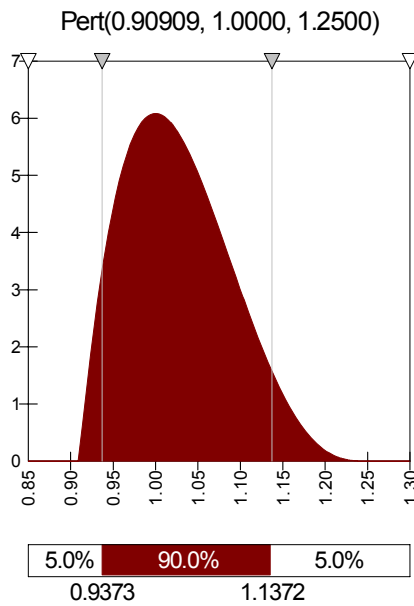


Figure A7.10 The distribution of the relative magnitude of ϵ_{ctm} due to differences in aggregate type

In addition, it is the value under sustained loading that is used in the assessment of crack risk and crack width. While the effect of creep K_1 is to increase ϵ_{ctm} the effect of the sustained loading K_2 is to reduce the tensile stress, and hence strain, at which failure occurs. Under sustained loading ϵ_{ctm} is increased by the factor K_2/K_1 . As both K_1 and K_2 are themselves subject to variability. The combined effect is shown in Figure A7.11.

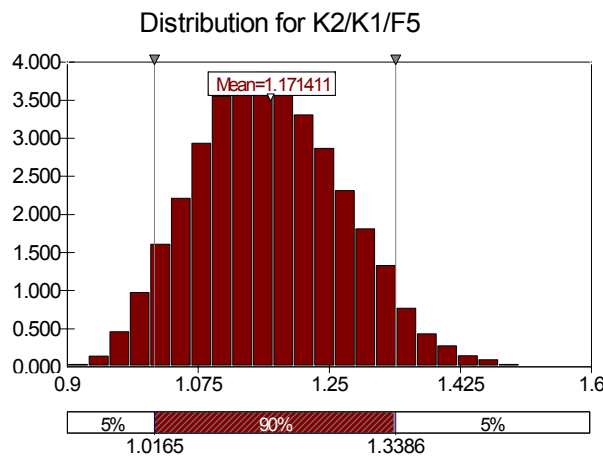


Figure A7.11 The distribution of the ratio K_2/K_1 applied ϵ_{ctm} for sustained loading

The tensile strain capacity increases with age as shown in Figure A7.12. Relative to the three day value used in the design ϵ_{ctm} which is about 70 per cent of the 28-day value, the range from one to six days is 0.5 to 0.8. Taking the three day value as unity, the 1 day and 6 day values are 0.7 to 1.15. This can be represented by a PERT distribution with relative minimum, mean and maximum values of 0.65, 1 and 1.20.

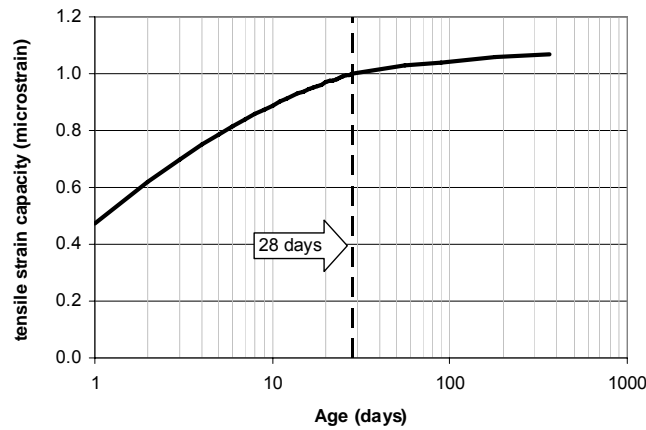


Figure A7.12 The development of tensile strain capacity with time relative to the 28-day value

A7.3.9 Probabilistic analysis to estimate the risk of early thermal cracking

At this stage the risk of the restrained strain being sufficient to cause cracking may be estimated. Consider a 3 m high, 500 mm thick retaining wall cast onto a 750 mm × 2000 mm base ($A_n/A_o = 1$). A C30/37 concrete is used with CEM I cement. The estimated binder content is 340 kg/m³. The input parameters are given in Table A7.3 together with estimated values of free strain and restrained strain in the short and long-term. Probability curves for early-age and long-term crack-inducing strains are shown in Figures A7.13 and A7.14.

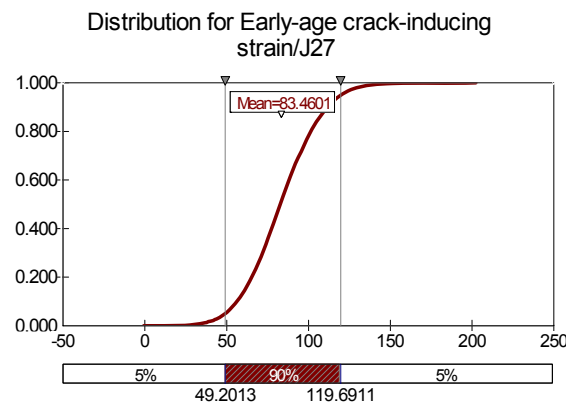


Figure A7.13 Probability distribution for early-age crack-inducing strain

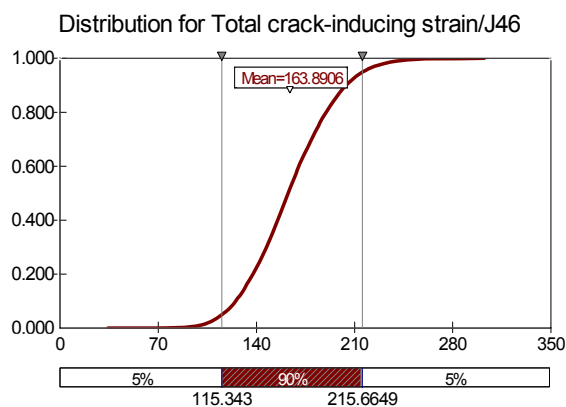


Figure A7.14 Probability distribution for total crack-inducing strain over the long-term

Table A7.3 Input data and results from a probabilistic analysis to determine the magnitude of crack-inducing strain and the risk of cracking

Input parameters	Symbol	Unit	Distribution	Input for probabilistic analysis			
				Min	Most likely	Max	SD
Strength class	$f_{ck}/f_{ck,cube}$	MPa			<u>C30/37</u>		
Age at cracking	t	days			<u>3</u>		
Tensile strength (calculated EN1992-1-1)	$f_{ctm}(t)$				1.73		
Elastic modulus (calculated EN1992-1-1)	E_{cm}	GPa			28.1		
Early-age strains							
Temperature drop	T_1	°C		25.4	<u>32</u>	36.5	
Model uncertainty in temperature drop		°C	NORMAL		<u>-0.7</u>		<u>3.4</u>
Coefficient of thermal expansion	α_c	$\mu\epsilon/^\circ\text{C}$	NORMAL	8.9	<u>10.5</u>	12.1	<u>1</u>
Autogenous shrinkage (calculated EN1992-1-1)	ϵ_{ca}	$\mu\epsilon$	NORMAL		15		4
Free contraction							
	ϵ_{free}	$\mu\epsilon$			347		
Restrained early-age strain							
E_n/E_o			NORMAL	0.62	<u>0.70</u>	0.78	<u>0.05</u>
A_n/A_o			Deterministic		<u>1.00</u>		
Restraint	R			0.56	0.59	0.62	
Coefficient for creep K_1	K_1		PERT	<u>0.50</u>	<u>0.60</u>	<u>0.70</u>	
Restrained contraction (short term)							
	ϵ_r	$\mu\epsilon$			122		
Crack-inducing early-age strain							
Tensile strain capacity, ϵ_{ctu} (rapid loading)	ϵ_{ctu}	$\mu\epsilon$			<u>62</u>		11.3
Effect of aggregate type			PERT	0.91	<u>1.00</u>	1.25	
Effect of sustained loading	K_2		NORMAL	0.60	<u>0.70</u>	0.80	<u>0.06</u>
Effect of age			PERT	0.70	<u>1.00</u>	1.15	
Tensile strain capacity, ϵ_{ctu} (sustained loading)	ϵ_{ctu}				72		
Crack-inducing strain (short term)							
	ϵ_{cr}	$\mu\epsilon$			87		
Risk of cracking	$\epsilon_r / \epsilon_{ctu}$				2.84		
Long term strain							
Long term temperature change	T_2	°C	PERT	<u>10</u>	<u>15</u>	<u>20</u>	
Residual autogenous shrinkage (3-28days)	ϵ_{ca}	$\mu\epsilon$	NORMAL		<u>18</u>		5
Drying shrinkage	ϵ_{cd}	$\mu\epsilon$	NORMAL	73	<u>143</u>	213	43
Free contraction (long term)							
	ϵ_{free}	$\mu\epsilon$			319		
Restrained long term strain							
E_n/E_o			Deterministic		<u>1</u>		
Restraint to long term strains	R_2				0.50		
Restraint to drying shrinkage	R_3				0.50		
Restrained strain (long term)							
	ϵ_r	$\mu\epsilon$			96		
Crack-inducing long term strain							
Tensile strain capacity (28 day)	ϵ_{ctu}	$\mu\epsilon$			103		
Residual tensile strain capacity	ϵ_{ctu}	$\mu\epsilon$			31		
Crack-inducing strain (long term)							
	ϵ_{cr}	$\mu\epsilon$			80		
Total strains							
Free contraction							
	ϵ_{free}	$\mu\epsilon$			665		
Restrained contraction							
	ϵ_r	$\mu\epsilon$			218		
Crack-inducing strain							
	ϵ_{cr}	$\mu\epsilon$			167		

The crack-inducing strain is the restrained strain minus the residual tensile strain in the concrete. Hence any value greater than zero indicates a risk of cracking. The results of this analysis demonstrate that there is very little chance of cracking being avoided.

The values of crack-inducing strain at early-age and in the long-term estimated using the full design method with conservative default assumptions were $157 \mu\epsilon$ and $294 \mu\epsilon$ indicating a significant margin of safety. Comparative values calculated using CIRIA R91 (Harrison, 1992) were $166 \mu\epsilon$ and $293 \mu\epsilon$. While the values are similar, the input assumptions differed. CIRIA R91 predicted lower values of free contraction with a larger proportion of this contraction generating crack-inducing strain.

A7.3 Estimating the minimum area of reinforcement, $A_{s,min}$

A7.3.1 The equation for $A_{s,min}$

Achieving the critical steel ratio is essential if cracking is to be controlled. To prevent yielding of the reinforcement at the location of cracks the steel should be able to accommodate the full load transferred from the concrete. To calculate the minimum reinforcement area $A_{s,min}$, EN1992-1-1 uses the expression

$$A_{s,min} \sigma_s = k_c k f_{ct,eff} A_{ct} \quad (A7.4)$$

where:

- $A_{s,min}$ is the minimum area of reinforcing steel within the tensile zone (previously defined by the critical steel ratio ρ_{crit})
- A_{ct} is the area of concrete within the tensile zone. The tensile zone is that part of the section which is calculated to be in tension just before formation of the first crack
- σ_s is the absolute value of the maximum stress permitted in the reinforcement after formation of a crack (usually taken as the yield strength of the steel f_{yk})
- $f_{ct,eff}$ is the mean value of the tensile strength of the concrete effective at the time when the cracks may first be expected to occur
- k is a coefficient which allows for “*the effect of non-uniform self-equilibrating stresses, which lead to a reduction in restraint forces*”
- k_c is a coefficient which takes account of the stress distribution within the section immediately prior to cracking and the change of the level arm.

Rearranging equation (A7.1) and substituting f_{yk} for σ_s gives

$$\frac{A_{s,min}}{k_c k A_{ct}} = \frac{f_{ct,eff}}{f_{yk}} (= \rho_{crit}) \quad (A7.5)$$

A7.3.2 The strength of the reinforcement

The value of f_{yk} has historically been assumed to have a characteristic value of 460 MPa. However, in a national survey (CARES, 2006) it was reported that the mean strength of reinforcement used in the UK was 530 MPa with a Standard Deviation (SD) of 32.1 MPa. This would yield a distribution as shown in Figure A7.15a with a range from below 440 MPa to above 620 MPa. However, the reported upper and lower limits were 474 MPa and 623 MPa. This indicates a skewed distribution with the mean being closer to the lower end. A better representation may be achieved, therefore, by the use of a PERT distribution with upper and lower bounds as reported and a mean value of 530 MPa. This results in a characteristic value of 493 MPa as shown in Figure A7.15b. This is close to the revised characteristic value of 500 MPa specified in EN1992-1-1:2004. The PERT distribution will therefore be used in the analysis.

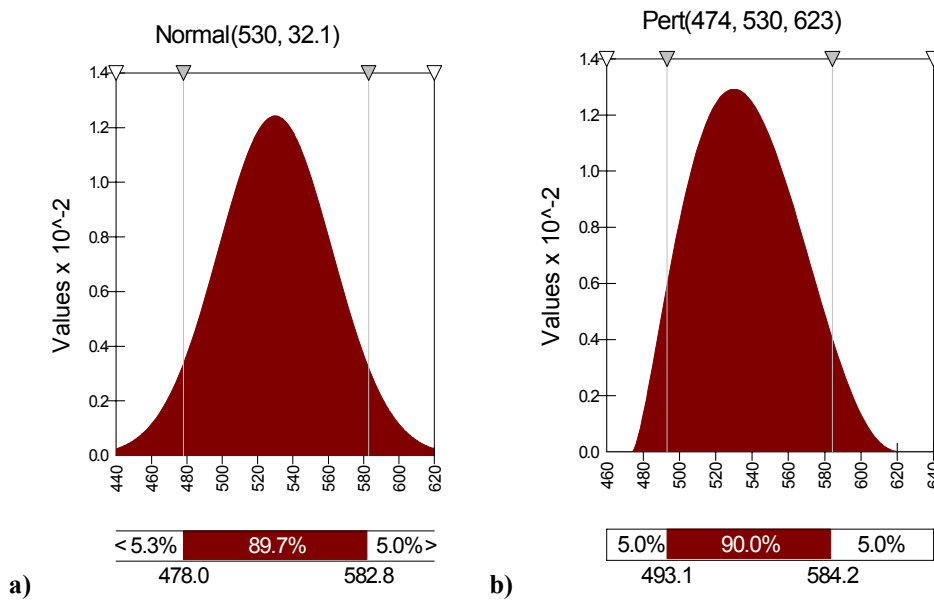


Figure A7.15 The distribution of the tensile strength of reinforcement expressed as a) Normal and b) Pert distributions, both using data from CARES (2005)

A7.3.3 Tensile strength of the concrete according to EN1992-1-1

In the evaluation of $A_{s,min}$ EN1992-1-1 recommends the use of the mean tensile strength effective at the time at which cracking occurs. However, it is the *in situ* tensile strength at the time of cracking that will determine the stress transferred to the steel. A detailed assessment of the *in situ* tensile strength is given in Appendix A10 and the estimated distributions at early-age and long-term for C30/37 concrete are given in Figures A7.16 and A7.17 respectively.

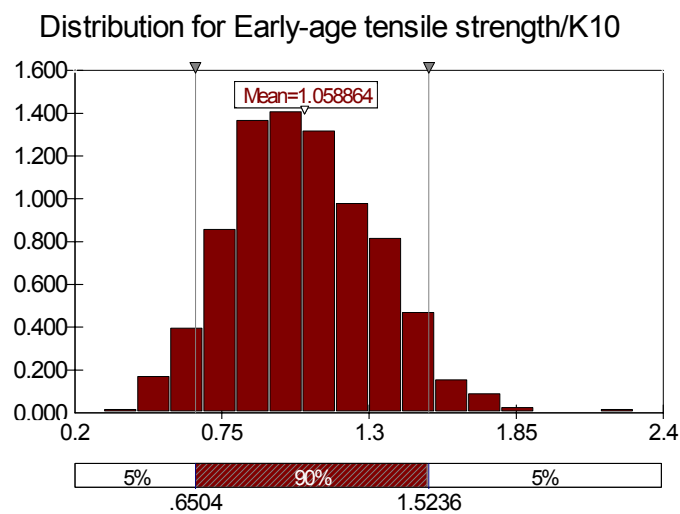


Figure A7.16 Distribution of early-age *in situ* tensile strength for C30/37 concrete

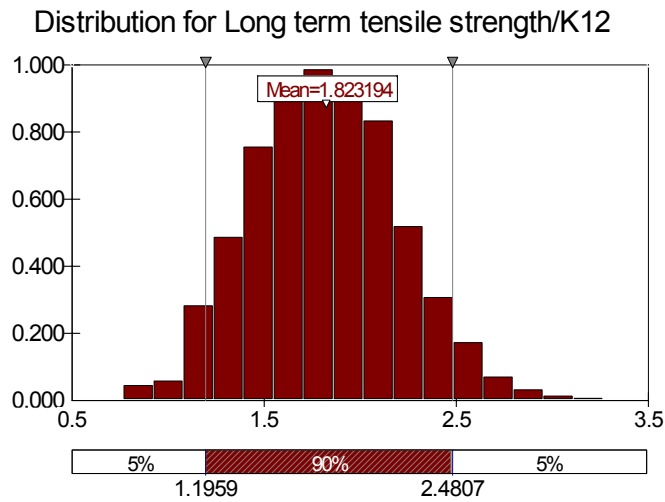


Figure A7.17 Distribution of long-term in situ tensile strength for C30/37 concrete

A7.3.4 The ratio of $f_{ctm}(t)/f_{yk}$

Probability distributions for $f_{ctm}(t)/f_{yk}$ have been estimated taking into account the variability in the tensile strength of both the steel and the concrete. Early-age and long-term values are show in Figures A7.18 and A7.19 respectively for C30/37 concrete.

Using the method of EN1992-1-1 $f_{ctm}(3) = 1.73 \text{ MPa}$; $f_{ctm}(28) = 2.9 \text{ MPa}$; and $f_{yk} = 500 \text{ MPa}$.
Using these values $f_{ctm}(t)/f_{yk} = 0.0035$ at early-age and 0.0058 in the long-term.

Based on the probabilistic analysis, the likelihood of higher values being required to control cracking are 0.04 and 0.11 per cent. This indicates that there may be some scope for reducing $f_{ctm}(t)/f_{yk}$ and hence the minimum area of reinforcement $A_{s,min}$ compared with that derived directly from EN1992-1-1. However, in view of the criticality of $A_{s,min}$ and the fact that the steel ratio A_s would normally be expected to be significantly higher than $A_{s,min}$ to ensure that the crack widths are acceptable, the safety factor inherent within the EN1992-1-1 approach should be maintained.

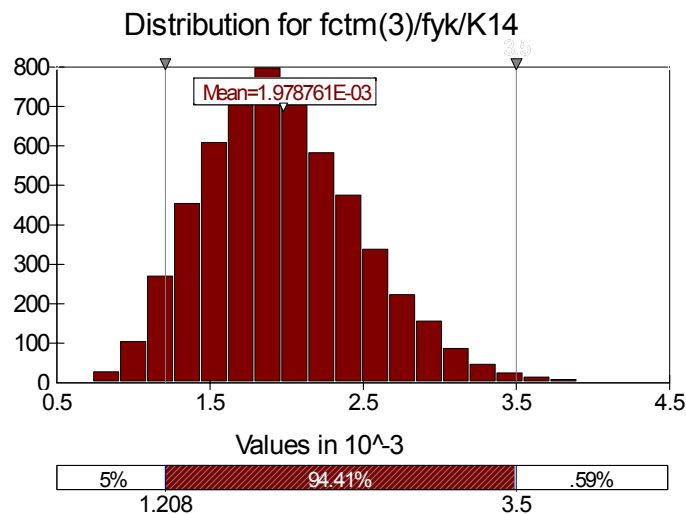


Figure A7.18 The probability distribution of $f_{ctm}(3)/f_{yk}$ at early-age

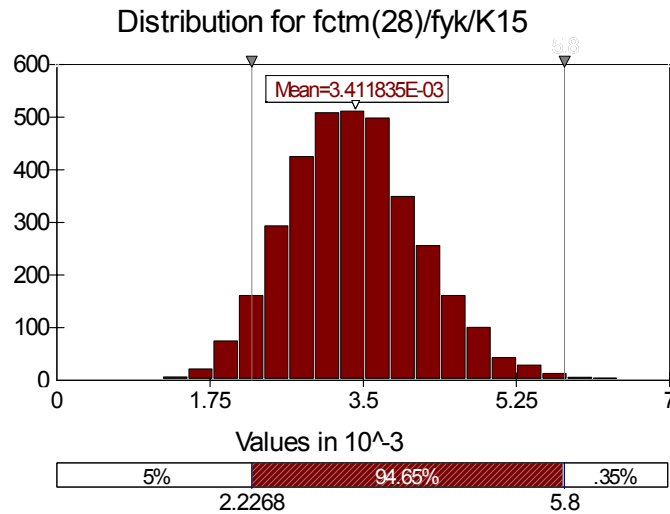


Figure A7.19 The probability distribution of $f_{ctm}(28)/f_{yk}$ in the long-term

A7.4 Estimating the crack width

A7.4.1 The predictive equations

The steel ratio determines the maximum crack spacing $S_{r,max}$ according to the expression

$$S_{r,max} = 3.4c + 0.425 \frac{k_1 \varphi}{\rho_{p,eff}} \quad (A7.6)$$

where:

- c is the cover to reinforcement
- k_1 is a coefficient which takes account of the bond properties of the reinforcement
- φ is the bar diameter
- $\rho_{p,eff}$ is the effect area of reinforcement $A_s / A_{c,eff}$ (see Appendix A8, Section A8.5.2).

From this, the crack width is calculated using the equation:

$$w_k = S_{r,max} R_{ax} \varepsilon_{free} \quad (A7.7)$$

R_{ax} , ε_{free} is the restrained strain ε_r estimated using equation (A7.1). It can be seen that equation A7.7 take no account of the fact that after cracking has occurred, there is a residual tensile strain in the concrete which does not contribute to the crack width. This is assumed to be half the tensile strain capacity of the concrete ε_{ctu} (see Appendix A8)

$$w_k = S_{r,max} (R_{ax} \varepsilon_{free} - 0.5 \varepsilon_{ctu}) \quad (A7.8)$$

To undertake the probabilistic analysis, each of the parameters in equations A7.6 and A7.8 should be expressed as a distribution. The coefficients 3.4 and 0.425 are NDP's and will therefore be assumed to be deterministic. In addition the bar diameter is unlikely to vary to the extent that it has a significant. Three factors, c , k_1 and $\rho_{e,eff}$ will therefore be considered.

A7.4.2 Cover c and the steel ratio $\rho_{e,eff}$

EN1992-1-1 requires that the nominal cover c_{nom} be calculated by adding an allowance Δc_{dev} to the minimum cover c for deviation in practice. The recommended value of Δc_{dev} is 10 mm.

Within the revised equation for $S_{r,max}$ cover has a significant impact in two respects. Firstly, there is the direct addition of $3.4 \times c$ through the additional term. The second term is also influenced by cover, although this is not immediately apparent. This term includes $\rho_{e,eff}$ which is calculated as $A_s/h_{e,ef}$ where $h_{e,ef}$ is equal to $h/2$ or $2.5(c+\phi/2)$ whichever is smaller. Hence $\rho_{e,eff} = A_s/[2.5(c+\phi/2)]$.

The effect of cover on the crack spacing is shown in Figure A7.20 based on a 500mm thick section with 20mm bars at 200mm centres on each face. The crack spacing increases by 500mm for every 25mm increase in cover. The impacts on the early-age and long-term crack widths are shown in Figure A7.21 for the same example.

Within the probabilistic analysis it will be assumed that the mean cover $c + 10$ mm and that the cover may vary by ± 10 mm about the mean.

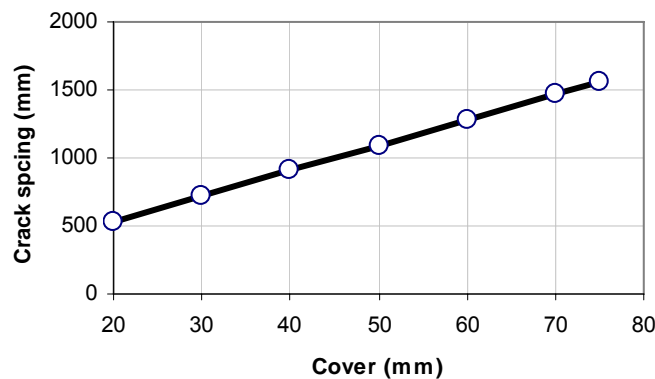


Figure A7.20 The effect of cover on crack spacing

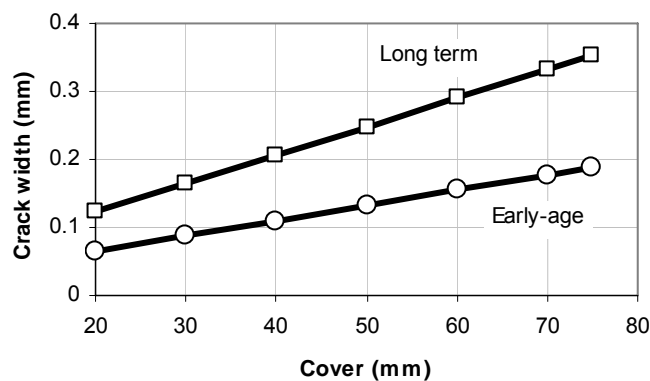


Figure A7.21 The effect of cover on crack width

A7.4.3 The ratio of tensile strength to bond strength, k_1

The coefficient k_1 represents both the ratio between the tensile strength and the bond strength of the reinforcement (0.6) and the ratio of the mean to the minimum crack spacing (1.33) and in combination lead to a value of $0.6 \times 1.33 = 0.8$ (see Appendix A8, Section A8.5.4). In BS8007 this was expressed as $f_{ct}/f_b = 0.67$ for high bond bars. As this term has an almost proportional effect on the crack spacing and width it is important that appropriate values are used.

In considering the development of the design equations in EN1992-1-1 further consideration was given to the k_f factor used in EN1992-1-1. The general assumption is that good bond is achieved around the whole bar perimeter. In addition, the data used in generating the expression for crack spacing have been derived from laboratory tests where this can be achieved. *In situ*, the achievement of good bond around horizontal bars may be more difficult, even with accepted good practice in placing the concrete. A common occurrence is for bleed water to accumulate below reinforcement resulting in a weak layer, and sometimes forming an air gap when the bleed water is reabsorbed into the concrete. In such cases EN1992-1-1 applies a factor of 0.7 and it has been recommended that this value be applied until experience with the use of EN1992-1-1 indicates that it may be omitted or revised. This increased k_f for 0.8 to 1.14.

For probabilistic analysis it will be assumed that k_f follows a PERT distribution with values between 0.8 and 1.14.

A7.4.4 Probabilistic analysis to estimate the crack width

The example started in Section A7.3 has been followed through to estimate early-age and long-term crack widths. The design data is used in conjunction with the estimated strains to derive the crack width. The input data are shown in Table A7.8 and probability distributions for early-age and long-term crack widths are shown in Figures A7.22 and A7.23.

The analysis has been carried out assuming 25 mm bars at 150 mm centres.

Table A7.7 Input data and results from a probabilistic analysis to determine the magnitude of early-age and long-term crack width

Input parameters	Symbol	Unit	Distribution	Input for probabilistic analysis			
				Min	Most likely	Max	SD
Reinforcement and crack spacing							
Section thickness	h	mm			500		
Bar diameter	ϕ	mm			25		
Bar spacing	S	mm			150		
Area of steel per face	A_s	mm ²			3272		
Coefficient	k_c				0.90		
Coefficient	k				1		
Surface zone for estimating $A_{s,min}$	$h_{s,min}$				225		
Strength of reinforcement	f_{ky}	MPa			500		
Critical steel ratio	ρ_{crit}				0.0035		
Minimum area of steel per face/m	$A_{s,min}$				780		
Cover	c	mm	PERT	40	50	60	
Effective surface zone for estimating $\rho_{p,eff}$	$h_{e,eff}$				156.25		
Steel ratio for estimating crack spacing	$\rho_{p,eff}$				0.02094		
Coefficient for bond characteristics	k_f		PERT	0.8	0.97	1.14	
Crack spacing	s_r	mm	PERT		662		
Early age crack width	w_k	mm			0.06		
Long term crack width	w_k	mm			0.11		

The values of early-age and long-term crack width estimated using the full design method with conservative default assumptions were 0.11 mm and 0.22 mm indicating a significant margin of safety. Comparative values calculated using CIRIA R91 (Harrison, 1992) were 0.12 mm and 0.19 mm. While the values are similar, the input assumptions differed. CIRIA R91 (Harrison, 1992) predicted lower values of free contraction with a larger proportion of this contraction generating crack-inducing strain.

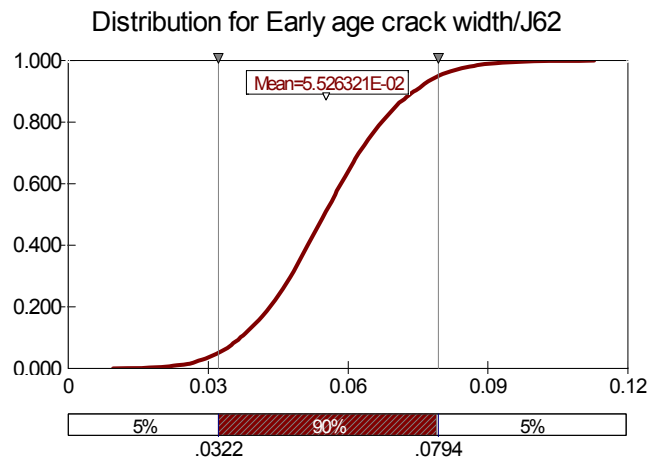


Figure A7.22 Probability distribution for early-age crack width

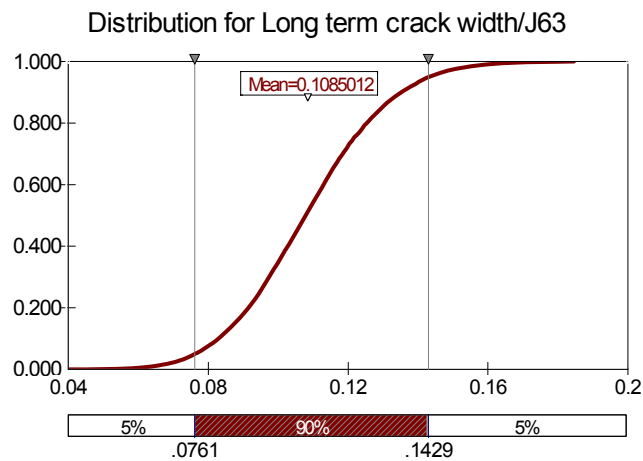


Figure A7.23 Probability distribution for long-term crack width

A7.5 Conclusions

Probabilistic analysis has been undertaken using a commercial software package, @RISK, which operates in Microsoft Excel. This approach has been used as follows:

- to derive safe values for the critical steel ratio
- to provide a method for estimating the risk of cracking
- to provide a basis for establishing safe levels of reinforcement in relation to crack widths.

The results indicate, assuming that the basic theory behind the calculation of crack widths is correct, that there is a significant margin of safety, in the order of 1.5, in the proposed method for design.

A7.6 References

- Altoubat, S A and Lange, D A (2001a)
 “Creep, shrinkage and cracking of restrained concrete at early-age”
ACI Materials Journal, July/August 2001 Vol. 98, No.4. pp 323-331
- Anson, M and Rowlinson, P M (1988)
 “Early-age strain and temperature measurements in concrete tank walls”
Magazine of Concrete Research, Vol. 40, No. 145, December 1988
- @RISK
 <www.palisade.com/risk/default.asp>
- Bamforth, P B (1982)
Early-age thermal cracking in concrete
 Institute of Concrete Technology, Technical Note TN/2, Slough
- van Breugle, K and Lokhorst, S J (2001)
 “The role of microstructural development on creep and relaxation of hardened concrete”
 In: *Proc RILEM PRO 23, Early-age cracking in cementitious systems*, 1, Haifa, Israel, pp 3-10
- Browne, R D and Blundell, R (1973)
 “Early-age behaviour of mass concrete pours”
 In: Symposium on *Large pours for R C structures*, University of Birmingham, Paper 6, September 1973, pp 42-65
- CARES (2006)
 CARES Website/Technical Information/reinforcement tensile test results
 <www.ukcares.co.uk/index.htm>
- Concrete Society (2004)
In situ strength of concrete – An investigation into the relationship between core strength and the standard cube strength
Working party of the Concrete Society, Project Report No 3, BCA, Camberley, Surrey, ISBN 0 94669 186 X
- Domone, P L J (1974)
 Uniaxial tensile creep and failure of concrete
Magazine of Concrete Research, 26 (No 88), Sept 1974, pp 144-152
- Fan, S C, Aw, K M and Tan, Y M (2004)
 “Peak temperature-rise for early-age concrete under tropical climatic conditions”
Journal of the Institution of Engineers, Singapore, Vol. 44, Issue 1, 2004
- Harrison, T (1992)
Early-age thermal crack control in concrete
 R91, CIRIA, London
- Price, W F (2006)
Production data provided by Lafarge Cement
 Lafarge Cement UK, Manor Court, Chilton, Oxon
- Reinhardt, H-W and Rinder, T (1998)
 “High strength concrete under sustained tensile loading”
Otto-Graf-Journal, Vol 9, 1998, pp 123-134

Vitharana, V and Sakai, K (1995)

“Early-age behaviour of concrete sections under strain induced loadings”

In: Proc 2nd Int. Conf. on *Concrete under severe conditions CONSEC '95*, (eds: Satai, K, Banthai, N, and Gjorv, O E) Sapporo, Japan, 2-4 August 1995, pp 1571-1581

British Standards

BS 8007:1987 *Design of concrete structures for retaining aqueous liquids*

Euro Codes

EN1992-1-1:2004 *Eurocode 2. Design of concrete structures. General rules and rules for buildings*

A8 Controlling crack widths with reinforcement

A8.1 Specifying acceptable crack widths

The calculated crack widths using the equations to follow, represents the characteristic “average” crack width. This is the crack width that would occur if the cracks were uniformly distributed at the characteristic crack spacing and of equal width. However, recognising the in-situ variability of concrete, there is a probability that some individual cracks will be greater than the calculated value. EN1992-1-1 recognises the design crack widths as characteristic values and hence it is recommended that conformance be established on the basis of an analysis taken over the full length of a particular pour and an estimated characteristic crack width at the 95 per cent level. Individual cracks that exceed this value need not be considered as non-compliant in relation to either design or construction practice but should, nevertheless be repaired if considered detrimental to the performance of the structure.

A8.2 General principles of reinforcement design according to EN1992-1-1 and EN1992-3

To achieve a state of controlled cracking requires that there is sufficient reinforcement to accommodate the stress transferred to it from the concrete when a crack develops. To define this value, EN1992-1-1 uses the minimum area of steel $A_{s,min}$. This is equivalent to the critical steel ratio ρ_{crit} previously used by BS8007. $A_{s,min}$ is estimated from equilibrium between the tensile forces in the concrete just before cracking and the tensile force in the steel at yielding.

While achieving $A_{s,min}$ will ensure that cracking occurs in a controlled manner it does not guarantee that the maximum acceptable crack width will be achieved and neither does it guarantee that crack widths will be small. With an area of steel ratio marginally higher than $A_{s,min}$ the stress in the steel when a crack occurs will be, by definition, close to the yield strength, ie approaching 500 MPa. At this level of stress, the strain in the steel at the crack will be about $2500 \mu\epsilon$ (assuming that the steel has an elastic modulus of 200 GPa). This will reduce to a level close to the tensile strength of the concrete ($< 100 \mu\epsilon$) over a length which may be in the order of 1m (see Section A8.5.3). Over this length the mean strain will be about $1300 \mu\epsilon$. This is equivalent to a crack width of 1.3mm. In this case, to achieve a crack width of 0.3 mm would require that A_s is 4-5 times $A_{s,min}$.

It should be appreciated that achieving a state of controlled cracking does not automatically mean achieving small cracks. This is likely to require an area of reinforcement A_s that is substantially higher than $A_{s,min}$.

While EN1992-1-1 provides general design guidance (replacing BS8110:1985), EN1992-3 deals specifically with the design of liquid retaining and containment structures (replacing BS8007:1987) and Informative Annex M considers two specific cases of restraint:

- 1 M.2 (a) Restraint of a member at its end.
- 2 M.2 (b) A long wall restrained along one edge.

The latter is the more common form of restraint. In each case, the crack width, w_k , is calculated using Expression 7.8 in EN1992-1-1. This states, very simply, that the crack width w_k is equal to the maximum crack spacing $S_{r,max}$ multiplied by the restrained component of strain ($\epsilon_{sm} - \epsilon_{cm}$) according to the equation:

$$\text{Crack width} \quad w_k = S_{r,max} (\epsilon_{sm} - \epsilon_{cm}) \quad (\text{A8.1})$$

where:

ϵ_{sm} is the mean strain in the reinforcement

ε_{cm} is the mean strain in the concrete between cracks.

EN1992-3 deals with the calculation of crack width for these two cases (of end restraint and edge restraint) differently in relation to the method for estimating the term $(\varepsilon_{sm} - \varepsilon_{cm})$ (see Section A8.6.2 and A8.6.3).

- for the condition of continuous edge restraint $(\varepsilon_{sm} - \varepsilon_{cm})$ is assumed to be determined by the magnitude of the restrained strain. In this case the restraint itself contributes to the control of cracking by limiting the extent to which strain relief occurs in relation to the crack location
- for the condition of end restraint $(\varepsilon_{sm} - \varepsilon_{cm})$ is determined by the tensile strength of the concrete at the time at which the crack occurs. In this case the magnitude of restrained strain has no effect on individual crack widths, but may affect the number of cracks that occur.

An important difference between EN1992-1-1 and BS8007 is in the calculation of the area of steel. The approach of BS8007:1987 uses the same surface zone (half the thickness or 250 mm, whichever is smaller) to estimate values of both $A_{s,min}$ and A_s . The approach of EN1992-1-1 uses different values as follows:

- $A_{s,min}$ which is used to determine the minimum area of reinforcement is estimated using the area of concrete in the tensile zone, A_{ct} . In sections greater than about 800 mm, EN1992-1-1 leads to higher values of $A_{s,min}$
- A_s which is used in the calculation of crack spacing and crack width is estimated using $A_{c,eff}$ the effective area of concrete in tension surrounding the reinforcement. This is assumed to be 2.5 times the distance to the centroid of the steel. For sections thicker than about, with normal cover and bar sizes, this leads to a significantly smaller surface zone when using EN1992-1-1 and hence the requirement for less reinforcement compared with BS8007.

In each case, the reinforcement requirement derived using EN1992-1-1 differs from the value derived using BS8007. The impacts of these differences are discussed in Section A8.4 and A8.5.

EN1992-2 deals with the design of bridges and refers to EN1992-1-1 for crack width design. The only additional requirement is that when estimating the crack width due to shrinkage, the tensile strength should not be assumed to be less than 2.9 MPa. This value is achieved by a C30/37 concrete after 28 days. As shrinkage occurs over the long term, and concrete used in bridge construction will generally be at least strength class C30/37, this requirement should be met without modification to the general approach of EN1992-1-1.

A8.3 Minimum reinforcement area

In order that cracking is controlled, the minimum area of reinforcement $A_{s,min}$ is required. Informative Annex M of EN1992-3 deals with “*Calculation of crack widths due to restraint of imposed deformations*” and refers to Clause 7.3.2 of EN1992-1-1 for estimation of $A_{s,min}$. The equation for calculating $A_{s,min}$ is as follows:

$$A_{s,min} \sigma_s = k_c k_{f_{ct,eff}} A_{ct} \quad (\text{A8.2})$$

where:

- $A_{s,min}$ is the minimum area of reinforcing steel within the tensile zone
- A_{ct} is the area of concrete within the tensile zone. The tensile zone is that part of the section which is calculated to be in tension just before formation of the first crack
- σ_s is the absolute value of the maximum stress permitted in the reinforcement after formation of a crack (usually taken as the yield strength of the steel f_{ky})

$f_{ct,eff}$ is the mean value of the tensile strength of the concrete effective at the time when the cracks may first be expected to occur, $f_{ctm}(t)$. For early-age thermal cracking the mean 3-day value $f_{ctm}(3)$ is used and for long term cracking the mean 28-day value is used, These are derived using the relationship with compressive strength age the age function provided in Section 3.1.2 of EN1992-1-1 and have been shown to be acceptable safe for estimating $A_{s,min}$ (see Appendix A10). Estimated values are as follows:

Strength class	C20/25	C25/30	C30/37	C35/45	C40/50	C45/55	C50/60	C55/67	C60/75
$f_{ctm}(3)$ (MPa)	1.32	1.53	1.73	1.92	2.10	2.27	2.44	2.52	2.61
$f_{ctm}(28)$ (MPa)	2.21	2.56	2.90	3.21	3.51	3.80	4.07	4.21	4.35

- k is a coefficient which allows for “the effect of non-uniform self-equilibrating stresses, which lead to a reduction in restraint forces”
- =1.0 for webs with $h \leq 300\text{mm}$ or flanges with widths less than 300mm
- =0.65 for webs with $h \geq 800\text{mm}$ or flanges with widths greater than 800mm
- intermediate values may be interpolated
- k_c is a coefficient which takes account of the stress distribution within the section immediately prior to cracking and the change of the level arm. For pure tension $k_c = 1.0$.

For sections less than 300 mm thick which are in direct tension both k and $k_c = 1$ and equation A8.2 reduces to:

$$A_{s,min} = \frac{f_{ct,eff}}{f_{ky}} A_{ct} \quad (\text{A8.3})$$

where A_{ct} is the gross section area. The ratio $f_{ct,eff}/f_{ky}$ is what was referred to in BS8007 as ρ_{crit} .

A8.4 Surface zones for estimating $A_{s,min}$

A8.4.1 Background to UK practice (BS8007)

BS8007 is very specific in the definition of the surface zone used to determine the minimum area of reinforcement (previously defined as ρ_{crit}) and the steel ratio used in the calculation of crack spacing. For walls < 500 mm thick, the gross section is used and for thicker sections a 250 mm surface zone is assumed. For ground slabs the same applies to the top face but the bottom face steel is reduced to 100 mm except in slabs < 300mm thick, where it is omitted. These values were used both in the estimation of the critical steel ratio ρ_{crit} associated with $A_{s,min}$ and in the design of reinforcement to control crack widths. The argument for this approach was that practice had shown that taking the gross-cross sectional area of sections thicker than 500 mm was both uneconomic and unnecessary for the control of surface crack widths. However, the author has witnessed cracking in thick sections (500-1000 mm) in which crack widths have been in excess of those predicted using the 250 mm zone of influence, even though the concrete has performed predictably in terms of temperature rise and thermal strain. This cracking behaviour was consistent either with insufficient steel or with the steel provided not acting effectively; and no specific reasons could be found for the latter.

A review of the background to the development of the approach of BS8007 was undertaken, therefore, to understand the basis for the zones of influence in relation to the way in which cracking develops during the early thermal cycle.

It is made very clear in BS8007 that when calculating ρ_{crit} the concrete section A_c is based on, “the gross concrete section required to distribute the cracking, “concrete section” being the surface zones

given....etc (eg $h/2$ or 250 mm whichever is smaller).” The intent of using zones of influence is to avoid wasteful reinforcement in areas that are not in tension. When an element is subjected to bending, or where the thermal stresses are caused by temperature differentials which generate tension at the surface and compression in the core, this approach is rational. Indeed, the handbook to BS5337 (the forerunner to BS8007 and the code within which the surface zones were proposed) states that “*The development of cracking in thick walls, however, is progressive from the surface and this fact can be utilized to effect economies in reinforcement*” ie when cracking is caused by thermal gradients or bending (Anchor,1979) The handbook adds further that “*Once the cracks have developed in the surface they can extend into the core, as the latter cools, without the need for additional distribution reinforcement*”. (Note that the principal applies to both walls and slabs. The handbook states that “*The Code extends the surface zone concept to ground slabs of all thicknesses*”).

These statements make it very clear that the surface zone concept is applicable only when cracking is initiated at the surface and when only that part of the concrete is in tension. It may not be applicable to members or parts of members that are externally restrained to the extent that the whole of the section is in tension.

The confusion may be due, at least in part, to the fact that BS8007 is concerned primarily with control of cracking which occurs as a result of external restraint to cooling, while tension in the surface develops due to internal restraint during the heating phase of the temperature cycle. Furthermore, one of the design assumptions in BS8007 is that the compressive stresses generated during heating are fully relieved by creep. If this were the case then the tensile stresses at the surface associated with the compressive stresses generated in the centre would also be relieved. And finally, because the centre of a section achieves the higher temperature it will be subjected to greater contraction than the surface. During cool down cracking is therefore most likely to be initiated at the centre where the tensile stresses are greatest as shown in Figure A8.1 and not at the surface, as assumed by BS8007.

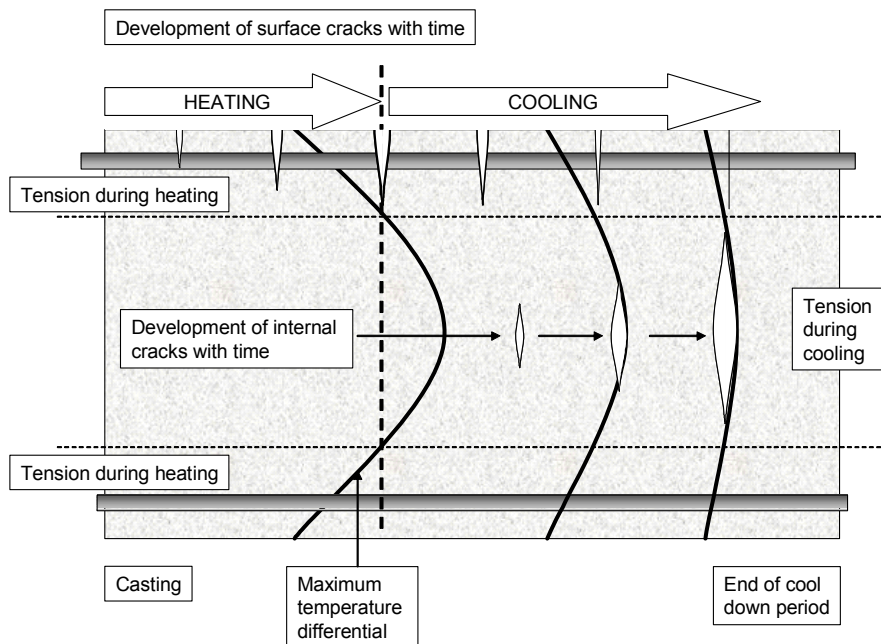


Figure A8.1 Section through a thick wall close to the joint where external restraint is high

A8.4.2 The approach of EN1992-1-1

In the calculation of $A_{s,min}$ EN1992-1-1 uses the coefficients k_c and k applied to the area of concrete in tension. This has been described in Section A8.3 and equation A8.2 may be rearranged as follows;

$$A_{s,min} = k_c k A_{ct} \frac{f_{ct,eff}}{f_{ky}} = (k_c k A_{ct} \rho_{crit}) \quad (A8.4)$$

A_{ct} represents the area of concrete in tension and the coefficients k_c and k are described in Section A8.3. For concrete in pure tension $k_c = 1$ and k varies with section thickness. To enable comparison with BS8007, the coefficients k_c and k may be considered as “area reduction factors”. When applied to A_{ct} this is equivalent to defining surface zones which are close to those required by BS 8007 up to a section thickness of about 800 mm, as shown in Figure A8.2. However, EN1992-1-1 requires significantly higher values for thicker sections. The difference is such that in a 1000 mm section the surface zone is about 25 per cent greater than that required by BS8007 and the difference increases in thicker sections. This leads to a higher value of $A_{s,min}$ being required by EN1992-1-1 in sections thicker than 800mm and subjected to external restraint. If the approach of BS8007 is correct, then design to EN1992-1-1 could result in a significant waste of steel. However, if the converse is true, the use of BS8007 may have resulted in under-design and subsequent uncontrolled cracking. This may be an explanation for cracking observed by the author in thick sections, subject to external restraint, that was in excess of that specified and predicted by the design process of BS8007.

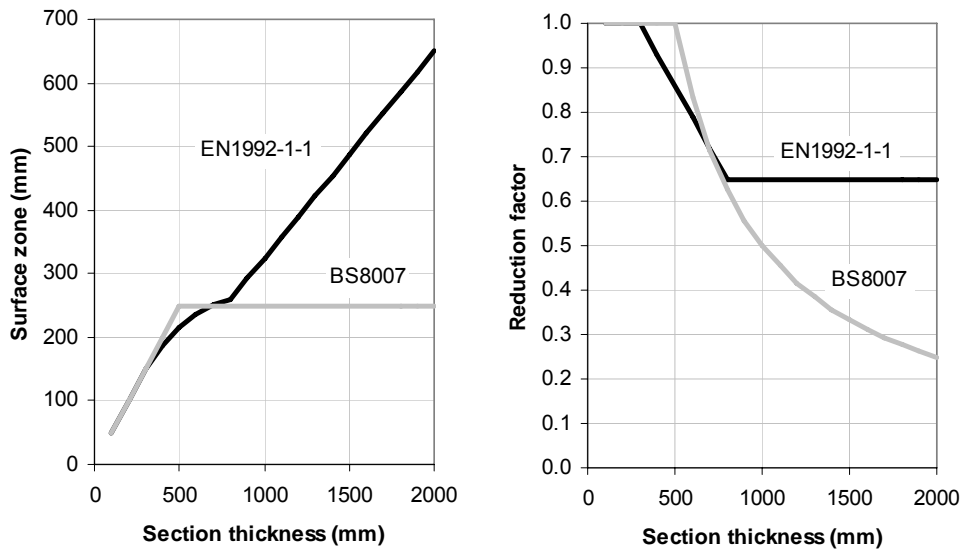


Figure A8.2 Surface zones (applicable to each face) and the area reduction factor

The Designers’ Guide to EN1992-1-1 and EN 192-1-2 (Naryanan and Beeby, 2005) makes it very clear that the factor k is based on the assumption that cracking is initiated by higher strains generated at the surface, stating that... “These effects (of restrained deformations) do not occur uniformly throughout the section, occurring more rapidly at the member surface. As a result, deformations at the surface concrete will be restrained by the interior concrete, and higher tensions will be developed near the surface”. The basic assumptions behind the approach of EN1992-1-1 are therefore consistent with those of BS8007; namely, that cracking will propagate from the surface where tension is highest.

However, as shown in Figure A8.1, it is more likely that during cool down, cracking will be initiated at the point where the temperature drop is the greatest, ie at the centre of the section. Once such a crack is initiated it is likely to propagate rapidly as, generally, there is no reinforcement at the centre of the section. The area of uncracked concrete will therefore diminish rapidly, transferring more tensile stress to the remaining uncracked section and eventually to the reinforcement. In such circumstances it would seem inappropriate to assume either that only the surface zone will be in tension or that cracking will initiate at the surface. Furthermore, all of the section may have been in tension prior to cracking and if this was the case then all of the tensile stress would be transferred to the steel.

Both BS8007 and EN1992-1-1 have used an effective surface zone principle for estimating the minimum area of reinforcement. This may be appropriate for members subjected predominantly to internal restraint within which tension develops only in the surface zone. However, within members that are subjected predominantly to external restraint all of the section may be in tension during cool down and cracking may be initiated at the centre where the drop in temperature, and hence the tensile stress, is highest. In this case, the surface zone concept may not be appropriate for estimating the minimum area of reinforcement and could lead to uncontrolled cracking.

A8.4.3 Members dominated by external restraint

Further consideration of the situation in which a thick section is subjected to external restraint may enable a reduction from the full thickness to be used when estimating the minimum area of reinforcement. In the design process, the thermal contraction is derived using the peak temperature. However, it will be the average tensile stress that is developed that will be transferred to the steel. This will be determined by the average temperature drop and the resulting thermal contraction of the section. A typical parabolic temperature distribution is illustrated in Figure A8.3 for a 700 mm thick section with a peak temperature of 65 °C and a differential of 25 °C.

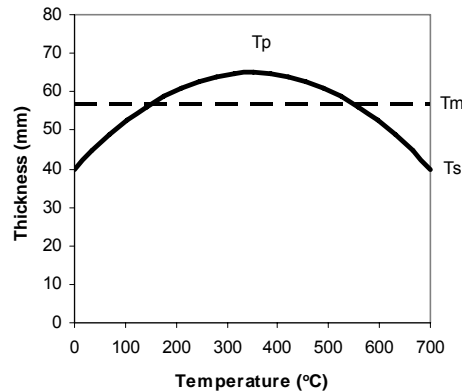


Figure A8.3 Parabolic temperature distribution through a 700mm thick wall

It can be seen that the mean temperature through the section is about 57 °C, about 8 °C below the peak value of 65°C. As a general rule, the mean of a parabola is 2/3 of its height, hence:

$$T_m = T_p - (T_p - T_s)/3 \quad (\text{A8.5})$$

A reduction factor $k_{t1} = (T_m - T_a)/T_1$ may be applied, therefore, to take account of the difference between the peak temperature and the mean temperature through the section. This reduction factor will be dependent on both the peak temperature and the differential from the centre to the surface and shown in Figure A8.4.

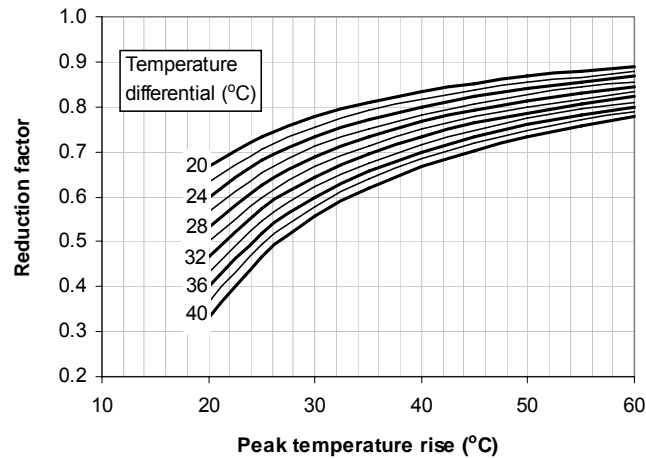


Figure A8.4 Proposed reduction factor k_{t1} to take account of the difference between the peak and the mean temperature

Comparisons of values obtained using this approach and those obtained using the reduction factor, k , recommended by EN1992-1-1 are shown in Figures A8.5 and A8.6. These are presented as both surface zones (for each face) and reduction factors and have been estimated for sections in which the centre to surface temperature differential is 20 °C and 30 °C respectively. In each case it is assumed that external restraint is sufficient to achieve tension through the thickness of the member and hence the surface zones are based on the gross section.

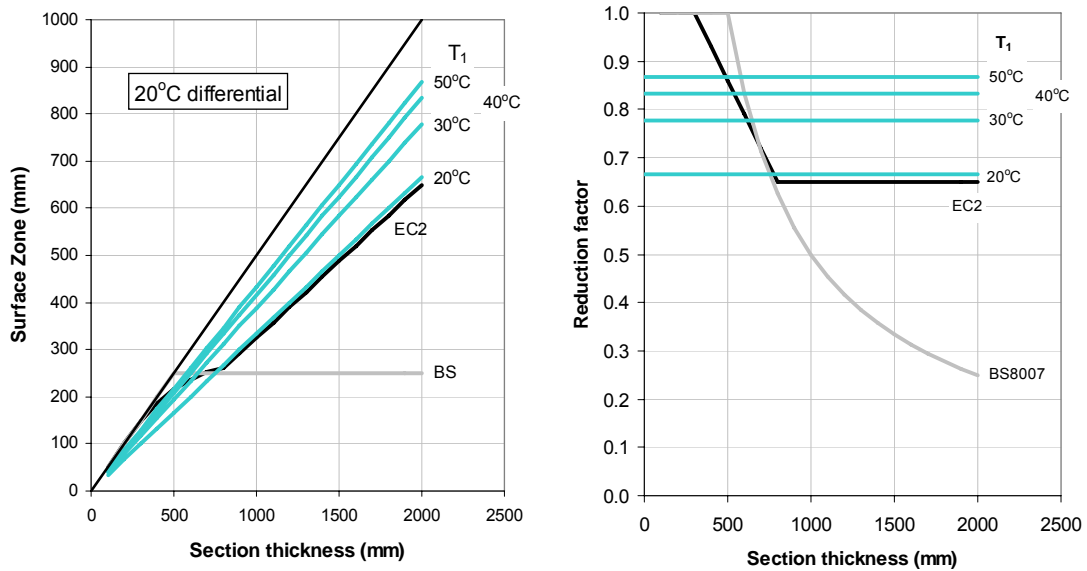


Figure A8.5 Surface zones of influence reduction factors in relation to the section thickness and temperature rise when the temperature differential is 20 °C

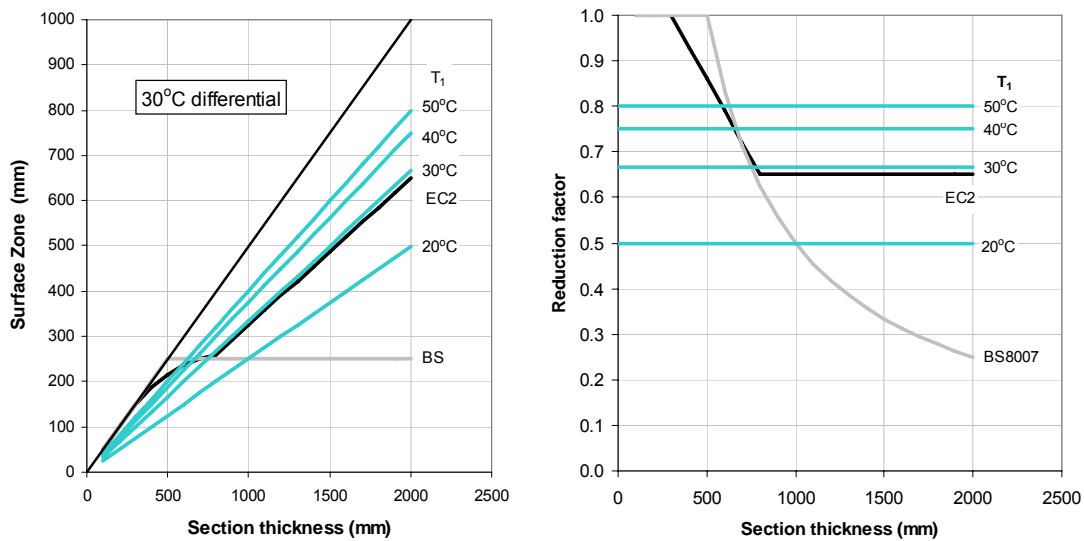


Figure A8.6 Reduction factors and zones of influence in relation to the section thickness and temperature rise when the temperature differential is 30 °C

It can be seen that by limiting the temperature differential to only 20 °C, the surface zone in very thick sections is generally higher than that recommended by EN1992-1-1 unless T_1 is relatively low (only 20 °C).

By permitting an increase in the allowable temperature differential where appropriate (ie when using concrete with a low coefficient of thermal expansion or where external restraint limits the development of strain differentials) a lower reduction factor can be allowed, thus achieving greater economies in reinforcement design.

In addition to using the peak rather than the mean temperature in the design process, it is also assumed that tensile stresses are developed as soon as the concrete starts to cool. This is again a conservative assumption. There is considerable evidence from stress rig measurements under laboratory conditions that compressive stresses (sometimes in excess of 1 MPa) may be generated and should be relieved before tensile stresses develop (Blundell and Bamforth, 1975, Kanstad *et al*, 2001, van Breugel and Lokhorst, 2001, van Beek *et al*, 2001, Pane and Hansen, 2002). A review of these data indicates that the temperature drop required to relieve the compressive stresses may vary between 10 and 30 per cent of the temperature drop T_1 and is typically in the range for 2 to 6 °C. An additional coefficient, k_{t2} (having a value in the range 0.7 to 0.9) may be applied, therefore, to the area reduction factors shown in Figure A8.4.

Based on the above analysis, equation (A.8.5) may be revised as follows:

$$A_{s, min} = k_c k_{t1} k_{t2} A_{ct} \frac{f_{ct, eff}}{f_{ky}} \tag{A8.6}$$

where:

k_{t1} is a coefficient which accounts for the difference between the peak temperature drop and the mean temperature drop (with values in the range from 0.5 to 0.9 in sections in which the temperature differential does not exceed 30 °C as shown in Figure A8.4)

k_{t2} is a coefficient which accounts for the fact that some compressive stresses should be relieved by a drop in temperature before tensile stress are generated (with a value in the range from 0.7 to 0.9).

The coefficients k_{t1} and k_{t2} may be combined into the single coefficient k . For those conditions in which early-age thermal cracking is most likely (ie sections with the higher temperature rise) k_{t1} is typically in the higher end of the range from 0.8 to 0.9. Combining this with a conservative value of k_{t2} also in the upper end of the range from 0.8-0.9, leads to a value of $k = 0.75$ which has only a 5 per cent chance of being exceeded.

It is recommended, therefore, that for sections thicker than 800 mm the coefficient $k = 0.75$ replaces the value 0.65 recommended by EN1992-1-1 in the calculation of $A_{s,min}$. Hence,

$$k = 1.0 \text{ for webs with } h \leq 300\text{mm or flanges with widths less than } 300 \text{ mm}$$

$$k = 0.75 \text{ for webs with } h \geq 800\text{mm or flanges with widths greater than } 800 \text{ mm}$$

Intermediate values may be interpolated.

As the whole section is in tension, to calculate the minimum area of reinforcement on each face, A_{ct} is taken as the area associated with $0.5 \times$ the full section thickness.

A comparison of the values obtained using this expression, expressed as an equivalent surface zone are shown in Figure A8.7 compared with those of the existing recommendations of EN1992-1-1 and BS8007.

In section with a thickness > 600 mm the increase in the effective surface zone will result in a requirement for an increase in A_s compared with the requirements of BS8007.

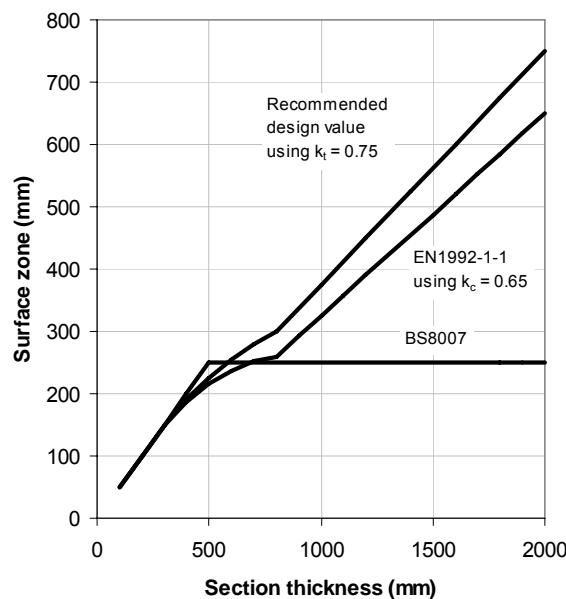


Figure A8.7 *Surface zones used in estimating $A_{s,min}$ in sections that are dominated by external restraint and subject to tension through the full thickness*

A8.4.4 Members within which internal restraint is dominant

When internal temperature differentials become the dominant form of restraint the stress distribution may be considered to be the same shape as the temperature profile through the section. Measurements (Bamforth, 1978) have shown that the temperature profiles generally approximate to a parabola as shown in Figure A8.8.

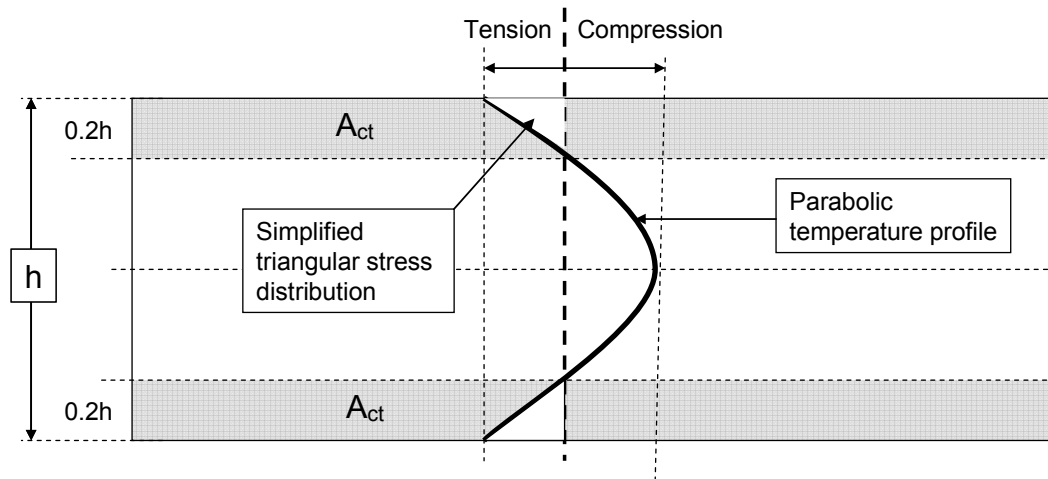


Figure A8.8 Simplified stress distribution used to determine the coefficient k_c for a member subjected to a temperature profile

In this stress condition, equilibrium requires that after cracking the tensile force in the concrete is carried by the reinforcement. The stress distribution in the tensile zone at the surface is approximately triangular and hence the coefficient k_c (which takes account of the stress distribution) may be taken as 0.5.

It would be sensible to adopt a conservative value of $k = 1$ as, in this case, the coefficient k_c as the coefficient k has already taken account of the self-equilibrating stresses. Equation A8.4 may be simplified to:

$$A_{s, min} = 0.5 A_{ct} \frac{f_{ct, eff}}{f_{ky}} \tag{A8.7}$$

With the assumed parabolic distribution shown in Figure A8.8, the tensile zone at the surface may be assumed to be approximately 20 per cent of the thickness ($= 0.2h$). On this basis, the surface zones derived using equation A8.7 are shown in Figure A8.9 compared with the previous requirements of BS8007. It is apparent that for conditions in which internal restraint is dominant, the surface zone (and hence the estimated value of $A_{s, min}$) is significantly lower when estimated using EN1992-1-1 than that previously required by BS8007 for section thicknesses up to about 1250 mm. For thicker sections EN1992-1-1 leads to higher values of surface zone and $A_{s, min}$.

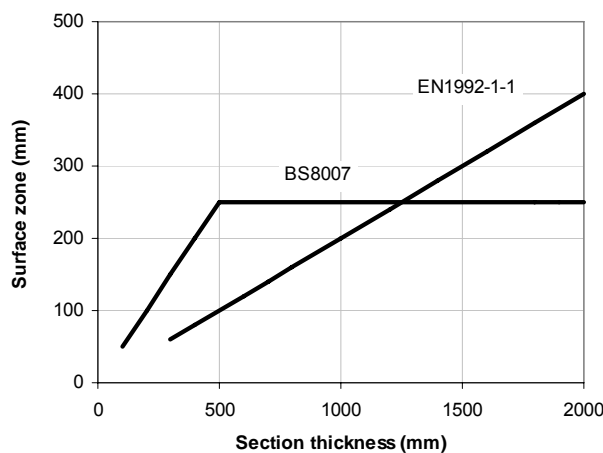


Figure A8.9 Surface zones used in estimating $A_{s, min}$ in sections that are dominated by internal restraint

A8.4.5 Summary of coefficients for estimating $A_{s,min}$

Based on the above analysis, the recommended values for use in the estimation of $A_{s,min}$ are given in Table A8.1. It is normal to estimate the area of steel on each face and this is reflected in the values for surface zone representing the area of concrete in tension.

Table 8.1 Coefficients used in the estimation of $A_{s,min}$ for different restraint conditions

		EXTERNAL restraint dominant	INTERNAL restraint dominant
Coefficient	k_c	1.0	0.5
Coefficient	k	= 1.0 for $h < 300\text{mm}$ = 0.75 for $h \geq 800\text{mm}$ intermediate values are interpolated	1.0
Surface zone representing the area of concrete in tension. Section thickness = h	h	Full section thickness ($0.5h$)	20% of section thickness ($0.2h$)

A8.5 Crack spacing

A8.5.1 The general equation

The maximum crack spacing $S_{r,max}$ is defined by expression 7.11 of EN1992-1-1 for situations where reinforcement is fixed at reasonably close centres $\leq 5(c + \varphi/2)$ as follows;

$$S_{r,max} = k_3 c + k_1 k_2 k_4 \frac{\varphi}{\rho_{p,eff}} \quad (\text{A8.8})$$

where:

- φ is the bar diameter
- c is the cover to the longitudinal reinforcement
- k_1 is a coefficient that takes account of the properties of bonded reinforcement. This is related to (but not equal to) the term f_{ct}/f_b used previously in CIRIA R92, 1992 and in BS8007. The EN1992-1-1 recommended value is 0.8
- k_2 is a coefficient that takes account of the distribution of strain.
 - = 1.0 for pure tension
 - = 0.5 for bending
- k_3 Recommended value of 3.4 to give a characteristic value of crack spacing (NDP)
- k_4 Recommended value of 0.425 to give a characteristic value of crack spacing (NDP)
- $\rho_{p,eff} = (A_s + \xi_1^2 A_p) / A_{c,eff}$
with reinforcement only (ie no prestress) $\rho_{p,eff} = A_s / A_{c,eff}$

$A_{c,eff}$ is the effective area of concrete in tension surrounding the reinforcement to a depth $h_{c,ef}$, where $h_{c,ef}$ is the lesser of $h/2$ or $2.5(h-d)$ as shown in Figure A8.10.

A8.5.2 The steel ratio used in calculating crack spacing, $\rho_{e,eff}$

The crack spacing estimated using equation A8.8 is generally in the order of 60-80 per cent of the value predicted using BS8007. This is due, principally, to the difference in the surface zones used in the calculation of the steel ratio. EN1992-1-1 derives $\rho_{p,eff}$ using the effective area of concrete in tension surrounding the reinforcement $A_{c,eff}$ based on the surface zone to a depth of $h_{e,ef} = 2.5(c + \phi/2)$ as shown in Figure A8.10, while the surface zone used by BS2007 is $h/2$ or 250 mm whichever is smaller.

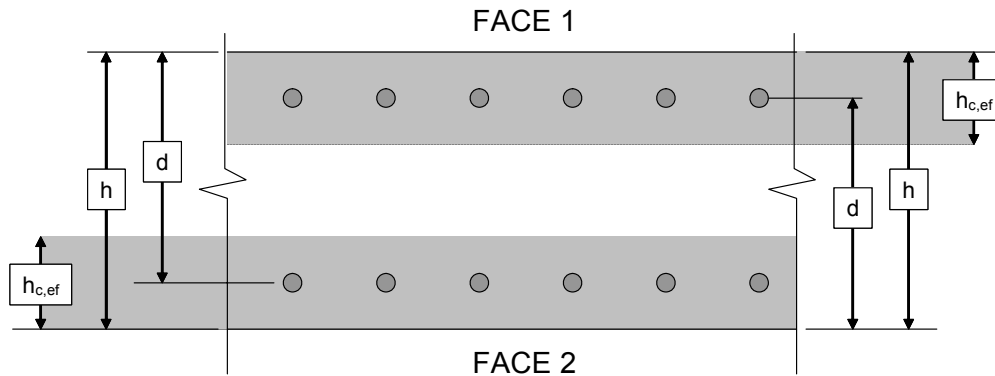


Figure A8.10 Parameters used in estimating the effective area of concrete in tension $A_{c,eff}$

Consider a 500 mm thick wall. With a typical cover depth of 40 mm and using 20 mm diameter bars, $h_{e,ef} = 125$ mm, only half the value of 250 mm used by BS8007. As the value of $\rho_{p,eff}$ is inversely proportional to $h_{e,ef}$ the use of a lower value by EN1992-1-1 will result in the steel ratio $\rho_{p,eff}$ being double the value used by BS8007, thus halving the value of the second term in equation A8.8. While this is partially offset by the first term which is related to cover, the effect is for values of early-age crack spacing estimated using EN1992-1-1 to be 20-40 per cent lower than values estimated using BS8007 and hence for the estimated crack width (see Section A8.6) to be lower also. With no other changes this would lead to a significant reduction in crack control reinforcement compared with that currently used.

Observations of early-age cracking suggest that the requirements of BS8007, while having been generally applicable, have occasionally led to crack spacing and crack widths in excess of those predicted and on this basis it would be unsafe to adopt a design that significantly reduces the current reinforcement requirements. Other factors have therefore been investigated to determine which factors may be most influential, in particular k_f (Section A8.13).

A8.5.3 Crack formation

Equation A8.8 has been developed on the assumption that the crack spacing is determined by the extent of bond slip between the steel and the concrete. The concrete is free to contract at the cracks, but as the bond increases, more and more of the potential concrete contraction becomes restrained as shown in Figure A8.11.

Consider the first crack which will occur within the region of highest restraint and at the location where the concrete has the lowest strain capacity (determined by normal variability). When the crack occurs, the strain in the immediate vicinity of the crack is relieved over a distance of S_0 . Within this zone the strain in the concrete can no longer exceed the strain capacity hence S_0 represents the minimum crack spacing. However, as the restraint is uniform over the length of the member (except close to the ends where it reduces), a high level of restrained strain will remain in the section beyond S_0 from the crack. A second crack will then occur at the next weakest location. If the second crack is within a distance of $2S_0$ from the first crack no intermediate cracks can occur as the restrained strain between these two cracks is relieved to the extent that the tensile strain capacity of the concrete cannot be exceeded. This is shown in

Figure A8.11a. However, if the second crack occurs at a distance of more than $2S_0$, there will remain, between the cracks, a zone within which there is still restrained strain that exceeds the strain capacity and further intermediate cracks may develop as shown in Figure A8.11b.

With sufficient restrained strain, the crack pattern will therefore form quickly and subsequent long term thermal contraction and shrinkage will cause the existing cracks to open rather than new cracks to form.

A8.5.4 The derivation of the equation for S_0

Consider, for simplicity, a restrained member with a cross sectional area, A_c , that is shrinking uniformly. After the first crack, the second crack may develop when the bond force between the steel and concrete exceeds the tensile capacity of the concrete, ie when:

$$f_b S_0 \pi \phi \geq f_{ct} A_c \quad (\text{A8.9})$$

where:

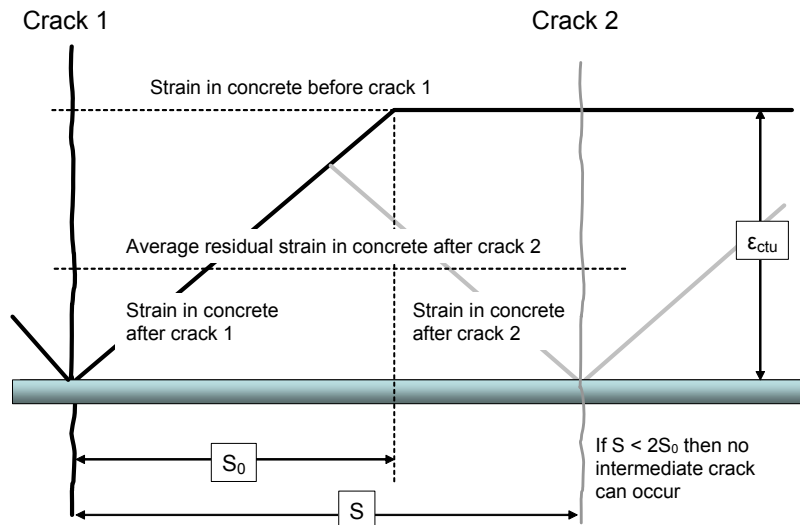
f_b is the bond stress

S_0 is the length of bar required to develop a stress in the concrete that is just equal to its tensile strength

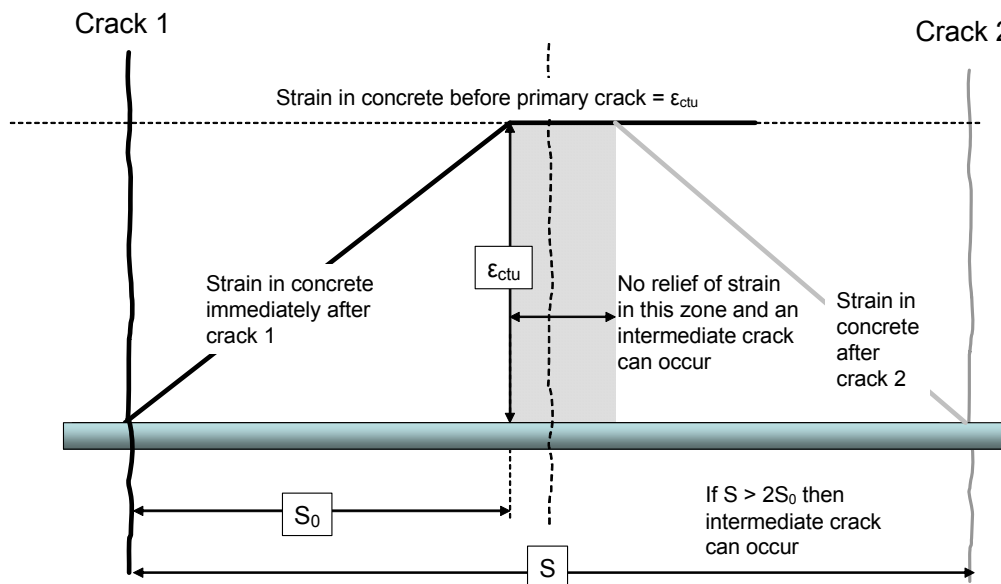
f_{ct} is the tensile strength of the concrete

Substituting for the effective steel ratio, $\rho = A_s / A_c = \pi \phi^2 / 4 A_c$ in Equation (A8.9) and rearranging gives:

$$S_0 = \frac{f_{ct} \phi}{f_b 4 \rho} \quad (\text{A8.10})$$



(a) 2nd crack forms within 2S₀ of 1st crack



(b) 2nd crack forms beyond 2S₀ from 1st crack, allowing intermediate crack to occur

Figure A8.11 The distribution of restrained contraction and the formation of cracks

The equality sign gives the minimum distance, S_0 , needed for the restrained contraction to equal the tensile strain capacity and therefore no secondary crack forms within S_0 . If crack 2 occurred at $2S_0$, the restrained strain at mid-span would just equal the tensile strain capacity of the concrete, so that any intermediate crack would not occur. At a crack spacing greater than $2S_0 = S_{r,max}$ the mid-span restrained strain could exceed the tensile strain capacity, and an intermediate crack could occur. Therefore, for a fully developed crack pattern, the crack spacing is between:

$$\frac{f_{ct}\phi}{f_b 2\rho} \geq S \geq \frac{f_{ct}\phi}{f_b 4\rho} \tag{A8.11}$$

$$\text{and } S_0 = \frac{f_{ct}\phi}{f_b 4\rho} \quad (\text{A8.12})$$

EN1992-1-1 uses the coefficient k_l to represent the relationship between tensile strength of the concrete and the bond strength. In addition, the crack spacing is presented as the mean value S_{rm} and equation A8.12 becomes:

$$S_{rm} = 0.25 \frac{k_l \phi}{\rho} \quad (\text{A8.13})$$

According to Beeby (1990) the mean crack spacing S_{rm} is not $1.5S_0$ as might be expected, but $1.33S_0$. In addition, the recommended value of the coefficient k_l is 0.8. To make the conversion from equation A8.12 to A8.13, implies therefore, that the assumed value of f_{ct}/f_b should have been $0.8/1.33 = 0.6$. This is marginally lower than the value of 0.67 previous used by BS8007, but it consistent with recent research (Sule, 2003) as shown in Figure A8.12 (Section A8.5.5).

EN1992-1-1 has also introduced an additional term for cover c which takes account of studies which have shown a better agreement with test results (Naryanan and Beeby, 2005). This leads to the expression,

$$S_{rm} = 2c + 0.25 \frac{k_l \phi}{\rho} \quad (\text{A8.14})$$

EN1992-1-1 then gives the maximum crack spacing $S_{r,max}$ using a characteristic value with only a 5 per cent chance of being exceeded. This is assumed to be 1.7 times the mean value. However, assuming that $S_{rm} = 1.33S_0$ this would lead to a characteristic crack spacing that is $1.33S_0 \times 1.7 = 2.26S_0$. It may seem surprising that the characteristic crack spacing exceeds the theoretical maximum spacing of $2S_0$. However, Beeby (1990) reasons that this is due to the fact that S_0 varies for each individual crack, depending on the rate at which stress can be transferred from the reinforcement to the concrete. This is highly variable, hence both the minimum and the maximum crack spacing may vary about their theoretical values.

Applying the multiplier of 1.7 gives the equation for maximum crack spacing.

$$S_{r,max} = 3.4c + 0.425 \left(\frac{k_l \phi}{\rho_{p,eff}} \right) \quad (\text{A8.15})$$

This is the same as equation A8.8 (expression 7.11 in EN1992-1-1) with numerical values of the coefficients k_3 and k_4 applied. The coefficient k_2 is 1 for direct tension and hence also applies for this condition.

Equation A8.15 only applies when the area of reinforcement A_s exceeds the minimum area of reinforcement $A_{s,min}$. In general, when the reinforcement is checked, if $A_{s,min}$ is not exceeded the area of steel would be increased. However, clause 7.3.4 (5) of EN1992-1-1 draws attention to the fact that, for walls subjected to early thermal contraction, if the designer chooses to use an amount of steel that does not exceed $A_{s,min}$ then $S_{r,max}$ is given as 1.3 times the wall height. For a 4 m high wall the maximum crack spacing is assumed to be 5.2m, this being broadly consistent with practice.

A8.5.5 The influence of bond strength

EN1992-1-1 provides information on bond in relation to anchor lengths. The ultimate bond stress is given by the equation,

$$f_{bd} = 2.25 \eta_1 \eta_2 f_{ctd} \quad (\text{A8.16})$$

where:

f_{bd} is the ultimate (design) bond stress

f_{ctd} is the design tensile strength defined as:

$$f_{ctd} = \alpha_{ct} f_{ctk,0.05} / \gamma_c$$

where γ_c is the partial safety factor for concrete = 1.5

α_{ct} is a coefficient taking account of long-term effects on the tensile strength and unfavourable effects resulting from the way the load is applied = 1 (NDP)

η_1 is a coefficient related to the quality of the bond condition and the position of the bar during concreting

= 1.0 for condition of good bond

= 0.7 for all other cases and for bars in structural elements built with slipforms

η_2 is related to bar diameter

= 1.0 for $\phi \leq 40$ mm (NDP)

= $(140 - \phi) / 100$ for $\phi > 40$ mm

Rearranging equation A8.16 and substituting for f_{ctd} , for good bond

$$\frac{f_{ctk,0.05}}{f_{bd}} = \frac{\gamma_c}{2.25 \alpha_{ct} \eta_1 \eta_2} = \frac{1.5}{2.25} = 0.67 \quad (\text{A8.17})$$

This is the value that has been used in the expression for crack spacing in BS8007 and would be applicable where it could be demonstrated that good bond would be achieved.

The review of the development of the expression for crack spacing indicated that this value has been reduced to 0.6 in EN1992-1-1, but includes an addition factor of 1.33, this being the ratio of the mean to minimum crack spacing (see Section A8.5.4).

Additional support for the value of 0.6 was provided in a laboratory study on the effect of reinforcement on early-age cracking (Sule, 2003). In this study the ratio of tensile strength to bond strength was found to reduce from a value of about 0.6 with increasing compressive strength (Figure A8.12). This behaviour is consistent with the bond strength being related more closely to the compressive strength of the concrete and might be explained if the bond slip is initially influenced by the bearing of the lugs against the concrete. As the ratio of tensile to compressive stress reduces with increasing strength to a greater extent than the ratio of bond strength to compressive strength, the ratio of tensile strength to bond strength would be expected to reduce also.

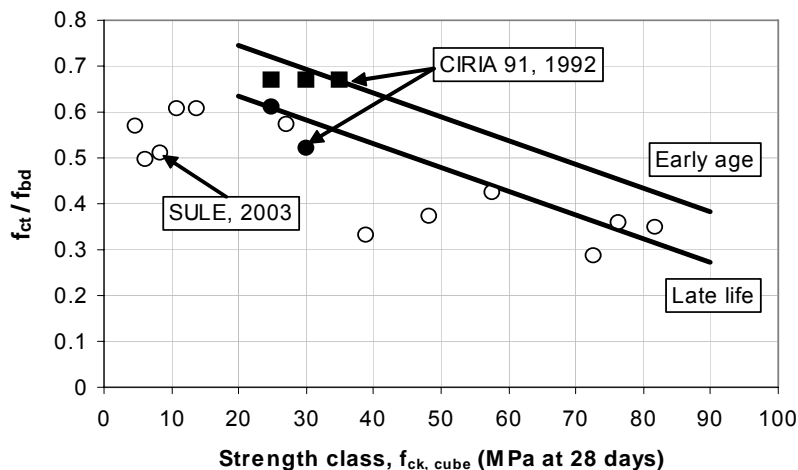


Figure A8.12 The ratio f_{ct}/f_b in relation to cube strength and age for bond stress at 0.05 mm slip

These results in Figure A8.12 indicate that it might be acceptable to reduce the f_{ct}/f_b ratio for concrete of a higher strength class. This would result in a reduced crack spacing and crack widths. However, used in conjunction with the change in the surface zone used to estimate the steel ratio, which already leads to a significant reduction in reinforcement requirements compared with BS8007, this could result in levels of reinforcement that are only about half those presently used.

Observations of early-age cracking suggest that the requirements of BS8007, while having been generally applicable, have occasionally led to crack widths in excess of those predicted. On this basis it would be unsafe to adopt a less robust design that significantly reduces the current reinforcement requirements.

Further consideration has therefore been given to the k_1 factor used in EN1992-1-1. The general assumption is that good bond is achieved around the whole bar perimeter. In addition, the data used in generating the expression for crack spacing have been derived from laboratory tests where this can be achieved. *In situ*, the achievement of good bond around horizontal bars may be more difficult, even with accepted good practice in placing the concrete. A common occurrence is for bleed water to accumulate below reinforcement resulting in a weak layer, and sometimes forming an air gap when the bleed water is reabsorbed into the concrete. In such cases it would be appropriate to apply the factor of 0.7, assuming that good bond cannot be guaranteed. The effect of this would be to offset the used of the reduced surface zone.

It is recommended, therefore, that k_1 should be increased to $0.8/0.7 = 1.14$ (this is effectively increasing the f_{ct}/f_b component of k_1 to $0.6/0.7 = 0.86$) until experience with the application of the approach of EN1991-1-1 to early-age thermal cracking indicates that a lower value is acceptable.

A8.6 Crack width

A8.6.1 The requirements of EN1992-3

With regard to the calculation of crack width, EN1992-3 considers two specific conditions;

- 1 Restraint of a member at its end.
- 2 A long wall restrained along one edge.

These conditions differ in the way in which cracks are formed and the influence of the cracks on the distribution of stresses within the element. Condition b), may also be applied to adjacent pours in a slab, where the edge restraint occurs along the joint. It is important to understand the nature of restraint as the resulting crack widths may differ significantly.

A8.6.2 Member restrained at its ends

In terms of the process of cracking, the differences between these two cases of restraint are discussed by Beeby and Forth (2005).

The underlying principles for crack control to BS8007 have been based on consideration of the forces in a fully restrained concrete specimen with a single central reinforcing bar. This method assumed that all possible cracks occur at once and that the crack width is proportional to the restrained component of strain. However, more recent investigations have shown these assumptions to be incorrect, with cracking occurring progressively. Beeby and Forth (2005) describe the process as follows:

1. The restrained strain increases until the tensile stress reaches the tensile strength of the concrete and the first crack forms.
2. The cracks results in a reduction in the stiffness of the member and a reduction in stress along its entire length.

3. Further increase in the restrained strain causes the first crack to widen and an increase in stress until the stress again reaches the tensile strength of the concrete, forming the second crack and again there is a reduction in stiffness and stress in the concrete. Note that, as the first crack will occur at the weakest point, progressively higher stress may be needed to induced subsequent cracks.
4. This process continues, as shown in Figure A8.13, until there is no further increase in restrained strain. If sufficient restrained strain is developed the stabilized crack phase is established, beyond which further restrained strain will simply cause the existing cracks to widen. However, the magnitude of restrained strain to achieve this state is about $1000 \mu\epsilon$ and this is unlikely to occur in practice.

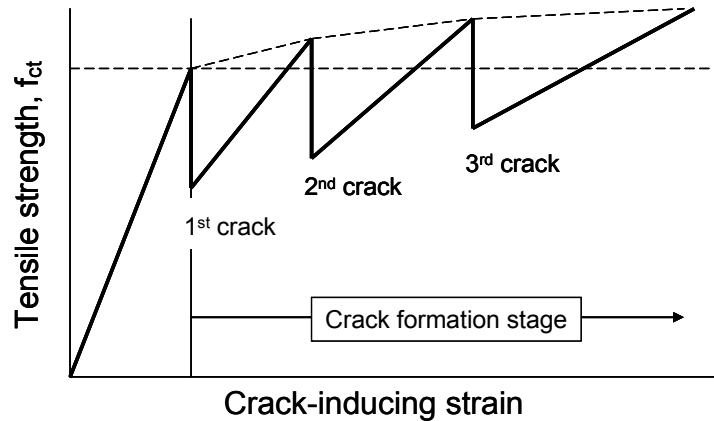


Figure A8.13 Schematic illustration of crack formation

For simplicity, the tensile strength of the concrete is assumed to be uniform and constant and the generation of cracks is assumed to follow the process shown in Figure A8.14.

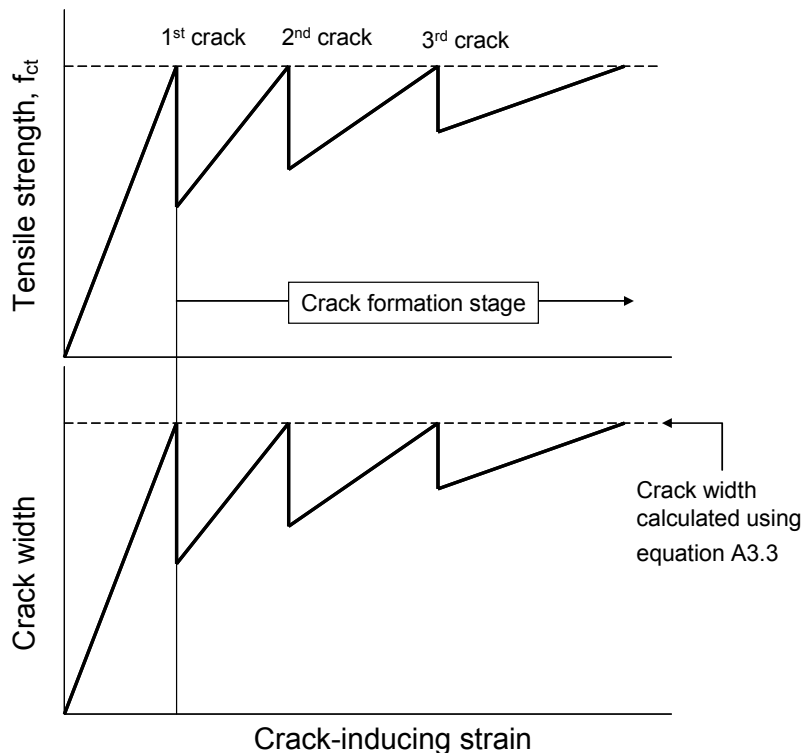


Figure A8.14 Schematic of the variation of crack width and concrete stress with increasing imposed strain for an element restrained at its ends (Beeby and Forth, 2005)

Under these conditions, Beeby (1990) derived the following equation for estimating crack width;

$$w_{max} = \frac{0.5\alpha_e f_{ct} S_{max}}{E_s} \left(1 + \frac{I}{\alpha_e \rho} \right) \quad (\text{A8.18})$$

where:

- α_e is the modular ratio
- f_{ct} is the tensile strength of the concrete when cracking occurs
- E_s is the elastic modulus of the reinforcement
- ρ is the steel ratio.

Beeby (1990) has reported good agreement between experimental results and crack widths (Jaccoud, 1986) derived using equation A8.16 and this provides the basis for the recommendation of EN1992-3 for a member restrained at its ends. The general term for estimating the crack inducing strain is given as expression M.1 in Informative Annex M of EN1992-3 as follows:

$$(\varepsilon_{sm} - \varepsilon_{cm}) = \frac{0.5\alpha_e k_c k f_{ct,eff}}{E_s} \left(1 + \frac{I}{\alpha_e \rho} \right) \quad (\text{A8.19})$$

The values of k_c and k are defined in Section A8.3 and the values given in Table A8.1 for the condition of external restraint dominant should be applied. In addition, steel ratio ρ is based on the full section thickness.

Substituting equation A8.19 in equation A8.1 gives Expression M.1 in EN1992-3 as follows;

Crack width (end restraint)	$w_k = \frac{0.5\alpha_e k_c k f_{ct,eff}}{E_s} \left(1 + \frac{I}{\alpha_e \rho} \right) S_{r,max}$	(A8.20)
-----------------------------	---	---------

The crack spacing $S_{r,max}$ is derived using equation A8.15. Hence to calculate crack width, two values of steel ratio are used; $\rho_{p,eff}$ is based on the effective area of concrete in tension surrounding the reinforcement to a depth $h_{c,ef}$; and ρ based on the area of concrete in tension, in this case the full section thickness. It is not clear how the mechanics of the system justifies the different values of steel ratio thus derived. However, it is assumed that in calibrating the crack spacing and crack width equations, these values have been used.

A8.6.3 A member restrained along one edge

This more common form of edge restraint differs significantly from the condition of end restraint. The principal difference is that, along with the steel, the adjacent concrete also acts as a crack distributor.

Consider the common case of a wall on a rigid foundation (Beeby and Forth, 2005). When a crack occurs, the relieved stress in the wall is transferred to the base by shear. While there is some reduction in stiffness local to the crack, at some distance from the crack the stresses will be unaffected and further cracks may form. Hence, even in an unreinforced section, there would be some distribution of cracking. EN1992-1-1 recommends that under conditions in which the steel area does not meet the minimum requirements, the maximum crack spacing may be assumed to be 1.3 times the height of the wall. This differs significantly for the case of end restraint where, in an under-reinforced section, all of the strain would be relieved at the first crack, with no additional cracks forming.

Now consider the influence of reinforcement on the cracks that would form in the unreinforced element. While the location of the cracks may not differ, the steel will improve the transfer of stress to concrete

with increasing distance from the crack compared with the unreinforced case. In this case, therefore, the crack pattern will tend to be established when the tensile stress first exceeds the tensile strength of the concrete, and additional restrained strain will result in the cracks widening.

Informative Annex M of EN1992-3 advises that a reasonable estimate of crack width can be obtained by using expression 7.8 of EN1992-1-1 (shown herein as equation A8.1) in which the value of $(\epsilon_{sm} - \epsilon_{cm})$ is given as,

$$(\epsilon_{sm} - \epsilon_{cm}) = R_{ax} \epsilon_{free} \quad (A8.21)$$

where:

R_{ax} is the restraint factor

ϵ_{free} is the strain which would occur if the structure was completely unrestrained.

Substituting equation A8.21 in equation A8.1 gives

$$w_k = S_{r,max} R_{ax} \epsilon_{free} \quad (A8.22)$$

$R_{ax} \epsilon_{free}$ represents the restrained component of contraction ϵ_r . EN1992-1-1 provide some guidance on factors that contribute to ϵ_{free} including methods for estimating autogenous and drying shrinkage and recommends a value of $10\mu\epsilon/^\circ\text{C}$ for the coefficient of thermal expansion of concrete. EN1992-3 gives some very general guidance on restraint factors, with a maximum value of 0.5 which has been adopted from BS8007 and includes the effect of creep. However, no information is given in either EN1992-1-1 or EN1992-3 on the likely temperature rise or temperature differential, the principle contributors to early age thermal cracking. Guidance on estimating ϵ_r is given in Chapter 3 of the Main Report with detailed input data provided in Chapter 4.

Substituting for $S_{r,max}$ in equation A8.22 and using $\epsilon_r = R_{ax} \epsilon_{free}$ gives the expression for estimating crack width as follows:

$$\text{Crack width } w_k = \left(3.4c + 0.425 \left(\frac{k_l \cdot \varphi}{\rho_{p,eff}} \right) \right) \epsilon_r \quad (A8.23)$$

It can be seen that equation A8.23 take no account of the fact that after cracking has occurred, there is a residual tensile strain in the concrete which does not contribute to the crack width. This residual strain will be determined by strain distribution along the reinforcement as affected by the bond. Measurements (Scott & Gill, 1987) indicate a linear distribution of strain in the reinforcement away from the first crack. As it is assumed for design purposes that the maximum crack spacing occurs, it is reasonable to assume also that the maximum strain between cracks would just equal the tensile strain capacity of the concrete ϵ_{ctu} . Hence the average strain in the concrete between the cracks will be $0.5 \epsilon_{ctu}$.

Hence the crack-inducing strain, $\epsilon_{cr} = \epsilon_r - 0.5 \epsilon_{ctu}$.

In this case equations A8.23 is modified as follows:

$$\text{Crack width (edge restraint) } w_k = \left(3.4c + 0.425 \left(\frac{k_l \cdot \varphi}{\rho_{p,eff}} \right) \right) (\epsilon_r - 0.5 \epsilon_{ctu}) \quad (A8.24)$$

A8.7 Conclusions

The approach to the design of reinforcement for the control of early-age cracking to EN1992-3 and EN1992-1-1 is similar to the approach used by BS8007 but differs in a number of specific respects as follows.

- 1 While BS8007 uses the same surface zone for estimating both the minimum reinforcement area (previously referred to as ρ_{crit}) and the crack spacing and width, EN1992-1-1 uses one area “*the area of concrete in the tensile zone*” for calculating the minimum reinforcement area $A_{s,min}$ and another “*the effective area of concrete in tension surrounding the reinforcement*” for calculating crack spacing and width.
- 2 The change in “*the area of concrete in the tensile zone*” leads to an increase in the minimum reinforcement area $A_{s,min}$ in sections > 600 mm which are subject to external restraint.
- 3 The change in the surface zone defined as “*the effective area of concrete in tension surrounding the reinforcement*” leads to a reduction in the required area of reinforcement A_s in most practical circumstances.
- 4 The expression in EN1992-1-1 for crack spacing differs from BS8007 in two principal respects. An additional term is included for cover and the steel ratio is calculated differently due to a change in the surface zone. The net effect is for the crack spacing estimated using EN1992-1-1 to be 20-40 per cent lower than values calculated using BS8007 and this leads to the estimated crack widths being lower by a similar amount. This leads to a reduction in the required reinforcement (subject to $A_{s,min}$ being exceeded) which may lead to an insufficiently robust design if no other changes are made to the design equation.
- 5 There is uncertainty about the value of k_f used in the equation for estimating crack spacing, and in particular the component of this term that relates to the ratio of tensile strength to bond strength. It is recommended that k_f be increased from 0.8 to 1.14 to take account of the fact that in many practical circumstances, even with good construction practice, good bond may not be achieved around the full perimeter of horizontal bars. Increasing k_f largely offsets the reduction in A_s due to the change in the surface zone.
- 6 While BS8007 only deals with the condition of edge restraint, EN1992-3 provides different methods for calculating the crack inducing strain depending on the form of restraint. For conditions of continuous edge restraint the approach is similar to that of BS8007, being determined by the magnitude of contraction and the level of restraint. For conditions of end restraint a different approach is used in which the crack-inducing strain is related to the tensile strength of the concrete at the time of cracking. In the former case it is assumed that the full crack pattern develops when the strain capacity of the concrete is exceeded and the cracks widen with continuing contraction. In the latter cases each crack is assumed to form to its full potential width and with continuing contraction additional cracks occur progressively. The result is the formation of fewer, larger cracks for the condition of end restraint. The difference in crack width is substantial and it is important that the nature of the restraint is properly defined.

A8.9 References

- Anchor, R D, Hill, A W and Hughes, B P (1979)
Handbook on BS 5337:1976 (The structural use of concrete for retaining aqueous liquids)
 Viewpoint. Publications, Cement and Concrete Association, Slough
- Bamforth, P B (1978)
 Advantages from temperature studies
 In: Proc paper presented at symposium *How hot is your concrete and does it matter?*
 Cement and Concrete Association, June 1978, C&CA Wexham Springs, now BCA, Camberley, Surrey
- Beeby, W (1990)
Fixings in cracked concrete – The probability of coincident occurrence and likely crack width
 TN136, CIRIA, London
- Beeby, W and FORTH, J P (2005)
 “Control of cracking walls restrained along their base against early thermal movements”
 In: *Proc 6th Int. Cong. on Global construction, ultimate concrete opportunities*, Dundee University, July 2005, pp 123-132. Published by Thomas Telford, London, ISBN 0 72773 387 7
- Van Beek, A, Baetens, B E J and Schlangen, E (2001)
 “Numerical model for prediction of cracks in concrete structures”
 In: *Proc RILEM PRO 23, Early-age cracking in cementitious systems*, **5**, Haifa, Israel, pp 39-48
- Blundell, R and Bamforth, P B (1975)
 “Humber tests prove Cemsave heat effect”
New Civil Engineer, 24 July 1975, 25-25
- van Breugle, K and Lokhorst, S J (2001)
 “The role of microstructural development on creep and relaxation of hardened concrete”
 In: *Proc RILEM PRO 23, Early-age cracking in cementitious systems*, **1**, Haifa, Israel, pp 3-10
- Harrison, T (1992)
Early-age thermal crack control in concrete
 R91, CIRIA, London
- Jaccoud, J P (1986)
Armature minimale pour le control de la fissuration des structures en beton
 Thesis, Department of Civil Engineering, Ecole Polytechnique Federale de Lausanne, December 1986
- Kandstad, T, Bjøntegaard, Ø, Sellevold, E and Hammer, T A (2001)
 “Crack sensitivity of bridge concretes with variable silica fume content”
Improved performance of Advanced Concrete Structures – IPACS, Report BE96-3843/2001:48-6, 2001,
 Selmer Skanska, Trondheim, Norway, ISBN 9 18958 077 X
- Narayanan, R S and Beeby, A W (2005)
Designers’ Guide to EN 1992-1-1 and EN 1992-1-2 Eurocode 2: Design of Concrete Structures. General rules and rules for buildings and structural fire design
 Thomas Telford, London ISBN 0 72773 105 X
- Pane, I and Hansen, W (2002)
 “Concrete Hydration and Mechanical Properties under Nonisothermal Conditions”
ACI Materials Journal, 99 (No 6), November/December 2002, 24–33pp, Detroit, Michigan
- Scott, R H and Gill, P A T (1987)
 “Short term distributions of strain and bond stress along tension reinforcement”
The Structural Engineer, 1987, Vol. 65B, No.2
- British Standards**

BS 8007:1987 Design of concrete structures for retaining aqueous liquids.

Euro Codes

EN1992-1-1:2004 *Eurocode 2. Design of concrete structures. General rules and rules for buildings. National Annex to BS EN 1992-1-1:2004*

EN1992-2:2005 *Eurocode 2. Design of concrete structures – Design of concrete structures – Concrete bridges – Design and retaining rules*

EN1992-3:2006 *Eurocode 2: Design of concrete structures – Part 3: Liquid retaining and containment structures*

EN1992-1-1:2004 *Eurocode 2. Design of concrete structures. General rules and rules for buildings*

A9 The effect of peak temperature on the *in situ* strength and durability of concrete

A9.1 Strength development

A9.1.1 Background data

It has been recognised for many years that if concrete is heated too rapidly during the early period of hydration, the long term properties may be adversely affected. This is demonstrated by the limits placed on the rate of heating for precast heat cured elements (Richardson, 2003). While it is difficult to control the rate of heat evolution *in situ*, the maximum peak temperature is commonly specified for massive sections and concretes likely to achieve a significant temperature rise during hydration. A commonly used value is 70 °C. One reason for this limit is to ensure that the *in situ* strength is not impaired significantly.

In a study of the influence of the natural heat cycle in very thick sections (Bamforth, 1980) significant changes in the rate of strength development of heat cycled concretes were observed. In particular the heat cycled 28-day strength for CEM I concrete was appreciably lower than that of standard cured cubes. Similar findings have been reported more recently by Barnett *et al* (2005), Sato *et al* (2001) and Sugiyama *et al* (2000). In the most extreme case, (Sato *et al*, 2001) the core strength at 56 days for concrete with a peak temperature of 70 °C was less than 50 per cent of cores removed from the same concrete with a peak temperature of 56 °C.

Sugiyama *et al* (2000) imposed a variety of temperature cycles on the concrete, with variation in the start time, the rate of temperature rise and fall and the peak temperature. The results, shown in Figure A9.1, were obtained for concrete subjected to a heat cycle that closely represented a natural early age heat cycle.

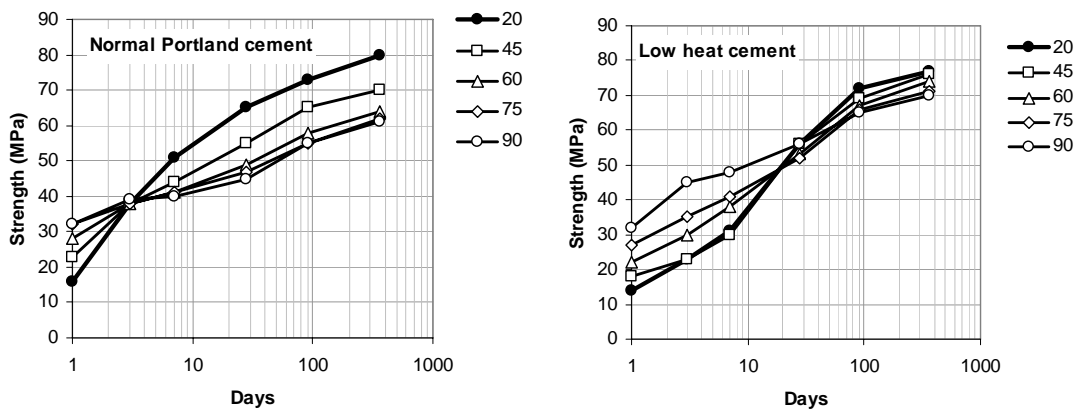


Figure A9.1 Strength development as affected by the peak temperature achieved during an early age heat cycle (Sugiyama *et al*, 2000)

It can be seen that for CEM I concrete, while the early temperature cycle resulted in acceleration of the strength development within the first few days, the subsequent rate of strength gain was reduced such that at 28 days, the heat cycled strength was up to 25 per cent below the strength of concrete cured at 20 °C. With low heat cement, however, the early benefit in strength development was still observed (during the initial 14 days) but without the long term strength development being impaired.

A9.1.2 The Concrete Society Study

In a comprehensive study of the *in situ* strength of concrete to establish the relationship between core and cube strength (Concrete Society, 2004) similar findings were reported. The testing was carried out to measure the *in situ* strength of a variety of concrete mixes cast into elements of differing geometry. The following factors were investigated

- concrete strength class - target strengths of 30MPa and 50MPa were used to represent low and medium strength concrete
- cement type – four cement types were used, CEM I, Portland limestone cement (LPC), 70 per cent CEM I/30 per cent fly ash and 50 per cent CEM I/50 per cent ggbs
- aggregate type – limestone and quartzite gravel
- element geometry – Concrete blocks (1.5 × 1.7 × 1.2m) insulated on all but one face, 300mm walls cast in plywood formwork and 200 mm thick slabs
- time of casting – winter and summer.

The early age temperature rise was measured in each of the specimens and cores were extracted for testing at 28, 42, 84 and 365 days. An example is shown in Figure A9.2 for the 30 MPa CEM I concrete using quartzite gravel aggregate cast in the summer into the different elements. The influence of the peak temperature on the rate of strength development is clear. In the section which achieved the highest peak temperature of about 60 °C, the core strength at 28 days was about 35 per cent lower than the cube strength. While these results were broadly in line with the findings of Bamforth (1980) and Sugiyama et al (2000) other researchers have reported less influence of the early heat cycle. Barrett *et al* (2005) reported a difference between heat cycled and standard cured cubes at 28 days of only 10 per cent. It is clear, however, that for CEM I cement concretes, the *in situ* strength may be adversely affected, and to a considerable extent, by permitting a high peak temperature.

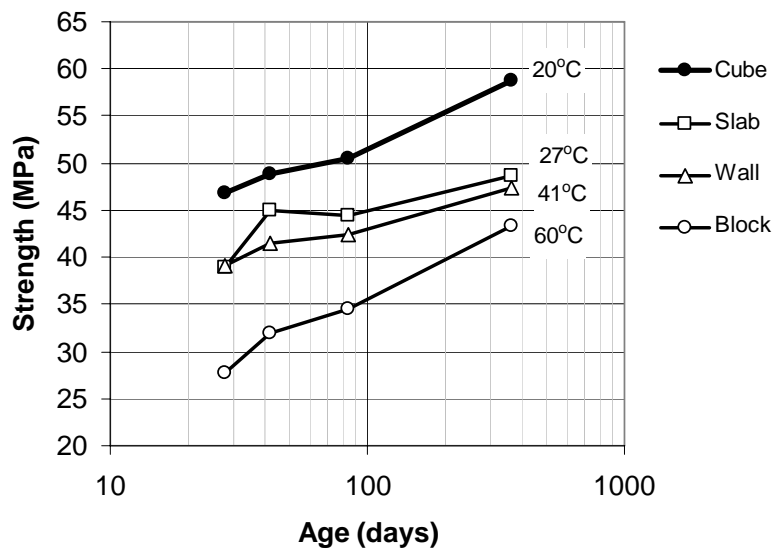


Figure A9.1 The strength development in elements of different size and achieving different peak temperatures (shown) during the early thermal cycle (Concrete Society, 2004)

Figure A9.3 shows the relationship between peak temperature T_p and the ratio of core/cube strength obtained from the Concrete Society study for the range of elements and concretes cast using CEM I concrete. This shows an approximately linear relationship between the peak temperature and the *in situ* strength expressed as a proportion of the 28-day cube strength.

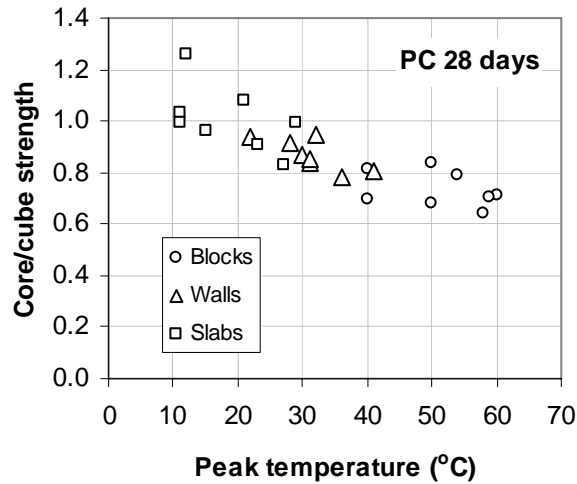


Figure A9.3 The effect of the peak early age temperature on the ratio of the core/cube strength at 28 days (Concrete Society, 2004)

In order to develop a better understanding of the way in which the peak temperature influences strength, the Concrete Society data have been analysed in more detail. Results are shown in Figure A9.4 (expressed as the ratio of the core strength achieved at 28, 42, 84 days and 1 year to the 28-day cube strength) for concretes using each of the four cement types. While there is some scatter to the results, clear trends are apparent. For example, the lower *in situ* strength achieved with higher peak temperature for CEM I concrete was also observed for Limestone Portland cement concrete, although at 28 days the reduction was less, being about 20 per cent at 60 °C. However, the performance of concretes containing fly ash and ggbs differed significantly from that of CEM I and LPC concretes in two principal respects. Firstly, at 28-days the *in situ* strength did not reduce with an increase in the peak temperature, with a trend for a higher *in situ* strength in those elements achieving the higher peak temperatures, at least up to about 60 °C. And secondly, the development of *in situ* strength over the long term was significantly higher for the fly ash and ggbs concretes. At 1 year, none of the elements containing pfa or ggbs exhibited strengths less than the 28-day cube strength, regardless of peak temperature, while for CEM I concrete, this was only achieved in concretes with peak early-age temperatures of less than about 40 °C.

Figure A9.5 illustrates more clearly the way in which the relative strength changes with age for concretes with the four cement types. Based on the best fit linear relationships derived for each data set, the results indicate that under conditions within which the peak temperature is likely to exceed 40 °C, concretes containing CEM I or Portland limestone cement are unlikely to achieve an *in situ* strength which exceeds the 28-day cube strength, even after one year. For the concretes containing fly ash and ggbs, however, the *in situ* strength had achieved the 28-day cube strength within 42 days, even when the peak temperature reached 60 °C. By comparison, CEM I concretes, even after 1 year, exhibited *in situ* strengths which were only about 85 per cent of the 28-day cube strength.

These findings are broadly consistent with those of Bamforth (1980) who measured the strength development for concretes containing fly ash (30 per cent) and ggbs (70 per cent) using temperature matched curing. Unlike CEM I concrete, for which the *in situ* strength was adversely affected at 28 days, in both cases the heat cycled strength exceeded the cube strength. This indicated that such mixes are far more tolerant to early temperature rise.

The difference between the performance of CEM I concrete and mixes containing fly ash and ggbs can have significant implications. It is clear from the results reported that for a given class of concrete, higher *in situ* strength will be achieved if the concrete contains fly ash or ggbs. In a study of fly ash concretes Bamforth (1984) indicated that in structural concrete in sections exposed to peak temperatures in the order of 70 °C, fly ash concrete achieves a heat cycled strength that may be 10MPa higher than the same class of concrete using CEM I. The converse of this is that to achieve the same *in situ* strength, a lower strength class may be used. Hence, under appropriate circumstances, it may be acceptable to not only benefit from the reduction in heat generation resulting from the inclusion of fly ash or ggbs, but also to

achieve a lower binder content associated with a lower strength class. This is similar in effect to specifying the strength at a later age, as sometimes occurs in practice.

An argument against utilizing the benefit from the early age temperature rise with fly ash and ggbs concretes has been that the surface is generally subjected to a lower temperature rise than the centre of a section. However, with the use of plywood formwork, the surface temperature may achieve a level at which it becomes significant and where knowledge is available on the construction process, consideration may be given to specifying either a lower strength class or later age compliance when using fly ash or ggbs concrete.

In order to understand the reasons for the observed scatter, the results have also been presented to show the effects of strength class (Figure A9.6), time of casting (Figure A9.7) and aggregate type (Figure A9.8).

Strength class

The results shown in Figure A9.6 indicate that the *in situ* strength for the lower strength concrete achieved a higher proportion of the cube strength at both 28 days and after 1 year. The difference is small but consistent across the range of mixes. The difference was most apparent for the fly ash concrete after one year and was least apparent for the ggbs concrete.

Time of casting

The results shown in Figure A9.7 indicate that the time of casting (winter or summer) had little effect on the relationship between *in situ* strength and cube strength for CEM I and PLC concretes. Similarly, after 1 year, the time of casting had little effect on the fly ash and ggbs concretes. However, the time of casting did have some effect on the *in situ* strength of these mixes at 28 days. As expected, the slower rate of hydration of these mixes resulted in lower early strengths, particularly when the peak temperature was low.

Aggregate type

Differences in the gradients of the best fit linear relationships between peak temperature and *in situ*/28-day cube strength indicate that the influence of peak temperature was more detrimental, (or less beneficial) in concrete containing limestone aggregate when compared with gravel aggregate concrete. This indicates that the effect of the early age temperature change is in part mechanical. The coefficient of thermal expansion of limestone is significantly lower than that of quartzite gravel and both are lower than the thermal expansion of cement paste. Hence changes in temperature in limestone aggregate concrete will result in greater differential expansion and contraction between the aggregate and cement paste, leading to localized thermal stresses that may cause micro-cracking and loss of strength. The average difference in the gradient was -0.0042 indicating that, over a temperature change of 40°C limestone aggregate concrete would achieve an *in situ* strength about 17 per cent less than achieved with a gravel aggregate concrete having the same strength at 20 °C. It was also observed, however, that the *in situ* strength of limestone aggregate concrete at 20 °C generally achieved a marginally higher proportion of the cube strength (by about 4 per cent), partially offsetting the effect of the subsequent change in temperature, which reduces to 13% on average at 60 °C.

A9.1.3 General conclusions relating to strength development

From the analysis of the Concrete Society study, the following may be concluded.

1. The strength development of CEM I concrete was adversely affected by the early temperature cycle to the extent that at 28 days the *in situ* strength may be only 65 per cent of the 28 day cube strength if the peak temperature reaches 60 °C. In the longer term the *in situ* strength increased but after 1 year it was still, on average, only about 85 per cent of the 28-day cube strength if the high peak temperature had been achieved.
2. Concrete containing Portland limestone cement was also adversely affected by the early thermal cycle but to a lesser extent than CEM I concrete. At 28 days the *in situ* strength was typically about 80 per cent of the 28 day cube strength, increasing to about 90 per cent after one year for concretes achieving 60 °C during the early thermal cycle.
3. The influence of the early thermal cycle on both fly ash and ggbs concretes was to enhance the *in situ* strength at 28 days such that it achieved 100 per cent of the 28 day cube strength within 42 days. After one year the *in situ* strength exceeded the 28-day cube strength by 10 per cent for

those concretes with the highest peak temperature and by a considerably higher margin for concretes experiencing lower peak temperatures.

4. For a given peak temperature, the lower grade of concrete achieved a higher proportion of the 28 day cube strength, with the difference being greatest during the early life of the concrete.
5. The time of casting (winter v summer) had little effect on the relationship between peak temperature and the *in situ* strength relative to the cube strength
6. The aggregate type was significant and indicates that the effect of the early temperature rise will be most detrimental (or less beneficial) for concrete containing lower thermal expansion aggregates (when comparing limestone with quartzite gravel).

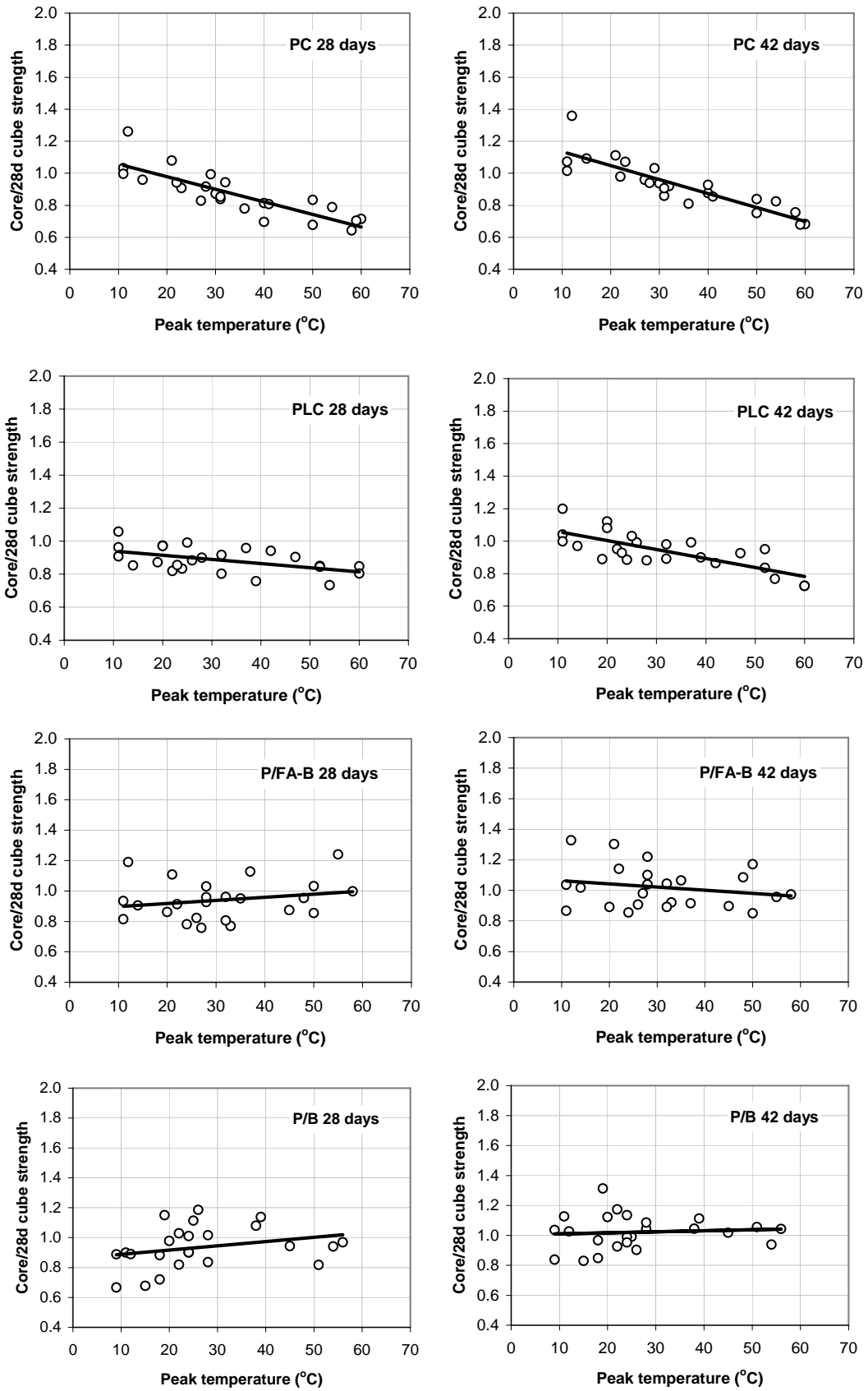


Figure A9.4 *The influence of the peak temperature achieved during the early thermal cycle on the *in situ* strength of concrete (at 28 and 42 days) expressed in relation to the 28-day cube strength*

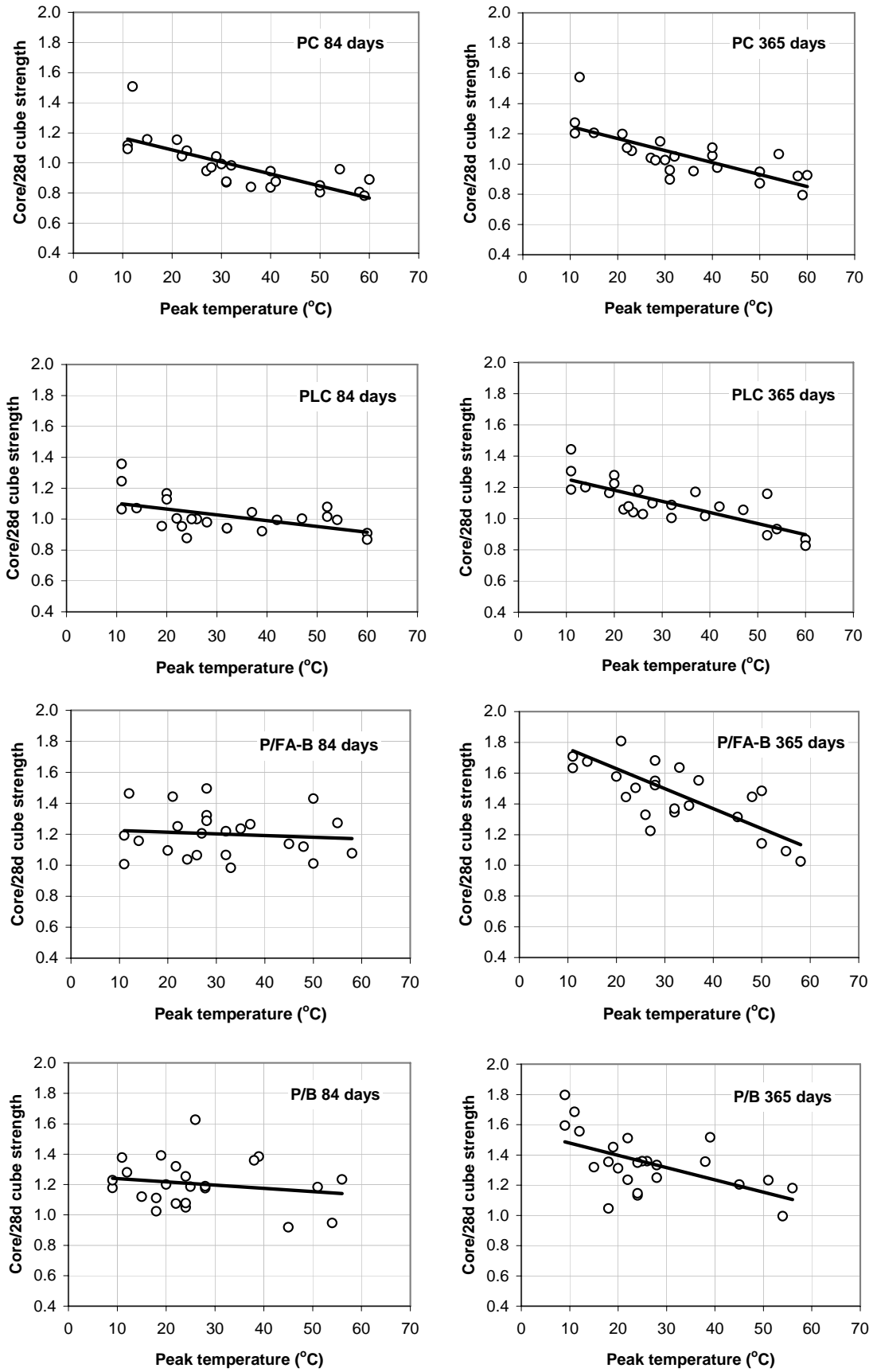


Figure A9.4 (contd) *The influence of the peak temperature achieved during the early thermal cycle on the insitu strength of concrete at 84 and 365 days expressed in relation to the 28-day cube strength*

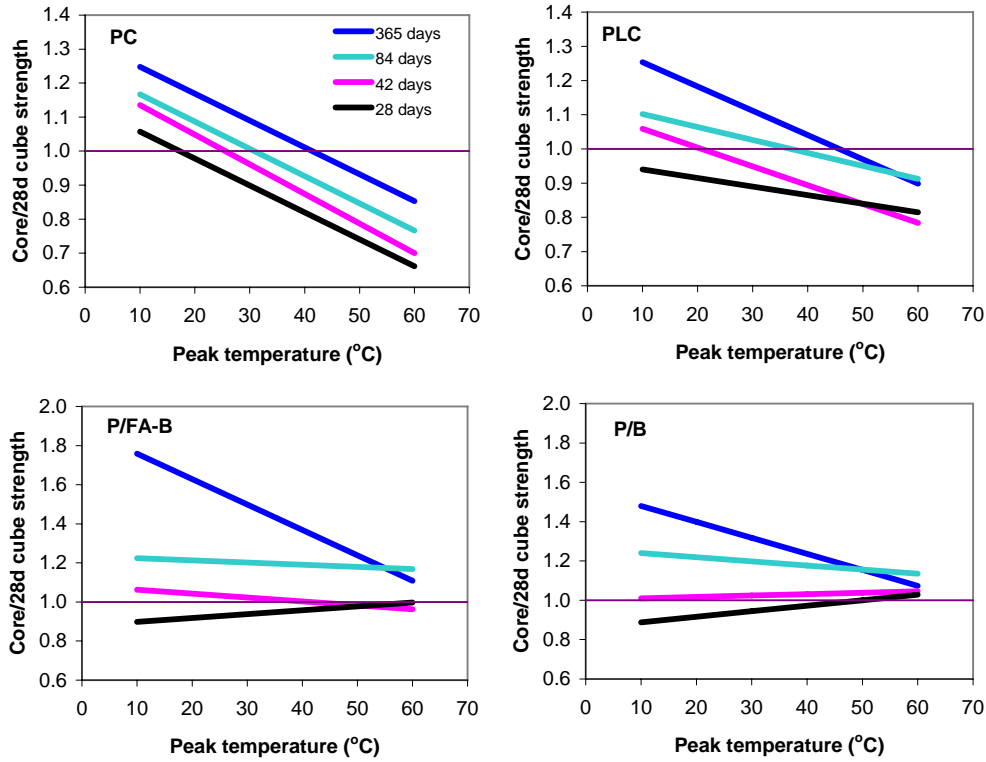


Figure A9.5 The relationship between the peak temperature and the strength (relative to the 28-day cube) using CEM I cement, Portland limestone cement (PLC), and combinations of CEM I cement with 30 per cent fly ash cement (P/FA-B) and 50 per cent ggbs (P/B)

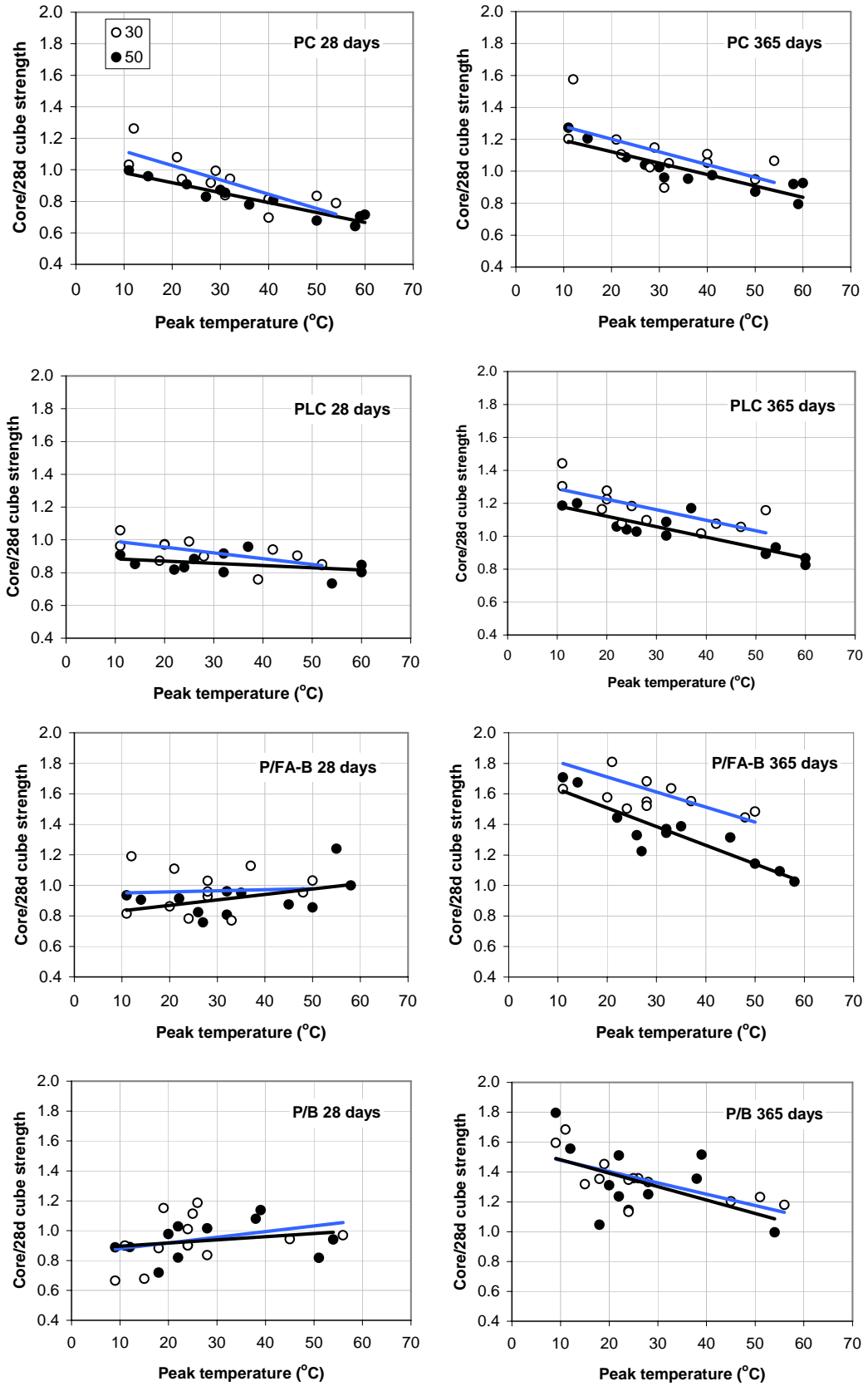


Figure A9.6 The relationship between peak temperature and strength as affected by concrete strength class

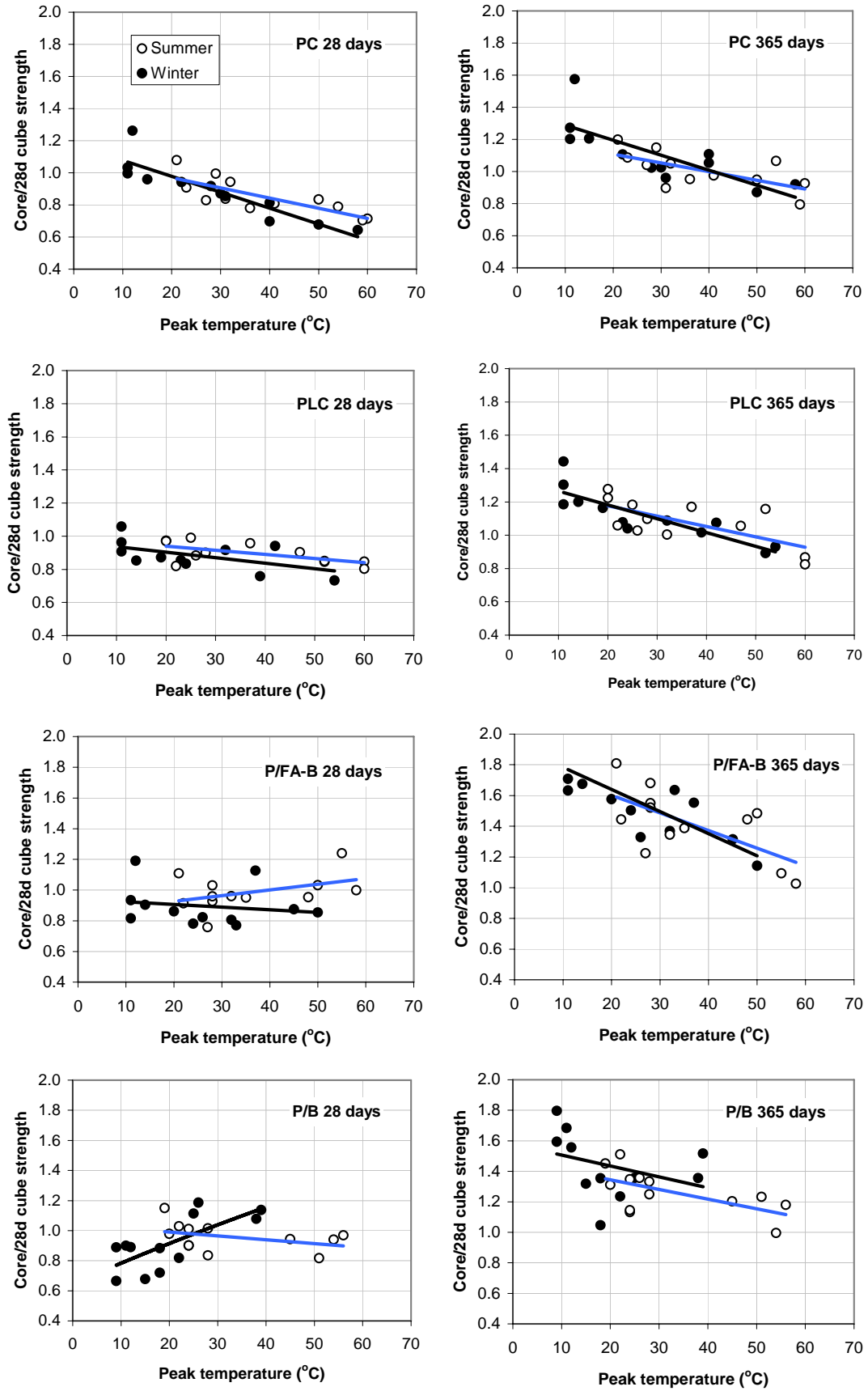


Figure A9.7 The relationship between peak temperature and strength as affected by the time of casting (summer v winter)

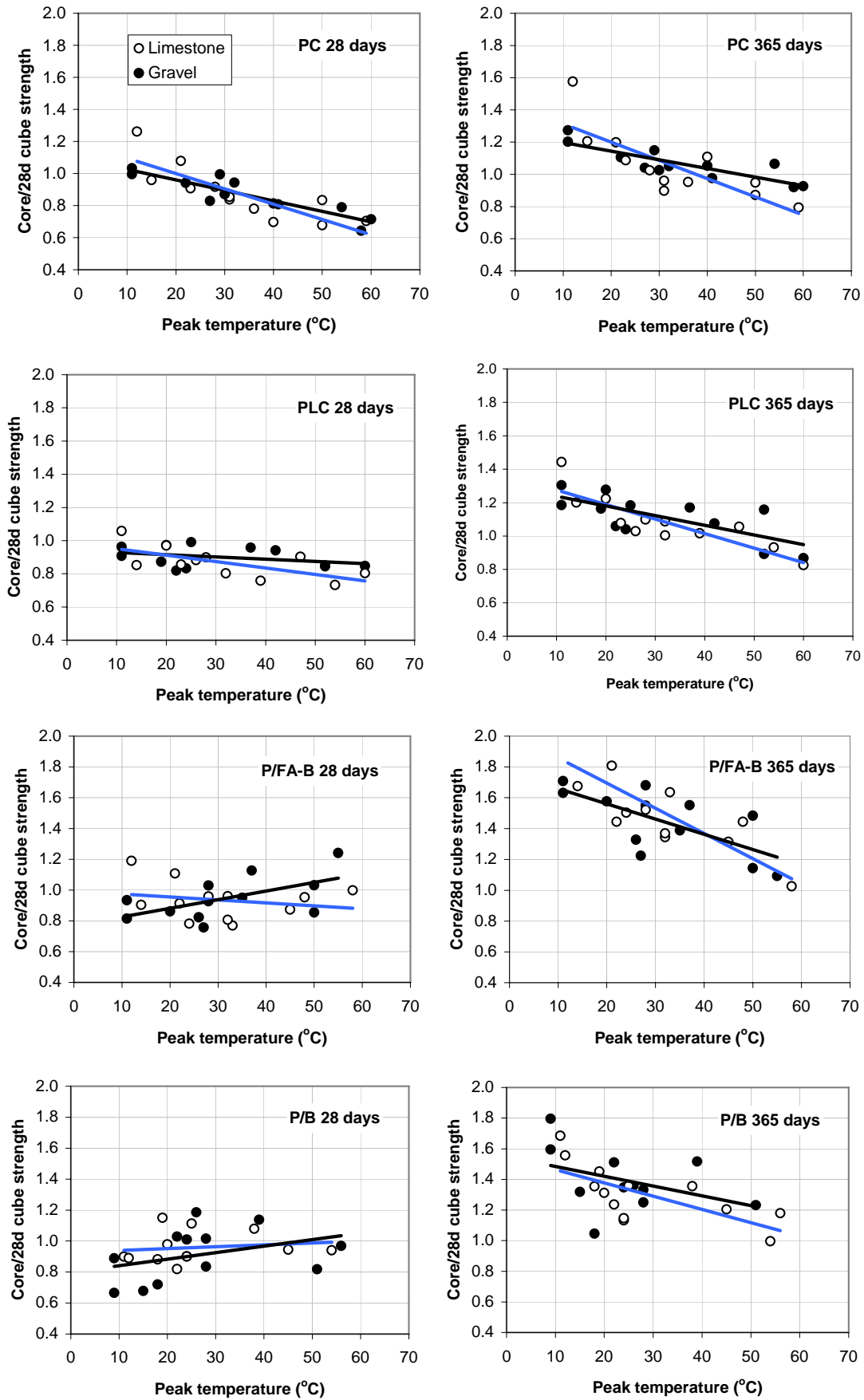


Figure A9.8 The relationship between peak temperature and strength as affected by the aggregate type (limestone v gravel)

A9.2 Durability

The influence of the early heat cycle on the durability of concrete does not appear to have been widely researched. If it is assumed that there is some correlation between durability and strength for a particular combination of constituent materials, it may be inferred from the Concrete Society study referred to in Section A9.1.2 that CEM I concrete may be adversely affected by the early thermal cycle, while concretes that contain fly ash and ggbs will benefit. However, there is not sufficient data to quantify the effect and enable its application in design.

In a study on high strength concrete containing fly ash, the influence of peak curing temperature on the Rapid Chloride Permeability was measured (Myers *et al*, 2000). An improvement was reported with increasing peak temperature up to about 88 °C. Interestingly, while there was a correlation between performance and peak temperature, no trend was observed with temperature rise. This suggests that the influence is most likely to have been related to chemical rather than physical processes.

A9.3 Delayed ettringite formation

Delayed ettringite formation (DEF) is a delayed form of sulphate attack and occurs in concrete which has a relatively high sulfate content and which has experienced high temperature during its early hydration. The high temperature decomposes the primary ettringite which is responsible for regulating set, and this reforms later in the life of the concrete. The following guidance is given in BRE IP11/01 (BRE, 2000) in relation to the risk of DEF.

- $T_p < 60$ °C no risk
- $T_p < 70$ °C very low risk
- $T_p < 80$ °C low risk

These above limits apply to Portland cement concretes. BRE IP11/01 states that pfa at levels of > 20 per cent or ggbs at levels of > 40 per cent will prevent DEF-induced expansion in concrete subject to peak temperatures of up to 100 °C.

Hence DEF may be prevented by limiting the peak temperature achieved during the early thermal cycle. The risk of DEF may be reduced most effectively by the use of fly ash or ggbs in suitable quantities which will have the combined effect of both reducing the temperature rise and increasing the temperature at which DEF will occur.

A9.4 Conclusions

The early-age peak temperature has a significant effect on the strength development of concrete. For concrete using CEM I the strength is impaired by the heat cycle such that at 28-days the heat cycled strength may be only 65 per cent of the standard cube strength. Concrete containing fly ash or ggbs are less adversely affected by the heat cycle and for the same class of concrete will achieve higher *in situ* strength. Hence, the same *in situ* compressive strength may be achieved with fly ash and ggbs concrete when using a lower strength class compared with CEM I concrete. For this reason it may be acceptable to measure compliance at an age later than 28 days (56 days is sometimes used) which is itself equivalent to using a lower strength class. This will enable a reduction in binder content, and hence a further reduction in temperature rise and the associated risk and/or extent of early-age thermal cracking.

A9.5 References

Bamforth, P B (1980)

“*In situ* measurement of the effects of partial Portland cement replacement using either fly ash or ground granulated slag on the performance of mass concrete”

Proc. Instn. Civ. Engrs. 69, Part 2, Sept 1980, pp 777-800

Bamforth, P B (1984)

“Heat of Hydration of Pfa Concrete and its Effect on Strength Development”

In: *Proc 2nd Int. Conf. Ash Technology and Marketing* (ASHTECH '84) London, September 1984

Barnett, S J, Soutsos, M N, Bungey, J H and Millard, S G (2005)

“The effect of ground granulated blastfurnace slag on the strength development and adiabatic temperature rise of concrete mixes”

In: Dhir R K, Harrison, T A and Newlands, M D (eds), *Proc Int Conf Cement combinations for durability*, University of Dundee, 5-7 July, Thomas Telford, pp 165-172

BRE

Delayed ettringite formation: In situ concrete

Information Paper IP 11/01, BRE 2001

Concrete Society (2004)

In situ strength of concrete – An investigation into the relationship between core strength and the standard cube strength

Working party of the Concrete Society, Project Report No 3, BCA, Camberley, Surrey, ISBN 0 94669 186 X

Myers, J J and Arrasquillo, R L (2000)

“Influence of hydration temperature on the durability and mechanical property performance of HPC prestressed/precast beams”

Journal of the Transportation Research Board. In: *Proc 5th Int. Bridge Engineering Conf.*, Publication 5B0038, Vol.1, No. 1696, pp 131-142, April 2000

Richardson, J (2003)

“Precast concrete structural elements”

Advanced Concrete Technology (ed Newman and Choo), Elsevier, Butterworth, Heinemann, Processes, 7, Precast Concrete, 2003

Sato, S, Hattori, K and Ogata, H (2001)

“Mechanical properties in massive concrete specimens with different initial curing conditions” In:

Banthai, N, Satai, K and Gjordv, O E (eds) *Proc 3rd Int. Conf. Concrete under severe conditions, CONSEC '01*, University of British Columbia, Vancouver, Canada, 18-20 June 2001, 1554-1561

Sugiyama, H, Masuda, Y and Abe, M (2000)

“Strength development of concrete cured under high temperature conditions at early-age”

In: *Proc 5th Int. Conf. Durability of concrete*, Spain, 2000, ACI SP 192-59, 965-982

A10 The tensile strength of concrete

A10.1 Introduction

The design approach for cracking combines the short-term early-age thermal movement and autogenous shrinkage, the long-term thermal movements, and drying shrinkage. The tensile strength of the concrete is important in the design process as it determines both the minimum area of reinforcement $A_{s,min}$ and the crack width for elements subjected to end restraint. It is important, therefore, to be able to predict the tensile strength of the concrete **in the structure** and how it changes with time.

A probabilistic approach has been used (Appendix A7) to determine the likely range of values of *in situ* tensile strength and to determine the margin of safety associated with the use of values of mean tensile strength f_{ctm} derived using the recommendations of EN1992-1-1.

A10.2 Estimating tensile strength according to EN1992-1-1

EN1992-1-1 provides an expression relating the 28-day mean tensile strength f_{ctm} to the compressive strength at 28 days and an age function which enables the estimation of the mean tensile strength, $f_{ctm}(t)$ at time t in relation to the 28-day value. For the estimation of $A_{s,min}$, EN1992-1-1 recommends the use of the mean value of the tensile strength effective at the time that cracking is first expected to occur, $f_{ct,eff}$.

EN1992-1-1 defines “ $f_{ct,eff} = f_{ctm}$ or lower $f_{ctm}(t)$ if cracking is expected earlier than 28 days”

According to EN1992-1-1, the mean tensile strength f_{ctm} at 28 days may be derived from the 28-day cylinder strength using the following equations:

$$\text{For strength class } \leq \text{C50/60} \quad f_{ctm} = 0.3 f_{ck}^{(2/3)} \quad (\text{A10.1})$$

$$\text{For strength class } > \text{C50/60} \quad f_{ctm} = 2.12 \ln(1 + f_{cm}/10) \quad (\text{A10.2})$$

where:

f_{ck} is the characteristic cylinder strength
 f_{ctm} is the mean cylinder strength.

The rate of strength development is determined using the expression:

$$f_{ctm}(t) = (\beta_{cc}(t))^\alpha f_{ctm} \quad (\text{A10.3})$$

$$\text{where } \beta_{cc} = \exp \left\{ s \left[1 - \left(\frac{28}{t} \right)^{0.5} \right] \right\} \quad (\text{A10.4})$$

$$\alpha = \begin{cases} 1 & \text{for } t < 28 \text{ days} \\ 2/3 & \text{for } t \geq 28 \text{ days} \end{cases}$$

s is a coefficient which depends on depends on cement type
 = 0.20 for cement of strength classes CEM 42.5R, CEM 52.5 N and CEM52.5 R
 = 0.25 for cement of strength classes CEM 32.5R, CEM 42.5 N (Class N)
 = 0.38 for cement of strength classes CEM 32.5N (Class S).

Values derived using these relationships for a range of concrete strength classes using CEM I (42.5 N) are shown in Figure A10.1.

EN1992-1-1 also notes that “*The development of tensile strength with time is strongly influenced by curing and drying conditions as well as the dimensions of the structural members*” and that where the development of tensile strength is important testing should be carried out. The expressions provided by EN1992-1-1 should therefore be applied with caution. This Appendix reviews the tensile strength of concrete in relation to its impact on early-age thermal cracking.

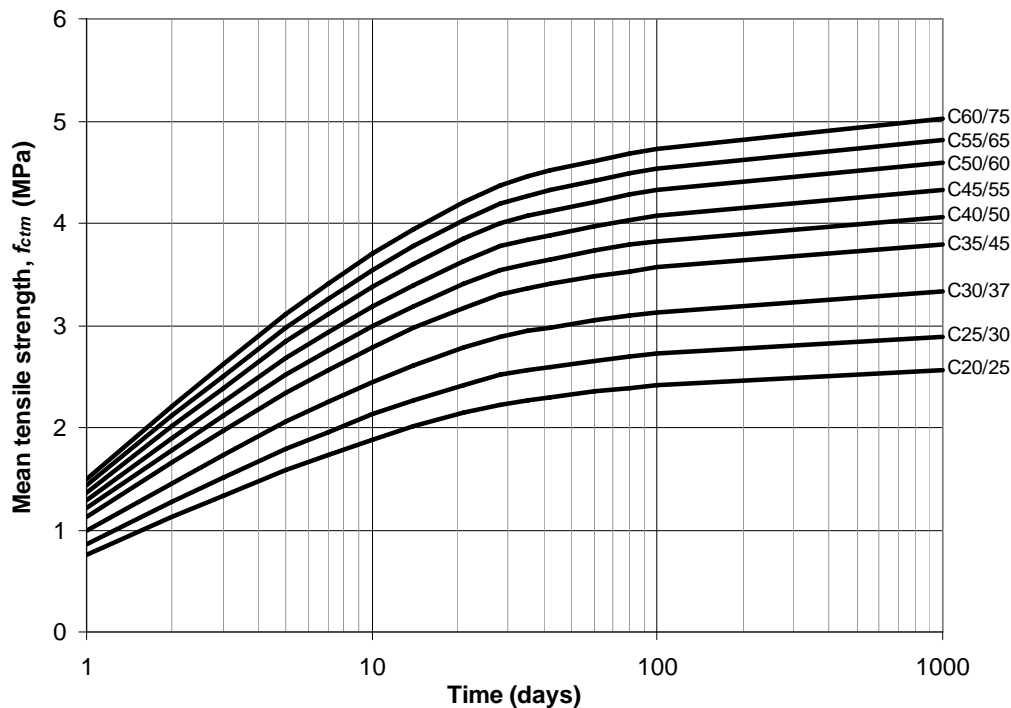


Figure A10.1 The mean tensile strength, f_{ctm} , for CEM I concrete according to EN1992-1-1

A10.3 Estimating the tensile strength of concrete *in situ*

A10.3.1 Influencing factors

EN1992-1-1 acknowledges that the tensile strength may vary considerably with the lower 5 per cent fractile and the upper 95 per cent fractile varying by ± 30 per cent from the mean. This is equivalent to a coefficient of variation of $0.3/1.64 = 0.18$. EN1992-1-1 also states that the age function only applies at 20 °C and for moist curing in accordance with EN12390. *In situ*, the variation may be greater as compaction and curing will be less than ideal, the peak temperature will influence strength gain (see Appendix A9) and the concrete will be under sustained loading. In addition, the precise time at which cracking occurs is difficult to predict.

In relation to the minimum area of reinforcement $A_{s,min}$ it is the *in situ* tensile strength at the time of cracking that will determine the stress transferred to the steel. An assessment of the *in situ* tensile strength $f_{ct(is)}$ has been undertaken and is represented using the following expression;

$$f_{ct(is)} = f_{ctm(t)} k_{cct} K_2 k_a \quad (\text{A10.5})$$

where:

$f_{ctm(t)}$ is the tensile strength estimated in accordance with EN1992-1-1. In the UK, 3 days has been the generally accepted early-age value for design (CIRIA R91, Harrison 1992, BS8007:1987)

k_{cct} is a coefficient to take account of compaction and curing, including temperature rise

K_2 is a coefficient to take account of the reduced tensile strength under sustained loading

k_a is a coefficient to take account of variation in the time of cracking.

A10.3.2 Effects of compaction and curing (k_{cct})

The *in situ* tensile strength will differ from that achieved in a test specimen as a result of differences in compaction and curing. In the latter case the peak temperature will be significant (Appendix A9).

While there are no data on the variation of *in situ* tensile strength of concrete, data are available for compressive strength. Assuming that the two are related according to the relationships given in equations A10.1 and A10.2, an assessment of the likely variation of *in situ* tensile strength may be derived from the variation in compressive strength. Data obtained at 28 days as part of the Concrete Society study on the relationship between core and cube strength (Concrete Society, 2004) have been analysed and a normal distribution has been fitted to the range of values of the ratio of core/cube strength as shown in Figure A10.2. The data were derived from concretes containing four cement types (including combinations with ground granulated blast-furnace slag and fly ash) and two aggregate types (limestone and quartzite gravel). In addition, peak temperatures varied from 9 °C to 60 °C. It can be seen that a mean value of ratio of core strength to cube strength was 0.9 with a SD of 0.128.

Based on the relationship between compressive and tensile strength (equations A10.1 and A10.2) and the results in Figure A10.2 the Standard Deviation for the ratio of *in situ* tensile strength/splitting test strength has been estimated to be 0.082 with a mean value of 0.9 and this has been used in the analysis.

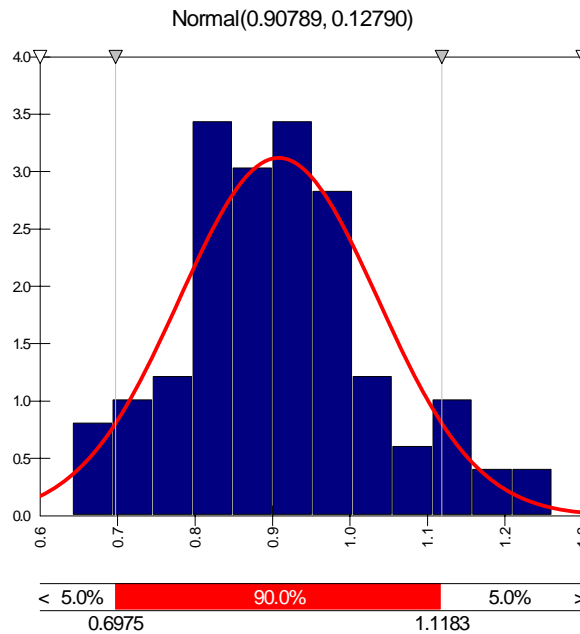


Figure A10.2 The variation in the ratio of core/cube strength at 28 days (Concrete Society, 2004)

A10.3.3 The effect of sustained loading K_2

Concrete that is maintained under a sustained tensile stress will fail at a load that is significantly lower than the load that may be sustained in a rapid load test. Under testing at constant load it has been demonstrated that when the stress exceeds about 80 per cent of the short term tensile strength, failure will almost certainly occur (Domone, 1974, Reinhardt and Rinder, 1998 van Breugel and Lokhorst, 2001) and some risk of failure is demonstrable at lower stress/strength ratios. Altoubat and Lange (2001) achieved failure in normal concretes at stress/strength ratios between 0.75 and 0.81 and Reinhardt and Rinder (1998) have reported data that shows failure at a stress/strength ratio of as low as 0.6. In probabilistic terms the risk of cracking in relation to the stress/strength ratio may be expressed as a PERT distribution with 0.6, 0.7 and 0.8 as minimum, mean and maximum values, shown in Figure A10.3. This represents

no chance of cracking if the stress/strength ratio is below 0.6, a 50 per cent chance of cracking when the stress/strength ratio exceeds 0.7 and certainty of cracking if the stress/strength ratio exceeds 0.8.

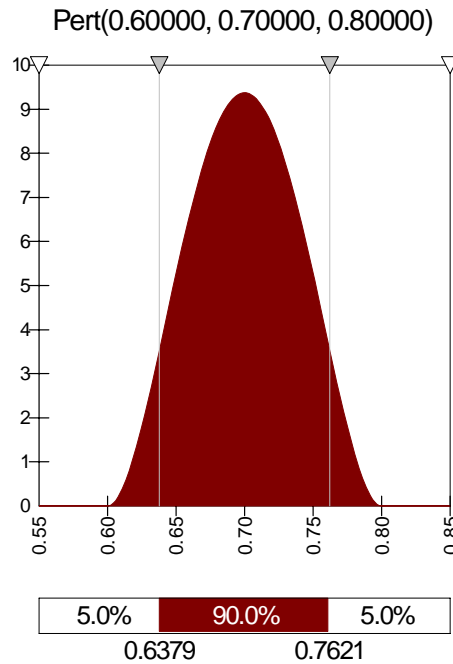


Figure A10.3 The probability of cracking in relation to the stress/strength ratio in tension.

A10.3.4 Age at cracking k_a

As the tensile strength of the concrete will increase with age, the time at cracking will be significant in determining the minimum area of reinforcement. A commonly used expression for “early-age tensile strength” in the UK (Highways Agency, 1989) is as follows;

$$f_{ct} = 0.12(f_{cu} + 10)^{0.7} \quad (\text{A10.4})$$

where f_{cu} is the characteristic 28-day cube strength.

Values obtained using this expression are given in Table A10.1. The 3-day tensile strength estimated using the expressions in EN1992-1-1 is also given and compared with values used by BS8007: 1987 and CIRA 91 (Harrison, 1992). The later were derived from the product of the critical steel ratio and the yield strength of the steel (assumed to be 460 MPa).

Table A10.1 Estimated values of “early-age” tensile strength (MPa)

Strength Class	Using equ. A10.4 HA BD 28/87	CIRIA 91, 1992	BS8007	EN1992-1-1 3 days
C20/25	1.45	1.15	-	1.32
C25/30	1.59	1.29	-	1.53
C28/35	1.72	1.61	1.60	1.66
C30/37	1.78	-	-	1.73
C35/45	1.98	-	-	1.92
C40/50	2.11	-	-	2.10
C45/55	2.23	-	-	2.27
C50/60	2.35	-	-	2.44

Values derived using equation A10.4 are similar to those derived using the expressions in EN1992-1-1. Both CIRIA R91 (Harrison, 1992) and BS8007:1987 have used values below that estimated using equation A10.4. In addition, CIRIA R91 uses a value of long-term tensile strength under sustained loading of 1.5 MPa for both C20/25 and C25/30 concrete, while the recommended critical steel ratio of 0.0037 indicates that the assumed value was $0.0037 \times 460 = 1.7$ MPa. In either case this is not significantly different from the assumed early-age tensile strength, indicating that no additional steel would be required to deal with late life cracking. Based on the results in Figure A10.1, this would appear to have been as unsafe assumption.

While it is common to base the estimate of the minimum area of reinforcement $A_{s,min}$ for the control of early-age cracking on the three day tensile strength, in practice, the time at which cracking occurs will vary, depending on a variety of factors. Observations by Alexander (2006) indicate that early-age cracking is most likely to occur within three to six days. An analysis of elements up to 1m thick using the model described in Appendix A2 indicates that the time for the temperature to drop sufficiently to cause cracking under restrained conditions (15 °C in some concretes with 50 per cent restraint (Bamforth and Price, 1995)) will be between 1 and 4 days as shown in Figure A10.4 for concretes with a range of cement contents.

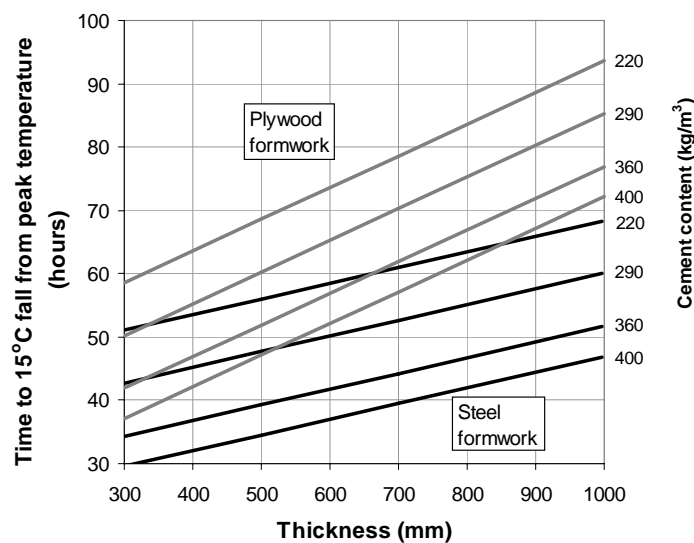
**Figure A10.4** Estimated times for a 15 °C fall from the peak temperature in relation to element thickness and cement content (kg/m^3) for CEM I concretes

Figure A10.1 indicates that within the first few days the tensile strength may increase significantly, Compared with the three day value it can be seen that the tensile strength may vary by -46 per cent to +28 per cent between one and six days. This can be expressed by a skewed PERT distribution as shown in Figure A10.5.

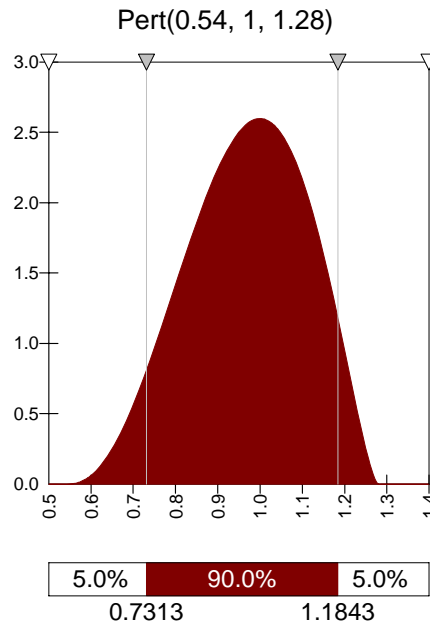


Figure A10.5 Distribution of early-age (1-6 days) tensile strength in relation to the three day value

In the long term the rate of increase in tensile strength development reduces as shown in Figure A10.1. As EN1992-1-1 recommends that for long-term cracking $f_{ct,eff} = f_{cm}(28)$ the effect of cracking before or after 28 days is considered. The data in Figure A10.1 show results up to 1000 days and indicates that under ideal curing, the tensile strength may increase by about 10 per cent beyond the 28-day value. *In situ* this continued development of strength is less likely but it is assumed in the analysis that this is the maximum increase that may occur. The possibility of cracking occurring before 28 days (but beyond 6 days) is taken into account by assuming a lower limit on long-term tensile strength which is 10 per cent below the 20-day value.

A10.4 Probabilistic analysis to derive *in situ* tensile strength

Input data for the probabilistic analysis are given in Table A10.2 for class C30/37 concrete.

Table A10.2 Input data for the probabilistic analysis for strength class C30/37

Input parameters		Distribution	Min	Mean	Max	SD
f_{cm} (EN1992-1-1) 28-day	MPa	NORMAL		2.90		0.53
f_{cm} (EN1992-1-1) 3-day	MPa	NORMAL		1.73		0.32
<i>In situ</i> effects	k_{is}	NORMAL		0.90		0.082
Sustained loading	k_s	PERT	0.6	0.70	0.8	
[Early] Age factor (relative to 3days)	k_a	PERT	0.54	1.00	1.28	
[Long-term] Age factor relative to 28 days	k_a	PERT	0.90	1.00	1.10	

Probability distributions for *in situ* strength have been estimated for both early-age and long-term cracking and are shown in Figures A10.6 and A10.7 respectively. The most likely value of *in situ* tensile strength at early-age is estimated to be about 1.1 MPa, with 90 per cent of the results falling in the range from about 0.7 to 1.5 MPa. In the long-term the most likely value of *in situ* tensile strength at early-age is about 1.8 MPa, with 90 per cent of the results falling in the range from about 1.1 to 2.5 MPa. In each case the mean value is about $2/3 f_{cm}(t)$.

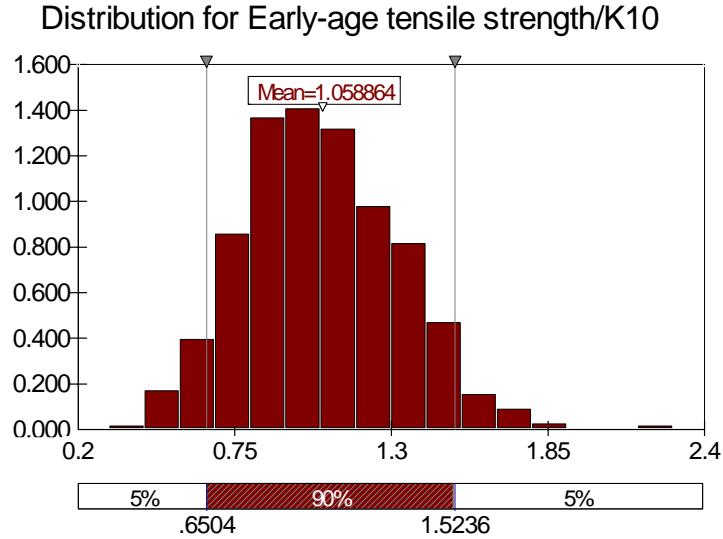


Figure A10.6 Distribution of early-age *in situ* tensile strength for C30/37 concrete

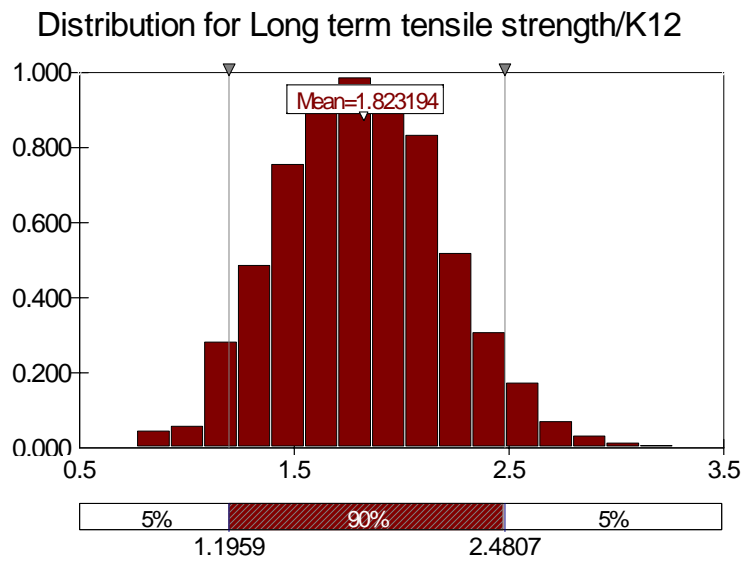


Figure A10.6 Distribution of long-term *in situ* tensile strength for C30/37 concrete

To determine the level of safety associated with the use of values of $f_{cm}(t)$, 95 and 99 percentile values have been estimated for a range of strength classes at 3 days and 28-days. The results are shown in Table A10.3 and indicate that if values derived according to EN1992-1-1 are used, there is less than a 1 per cent chance of these values being exceeded *in situ*. These values are therefore safe with regard to the estimation of both $A_{s,min}$ and crack width for end-restrained elements.

Table A10.3 *Estimated in situ tensile strength at early-age and long-term compared with values calculated in accordance with EN1992-1-1*

Strength class	Early-age (3 days)			Long-term (28 days)		
	In-situ values		EN1992-1-1	In-situ values		EN1992-1-1
	95%	99%		95%	99%	
C20/25	1.16	1.30	1.33	1.92	2.17	2.28
C25/30	1.30	1.46	1.51	2.17	2.49	2.58
C30/37	1.52	1.70	1.73	2.48	2.81	2.90
C35/45	1.72	1.94	1.98	2.84	3.19	3.30
C40/50	1.83	2.05	2.12	3.06	3.41	3.54
C45/55	1.95	2.17	2.26	3.25	3.73	3.77
C50/60	2.06	2.34	2.39	3.43	3.90	4.00
C55/67	2.15	2.44	2.51	3.63	4.05	4.20
C60/75	2.27	2.52	2.62	3.76	4.23	4.38

A10.5 Conclusions

1. The *in situ* tensile strength of concrete is affected by numerous factors including the compaction and curing, the peak temperature achieved during the early thermal cycle, the age of the concrete and the effect of sustained loading.
2. A probabilistic analysis has been undertaken to determine the likely range of *in situ* tensile strength at early-age and in the long-term. It is estimated that the most likely value of *in situ* tensile strength is about 2/3 of the mean value of tensile strength $f_{cm}(t)$ calculated using the expressions given in EN1992-1-1.
3. Based on the probabilistic analysis it is estimated that the use of three day and 28-day values of $f_{cm}(t)$ will result in less than a 1 per cent chance of these values being exceeded at early-age or in the long-term respectively. The use of $f_{cm}(3)$ and $f_{cm}(28)$ will therefore provide a sufficiently safe basis upon which to calculate the minimum area of reinforcement and crack widths.

A10.6 References

Alexander, S J (2006)

“Why does our concrete still crack and leak”

The Structural Engineer, 5 December 2006, pp 40-43, London

<<http://www.istructe.org/thestructuralengineer>>

Altoubat, S A and Lange, D A (2001a)

“Creep, shrinkage and cracking of restrained concrete at early-age”

ACI Materials Journal, July/August 2001, 98 (No.4), pp 323-331

Bamforth, P B and Price, W F (1995)

Concreting deep lifts and large volume pours

Report 135, CIRIA, London

van Breugle, K and Lokhorst, S J (2001)

“The role of microstructural development on creep and relaxation of hardened concrete”

In: *Proc RILEM PRO 23, Early-age cracking in cementitious systems*, 1, Haifa, Israel, pp 3-10

Concrete Society (2004)

In situ strength of concrete – An investigation into the relationship between core strength and the standard cube strength

Working party of the Concrete Society, Project Report No 3, BCA, Camberley, Surrey, ISBN 0 94669 186 X

Domone, P L J (1974)

Uniaxial tensile creep and failure of concrete

Magazine of Concrete Research, 26 (No 88), Sept 1974, pp 144-152

Harrison, T (1992)

Early-age thermal crack control in concrete

R91, CIRIA, London

Highways Agency (1989)

“Early thermal cracking of concrete”

Design manual for roads and bridges, Vol 1 Highways structures: Approval procedures and general design, Section 3: General design, HA BD 28/87, Incorporating Amendment No1, HMSO

Reinhardt, H W and Rinder, T (1998)

“High strength concrete under sustained tensile loading”

Ototo-Graf-Journal, 9, pp 123-134

<www.mpa.unistuttgart.de/publikationen/otto_graf_journal/ogj_1998/beitrag_reinhardt_rinder.pdf>

British Standards

BS 8007:1987 *Design of concrete structures for retaining aqueous liquids*

Euro Codes

EN1992-1-1:2004

Eurocode 2. Design of concrete structures. General rules and rules for buildings